ISSN 2518-1726 (Online),
ISSN 1991-346X (Print)

ҚАЗАҚСТАН РЕСПУБЛИКАСЫ
ҰЛТТЫҚ ҒЫЛЫМ АКАДЕМИЯСЫНЫҢ
Әль-фараби атындағы Қазақ ұлттық университетінің

Х А Б А Р Л А Р Ы

ИЗВЕСТИЯ

НАЦИОНАЛЬНОЙ АКАДЕМИИ НАУК
РЕСПУБЛИКИ КАЗАХСТАН
Казахский национальный университет
имени Аль-фараби

N E W S

OF THE NATIONAL ACADEMY OFSCIENCES
OF THE REPUBLIC OF KAZAKHSTAN
Al-farabi kazakh
national university

SERIES
PHYSICO-MATHEMATICAL

4 (326)

JULY-AUGUST 2019

PUBLISHED SINCE JANUARY 1963

PUBLISHED 6 TIMES A YEAR

ALMATY, NAS RK

«ҚР ҰҒА Хабарлары. Физика-математикалық сериясы».

ISSN 2518-1726 (Online), ISSN 1991-346X (Print)

Меншіктенуші: «Қазақстан Республикасының Ұлттық ғылым академиясы» РҚБ (Алматы қ.)
Қазақстан республикасының Мәдениет пен ақпарат министрлігінің Ақпарат және мұрағат комитетінде 01.06.2006 ж. берілген **№5543-Ж** мерзімдік басылым тіркеуіне қойылу туралы куәлік

Мерзімділігі: жылына 6 рет.
Тиражы: 300 дана.

Редакцияның мекенжайы: 050010, Алматы қ., Шевченко көш., 28, 219 бөл., 220, тел.: 272-13-19, 272-13-18, http://physics-mathematics.kz/index.php/en/archive

---

Типографияның мекенжайы: «Аруна» ЖК, Алматы қ., Муратбаева көш., 75.

«Известия НАН РК. Серия физико-математическая».

ISSN 2518-1726 (Online), ISSN 1991-346Х (Print)

Собственник: РОО «Национальная академия наук Республики Казахстан» (г. Алматы)
Свидетельство о постановке на учет периодического печатного издания в Комитете информации и архивов Министерства культуры и информации Республики Казахстан **№5543-Ж**, выданное 01.06.2006 г.

Периодичность: 6 раз в год.
Тираж: 300 экземпляров.

Адрес редакции: 050010, г. Алматы, ул. Шевченко, 28, ком. 219, 220, тел.: 272-13-19, 272-13-18,
http://physics-mathematics.kz/index.php/en/archive

Адрес типографии: ИП «Аруна», г. Алматы, ул. Муратбаева, 75.

News of the National Academy of Sciences of the Republic of Kazakhstan. Physical-mathematical series.

ISSN 2518-1726 (Online), ISSN 1991-346X (Print)

Owner: RPA "National Academy of Sciences of the Republic of Kazakhstan" (Almaty)
The certificate of registration of a periodic printed publication in the Committee of information and archives of the Ministry of culture and information of the Republic of Kazakhstan N 5543-Ж, issued 01.06.2006

Periodicity: 6 times a year
Circulation: 300 copies

Editorial address: 28, Shevchenko str., of. 219, 220, Almaty, 050010, tel. 272-13-19, 272-13-18,
http://physics-mathematics.kz/index.php/en/archive

Address of printing house: ST "Aruna", 75, Muratbayev str, Almaty

N E W S
OF THE NATIONAL ACADEMY OF SCIENCES OF THE REPUBLIC OF KAZAKHSTAN
PHYSICO-MATHEMATICAL SERIES
ISSN 1991-346X **https://doi.org/10.32014/2019.2518-1726.38**
Volume 4, Number 326 (2019), 5 – 13

D. M. Zazulin[1,2], N.Burtebayev[1,2], R. J. Peterson[3], S. V. Artemov[4], S. Igamov[4], Zh.K. Kerimkulov[1], D. K. Alimov[1], E. S. Mukhamejanov[1,2], Maulen Nassurlla[1,2], A. Sabidolda[1], Marzhan Nassurlla[1,2], R. Khojayev[1,2]

[1]Institute of Nuclear Physics, Almaty, Kazakhstan;
[2]Al-Farabi Kazakh National University, Almaty, Kazakhstan;
[3]University of Colorado, Boulder, Colorado, USA;
[4]Institute of Nuclear Physics, Tashkent, Uzbekistan
nburtebayev@yandex.ru; denis_zazulin@mail.ru; nburtebayev@yandex.ru; jerry.peterson@colorado.edu; artemov1943@gmail.com; igamov@inp.uz; zhambul-k@yandex.ru; diliyo@mail.ru; craftinho@mail.ru; morzhic@mail.ru; nespad@mail.ru; asabidolda@mail.ru; ramazan_inp@mail.ru

NEW RESULTS FOR THE P-^{12}C RADIATIVE CAPTURE AT LOW ENERGIES

Abstract. New measurements of the differential cross sections of the ^{12}C(p,γ)^{13}N radiative capture reaction at the angle 0^0 for the transition to the ground state in ^{13}N have been made at the energies of incident protons from 1088 to 1390 keV (uncertainties of about 12%). Based on the obtained differential cross sections and on the assumption that the angular distributions are isotropic in this energy region, the ^{12}C(p,γ)^{13}N reaction astrophysical S-factors have been determined for the transition to the ground state in ^{13}N with an uncertainties of about 16%. Within the limits of uncertainties, our experimental results are consistent with the previous data. Analysis of the ^{12}C(p,γ)^{13}N reaction astrophysical S-factor at low energies has been carried out within the modified R-matrix approach by using previously measured asymptotic normalization coefficient of the overlap integral of the wave functions of ^{12}C and ^{13}N nuclei bound states to minimize the uncertainties due to calculation of the direct capture part of the ^{12}C(p,γ)^{13}N reaction astrophysical S-factor at extremely low energies. For the energies of 0.25 and 50 keV in center of mass frame the calculated values of the ^{12}C(p,γ)^{13}N reaction S-factors for the transition to the ground state in ^{13}N are presented. In the temperature range from 0 to 10^{10} K the rates of the ^{12}C(p,γ)^{13}N fusion reaction have been obtained. The results of our calculations are compared with the experimental and calculated results of previous works.

Keywords: differential cross sections, total cross sections, astrophysical S-factor, asymptotic normalization coefficient, reaction rates.

Introduction

It is well known that, in addition to the hydrogen pp chain, in stars more massive than the Sun, hydrogen can burn in the reactions of the carbon-nitrogen cycle (CNO cycle) [1]. The sequence of the cold CNO cycle consists of the following reactions: ^{12}C(*p,γ*)^{13}N(→^{13}C+ e^+ +ν_e) ^{13}C(*p,γ*)^{14}N(*p,γ*)^{15}O(→^{15}N+ e^+ +ν_e) ^{15}N*(p,α)*^{12}C. In this sequence, four protons are transformed into α particle (4 p → α) and as a result the energy of 26.73 MeV is released. Approximately 1.7 MeV of this energy is carried away by the neutrinos. As calculations show, the rate of energy release in the CNO cycle with increasing temperature (T ~ 10^7 K) increases much faster than the rate of energy release in the *pp*-chain.

The ^{12}C(p,γ)^{13}N reaction is the first reaction of the hydrogen-burning CNO cycle and plays an important role as a source of generation of both nuclear energy [1] and low-energy neutrinos [2-5] in massive stars. In the low-energy region, the ^{12}C(p,γ)^{13}N radiative capture reaction with formation of ^{13}N nucleus in the ground state mainly goes via both direct and resonant (E^* = 2.365 MeV, J^π = $1/2^+$ and E^* = 3.502 MeV, J^π = $3/2^-$) captures. Therefore, calculations of the ^{12}C(p,γ)^{13}N reaction astrophysical S-factor, which is based on the analysis of experimental data, should take into account the contributions of the abovementioned two resonant and direct radiative captures, as well as their interference, in the energy region $E_{c.m.}$ < 2.5 MeV (c.m. here is the center of mass frame). Unfortunately, in the energy region between these two resonances, the available experimental data have large uncertainties [1].

Therefore, in this region $E_{p,\ lab.}$ = 1100- 1400 keV (lab. here is the laboratory frame), we have made new experimental measurements of the astrophysical S-factor for the $^{12}C(p,\gamma)^{13}N$ radiative capture reaction with an uncertainty of about 16%. The calculation of the astrophysical S-factor, including the analysis of our new experimental data, has been made within the modified R-matrix method proposed previously in [6-9].

Experimental method and results of the measurements

The experimental part of our work was done on the electrostatic tandem accelerator UKP-2-1 of the Institute of Nuclear Physics ME RK in Almaty [10]. Protons were accelerated to energies $E_{p,\ lab.}$ = 340-1400 keV. Calibration of proton energies in the beam was made with uncertainties of ± 1 keV according to the $^{19}F(p,\alpha\gamma)^{16}O$ and $^{27}Al(p,\gamma)^{28}Si$ reactions with many well-separated resonances in the region of $E_{p,\ lab.}$ = 340-1400 keV [11, 12].

In our experiments, a specially made reaction chamber [6] with indium vacuum seals, a water-cooled target holder, and a quartz glass for obtaining a luminous image of the beam shape in front of the target were used. By an external handle, the quartz glass could be placed in front of the target for alignment. The γ-ray registration system was realized by using high-pure Germanium (HPGe) γ-detector with a Ge-crystal of volume of 111 cm^3. To reduce the room and cosmic ray background the γ-detector was surrounded by 6 cm thick lead shield. The resolution of the γ-detector was about 5 keV at E_γ = 2200 - 3250 keV. The target was produced by sputtering natural carbon onto a 2 mm thick Cu substrate (thickness ≈ 2 mm, length ≈ 30 mm, and width ≈ 15 mm). The thickness of the carbon film sputtered onto the substrate was 110 ± 8.8 $\mu g/cm^2$. The detailed description of the reaction chamber, the target production technology, and the target thickness determination method can be found in Refs. [6, 13, 14].

The absolute detector γ-ray efficiency for E_γ = 2200 - 3250 keV was determined by using γ-lines (E_γ = 2034.92, 2598.58 and 3253.6 keV) of a calibrated ^{56}Co source, with γ-lines intensities known to better than 4.5% [15].

When measuring the absolute efficiency, the detector and the ^{56}Co source were located precisely in the geometry of the experiment. At the same time, the statistical uncertainty in determining the number of counts for each γ-line was no more than 2%, and the electronics dead time did not exceed 1%.

The experimental differential cross sections of radiative capture were obtained at the measurement complex of INP [6], which allow to study the yields of the nuclear reactions on the extracted beams of the cyclotrons of the institute at the low and ultra low energies for the astrophysical and thermonuclear applications, see papers [6, 13, 14, 16].

During the measurements, γ-detector was about 8 cm away from the beam spot on the target. The γ-detector and ^{56}Co source were located with an uncertainty of about 1 mm. The dependence of the γ-ray registration rate on the source-detector distance was determined using ^{56}Co source. It was determined that at a distance of 8 cm, a deviation of ± 1 mm leads to a change in the γ-ray registration rate by ± 3%. Thus, uncertainties in the source and detector positions, dead time, γ-lines intensities, and counting statistics lead to an overall uncertainty of 6% for the detector efficiency over the entire energy interval of registered γ-rays (i.e. from 2200 to 3250 keV).

The differential cross sections of the $^{12}C(p,\gamma)^{13}N$ reaction for the transition to the ground state were determined at $E_{p,\ lab.}$ = 1100, 1150, 1250 and 1400 keV and at $\theta_{\gamma,\ lab.} = 0^0$.

Beam currents ranged from 5 to 8 μA. The energy spread of the beam was determined by the width of the front of the $^{27}Al(p,\gamma)^{28}Si$ reaction yield curve near the resonance at $E_{p,\ lab.}$ = 992 keV (resonance width < 0.1 keV) and did not exceed 1.5 keV. The accumulated charges on the target with an uncertainty of 3% were 0.28, 1.26, 1.51 and 1.4 Coulomb for $E_{p,\ lab.}$ = 1100, 1150, 1250 and 1400 keV, respectively. Dead-time effects were kept below 1.5% at all beam energies.

Figure 1 shows the γ-ray spectrum obtained at $E_{p,\ lab.}$ = 1100 keV and $\theta_{\gamma,lab.} = 0^0$. The energy calibration of the spectrometer was determined using well-known γ-lines of the ^{56}Co source and the room background γ-lines at 1461 keV (^{40}K) and at 2614 keV (Th).

The number of counts in the spectral peak with preliminarily subtracted background (trapezium shaped) divided by the calibrated integrator counter value was taken as the yield of the $^{12}C(p,\gamma)^{13}N$ capture reaction. Statistical uncertainties in the determination of the yields (including uncertainties introduced by backgrounds subtracted) were about 15% for the measurement at $E_{p,\ lab.}$ = 1100 keV and about 6% for the measurements at all other energies.

During each measurement, we computed the number of registered γ -rays of the transition to the ground state in ^{13}N (N_γ) over the integrator counter (N_p) as the yield per proton. For each of the energies presented in the work, the dependence of N_γ on N_p represented a straight line within the current statistical uncertainty of determining N_γ, which indicated the stability of the target and the stability of the beam position on it during the whole exposure.

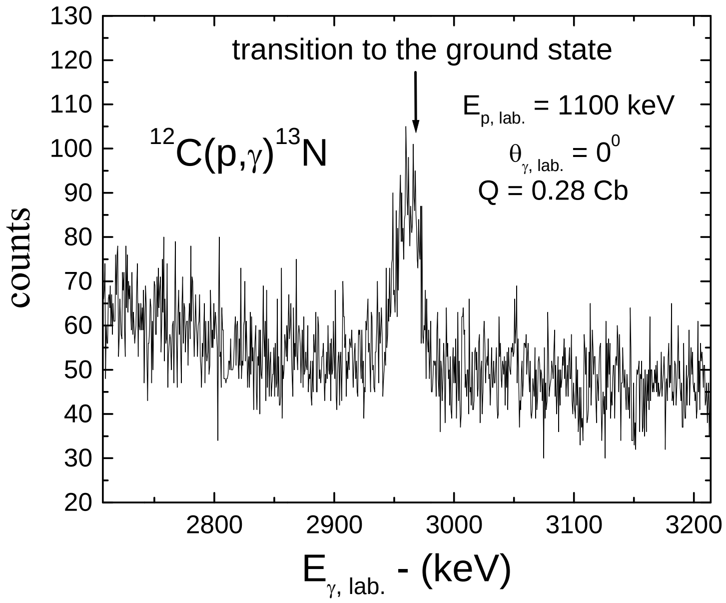

Figure 1 - γ-ray spectrum of the ^{12}C(p,γ)^{13}N reaction for the radiative capture transition to the ground state in ^{13}N as obtained at the laboratory proton energy of 1100 keV ($\theta_{\gamma,\ lab.} = 0^0$) by our HPGe γ-detector of volume 111 cm^3, located 8 cm. from the reaction region

Since, in the region $E_{p,\ lab.}$ = 1000-1400 keV the differential cross sections change only slightly with energy, as can be seen, for example, from previous works [6, 17], the effective laboratory energies were found using the expression $E_{p,\ eff} = E_{p,\ lab} - 0.5\Delta_{lab}(E_{p,\ lab})$, where Δ_{lab} is the energy loss of protons in the target.

Because the γ-detector energy resolution and the proton beam energy spread are significantly less than the energy losses of protons in the target, the upper part of the ^{12}C(p,γ)^{13}N reaction γ-line, for example, shown in Figure 1, repeats the course of the ^{12}C(p,γ)^{13}N reaction yield curve in the corresponding energy region (the spectrum in Figure 1 has too big statistical uncertainties), and the width of this γ-line is largely due to the target thickness. This circumstance allowed us to determine the target thickness also by analyzing the ^{12}C(p,γ)^{13}N reaction γ-lines shapes (i.e. as a second independent method) and to confirm the value obtained by the first method within the uncertainties. Moreover, the second method allowed us to check the uniformity of the target thickness for all the spectra obtained.

The differential cross sections of the ^{12}C(p,γ)^{13}N reaction for radiative capture to the ground state of ^{13}N at $\theta_{\gamma,\ lab} = 0^0$ were determined by using the relation

$$\frac{d\sigma}{d\Omega}(E_{p,\ eff.}, 0^0) = \frac{N_\gamma}{N_p\ N_{C^{12}}\ \varepsilon(E_{\gamma,\ eff.})}$$

where N_γ is the number of counts observed for the capture transition, $\varepsilon(E_{\gamma,\ eff.})$ is the absolute detector γ-ray efficiency, $E_{\gamma,\ eff.} = E_{p,\ lab.}\frac{12}{13} + 1941 - 0.5\,\Delta_{lab.}(E_{p,\ lab.})$, N_p is the number of incident protons, and $N_{C^{12}}$ is the areal density of ^{12}C atoms.

As an additional test of the method for obtaining the absolute values of the differential cross sections, we have measured the yields over the $^{12}C(p,\gamma)^{13}N$ resonance at $E_{p,\ lab.}$ = 457 keV (the differential cross sections in this energy range are known, for example, from [6, 17] with uncertainties of no more than 10%). Due to the energy losses of protons in the target in this energy region match with the resonance width (which is about 40 keV) the yields in the resonance region were determined by the relation

$$N_\gamma = N_p\ N_{C^{12}} \int_{E_{p,\ exit}}^{E_{p,\ lab.}} \frac{d\sigma}{d\Omega}(E, 0^0)\ \varepsilon(E)\ \frac{d\Delta}{dE}(E)\ dE$$

where $E_{p,\ lab.}$ is the proton energy at the target entrance ($E_{p,\ lab.}$ = 440, 450, 460, 470, 480 keV), $E_{p,\ exit}$ is the corresponding proton energy at the target exit, $\frac{d\sigma}{d\Omega}(E, 0^0)$ is the differential cross section of the $^{12}C(p,\gamma)^{13}N$ reaction for the capture to the ground state of ^{13}N at $\theta_{\gamma,\ lab.} = 0^0$ (the experimental data were taken from [6, 17]), $\frac{d\Delta}{dE}(E)$ is the stopping power of protons in carbon (calculated by the LISE++ program [18]). Such measurements were carried out before and after the main experiments, and the calculated and measured yields matched within the uncertainties.

The differential cross sections obtained in present work are given in the second row of Table 1. Assuming isotropy in the angular distributions of the $^{12}C(p,\gamma)^{13}N$ reaction in the energy region of incident protons from 400 to 1390 keV (which is confirmed with uncertainties of 10% in the works [6, 17]) in the present work, the total sections are calculated according to the formula:

$$\sigma(E_{p,\ eff.}) = 4\pi \frac{d\sigma}{d\Omega}(E_{p,\ eff.}, 0^0)$$

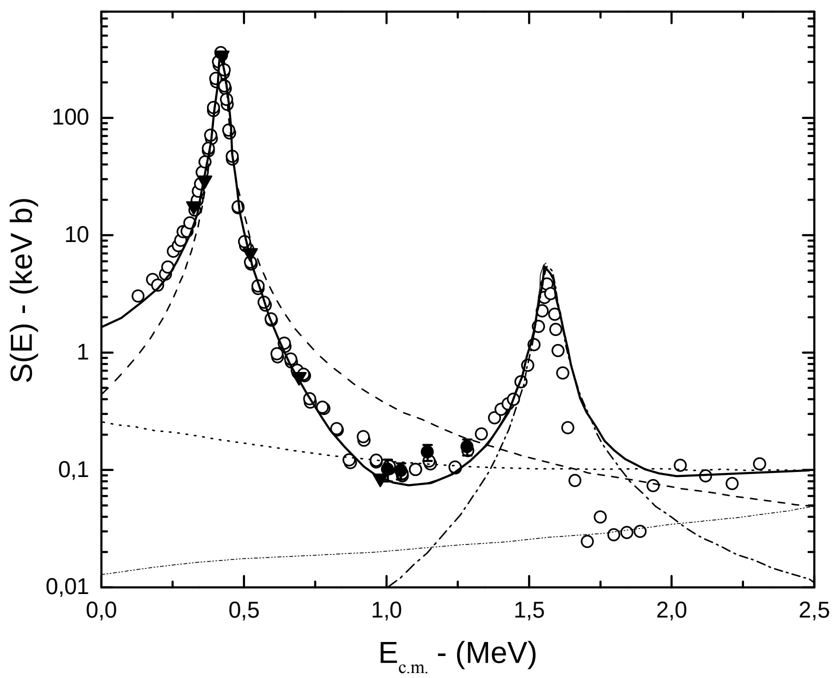

Figure 2 - The astrophysical S-factor for the $^{12}C(p,\gamma)^{13}N$ reaction. The experimental data: filled circles are the result of the present work, filled triangles are the data from [6] and open circles are the data from [17]. The solid line is our fit, dotted line is our calculated contribution for the direct radiative capture, dashed (dashed-dotted) line shows our calculated contribution for the first (second) resonance and dashed-dotted-dotted line presents our calculated contribution for the third (E^* = 10.250 MeV, $J^\pi = 1/2^+$) γ-resonance tail

Further, according to the relation:

$$S(keV\ b) = \sigma(b)\ E(keV)\ \exp(\frac{180.29}{\sqrt{E(keV)}})$$

the astrophysical S-factors were calculated, which are given in the third row of Table 1 and are shown in Figure 2 in comparison with the results of previous works. From Figure 2, it is clear that the experimental data of our work are in good agreement with the results obtained in [6, 17].

Table 1 + Experimental differential cross sections and experimental astrophysical S - factors of the $^{12}C(p,\gamma)^{13}N$ reaction for radiative capture to the ground state of ^{13}N

$E_{p,\ eff.}$ (keV)	1088	1138.5	1239.3	1390
$\frac{d\sigma}{d\Omega}^{exp.}(E,0^0)$ – ($\frac{\mu b}{sr}$)	0.027±0.0049	0.029±0.0035	0.048±0.0058	0.064±0.0077
$S^{exp.}(E)$ – (MeV b)	0.1±0.02	0.098±0.015	0.14±0.022	0.16±0.025

Results of the $^{12}C(p,\gamma)^{13}N$ reaction astrophysical S-factor calculation by the modified R-matrix analysis method

The detailed description of the modified R-matrix method that was used in the calculations can be found in [6-9, 19, 20]. The input parameters required for calculating the $^{12}C(p,\gamma)^{13}N$ reaction astrophysical S-factor for transition to the ground state of ^{13}N (channel radius, proton width and radiative widths of the first and second resonance states) were taken from [6]. The experimental results of this work and the experimental results of [6, 17] were used as experimental data. The asymptotic normalization coefficient (ANC) value was taken equal to 1.43 ± 0.09 $fm^{-1/2}$ [21, 22] as in [6].

The results of our calculations of the $^{12}C(p,\gamma)^{13}N$ reaction astrophysical S-factor taking into account the analysis of new experimental data completely repeat our earlier results [6] and are shown in Figure 2, where the contributions of direct radiative capture (dotted line), first resonance (dashed line) and second resonance (dashed-dotted line) are given separately. The inclusion of the third resonant state (E^* = 10.250 MeV, $J^\pi = 1/2^+$, the proton width Γ_3^p = 280 keV [23] and the radiation width Γ_3^γ = 6000 eV [6]) tail part contribution in the calculations significantly improved the theoretical description of the experimental data (dashed-dotted-dotted line). The values of the resonant parameters used in present work are listed in Table 2 of [6].

The results of our calculations of the $^{12}C(p,\gamma)^{13}N$ reaction astrophysical S-factors for the transition to the ground state of ^{13}N at the most important energies for astrophysics E = 0; 25 and 50 keV are S(0 keV) = 1.62 ± 0.20 keVb, S(25 keV) = 1.75 ± 0.22 keVb and S(50 keV) = 1.88 ± 0.24 keVb, respectively. The uncertainties quoted for these astrophysical S-factors are due to those of the parameters of proton and γ widths and ANC given earlier [6]. Our central value for S(25 keV) within the specified uncertainty is consistent with the values of S(25 keV) = 1.54 ± 0.08 keVb obtained in [24] and S(25 keV) = 1.45 ± 0.20 keVb obtained in [17], and in satisfactory agreement with the value of S(25 keV) = 1.33 ± 0.15 keVb obtained in [25, 26]. However, our result for S(0 keV) is noticeably larger than that of S(0 keV) = 1.0 and 1.3 keVb obtained in [27] using the Minnesota and V2 forms of the NN potential, respectively, as well as the value of S(0 keV) = 1.4 keVb recommended in [28]. It should be emphasized that a value of S(25 keV) = 1.54 ± 0.08 keVb in [24] has been also obtained within the R-matrix approach [7, 9]. In contrast to our work in [24], the ANC, which is responsible for the contribution of direct radiative capture, was a fitting parameter in order to better describe the experimental data at first resonance region. As a result, this artificial overestimation of the ANC value led to resonance (Γ_1^γ = 0.50 ± 0.05 eV) decrease in the total amplitude of the radiative capture process, which led to an underestimated value of S(25 keV). In our present work, we used the fixed ANC value obtained independently from the analysis of the peripheral proton transfer reaction [21, 22], which allowed us earlier in [6] to carry out fitting of resonant width parameters (for example, Γ_1^γ = 0.65 ± 0.07 eV) in a correct way.

$^{12}C(p,\gamma)^{13}N$ reaction rate

The calculated astrophysical S-factors, as well as the data of [6, 17], were used for calculating the rate of ^{13}N nucleus formation in the stellar interior as a function of stellar temperature T_9, where $T_9 = T \times 10^9$ K. The Maxwellian-averaged reaction rates $N_A(\sigma v)$ as a function of temperature are defined by

$$N_A(\sigma\upsilon) = N_A\left(\frac{8}{\pi\mu}\right)^{1/2}(k_B T)^{-3/2}\int_0^{\infty}\sigma(E)\exp(-E/k_B T)EdE\,,$$

where N_A is Avogadro's number, k_B is the Boltzmann constant, and $\vartheta = \sqrt{2E/\mu}$ is the relative velocity of the colliding particles. The calculation performed in the present work matches with the results we obtained in [6]. Figure 3(a) shows the reaction rates of our calculation (solid line) and its comparison with the experimental data of [29]. It is seen that the result of our calculation is in good agreement with those recommended in [29]. That work used a very different method, with independent systematic uncertainties, and cited uncertainties equal to the estimated values for unobserved energies. The ratio of our calculation of reaction rates $N_A(\sigma v)$ to the result recommended in [30] (solid line) is also given in Figure 3(b). As is seen from Figure 3(b) there is a noticeable difference (up to ≈ 20%) between our recommended results and those given in [30] within a wide interval of stellar temperatures. The probable reason for the observed difference is that in [30] the calculation of the reaction rates included all the experimental astrophysical S-factors obtained in [17, 25, 26, 30], some of which have uncertainties up to 40%, by a smooth spline fit. Moreover, it was assumed in [30] that the spectroscopic factor for the ground state of the ^{13}N nucleus in (^{12}C + p) - configuration is 1. However, as can be seen from [31], this assumption is not justified and, in fact, the empirical value of the spectroscopic factor is 0.55 ± 0.18. It can be considered that the result in [30] is model-dependent, while our calculation of the reaction rate does not contain free parameters and in this sense it can be regarded as more reliable.

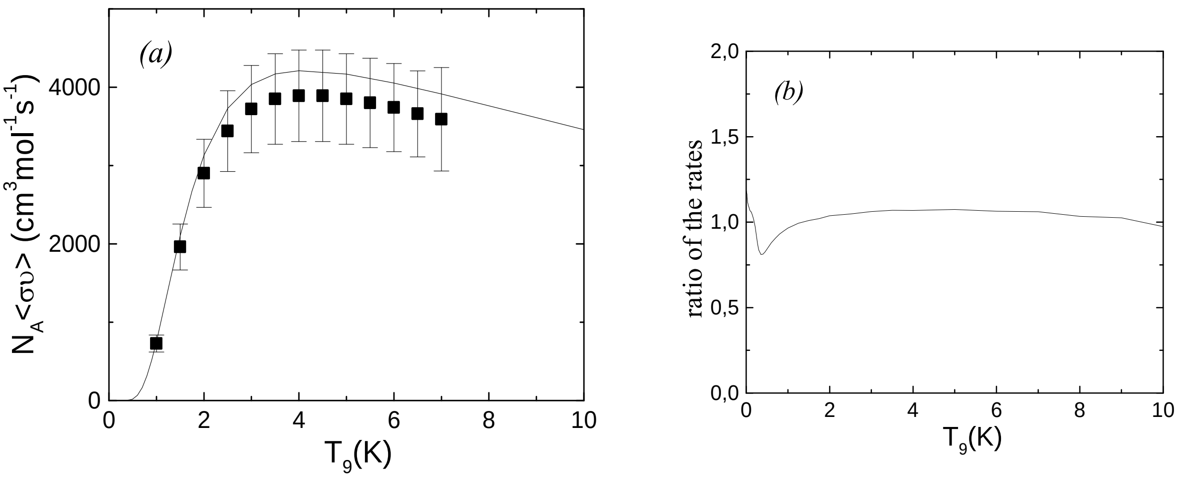

Figure 3 - (a) The $^{12}C(p,\gamma)^{13}N$ reaction rate calculated in present work (solid line) and points taken from [29].
(b) The ratio of the $^{12}C(p,\gamma)^{13}N$ reaction rates N_A ($\sigma\upsilon$) of present work to those from [30] (solid line)

Conclusion

In this work new experimental data on the differential cross sections of the $^{12}C(p,\gamma)^{13}N$ reaction for the transition to the ground state of ^{13}N have been obtained at four energies from 1088 to 1390 keV in the laboratory system at an angle of 0^0 with uncertainties of about 12%. The astrophysical S-factors for radiative capture of a proton to the ground state of ^{13}N (the only bound state of this nucleus) have been determined with uncertainties of about 16% at these energies. Our experimental data are in good agreement with those previously obtained in [6, 17].

We have analyzed the new experimental data on $^{12}C(p,\gamma)^{13}N$ reaction astrophysical S-factors for the transition to the ground state of ^{13}N at extremely low energies within the one-level R-matrix approach where the direct part of the amplitude is expressed in terms of the ANC for ^{13}N in the (p + ^{12}C) channel. Such a parametrization allowed us to calculate the direct capture part of the amplitude in a correct way using the indirectly measured value of ANC found previously in [21, 22] from the analysis of the peripheral $^{12}C(^{3}He,d)^{13}N$ reaction.

It is shown that using information about ANC value provides good fitting of the experimental astrophysical S-factor of the $^{12}C(p,\gamma)^{13}N$ reaction for the transition to the ground state of ^{13}N and reduces to a minimum the model dependence of the calculated direct capture part of the astrophysical S-factor on the parameters of the R-matrix approach . In general, the results of the new analysis of the experimental astrophysical S-factors match with the results of our previous work [6].

We have also calculated the rates of the $^{12}C(p,\gamma)^{13}N$ reaction for the astrophysically important transition to the ground state of ^{13}N in the low energy region. It has been shown that these present reaction rates (as well as the rates of [6]) are in good agreement with those recommended in [29] using a very different technique from that described in present work, whereas a notable difference (up to ≈ 20%) occurs between our result (as well as the result of [6]) and that given in [30] within a wide interval of stellar temperatures.

Acknowledgments

The authors would like to thank the UKP-2-1 staff for assistance with the experiment. This work was supported by program targeted funding titled “Development of the complex scientific research activities in nuclear and radiation physics based on the Kazakhstan’s accelerator facilities” # 0118PK01174.

Д.М. Зазулин[1,2], Н. Буртебаев[1,2], Р.Ж. Петерсон[3], С.В. Артемов[4], С. Игамов[4], Ж.К. Керимкулов[1], Д.К. Алимов[1], Е.С. Мухамеджанов[1,2], Маулен Насурлла[1,2], А. Сабидолда[1], Маржан Насурлла[1,2], Р. Ходжаев[1,2]

[1]Ядролық физика институты, Алматы, Қазахстан;
[2] аль-Фараби атындағы ҚазҰУ, Алматы, Қазахстан;
[3] Колорадо Университеті, Болдер, Колорадо, АҚШ;
[4]Ядролық физика институты, Ташкент, Узбекистон

ТӨМЕН ЭНЕРГИЯЛАРДАҒЫ P-^{12}C РАДИАЦИЯЛЫҚ ҚАРПУЫНЫҢ ЖАҢА НӘТИЖЕЛЕРІ

Аннотация. Жұмыста үдетілінген протондардың 1088 – 1390 кэВ энергияларында 0^0 бұрышта $^{12}C(p,\gamma)^{13}N$ радиациялық қарпуы реакциясының ^{13}N ядросының негізгі күйіне көшуінің дифференциалдық қимасының жаңа өлшеулер нәтижелері (12% дәлдікпен) ұсынылды. Алынған дифференциалдық қималар және осы энергия аймағындағы бұрыштық таралулардың изотроптық қасиетке ие болатындығына негізделе отырып, 16 % дәлдікпен $^{12}C(p,\gamma)^{13}N$ реакциясы үшін ^{13}N негізгі күйге ауысуының астрофизикалық S факторы анықталды. Қателер шегінде, осы жұмыстың эксперименттік нәтижелері бұрынғы жұмыстардың деректерімен сәйкес келеді. Модификацияланған R - матрицалық әдісті пайдалана отырып, астрофизикалық S-фактор бойынша эксперименттік мәліметтер талданды. Аса төменгі энергияларда ^{12}C ядросымен протондардың тікелей қарпылуына байланысты есептеу қәтеліктерін азайту мақсатында талдау барысында ^{12}C және ^{13}N ядроларының байланысқан күйлерінің толқындық функцияларының қабаттасу интегралының өлшенілген асимптотикалық нормалау коэффициентінің мәні пайдаланылды. Массалар орталығы жүйесінде E = 0,25 және 50 кэВ энергияларда $^{12}C(p,\gamma)^{13}N$ реакциясынан ^{13}N ядросының негізгі күйге ауысуы үшін S-фактордың есептік мәндері келтірілген. 0 - 10^{10} К температура аймағында $^{12}C(p,\gamma)^{13}N$ термоядролық реакциясының жылдамдықтары анықталды. Бұл жұмыстың есептеу нәтижелері бұрынғы жұмыстардың эксперименттік және есептік мәліметтерімен салыстырылды.

Түйін сөздер: дифференциалдық қималар, толық қима, астрофизикалық S-фактор, асимптотикалық нормалау коэффициенті, реакцияның жылдамдықтары.

УДК 524.1; 539.14/.17

Д.М. Зазулин[1,2], Н. Буртебаев[1,2], Р.Ж. Петерсон[3], С.В. Артемов[4], С. Игамов[4], Ж.К. Керимкулов[1], Д.К. Алимов[1], Е.С. Мухамеджанов[1,2], Маулен Насурлла[1,2], А. Сабидолда[1], Маржан Насурлла[1,2], Р. Ходжаев[1,2]

[1]Институт ядерной физики, Алматы, Казахстан;
[2]КазНУ им. аль-Фараби, Алматы, Казахста;
[3]Университет Колорадо, Болдер, Колорадо, США;
[4]Институт ядерной физики, Ташкент, Узбекистан

НОВЫЕ РЕЗУЛЬТАТЫ ДЛЯ РАДИАЦИОННОГО ЗАХВАТА p-^{12}C ПРИ НИЗКИХ ЭНЕРГИЯХ

Аннотация. Представлены результаты новых измерений дифференциальных сечений реакции ^{12}C(p,γ)^{13}N радиационного захвата на основное состояние ^{13}N для угла 0^0 и при энергиях налетающих протонов от 1088 до 1390 кэВ (точность около 12%). На основе полученных дифференциальных сечений и в предположении об изотропном характере угловых распределений в данной области энергий с точностью около 16% определены астрофизические S – факторы реакции ^{12}C(p,γ)^{13}N для перехода на основное состояние ^{13}N. В пределах погрешностей экспериментальные результаты настоящей работы согласуются с данными более ранних работ. С использованием модифицированного R – матричного метода проведен анализ экспериментальных данных по астрофизическому S – фактору. В целях минимизации вычислительной неопределенности, связанной с прямым захватом протона ядром ^{12}C для самых низких энергий, при анализе использовалось значение измеренного раннее асимптотического нормировочного коэффициента интеграла перекрытия волновых функций связанных состояний ядер ^{12}C и ^{13}N. Для энергий E = 0,25 и 50 кэВ в системе центра масс приведены вычисленные значения S – фактора реакции ^{12}C(p,γ)^{13}N для перехода на основное состояние ^{13}N. В области температур от 0 до 10^{10} К получены скорости термоядерной реакции ^{12}C(p,γ)^{13}N. Результаты расчетов настоящей работы сравниваются с экспериментальными и расчетными данными предыдущих работ.

Ключевые слова: дифференциальные сечения, полные сечения, астрофизический S-фактор, асимптотический нормировочный коэффициент, скорости реакции.

Information about authors:

Zazulin Denis Michailovich - Institute of Nuclear Physics, Almaty, Kazakhstan, Senior Researcher, candidate of physical and mathematical sciences, denis_zazulin@mail.ru, experimental data processing and analyzing of data;

Burtebayev Nassurlla - Institute of Nuclear Physics, Almaty, Kazakhstan, Head of laboratory, Doctor of physical and mathematical sciences, Professor of Physics, nburtebayev@yandex.ru, setting and planning tasks;

Peterson Roy Jerome – University of Colorado, Boulder, Colorado, USA, Professor of Physics, jerry.peterson@colorado.edu, setting and planning tasks;

Artemov Sergey Viktorovich - Institute of Nuclear Physics, Tashkent, Uzbekiston, Doctor of physical and mathematical sciences, professor, artemov1943@gmail.com, setting and planning tasks;

Igamov Sayram - Institute of Nuclear Physics, Tashkent, Uzbekistan, candidate of physical and mathematical sciences, professor, igamov@inp.uz, theoretical calculations;

Kerimkulov Zhambul Kuanyshbekovich - Institute of Nuclear Physics, Almaty, Kazakhstan, Senior Researcher, candidate of physical and mathematical sciences, zhambul-k@yandex.ru, experimental data processing and analyzing of data;

Alimov Dilshod Kamalovich - Institute of Nuclear Physics, Almaty, Kazakhstan, Senior Researcher, PhD, diliyo@mail.ru, analysis of experimental data;

Mukhamejanov Yerzhan Serikovich - Institute of Nuclear Physics, Almaty, Kazakhstan, Senior Researcher, PhD, craftinho@mail.ru, analysis of experimental data;

Marzhan Nassurlla - Institute of Nuclear Physics, Almaty, Kazakhstan, Senior Researcher, PhD, morzhic@mail.ru, analysis of experimental data;

Nassurlla Maulen - al-Farabi Kazakh National University, Almaty, Kazakhstan, PhD student, nespad@mail.ru, experimental data processing and analyzing of data;

Sabidolda Auganbek - Institute of Nuclear Physics, Almaty, Kazakhstan, engineer, asabidolda@mail.ru, obtaining experimental data.

Khojayev Romazan - Institute of Nuclear Physics, Almaty, Kazakhstan, engineer, ramazan_inp@mail.ru, obtaining experimental data.

REFERENCE

[1] Rolfs C and Rodney WS (1988) Cauldrons in the Cosmos, The University of Chicago Press, Chicago and London. ISBN- 13: 978-0226724577

[2] Bahcall JN and Pinsonneault MH (1992) Standard solar models, with and without helium diffusion, and the solar neutrino problem, Rev Mod Phys, 64: 885. DOI: 10.1103/RevModPhys.64.885 (in English).

[3] Bahcall JN, Basu S and Pinsonneault MH (1998) How uncertain are solar neutrino predictions?, Phys Lett B, 433: 1-8. DOI: 10.1016/S0370-2693(98)00657-1 (in English).

[4] Adelberg EG et al (1998) Solar fusion cross sections, Rev Mod Phys, 70:1265. DOI: 10.1103/RevModPhys.70.1265 (in English).

[5] Kirsten TA (1999) Solar neutrino experiments: results and implications, Rev Mod Phys 71:1213. DOI: 10.1103/RevModPhys.71.1213 (in English).

[6] Burtebaev N, Igamov SB, Peterson RJ, Yarmukhamedov R and Zazulin DM (2008) New measurements of the astrophysical S factor for $^{12}C(p,\gamma)^{13}N$ reaction at low energies and the asymptotic normalization coefficient (nuclear vertex constant) for the $p+^{12}C\rightarrow^{13}N$ reaction, Phys Rev C,78: 035802. DOI: 10.1103/PhysRevC.78.035802 (in English).

[7] Artemov SV, Bajajin AG, Igamov SB, Nie GK, Yarmukhamedov R (2008) Nuclear asymptotic normalization coefficients for $^{14}N \rightarrow {}^{13}C + p$ configurations and astrophysical S factor for radiative proton capture, Physics of Atomic nuclei, 71:998. DOI: 10.1134/S1063778808060045 (in English).

[8] Artemov SV, Igamov SB, Tursunmakhatov QI, Yarmukhamedov R (2012) Extrapolation of astrophysical S factors for the reaction $^{14}N((p, \gamma)\ ^{15}O$ to near-zero energies, Phys Atom Nucl, 75: 291. DOI: 10.1134/S1063778812020032 (in English).

[9] Igamov SB, Artemov SV, Yarmukhamedov R, Burtebayev N, Sakuta SB (2016) Astrophysical S factors for the reaction $^{6}Li(p, \gamma)^{7}Be$ at ultralow energies, Bulletin of National Nuclear Centre of the Republic of Kazakhstan [Vestnik Nazionalnogo Yadernogo Centra RK] 56:82. (in English).

[10] Arzumanov AA (1992) Proceedings of the 13th particle accelerator conference, Dubna, Russia. P. 118.

[11] Butler JW (1959) Table of (p, γ) Resonances, NRL Report, 5282. (in English).

[12] Lyons PB, Toevs JW and Sargood DG (1969) Total yield measurements in $^{27}Al(p, \gamma)\ ^{28}Si$, Nucl Phys A, 130: 1. DOI: 10.1016/0375-9474(69)90954-3 (in English).

[13] Dubovichenko SB, Burtebaev N, Zazulin DM, Kerimkulov ZhK and Amar ASA (2011) Astrophysical S factor for the radiative-capture reaction $p\ ^{6}Li \rightarrow {}^{7}Be\gamma$, Phys Atom Nucl, 74: 984. DOI: 10.1134/S1063778811050073 (in English).

[14] Dubovichenko S, Burtebayev N, Dzhazairov-Kakhramanov A, Zazulin D, Kerimkulov Zh, Nassurlla M, Omarov C, Tkachenko A, Shmygaleva T, Stanislaw Kliczewski S, Sadykov T (2017) New measurements and phase shift analysis of $p^{16}O$ elastic scattering at astrophysical energies, Chinese Physics C, 41: 014001. DOI: 10.1088/1674-1137/41/1/014001 (in English).

[15] Barker PH and Connor RD (1967) ^{56}Co as a calibration source up to 3.5 MeV for gamma ray detectors, Nucl Inst And Meth, 57:147. DOI: 10.1016/0029-554X(67)90513-7 (in English).

[16] Maulen Nassurlla, Burtebayev N, Kerimkulov Zh K, Suzuki T, Sakuta SB, Marzhan Nassurlla, Khojayev R (2018) Investigation of deuteron scattering by ^{7}Li nuclei at energy of 14.5 MeV , News of the National Academy of Sciences of the Republic of Kazakhstan. series physico-mathematical [Izvestija Nazionalnoi Akademii Nauk RK serija fizicheskaja] 6:15-22. https://doi.org/10.32014/2018.2518-1726.12 (in English).

[17] Rolfs C and Azuma RE (1974) Interference effects in $^{12}C(p, \gamma)^{13}N$ and direct capture to unbound states , Nucl Phys A, 227: 291. DOI: 10.1016/0375-9474(74)90798-2 (in English).

[18] http://lise.nscl.msu.edu/lise.html

[19] Barker FC and Kajino T (1991) The $^{12}C(\alpha,\gamma)^{16}O$ cross section at low energies, Aust J Phys, 44: 369. DOI: 10.1071/PH910369 (in English).

[20] Holt RJ, Jackson HE, Laszewski RM, Monahan JE, Specht JR (1978) Effects of channel and potential radiative transitions in the $^{17}O(\gamma, n_0)^{16}O$ reaction, Phys Rev C, 18: 1962. DOI: 10.1103/PhysRevC.18.1962 (in English).

[21] Yarmukhamedov R (1997) Influence of the three-particle Coulomb effects on the spectroscopic information extracted from analysis of the $^{12,13}\ (^{3}He, d)^{13,14}\ N$ surface reactions, Nuclear Physics [Yadernaya Fizika] 60: 1017. (in Russian).

[22] Artemov SV, Zaparov EA, Nei GK, Nadirbekov M, and Yarmukhamedov R (2002) Influence of the three-body coulomb effects on extracted value of nuclear vertex constants from transfer reactions, Bulletin of the Russian Academy of Sciences [Izvestija Akademii Nauk Rossii serija fizicheskaja] 66:60. (in Russian).

[23] Ajzenberg–Selove F (1986) Energy levels of light nuclei A = 13−15, Nucl Phys A, 449: 1-15. DOI: 10.1016/0375-9474(86)90119-3 (in English).

[24] Barker FC and Ferdous N (1980) The first excited state of ^{9}B, Aust J Phys, 33: 691. DOI: 10.1071/PH870307 (in English).

[25] Hebbard DF and Vogl JL (1960) Elastic scattering and radiative capture of protons by C^{13}, Nucl Phys, 21: 652. DOI: 10.1016/0029-5582(60)90084-5 (in English).

[26] Vogl JL (1963) Ph.D. thesis, California Institute of Technology. (in English).

[27] Dufour M and Descouvemont P (1997) Multicluster study of the 12C+n and 12C+p systems, Phys Rev C, 56: 1831. DOI: 10.1103/PhysRevC.56.1831 (in English).

[28] Caughlan GR and Fowler WA (1988) Thermonuclear reaction rates V , At Data Nucl Data Tables, 40: 283. DOI: 10.1016/0092-640X(88)90009-5 (in English).

[29] Roughton NA, Fritts MR, Peterson RJ, Zaidins CS, and Hansen CJ (1979) Thick-target measurements and astrophysical thermonuclear reaction rates: Proton-induced reactions , At Data Nucl Data Tables, 23: 177. DOI: 10.1016/0092-640X(79)90004-4 (in English).

[30] Angulo C, Arnould M et al (1999) A compilation of charged-particle induced thermonuclear reaction rates, Nucl Phys A, 656: 3. DOI: 10.1016/S0375-9474(99)00030-5 (in English).

[31] King JD, Azuma RE, Vise JB et al (1994) Cross section and astrophysical S-factor for the $^{13}C(p, \gamma)^{14}N$ reaction, Nucl Phys A, 567: 354. DOI: 10.1016/0375-9474(94)90154-6 (in English).

N E W S
OF THE NATIONAL ACADEMY OF SCIENCES OF THE REPUBLIC OF KAZAKHSTAN
PHYSICO-MATHEMATICAL SERIES
ISSN 1991-346X **https://doi.org/10.32014/2019.2518-1726.39**
Volume 4, Number 326 (2019), 14 – 21

УДК 517.9: 515.16
МРНТИ 27.31.21

A.A. Zhadyranova

Eurasian International Center for Theoretical Physics and Department
of General & Theoretical Physics, Eurasian National University, Astana 010008, Kazakhstan
a.a.zhadyranova@gmail.com

HIERARCY OF WDVV ASSOCIATIVITY EQUATIONS FOR $n=3$ AND $N=2$ CASE WHEN $V_0=0$ WITH NEW SYSTEM a_t, b_t, c_t

Abstract. We investigate solutions of Witten-Dijkgraaf-E.Verlinde-H.Verlinde (WDVV) equations. The article discusses nonlinear equations of the third order for a function f = f(x,t)) of two independent variables x,t. The equations of associativity reduce to the nonlinear equations of the third order for a function f = f(x,t)) when prepotential F dependet of the metric η. In this work we consider the WDVV equation for n = 3 case with an antidiagonal metric η. The solution of some cases of hierarchy equations of associativity illustrated. Lax pairs for the system of three equations, that contains the equation of associativity are written to find the hierarchy of associativity equation. Using the compatibility condition are found the relations between the matrices U, V_2, V_1. The elements of matrix V_2 are found with the expression of z_{ij} and independent and dependent variables for the matrix V_2. Also solving elements of matrix V_1 expressed through y_{ij} and independent and dependent variables for the matrix V_1. We accepted that elements of matrix V_0 are zero. In the physical setting the solutions of WDVV describe moduli space of topological conformal field theories [1, 2]. Let us introduce new variables a, b, c. In the above variables the nonlinear equations of the third order for a function f = f(x,t)) we rewritten as a new system of three equations. Expressed are variables a_t ,b_t ,c_t of three equations are written with the help of matrix elements z_{ij} ,y_{ij}.

Key words: equations of Witten-Dijkgraaf-E.Verlinde-H.Verlinde, the equations of associativity, nonlinear equations of the third order, antidiagonal metric, the Lax pair, the compatibility condition, independent elements, dependent variables, system with equations.

Introduction. The WDVV equations, in general, have the following form [3, 4, 5]:

$$\frac{\partial^3 F}{\partial t^i \partial t^j \partial t^p}\eta^{pq}\frac{\partial^3 F}{\partial t^q \partial t^k \partial t^r}=\frac{\partial^3 F}{\partial t^j \partial t^k \partial t^p}\eta^{pq}\frac{\partial^3 F}{\partial t^i \partial t^q \partial t^r}, \quad \forall i,j,k,r\in\{1,...,n\},$$

where F is a prepotential, η is a metric. The coordinates t^i can be linearly rearranged so that the metric, η, is antidiagonal [6], i.e.

$$\eta=\begin{pmatrix}0 & 0 & 1\\ 0 & 1 & 0\\ 1 & 0 & 0\end{pmatrix}.$$

In this work we consider the WDVV equation for $n=3$ case with an antidiagonal metric η [7]. In this case, two types of dependence of the function F on the fixed variable t^1 were found by Dubrovin [8, 9, 10] which are

$$F = \frac{1}{2}(t^1)^2 t^3 + \frac{1}{2} t^1 (t^2)^2 + f(t^2, t^3) \quad (1)$$

and

$$F = \frac{1}{6}(t^1)^3 + t^1 t^2 t^3 + f(t^2, t^3).$$

For these cases the equations of associativity reduce to the following two nonlinear equations of the third order for a function $f = f(x,t)$) of two independent variables ($x = t^2, t = t^3$):

$$f_{ttt} = f_{xxt}^2 - f_{xxx} f_{xtt} \quad (2)$$

and

$$f_{xxx} f_{ttt} - f_{xxt} f_{xtt} = 1,$$

correspondingly.

The function F in equation (1) has the form from the law of multiplication in the three-dimensional algebra A_t with the basis $e_1 = 1$, e_2 ,e_3 [3]. Every basis is a complete uniformly minimal system [11].

In this work, we consider the solution (1). Let us introduce new variables a, b, c as follows [12, 13]:

$$a = f_{xxx}, \quad b = f_{xxt}, \quad c = f_{xtt}.$$

In the above variables the equation (2) can be rewritten as a system of three equations as follows:

$$\begin{aligned} a_t &= b_x, \\ b_t &= c_x, \\ c_t &= (b^2 - ac)_x. \end{aligned} \quad (3)$$

The Lax pair for the system (3) is given by [8]

$$\begin{aligned} \Psi_x &= \lambda U \Psi, \\ \Psi_t &= \lambda V \Psi, \end{aligned} \quad (4)$$

where U is given by

$$U = \begin{pmatrix} 0 & 1 & 0 \\ b & a & 1 \\ c & b & 0 \end{pmatrix}$$

and V is given by

$$V = \begin{pmatrix} 0 & 0 & 1 \\ c & b & 0 \\ (b^2 - ac) & c & 0 \end{pmatrix}.$$

The compatibility condition for the system (4) is given by

$$\begin{aligned} U_t &= V_x, \\ [U, V] &= 0. \end{aligned}$$

In the following sections we work with the new system (3).

Methods. The solution to a hierarchy for $N = 1$ case corresponds to the system of equations (3). Hierarchy for $N = 2$ case when $V_0 \neq 0$ is given in the work [14]

In this section we consider a hierarchy for $N=2$ case when $V_0=0$ and the following system

$$\begin{aligned} a_t &= \varepsilon_1 b_x + \varepsilon_2 F_x, \\ b_t &= \varepsilon_1 c_x + \varepsilon_2 H_x, \\ c_t &= \varepsilon_1 (b^2 - ac)_x + \varepsilon_2 G_x. \end{aligned} \tag{5}$$

The Lax representation of the above system is same as before in the work [13].

In particular, for $N=2$ case when $V_0=0$ we have

$$\begin{aligned} \Psi_x &= \lambda U \Psi, \\ \Psi_t &= (\lambda^2 V_2 + \lambda V_1)\Psi = V\Psi \end{aligned}$$

The compatibility condition of (4) is given by

$$\lambda U_t - V_x + \lambda [U,V] = 0.$$

The compatibility condition of the Lax representation is given by the system

$$[U,V_2] = 0, \tag{6}$$

$$U_t = V_{1x}, \tag{7}$$

$$V_{2x} = [U,V_1]. \tag{8}$$

Statement of problem. We first consider the second equation of the system and let V_1 to be given by

$$V_1 = \begin{pmatrix} y_{11} & y_{12} & y_{13} \\ y_{21} & y_{22} & y_{23} \\ y_{31} & y_{32} & y_{33} \end{pmatrix}.$$

From the above system it follows that $y_{11}, y_{12}, y_{13}, y_{23}, y_{33}$ are constants w.r.t. x. Writing a system with equations for a_t, b_t, c_t only yields

$$\begin{aligned} a_t &= y_{22x}, \\ b_t &= y_{21x}, \\ b_t &= y_{32x}, \\ c_t &= y_{31x}. \end{aligned} \tag{9}$$

Now we equate similar terms in the systems (5) and (9), i.e. we have a system

$$\begin{aligned} a_t &= y_{22x} = \varepsilon_1 b_x + \varepsilon_2 F_x, \\ b_t &= y_{21x} = \varepsilon_1 c_x + \varepsilon_2 H_x, \\ b_t &= y_{32x} = \varepsilon_1 c_x + \varepsilon_2 H_x, \\ c_t &= y_{31x} = \varepsilon_1 (b^2 - ac)_x + \varepsilon_2 G_x. \end{aligned} \tag{10}$$

Scheme of the method and reduction to equivalent problem. From the above system (10) we find the following

$$\begin{aligned} y_{22} &= \varepsilon_1 b + \varepsilon_2 F, \\ y_{21} &= \varepsilon_1 c + \varepsilon_2 H, \\ y_{32} &= \varepsilon_1 c + \varepsilon_2 H, \\ y_{31} &= \varepsilon_1 (b^2 - ac) + \varepsilon_2 G. \end{aligned}$$

Thus the matrix V_1 has the form

$$V_1 = \begin{pmatrix} y_{11} & y_{12} & y_{13} \\ \varepsilon_1 c + \varepsilon_2 H & \varepsilon_1 b + \varepsilon_2 F & y_{23} \\ \varepsilon_1 (b^2 - ac) + \varepsilon_2 G & \varepsilon_1 c + \varepsilon_2 H & y_{33} \end{pmatrix}. \tag{11}$$

Now we solve the equation (6). Denote V_2 as follows:

$$V_2 = \begin{pmatrix} z_{11} & z_{12} & z_{13} \\ z_{21} & z_{22} & z_{23} \\ z_{31} & z_{32} & z_{33} \end{pmatrix},$$

Plugging U, V_2 into (6) we obtain the following relations:

$$\begin{aligned} z_{23} &= z_{12}, \\ z_{32} &= z_{21}, \\ z_{33} &= z_{11}. \end{aligned}$$

Hence, we are left with the equations

$$\begin{aligned} z_{21} &= b z_{12} + c z_{13}, \\ z_{22} &= z_{11} + a z_{12} + b z_{13}, \\ z_{31} &= c z_{12} + (b^2 - ac) z_{13}. \end{aligned}$$

Thus the matrix V_2 has the form

$$V_2 = \begin{pmatrix} z_{11} & z_{12} & z_{13} \\ b z_{12} + c z_{13} & z_{11} + a z_{12} + b z_{13} & z_{12} \\ c z_{12} + (b^2 - ac) z_{13} & b z_{12} + c z_{13} & z_{11} \end{pmatrix}.$$

Hence, only z_{11}, z_{12}, z_{13} are independent elements of V_2, and the other elements can be written in terms of them.

Now let us find the elements of V_1 in (11). To do so we use the equation (8). First we evaluate $[U, V_1]$.

We have elementwise yields the following system:

11 : $z_{11x} = \varepsilon_1 c + \varepsilon_2 H - by_{12} - cy_{13}$,
12 : $z_{12x} = \varepsilon_1 b + \varepsilon_2 F - y_{11} - ay_{12} - by_{13}$,
13 : $z_{13x} = y_{23} - y_{12}$,
21 : $b_x z_{12} + bz_{12x} + c_x z_{13} + cz_{13x} = by_{11} + a(\varepsilon_1 c + \varepsilon_2 H) + (\varepsilon_1(b^2 - ac) + \varepsilon_2 G) - b(\varepsilon_1 b + \varepsilon_2 F) - cy_{23}$,
22 : $z_{11x} + a_x z_{12} + az_{12x} + b_x z_{13} + bz_{13x} = by_{12} - by_{23}$,
23 : $z_{12x} = by_{13} + ay_{23} + y_{33} - (\varepsilon_1 b + \varepsilon_2 F)$,
31 : $c_x z_{12} + cz_{12x} + (b^2 - ac)_x z_{13} + (b^2 - ac) z_{13x} = cy_{11} - cy_{33}$,
32 : $b_x z_{12} + bz_{12x} + c_x z_{13} + cz_{13x} = cy_{12} + b(\varepsilon_1 b + \varepsilon_2 F) - (\varepsilon_1(b^2 - ac) + \varepsilon_2 G) - a(\varepsilon_1 c + \varepsilon_2 H) - by_{33}$,
33 : $z_{11x} = cy_{13} + by_{23} - (\varepsilon_1 c + \varepsilon_2 H)$.

Now let us express $\varepsilon_1 c + \varepsilon_2 H$, $\varepsilon_1 b + \varepsilon_2 F$, y_{23} in the element 11, 12, 13 of the above system.

$$\begin{aligned} \varepsilon_1 c + \varepsilon_2 H &= z_{11x} + by_{12} + cy_{13}, \\ \varepsilon_1 b + \varepsilon_2 F &= z_{12x} + y_{11} + ay_{12} + by_{13}, \\ y_{23} &= z_{13x} + y_{12}. \end{aligned}$$

Now let us express $\varepsilon_1(b^2 - ac) + \varepsilon_2 G$ in the element 21 and substitute the values for $\varepsilon_1 c + \varepsilon_2 H$, $\varepsilon_1 b + \varepsilon_2 F$, y_{23}

$$\varepsilon_1(b^2 - ac) + \varepsilon_2 G = b_x z_{12} + bz_{12x} + c_x z_{13} + 2cz_{13x} - az_{11x} + bz_{12x} + (b^2 - ac) y_{13} + cy_{12}$$

Now let us express y_{33} in the element 23 and substitute the values for $\varepsilon_1 b + \varepsilon_2 F$, y_{23}

$$y_{33} = 2z_{12x} - az_{13x} + y_{11}$$

Hence, dependent elements of V_1 are given by:

$$\begin{aligned} &\varepsilon_1(b^2 - ac) + \varepsilon_2 G = b_x z_{12} + bz_{12x} + c_x z_{13} + 2cz_{13x} - az_{11x} + bz_{12x} + (b^2 - ac) y_{13} + cy_{12}, \\ &\varepsilon_1 c + \varepsilon_2 H = z_{11x} + by_{12} + cy_{13}, \\ &\varepsilon_1 b + \varepsilon_2 F = z_{12x} + y_{11} + ay_{12} + by_{13}, \\ &y_{23} = z_{13x} + y_{12}, \\ &y_{33} = 2z_{12x} - az_{13x} + y_{11}. \end{aligned} \quad (12)$$

Now let us rewrite the element 22 by substituting the values for y_{23}. So we have

$$z_{11x} + 2bz_{13x} + a_x z_{12} + az_{12x} + b_x z_{13} = 0$$

Now let us rewrite the element 31 by substituting the values for y_{33}. So we have

$$c_x z_{12} + 3cz_{12x} + (b^2 - ac)_x z_{13} + (b^2 - 2ac) z_{13x} = 0$$

Now let us rewrite the element 32 by substituting the values for $\varepsilon_1 b + \varepsilon_2 F$, $\varepsilon_1(b^2 - ac) + \varepsilon_2 G$, $\varepsilon_1 c + \varepsilon_2 H$, y_{33}. So we have

$$2b_x z_{12} + 4bz_{12x} + 2c_x z_{13} + (3c - ab) z_{13x} = 0$$

Now let us rewrite the element 33 by substituting the values for y_{23}, $\varepsilon_1 c+\varepsilon_2 H$

$$2z_{11x}-bz_{13x}=0$$

Also, the independent variables z_{11},z_{12},z_{13} of the matrix V_2 have to satisfy the following system of equations:

$$\begin{aligned}
z_{11x}+2bz_{13x}+a_x z_{12}+az_{12x}+b_x z_{13} &= 0,\\
c_x z_{12}+3cz_{12x}+(b^2-ac)_x z_{13}+(b^2-2ac)z_{13x} &= 0,\\
2b_x z_{12}+4bz_{12x}+2c_x z_{13}+(3c-ab)z_{13x} &= 0,\\
2z_{11x}-bz_{13x} &= 0.
\end{aligned} \tag{13}$$

From the above system (13) it follows that

$$z_{13x}=\left(\frac{4a_x b-2ab_x}{3ac-a^2b-10b^2}\right)z_{12}+\left(\frac{4bb_x-2ac_x}{3ac-a^2b-10b^2}\right)z_{13} \tag{14}$$

$$z_{12x}=\left(-\frac{c_x}{3c}-\frac{b^2-2ac}{3c}\cdot\frac{4a_x b-2ab_x}{3ac-a^2b-10b^2}\right)z_{12}+\left(-\frac{b^2-2ac}{3c}\cdot\frac{4bb_x-2ac_x}{3ac-a^2b-10b^2}-\frac{(b^2-ac)_x}{3c}\right)z_{13} \tag{15}$$

Results. Using necessary terms in the system (12) in (10), we obtai

$$\begin{aligned}
a_t &= \frac{a_x z_{13x}}{2}+a_x y_{12}+b_x y_{13},\\
b_t &= \frac{b_x z_{13x}}{2}+b_x y_{12}+c_x y_{13},\\
c_t &= b_{xx}z_{12}+3b_x z_{12x}+c_{xx}z_{13}+(a_x b+3c_x-\frac{ab_x}{2})z_{13x}-a_x z_{11x}+(b^2-ac)_x y_{13}+c_x y_{12}
\end{aligned} \tag{16}$$

We plug z_{11x},z_{12x},z_{13x} in (13), (15), (14) into (16) and obtain the following equation

$$\begin{aligned}
a_t &= \left(\frac{2ba_x^2-aa_xb_x}{3ac-a^2b-10b^2}\right)z_{12}+\left(\frac{2ba_xb_x-aa_xc_x}{3ac-a^2b-10b^2}\right)z_{13}+a_xy_{12}+b_xy_{13},\\
b_t &= \left(\frac{2ba_xb_x-ab_x^2}{3ac-a^2b-10b^2}\right)z_{12}+\left(\frac{2bb_x^2-ab_xc_x}{3ac-a^2b-10b^2}\right)z_{13}+b_xy_{12}+c_xy_{13},\\
c_t &= \left(b_{xx}-\frac{b_xc_x}{c}+\frac{5abca_xb_x-4b^3a_xb_x+2ab^2b_x^2-3a^2cb_x^2+2b^2ca_x^2+12bca_xc_x-6acb_xc_x}{3ac^2-a^2bc-10b^2c}\right)z_{12}\\
&+\left(c_{xx}-\frac{b_x(b^2-ac)_x}{c}+\frac{6abcb_x^2-4b^3b_x^2+2ab^2b_xc_x-3a^2cb_xc_x+2b^2ca_xb_x+12bcb_xc_x-abca_xc_x-6acc_x^2}{3ac^2-a^2bc-10b^2c}\right)z_{13}\\
&+(b^2-ac)_xy_{13}+c_xy_{12}
\end{aligned} \tag{17}$$

Conclusion. The solution to a hierarchy for $N=2$ case when system is given by (5) corresponds to the system of equations (17).

So, we considered of some cases of hierarchy of WDVV associativity equations. Lax pairs for the system of three equations, that contained the equation of associativity written to find the hierarchy of associativity equation. Using the compatibility condition are found the relations between the matrices U, V_2, V_1. Thus, we obtained the elements of the matrices V_2, V_1 for case N = 2 when V_0=0 and the above system a_t,b_t,c_t. It was found, that only z_{11} ,z_{12} ,z_{13} are independent elements of V_2, and the other elements can be written in terms of them. From the above system it follows that $y_{11},y_{12},y_{13},y_{23},y_{33}$

are constants w.r.t. x. It is found, that y_{11}, y_{12}, y_{13} are independent elements of V_1, and the other elements can be written in terms of them and z_{11}, z_{12}, z_{13}. Expressed are variables a_t, b_t, c_t of three equations are written with the help of matrix elements z_{ij}, y_{ij}.

Acknowledgments. I express gratitude to Professor R. Myrzakulov for useful discussions and advices. The work is performed under the financial support of the scientific and technical program BR05236277 "Investigation of some problems of astrophysics and cosmology in the framework of the Einstein and non-Einstein theories of gravity", 2018.

УДК 517.9: 515.16
МРНТИ 27.31.21

А.А. Жадыранова[1]

[1]Л.Н.Гумилев атындағы Еуразия ұлттық университетінің жалпы
және теориялық физика кафедрасы, Астана, Қазақстан

n = 3 ЖӘНЕ N = 2 ЖАҒДАЙЛАРЫ ҮШІН ЕНГІЗГІЗІЛГЕН ЖАҢА ЖҮЙЕ a_t, b_t, c_t V_0= 0 БОЛҒАНДАҒЫ WDVV АССОЦИАТИВТІЛІК ТЕҢДЕУІНІҢ ИЕРАРХИЯСЫ

Аннотация. Берілген мақалада Виттен – Диджкграф - Е.Верлинде - Г.Верлинде (ВДВВ) теңдеулері зерттеледі. Бұл жұмыста x, t тәуелсіз айнымалыларынан тұратын f = f(x,t) функциясы үшін үшінші ретті сызықты емес теңдеулер талқыланады. Тәуелсіз x, t айнымалыларынан тұратын f = f(x,t) функциясы үшін үшінші ретті сызықты емес теңдеулер F потенциалы η метрикасымен байланысты болғанда келтіріледі. Сонымен қатар ассоциативтілік теңдеулер иерархиясының бірнеше шешімдері сипатталады. Ассоциативтілік теңдеулерінің иерархиясын табу мақсатында ассоциативтілік теңдеулерінен құралған теңдеулер жүйесі үшін Лакс жұптары жазылды. Сәйкестік шартының қолдану арқылы U, V_2, V_1 матрицалары арасындағы қатынастар анықталды. z_{ij} арқылы өрнектелген V_2 матрицасының элементтері мен V_2 матрицасының тәуелді және тәуелсіз айнымалылары есептелінді. y_{ij} арқылы өрнектелген V_1 матрицасының элементтері мен V_1 матрицасының тәуелді және тәуелсіз айнымалылары табылды. Сонымен қатар V_0 матрицасының элементтері нөлге тең деп алынды. Физикалық қолданылуда WDVV ассоциативтілік теңдеуінің шешімі өрістің топологиялық конформдық теориясының модульдерінің кеңістігін сипаттайды. Жаңа айнымалылар енгізілген. Жаңа айнымалыларда f=f(x,t) функциясы үшін үшінші ретті сызықты емес теңдеулер жаңа жүйе арқылы жазылған. Теңдеулер жүйесінен тұратын a_t, b_t, c_t айнымалылары z_{ij}, y_{ij} матрицалық елементтері арқылы өрнектеліп жазылды.

Түйін сөздер: Виттен-Диджграф-Е.Верлинде-Г.Верлинде теңдеулері, ассоциативтілік теңдеуі, үшінші ретті сызықты емес теңдеулер, антидиагональ метрика, Лакс жұптары, үйлесімділік шарты, тәуелсіз элементтер, тәуелді айнымалылар, теңдеулер жүйесі.

УДК 517.9: 515.16
МРНТИ 27.31.21

А.А. Жадыранова[1]

[1]Кафедра общей и теоретической физики Евразийского национального университета имени Л.Н.Гумилева,
Астана, Казахстан

ИЕРАРХИЯ УРАВНЕНИЙ АССОЦИАТИВНОСТИ WDVV ДЛЯ СЛУЧАЯ n = 3 И N = 2 ПРИ V_0= 0 С НОВОЙ СИСТЕМОЙ a_t, b_t, c_t

Аннотация. В данной статье исследуются уравнения Виттена-Диджкграфа-Е.Верлинде-Г.Верлинде (ВДВВ). В работе обсуждаются нелинейные уравнения третьего порядка для функции f = f(x,t) двух независимых переменных x,t. Уравнения ассоциативности сводятся к нелинейным уравнениям третьего порядка для функции f = f(x,t) когда потенциал функии F связан с метрикой η. В этой работе рассматривается уравнение WDVV для случая n = 3 с антидиагональной метрикой η. Описано решение некоторых случаев иерархии уравнений ассоциативности. Для нахождения иерархии уравнений ассоциативности были записаны пары Лакса для системы из трех уравнений, которая содержит уравнения ассоциативности. С применением условия совместности найдены соотношения между матрицами U, V_2, V_1. Были вычислены элементы матрицы V_2, выраженные через z_{ij}, независимые и зависимые переменные матрицы V_2. Также были найдены элементы матрицы V_1, выраженные через y_{ij} , независимые и зависимые переменные матрицы V_1. Элементы матрицы V_0 равны 0. В физическом приложении решение уравнения ассоциативности WDVV описывает пространство модулей топологических конформных теорий поля. Введены новые переменные a, b, c. В новых переменных нелинейные уравнения третьего порядка для функции f = f(x,t) записаны через новую систему трёх уравнений. Выраженные переменные a_t, b_t, c_t системы из трех уравнений были записаны через матричные элементы z_{ij}, y_{ij}.

Ключевые слова: уравнения Виттена-Дижграфа-Е.Верлинде-Г.Верлинде, уравнения ассоциативности, нелинейные уравнения третьего порядка, антидиагональная метрика, пары Лакса, условие совместности, независимые элементы, зависимые переменные, система с уравнениями.

Information about authors:

Zhadyranova A.A. - PhD student of the department of general and theoretical physics, L.N. Gumilyov Eurasian National University, Satpayev str., Astana, Kazakhstan. E-mail: a.a.zhadyranova@gmail.com

REFERENCES

[1] Kontsevich M., Manin Yu., Gromov-Witten classes, quantum cohomology and enumerative geometry, Mirror symmetry, II, 607-653, AMS/IP Stud. Adv. Math., 1, Amer. Math. Soc., Providence, RI, (1997).

[2] Kontsevich M., Manin Yu., Relations between the correlators of the topological sigma-model coupled to gravity, Comm. Math. Phys., 196 (1998), no. 2, 385-398.

[3] Dubrovin B.A. Geometry of 2D topological field theories, Springer Lecture Notes in Math. 1620, 120-348, 1996. [arXiv:hep-th/9407018]

[4] Dijkgraaf R., Verlinde E., Verlinde H., Notes on topological string theory and 2D quantum gravity, Nucl. Phys. B 352 (1991) 59.

[5] Witten E., On the structure of the topological phase of two-dimensional gravity, Nucl. Phys.B 340 (1990) 281-332.

[6] Hertling C., Frobenius manifolds and moduli spaces for singularities, Cambridge University Press, Cambridge (UK), 2002.

[7] Hertling C., Manin Y., Weak Frobenius manifolds, Internat. Math. Res. Notices, no. 6 (1999), 277-286.

[8] Mokhov O.I., Ferapontov Y.V. Equations of Associativity in Two-Dimensional Topological Field Theory as Integrable Hamiltonian Nondiagonalizable Systems of Hydrodynamic Type, Functional analysis and its applications 30(3), 1995. [arXiv:hep-th/9505180]

[9] Dubrovin B.A., Novikov S.P., Hydrodynamics of weakly deformed soliton lattices. Differential geometry and Hamiltonian theory, Uspekhi Mat.Nauk. 44 (1989), 29-98. English translation in Russ. Math. Surveys 44 (1989), 35-124.

[10] Dubrovin B.A., On almost duality for Frobenius manifolds, Amer. Math. Soc. Transl. 212 (2004) 75-132.

[11] A.Sh. Shaldanbayev , A.A. Shaldanbayeva , B.A. Shaldanbay (**2019**) On projectional orthogonal basis of a linear non-self -adjoint operator. News of the National Academy of Sciences of the Republic of Kazakhstan. Physical-mathematical series. Volume 2, Number 324 (2019), PP, 79–89. https://doi.org/10.32014/2019.2518-1726.15 ISSN 2518-1726 (Online), ISSN 1991-346X (Print).

[12] Mokhov O.I. Symplectic and poisson geometry on loop spaces of manifolds and nonlinear equations, Translations of the American Mathematical Society-Series 2 170, 121-152, 1995. [arXiv:hep-th/9503076]

[13] Ferapontov E.V., Mokhov O.I., Nonlocal Hamiltonian operators of hydrodynamic type that are connected with metrics of constant curvature, Russ. Math. Surv. 45 (1990), no. 3, 218-219.

[14] A.A. Zhadyranova, Zh.R. Myrzakul, Y.Ye. Anuarbekova Hierarchy of WDVV associativity equations for n = 3 case and N = 2 when V0≠0 [Ierarchiya WDVV uravneniya dlya n = 3 i N = 2 sluchaya, kogda V0≠0] Bulletin of L.N. Gumilyov Eurasian National University [Vestnik Evrazijskogo nacional’nogo universiteta imeni L.N. Gumileva]. 4(125), 60-66, 2018.

N E W S
OF THE NATIONAL ACADEMY OF SCIENCES OF THE REPUBLIC OF KAZAKHSTAN
PHYSICO-MATHEMATICAL SERIES
ISSN 1991-346X **https://doi.org/10.32014/2019.2518-1726.40**
Volume 4, Number 326 (2019), 22 – 29

UDK 517.929

A.Sh.Shaldanbayev[1], M.I.Akylbayev[2], A.A.Shaldanbayeva[2], A.Zh.Beisebayeva[3]

[1]Silkway International University, Shymkent, Kazakhstan;
[2]Regional social-innovative University, Shymkent, Kazakhstan;
[3]South Kazakhstan State University M.Auezova, Shymkent, Kazakhstan
shaldanbaev51@mail.ru, musabek_kz@mail.ru, altima_a@mail.ru, akbope_a@mail.ru

ON THE SPECTRAL PROPERTIES OF A WAVE OPERATOR PERTURBED BY A LOWER-ORDER TERM

Abstract. The incorrectness of the minimal wave operator is well known, since zero is an infinite-to-one eigenvalue for it. As our study showed, the situation changes if the operator is perturbed by a low-order term containing the spectral parameter as a coefficient, and eventually the problem takes the form of a beam of operators. The resulting beam of operators is easily factorized by first-order functional-differential operators which spectral properties are easily studied by the classical method of separation of variables. Direct application of the method of separation of variables to the original beam of operators encounters the insurmountable difficulties.

Keywords: deviating argument, beam of operators, strong solvability, spectrum, functional - differential operator.

Introduction.

Investigations of the Dirichlet problem for the string oscillation equation in a bounded domain go back to J. Hadamard [1], who for the first time noted nonuniqueness of solution of the Dirichlet problem for a wave equation in a rectangle. Burgin and Duffin [2] considered the Dirichlet problem for the equation $Uxx = Utt$ in the rectangle $\{0< x < X ; 0<t<T\}$. It was described that the nonuniqueness of a solution in a specified space arises if and only if the ratio X/T is rational. By using Laplace transformation, they showed that if the number X/T is irrational, then there is the uniqueness of the solution of the problem in the class of continuously differentiable functions with the second derivatives integrable according to Lebesgue.

Later these results were refined and generalized by various authors (see, for example, [3], [4], [5], [6]). S.L. Sobolev [7] constructed an example of a well-posed boundary-value problem in a rectangle for a hyperbolic system of equations. Yu.M. Berezanskii [8] constructed a class of regions with angles, a change in the domain inside which leads to a continuous change in the solution of the Dirichlet problem.

For domains with a smooth boundary in smooth spaces, only the question of the uniqueness of the solution of the Dirichlet problem was studied (see, for example, the paper of Aleksandryan [9]). In paper [3] V.I. Arnol'd, applying his results on the mapping of the circle into itself, refines the results of [2], indicating that the proof of theorems on the existence of classical solutions of the Dirichlet problem can be carried over to the case of an ellipse. A number of studies by T.Sh. Kal'menov and M.A. Sadybekov are also devoted to boundary value problems of hyperbolic equations [10] - [12].

In [13], using the new general method, the properties of solutions of the Cauchy problem, as well as of the first, second and third boundary-value problems in the disk for a second-order hyperbolic equation with constant coefficients are investigated. The application of this method to higher-order equations can be found in [14]. A new and relatively simple method for constructing a system of polynomial solutions of the Dirichlet problem for second-order hyperbolic equations with constant coefficients in the disk is proposed in [15], and it is also proposed to construct a complete set of eigenfunctions for the Dirichlet problem for the string oscillation equation. The eigenfunctions constructed in this paper coincide with the eigenfunctions constructed earlier in the work of R.A. Aleksandaryan [9]. In this paper, the spectral properties of a beam of operators with a wave operator in the principal part were studied by the methods of [16]–[21].

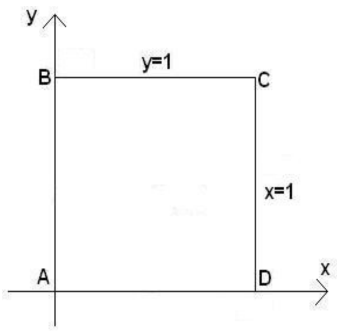

Figure 1

1. Setting of a Problem.

Let $\Omega \subset R^2$ be a quadrangle bounded by following segments: $AB: 0 \le y \le 1, x = 0$; $BC: 0 \le x \le 1,\ y = 1$; $CD: 0 \le y \le 1,\ x = 1$; $DA: 0 \le x \le 1,\ y = 0$. /See fig.1/

We denote by $C^{1,1}(\Omega)$ the set of functions $u(x,t)$ that are twice continuously differentiable with respect to the variables x and t. The boundary of the area Ω is a set of segments $\Gamma = AB \cup BC \cup CD \cup DA$.

We investigate the spectral properties of the operator beam

$$u_{xx} - u_{yy} = -2\lambda u_x + \lambda^2 u, \tag{1}$$

$$u\big|_{y=0} = 0, \tag{2}$$

$$u\big|_{x=0} = \alpha u\big|_{x=1}, \qquad |\alpha| = 1. \tag{3}$$

2. Research Methods.

We shall need the following lemmas.

Lemma 2.1. [22]. Let A be a densely defined operator in a Hilbert space H. Then

(a) A^* exists and is closed;

(b) A admits a closure if and only if $D(A^*)$ is dense in H, and in this case $\overline{A} = A^{**}$.

Lemma 2.2. The set of functions that are finite in the domain Ω is dense in the space $L^2(\Omega)$ [23].

Lemma 2.3. If the symmetric operator A has a complete system of eigenvectors, then the closure of this operator $\overline{A}$ is self-adjoint in H, in other words, the operator A is an essentially self-adjoint in H [22].

Lemma 2.4. Operator

$$Lu = iu_x(x,y) + u_y(x,1-y) \tag{4}$$

$$D(L) = \{u \in C^{1,1}(\Omega) \cap C(\overline{\Omega});\ u\big|_{y=0} = 0,\ u\big|_{x=0} = \alpha u\big|_{x=1}, |\alpha| = 1\}. \tag{5}$$

is a symmetric operator in space $L^2(\Omega)$.

{**The proof** is omitted, because it is done in the standard way}.

Proof. Let $u, v \in D(L)$, then

$$(Lu, v) = \int_0^1\int_0^1 [iu_x(x,y) + u_y(x,1-y)] \cdot \overline{v}(x,y)dxdy = \int_0^1\int_0^1 iu_x(x,y)\overline{v}(x,y)dxdy +$$

$$\int_0^1\int_0^1 u_y(x,1-y)\overline{v}(x,y)dxdy = J_1 + J_2 .$$

Using Fubini's theorem and integrating by parts, we transform the integrals J_1, J_2.

$$J_1 = \int_0^1\int_0^1 iu_x(x,y)\overline{v}(x,y)dxdy = \int_0^1\left[\int_0^1 iu_x(x,y)\overline{v}(x,y)dx\right]dy = \int_0^1\left[\int_0^1 i\overline{v}(x,y)d_x u\right]dy =$$

$$\int_0^1\left[i\overline{v}(x,y)u(x,y)\Big|_0^1 - i\int_0^1 u(x,y)\overline{v}_x(x,y)dx\right]dy = \int_0^1\left[\int_0^1 u(x,y)\overline{iv_x(x,y)}dx\right]dy =$$

$$\int_0^1\int_0^1 u(x,y)\overline{iv_x(x,y)}dxdy;$$

$$J_2 = \int_0^1\int_0^1 u_y(x,1-y)\overline{v}(x,y)dxdy = \int_0^1\left[\int_0^1 u_y(x,1-y)\overline{v}(x,y)dy\right]dx = \int_0^1\left[-\int_0^1 \overline{v}(x,y)d_y u(x,1-y)\right]dx =$$

$$\int_0^1\left[-\overline{v}(x,y)u(x,1-y)\Big|_0^1 + \int_0^1 u(x,1-y)\overline{v}_y(x,y)dy\right]dx = \int_0^1\left[\int_0^1 u(x,1-y)\overline{v_y}(x,y)dy\right]dx =$$

$$\int_0^1\int_0^1 u(x,y)\overline{v_y}(x,1-y)dxdy;$$

Consequently, $$(Lu, v) = \int_0^1\int_0^1 u(x,y)\overline{[iv_x(x,y) + v_y(x,1-y)]}dxdy = (u, Lv)$$

Lemma 2.5. The spectral problem

$$Lw = -w''(y) = \nu^2 w(y),$$
$$w(0) = w'(1) = 0$$

has an infinite set of eigenvalues

$$\nu_n = n\pi - \frac{\pi}{2}, \quad n = 1,2,...$$

and corresponding eigenfunctions

$$w_n(y) = \sqrt{2}\sin\left(n\pi - \frac{\pi}{2}\right)y, \; n = 1,2,...,$$

which form an orthonormal basis of the space $L^2(0,1)$ [24].

Lemma 2.6. The spectral problem

$$iv_x = \mu v(x), v(0) = \alpha v(1), |\alpha| = 1 \tag{6}$$

has an infinite set of real eigenvalues

$$\mu_m = arg\alpha + 2m\pi i, \; m = 0, \pm 1, \pm 2, ... \tag{7}$$

and their corresponding eigenfunctions

$$v_m(x) = exp[-i(arg\alpha + 2m\pi)x], \ m = 0, \pm1, \pm2, ... \quad (8)$$

which form an orthonormal basis of space $L^2(0,1)$ [16].

Lemma 2.7. If the orthogonal systems $\{\Phi_n(x)\}$ and $\{\psi_n(x)\}$, $n = 1,2, ...$ are complete in space $L^2(0,1)$, then their product $\{\Phi_n(x) \cdot \psi_n(x)\}$, $m, n = 1,2, ...$ is complete in the space $L^2(0,1)$, where $\Omega = [0,1]\times[0,1]$ [25].

3. Results of the research.

Theorem 1. The boundary value problem

$$Lu = iu_x(x,y) + u_y(x,1-y) = f(x,y), \quad (9)$$

$$u\big|_{y=0} = 0, \ u\big|_{x=0} = \alpha u\big|_{x=1}, \quad |\alpha| = 1, \quad (10)$$

has an infinite set of real eigenvalues

$$\lambda_{mn} = \arg\alpha + 2m\pi + (-1)^{n+1}\left(n\pi - \frac{\pi}{2}\right), , , \ n = 1,2,... \ m = 0,\pm1,\pm2,... \quad (11)$$

and the corresponding eigenfunctions

$$u_{mn}(x,y) = \sqrt{2}\exp[-i(\arg\alpha + 2m\pi)x]\cdot\sin\left(n\pi - \frac{\pi}{2}\right)y \quad (12)$$

which form an orthonormal basis of space $L^2(0,1)$.

Proof. Let $Su(x,y) = u(x,1-y)$, then

$$iu_x(x,y) + u_y(x,1-y) = \left(i\frac{\partial}{\partial x} + S\frac{\partial}{\partial y}\right)u(x,y)$$

we use this formula in the calculations.

Let $u_{mn}(x,y) = \sqrt{2}\exp[-i(\arg\alpha + 2m\pi)x]\cdot\sin\left(n\pi - \frac{\pi}{2}\right)y$, $n = 1,2,...$, $m = 0,\pm1,\pm2,...$.

Then the following formulas hold:

$$i\frac{\partial}{\partial x}u_{mn}(x,y) = (\arg\alpha + 2m\pi)u_{mn}(x,y);$$

$$S\frac{\partial}{\partial y}u_{mn}(x,y) = \sqrt{2}\left(n\pi - \frac{\pi}{2}\right)\exp[-i(\arg\alpha + 2m\pi)]\cdot\cos\left(n\pi - \frac{\pi}{2}\right)(1-y) =$$

$$\sqrt{2}\left(n\pi - \frac{\pi}{2}\right)\exp[-i(\arg\alpha + 2m\pi)x]\cdot(-1)^{n+1}\sin\left(n\pi - \frac{\pi}{2}\right)y = (-1)^{n+1}\left(n\pi - \frac{\pi}{2}\right)u_{mn}(x,y),$$

$$\left(i\frac{\partial}{\partial x} + S\frac{\partial}{\partial y}\right)u_{mn}(x,y) = \left[\arg\alpha + 2m\pi + (-1)^{n+1}\left(n\pi - \frac{\pi}{2}\right)\right]u_{mn}(x,y).$$

Consequently, $$i\frac{\partial}{\partial x}u_{mn}(x,y) + u_{mny}(x,1-y) = \lambda_{mn}u_{mn}(x,y),$$

where

$$\lambda_{mn} = \arg\alpha + 2m\pi + (-1)^{n+1}\left(n\pi - \frac{\pi}{2}\right), \ n = 1,2,..., \ m = 0,\pm1,\pm2,... .$$

Theorem 2. The operator

$$Lu = iu_x(x,y) + u_y(x,1-y), \tag{13}$$

$$D(L) = \{u \in C^{1,1}(\Omega) \cap C(\overline{\Omega}); u\big|_{y=0} = 0, u\big|_{x=0} = \alpha u\big|_{x=1}, |\alpha| = 1\} \tag{14}$$

is essentially self-adjoint in the space $L^2(\Omega)$.

Proof. This theorem is a simple consequence of Theorem 1, Lemma 2.3 and Lemma 2.4.

Up to the present time, we have not deliberately spoken about the spectrum of the operator L, because this concept is inherent only in a closed operator, and our operator has until now been not closed. In virtue of the Theorem 2 the equality $\overline{L} = L^*$ holds.

Further, by an operator L we mean the closure of the operator (13) – (14) and investigate its spectrum. The eigenvalues of this operator have the form:

$$\lambda_{mn} = \arg\alpha + 2m\pi + (-1)^{n+1}\left(n\pi - \frac{\pi}{2}\right),\ n = 1,2,...,\ m = 0,\pm1,\pm2,... .$$

a) Let $n = 2k$, $k = 1,2,...$, then

$$\lambda_{m,2k} = \arg\alpha + 2m\pi - \left(2k\pi - \frac{\pi}{2}\right) = \pi\left[\frac{\arg\alpha}{\pi} + 2(m-k) + \frac{1}{2}\right] = \pi\left[\frac{\arg\alpha}{\pi} + \frac{1}{2} + 2(m-k)\right].$$

The value $2(m-k)$ runs through all even numbers, the argument α lies within $0 \le \arg\alpha \prec 2\pi$, therefore

$$0 \le \frac{\arg\alpha}{\pi} \prec 2,\quad \frac{1}{2} \le \frac{\arg\alpha}{\pi} + \frac{1}{2} \prec \frac{5}{2}.$$

Between the numbers $\frac{1}{2}$ and $\frac{5}{2}$ there is only one even number 2, which is reached at $\frac{\arg\alpha}{\pi} = \frac{3}{2}$.

b) Let $n = 2k-1$, $k = 1,2,...$, then

$$\lambda_{m,2k-1} = \arg\alpha + 2m\pi(2k-1)\pi - \frac{\pi}{2} = \pi\left[\frac{\arg\alpha}{\pi} + 2m + 2k - 1 - \frac{1}{2}\right] = \pi\left[\frac{\arg\alpha}{\pi} - \frac{3}{2} + 2(m+k)\right];$$

The quantity $2(m+k)$ runs through all even integers. The following inequality holds:

$$-\frac{3}{2} \le \frac{\arg\alpha}{\pi} - \frac{3}{2} \prec \frac{1}{2}.$$

Between the numbers $-\frac{3}{2}$ and $\frac{1}{2}$ there is only one even number 0, which is reached when $\frac{\arg\alpha}{\pi} = \frac{3}{2}$.

Theorem 3. The spectrum of the operator (13)-(14) consists of two series of infinite eigenvalues:

a) $\lambda_m^{(1)} = \pi\left[\frac{\arg\alpha}{\pi} + \frac{1}{2} + 2m\right], m = 0,\pm1,\pm2,...;$

b) $\lambda_m^{(2)} = \pi\left[\frac{\arg\alpha}{\pi} - \frac{3}{2} + 2m\right],\ m = 0,\pm1,\pm2,...$

i.e. each of these values is taken an infinite number of times, the corresponding eigenfunctions form an orthonormal basis of the space $L^2(\Omega)$.

The inverse operator L^{-1} exists if and only if

$$\frac{\arg\alpha}{\pi} \neq \frac{3}{2} \tag{15}$$

Theorem 4. The boundary-value problem

$$Lu = iu_x(x,y) + u_y(x,1-y) = f(x,y),(x,y) \in \Omega ;$$
$$u\big|_{y=0} = 0, \; u\big|_{x=0} = \alpha u\big|_{x=1}, \quad |\alpha| = 1,$$

is strongly solvable in space $L^2(\Omega)$ if and only if

$$\frac{\arg\alpha}{\pi} \neq \frac{3}{2}.$$

When condition (15) is satisfied, the inverse operator $(\overline{L})^{-1}$ exists, is bounded, but not compact, since there is a continuous spectrum of the operator $\overline{L}$.

Theorem 5. The spectral problem (1)-(3) has an infinite set of eigenvalues

$$\lambda_{mn} = \arg\alpha + 2m\pi + (-1)^{n+1}\left(n\pi - \frac{\pi}{2}\right), \; n = 1,2,\ldots, \; m = 0,\pm1,\pm2,\ldots,$$

and the corresponding eigenfunctions

$$u_{mn}(x,y) = \sqrt{2}\exp[-i(\arg\alpha + 2m\pi)x]\cdot\sin\left(n\pi - \frac{\pi}{2}\right)y,$$

which form an orthonormal basis of space $L_2(\Omega)$.

The spectrum of the beam of operators (1)-(3) consists of two series of infinite eigenvalues:

a) $\lambda_m^{(1)} = \pi\left[\frac{\arg\alpha}{\pi} + \frac{1}{2} + 2m\right], m = 0,\pm1,\pm2,\ldots;$

b) $\lambda_m^{(2)} = \pi\left[\frac{\arg\alpha}{\pi} - \frac{3}{2} + 2m\right], \; m = 0,\pm1,\pm2,\ldots$

each of these values is taken an infinite number of times, the corresponding eigenfunctions form an orthonormal basis of the space $L^2(\Omega)$.

The proof of the theorem follows easily from the above Theorems 1 - 4. For this it is sufficient to note that the equation coincides with the equation (1), where

$$\mathrm{Lu} = \mathrm{iu_x(x,y)} + \mathrm{u_y(x,1-y)} = \mathrm{i}\left(\frac{\partial}{\partial \mathrm{x}} + \mathrm{S}\frac{\partial}{\partial \mathrm{x}}\right)\mathrm{u(x,y)},$$

and $\mathrm{Su(x,y)} = \mathrm{u(x,1-y)}$.

4. Conclusions.

Note that the operator (13)-(14) is a two-dimensional generalization of the operator discussed in [16] - [17], which has found application to singularly perturbed Cauchy problem [18], to the operator of the heat conductivity in [19], and to the ill-posed problems of mathematical physics in [20] - [21], and Volterra problems in [26] - [27].

The spectral properties of the wave operator change dramatically if it is perturbed by the low order term containing the spectral parameter, in particular, it turns out to be reversible for certain values of the coefficient of the boundary condition. Zero is an infinite eigenvalue of the Dirichlet problem of the wave equation. Adding a low-order term with a spectral parameter and expanding the domain of definition change the situation, the operator becomes reversible.

Authors thank the leadership of the International *Silkway University* and the *Regional Social Innovation University of Shymkent* for the partial funding of the research.

ӘОЖ 517.929

А.Ш.Шалданбаев[1], М.И.Ақылбаев[2], А.А.Шалданбаева[2], А.Ж.Бейсебаева[3]

[1]Халықаралық Silkway университеті, Шымкент, Қазақстан;
[2]Аймақтық әлеуметтік-инновациялық университеті, Шымкент, Казахстан;
[3]М.О.Әуезов атындағы Оңтүстік Қазақстан мемлекеттік университеті, Шымкент, Қазақстан

КІШІ МҮШЕЛІ ТОЛҚЫН ОПЕРАТОРЫНЫҢ СПЕКТРӘЛДІК ҚАСИЕТТЕРІ

Аннотация. Толқындық кішік оператордың жайсыз екені көпке мәлім, себебі нөл нүктесі шексіз еселі меншікті мән.Біздің зерттеулеріміздің көрсетуінше,жағдайды өзгертуге болады, бұл, үшін операторды спектрәлді параметрге көбейтілген кіші мүшемен тітіркендіру жеткілікті,сонда есебіміз операторлар шоғырының кейпіне енеді.Бұл операторлар шоғыры қарапайым операторлардың көбейтіндісіне жіктеледі,ал ол операторлар оңай зерттеледі.

Тірек сөздер: ауытқыған аргумент, әлді шешілу, спектр, операторлар шоғыры, функционал-дифференциал оператор.

УДК 517. 929

А.Ш. Шалданбаев[1], М.И. Ақылбаев[2], А.А. Шалданбаева[2], А.Ж. Бейсебаева[3]

[1]Международный университет Silkway, г. Шымкент, Казахстан;
[2]Региональный социально-инновационный университет, г. Шымкент, Казахстан;
[3]Южно-Казахстанский Государственный университет им.М.Ауезова, г.Шымкент, Казахстан

О СПЕКТРАЛЬНЫХ СВОЙСТВАХ ВОЛНОВОГО ОПЕРАТОРА, ВОЗМУЩЁННОГО МЛАДШИМ ЧЛЕНОМ

Аннотация. Некорректность минимального волнового оператора общеизвестна, так как нуль для него является бесконечнократным собственным значением. Как показали наши исследования, положение изменится, если возмутить его младшим членом, содержащим в качестве коэффициента спектральный параметр, в итоге задача принимает вид операторного пучка. Полученный пучок операторов легко факторизуется с помощью функционально– дифференциальных операторов первого порядка, спектральные свойства которых легко изучаются классическим методом разделения переменных. Непосредственное применение метода разделения переменных к исходному пучку операторов наталкивается на непреодолимые трудности.

Ключевые слова: отклоняющиеся аргумент, сильная разрешимость, спектр, пучок операторов, функционально-дифференциальный оператор

Information about authors:

Shaldanbayev A. Sh. - doctor of physico-mathematical Sciences, associate Professor, head of the center for mathematical modeling Silkway International University, Shymkent, Kazakhstan; http://orcid.org/0000-0002-7577-8402;

Akylbaev M. I. - candidate of technical Sciences, associate Professor, Vice-rector for research of the Regional socio-innovative University, Shymkent, Kazakhstan, https://orcid.org/0000-0003-1383-4592;

Shaldanbayeva A.A. - master of science, "Regional Social-Innovative University", Shymkent; https://orcid.org/0000-0003-2667-3097;

Beisebayeva A.Zh. - senior lecturer of Mathematics, South Kazakhstan state University named after M.O.Auezova, Shymkent, Kazakhstan, https://orcid.org/0000-0003-4839-9156

REFERENCES

[1] J. Hadamard. On some topics connected with linear partial differential equations, Proc.Benares Math. Soc, 1921, 3, p. 39-48.

[2] D.G. Bourgin, R. Duffin. The Dirichlet problem for the vibrating string equation. Bull.Amer.Math.Soc., 45 (12) (1939), pp.851-858.

[3] V.I. Arnold. Small denominators. I: Mappings of the circumference onto itself. Izv. Akad. Nauk SSSR Ser. Mat., 25 (1) (1961), pp. 21–86 [Am. Math. Soc., Transl., II. Ser. 46, 213284 (1965)].

[4] O.I. Bobik, P.I. Bondarchuk, B.I. Ptashnik. Elements of the Qualitative Theory of Partial Differential Equations. Kiev, 1972. 175 p.(In Russian).

[5] B. D. Sleeman. Boundary value problems for the vibrating string equation. Proc. Roy.Soc. Edinburgh, 1981, v. A–88, Us. 1-2, p. 185-194. (in Eng.).

[6] P. P. Mosolov. The Dirichlet problem for partial differential equations, Izv. Vyssh. Uchebn. Zaved. Mat., 1960, no. 3, 213-218.(In Russian).

[7] S.L.Sobolev. An example of a correct boundary-value problem for the equation of oscillation of a string with data on the entire boundary. Dokl. AN SSSR, 1956, v. 109, No. 4, p. 707–709. (In Russian).

[8] Yu.M. Berezanskii. Expansions in Eigenfunctions of Self-Adjoint Operators. Kiev: Naukova Dumka (1965), 799 pp. [in Russian].

[9] R.A. Aleksandryan. Spectral properties of operators arising from systems of differential equations of Sobolev type, Tr. Mosk. Mat. Obs., 9, 1960, 455-505. (In Russian)

[10] T.Sh. Kal'menov. Regular boundary value problems for the wave equation, Differ. Uravn., 17:6 (1981), 1105-1121. [in Russian].

[11] T.Sh. Kal'menov. On the Spectrum of a Self-Adjoint Problem for the Wave Equation, Vestnik Akad. Nauk KazSSR, 1982, N2, p.63–66.(In Russian).

[12] T.Sh. Kal'menov, M.A. Sadybekov. The Dirichlet problem and nonlocal boundary value problems for the wave equation, Differential Equations, 26:1 (1990), 55-59. (In Russian).

[13] V.P. Burskiy. Boundary value problems for a second-order hyperbolic equation in a disk, Izv. Vyssh. Uchebn. Zaved. Mat., 1987, no. 2, 22-29. (In Russian).

[14] V.P. Burskiy. On the kernel of a differential operator with constant coefficients of lower order in the disk. -VINITI, No. 3792–82 Dep., 1982. (In Russian).

[15] G.A. Sargsyan. Polynomial solutions of the Dirichlet problem for hyperbolic equations with constant coef- ficients in the disk, Reports of the National Academy of Sciences of Armenia, Volume 112, 2012, N 4. (In Russian).

[16] T.Sh. Kal'menov, S.T. Akhmetova, A.Sh. Shaldanbaev. To the spectral theory of equations with deviating argument // Mathematical Journal, Almaty, 2004, Vol.4, No. 3 (13). Pp. 41–48. (In Russian).

[17] M. T. Shomanbayeva. On the basis property of the eigenfunctions of the heat equation with a deviating argument, "Poisk", Almaty, 2, 2006. (In Russian).

[18] T. Sh. Kal'menov, A.Sh. Shaldanbaev. On a recurrence method for solving a singularly perturbed Cauchy problem for a second order equation, Mat. Tr., 13:2 (2010), 128-138. (In Russian).

[19] Orazov, A. Shaldanbayev, and M. Shomanbayeva. About the nature of the spectrum of the periodic problem for the heat equation with a deviating argument. Hindawi Publishing Corporation. Abstract and Applied Analysis. Volume 2013, Article ID 128363, 6 pages. (in Eng.).

[20] T.Sh. Kal'menov and A.Sh. Shaldanbaev. On a criterion of solvability of the inverse problem of heat conduction. Journal of Inverse and Ill-Posed Problems 18:4, 352-369 (2010). (in Eng.).

[21] Sh. Shaldanbayev, I. Orazov, and M.T. Shomanbayeva. On the restoration of an operator of Sturm- Liouville by one spectrum. AIP Conference Proceedings 1611, 53 (2014); doi: 10.1063/1.4893803. (in Eng.).

[22] M. Reed and B. Simon. Methods of Modern Mathematical Physics-vol. 1-Functional Analysis, Academic Press, London, UK, 1972. (in Eng.).

[23] S.G. Mikhlin. Course of Mathematical Physics, M., "Nauka", 1968. 576 pp. [in Russian].

[24] V.A. Marchenko. Operators of Sturm-Liouville and their applications. Kiev: Naukova Dumka (1977), 330 pp.[in Russian].

[25] A.N. Kolmogorov, S.V. Fomin. Elements of the theory of functions and functional analysis. M., "Nauka". 1976, 543 pp. [in Russian].

[26] Akylbayev M.I., Beysebayeva A., Shaldanbayev A. Sh. On the Periodic Solution of the Goursat Problem for a Wave Equation of a Special Form with Variable Coefficients. News of the National Academy of Sciences of the republic of Kazakhstan. Volume 1, Number 317 (2018), 34 – 50. (in Eng.).

[27] Shaldanbaeva A. A., Akylbayev M.I., Shaldanbaev A. Sh., Beisebaeva A.Zh. The Spectral Decomposition of Cauchy Problem's Solution for Laplace Equation. News of the National Academy of Sciences of the republic of Kazakhstan. Volume 5, Number 321 (2018), 75 – 87. https://doi.org/10.32014/2018.2518-1726.10 (in Eng.).

N E W S
OF THE NATIONAL ACADEMY OF SCIENCES OF THE REPUBLIC OF KAZAKHSTAN
PHYSICO-MATHEMATICAL SERIES
ISSN 1991-346X **https://doi.org/10.32014/2019.2518-1726.41**
Volume 4, Number 326 (2019), 30 – 41

UDK 517

A.Sh.Shaldanbayev[1], A.A.Shaldanbayeva[2], B.A.Shaldanbay[3]

[1]Silkway International University, Shymkent, Kazakhstan;
[2]Regional social-innovative University, Shymkent, Kazakhstan;
[3]South Kazakhstan State University M.O.Auezov, Shymkent, Kazakhstan
shaldanbaev51@mail.ru, altima_a@mail.ru, baglan.shaldanbayev@bk.ru

INVERSE PROBLEM OF THE STURM-LIOUVILLE OPERATOR WITH UNSEPARATED BOUNDARY VALUE CONDITIONS AND SYMMETRIC POTENTIAL

Abstract. In the paper we prove the uniqueness theorem on a single spectrum for the Sturm-Liouville operator with unseparated boundary value conditions and real continuous symmetric potential. The research method is different from all known methods, and is based on the internal symmetry of the operator generated by invariant subspaces.

Keywords: Sturm - Liouville operator, spectrum, Sturm - Liouville inverse problem, Borg theorem, Ambartsumian theorem, Levinson theorem, unseparated boundary value conditions, symmetric potential, invariant subspaces.

1. Introduction. By inverse problems of spectral analysis, we understand the problems about restoration of a linear operator according to one or another of its spectral characteristics.

The first significant result in this direction was obtained in 1929 by V.A. Ambartsumyan [1]. He proved the following theorem.

By $\lambda_0 < \lambda_1 < \lambda_2 < \cdots$ we denote eigenvalues of the following Sturm-Liouville problem

$$-y'' + q(x)y = \lambda y, \tag{1.1}$$

$$y'(0) = 0,\ y'(\pi) = 0; \tag{1.2}$$

where $q(x)$ is a real continuous function. If

$$\lambda_n = n^2\ (n = 0,1,2,\dots)\ \text{ then } q(x) \equiv 0.$$

The first mathematician who drew attention to importance of the V.A.Ambartsumian's result was the Swedish mathematician Borg. He also performed the first systematic study of one of the important inverse problems, namely, inverse problem for the classical Sturm-Liouville operator of the form (1.1) by spectra [2]. Borg showed that, in general case, one spectrum of the Sturm-Liouville operator does not define it, so Ambartsumian's result is an exception from the general rule. In the same paper [2], Borg shows that two spectra of the Sturm – Liouville operator (with different boundary conditions) uniquely determine it. More precisely, Borg proved the following theorem.

Borg Theorem.

Suppose that the following equations

$$-y'' + q(x)y = \lambda y, \tag{1.1}$$

$$-z'' + p(x)z = \lambda z, \tag{1.3}$$

have the same spectrum under the boundary value conditions

$$\begin{cases}\alpha y(0) + \beta y'(0) = 0,\\ \gamma y(\pi) + \delta y'(\pi) = 0;\end{cases} \quad (1.4)$$

and under the boundary value conditions

$$\begin{cases}\alpha y(0) + \beta y'(0) = 0,\\ \gamma' y(\pi) + \delta' y'(\pi) = 0.\end{cases} \quad (1.4)'$$

Then $q(x) = p(x)$ almost everywhere on the segment $[0, \pi]$, if

$$\delta \cdot \delta' = 0, \qquad |\delta| + |\delta'| > 0.$$

Shortly after Borg's work, important studies on the theory of inverse problems were performed by Levinson [3], in particular, he proved that if $q(\pi - x) = q(x)$, then the Sturm-Liouville operator

$$-y'' + q(x)y = \lambda y, \quad (1.1)$$

$$\begin{cases}y'(0) - hy(0) = 0,\\ y'(\pi) + hy(\pi) = 0\end{cases} \quad (1.5)$$

is reconstructed by one spectrum.

A number of works by B.M. Levitan [4], [5] are devoted to reconstructing the Sturm-Liouville operator by one and two spectra. These studies have found continuations in [6] - [20]. Sources [21] - [28] are introductory.

This paper is devoted to generalization of Ambartsumian [1] and Levinson [3] theorems, in particular, our results contain the results of these authors.

2. Research Methods.

Idea of this work is very simple. Analysis of contents of [1, 3] showed that both of these operators have an invariant subspace. If for a linear operator L the following formulas hold

$$LP = PL^*, \qquad QL = L^*Q,$$

where P, Q are orthogonal projections, satisfying the condition $P + Q = I$, then the operators L and L^* have invariant subspaces, sometimes restriction of these operators to these invariant subspaces, under certain conditions, form a Borg pair.

3. Research Results.

In the Hilbert space $H = L^2(0, \pi)$ we consider the Sturm-Liouville operator

$$Ly = -y'' + q(x)y; \quad (3.1)$$

$$\begin{cases}a_{11}y(0) + a_{12}y'(0) + a_{13}y(\pi) + a_{14}y'(\pi) = 0,\\ a_{21}y(0) + a_{22}y'(0) + a_{23}y(\pi) + a_{24}y'(\pi) = 0\end{cases} \quad (3.2)$$

where $q(x)$ is a continuous complex function, a_{ij} $(i = 1,2;\ j = 1,2,3,4)$ are arbitrary complex coefficients, and by Δ_{ij} $(i = 1,2;\ j = 1,2,3,4)$ we denote the minors of the boundary matrix:

$$A = \begin{pmatrix} a_{11} & a_{12} & a_{13} & a_{14} \\ a_{21} & a_{22} & a_{23} & a_{24} \end{pmatrix}.$$

Assume that $a_{24} \neq 0$, then the Sturm-Liouville operator (3.1) – (3.2) takes the following form

$$Ly = -y'' + q(x)y,\ x \in (0, \pi); \quad (3.1)$$

$$\begin{cases}\Delta_{14}y(0) + \Delta_{24}y'(0) + \Delta_{34}y(\pi) = 0,\\ \Delta_{12}y(0) + \Delta_{32}y(\pi) - \Delta_{24}y'(\pi) = 0\end{cases} \quad (3.3)$$

and its adjoint operator L^+ takes the form

$$L^+z = -z'' + \overline{q(x)}z,\ x \in (0, \pi); \quad (3.1)^+$$

$$\begin{cases}\overline{\Delta_{14}}z(0)+\overline{\Delta_{24}}z'(0)+\overline{\Delta_{12}}z(\pi)=0,\\ \overline{\Delta_{34}}z(0)+\overline{\Delta_{32}}z(\pi)-\overline{\Delta_{24}}z'(\pi)=0.\end{cases} \quad (3.3)^{+}$$

Let P and Q be orthogonal projections, defined by the formulas

$$Pu(x)=\frac{u(x)+u(\pi-x)}{2},\ Qv(x)=\frac{v(x)-v(\pi-x)}{2} \quad (3.4)$$

The main result of the paper is the following theorem.

Theorem 3.1. If $\Delta_{24}\neq 0$, and

1) $PL=L^{+}P$;
2) $LQ=QL^{+}$;
3) $\Delta_{12}=-\Delta_{34}$;

then the Sturm-Liouville operator (3.1) – (3.3) reconstructed by one spectrum.

4. Discussion.

In this section we prove the theorem and discuss the obtained results. Following Lemmas 4.1, 4.2 may have independent meanings.

Lemma 4.1. If for a linear and discrete operator L the following equalities hold

1) $PL=L^{+}P$;
2) $LQ=QL^{+}$;
3) $P+Q=I$;

where P,Q are orthogonal projections, and I is identity operator, then all its eigenvalues are real.

Proof.

Let $PL=L^{+}P$, $LQ=QL^{+}$; then

$$(PL)^{*}=L^{*}P^{*}=L^{*}P=PL;$$

$$(LQ)^{*}=Q^{*}L^{*}=QL^{*}=LQ;$$

i.e. operators PL and LQ are self-adjoint, therefore, their eigenvalues are real.

Further, if $Ly=\lambda y,\ y\neq 0$, then $PLy=\lambda Py,\ L^{+}Py=\lambda Py,\ L^{+}P(Py)=\lambda Py$, consequently, if $Py\neq 0$, then λ is a real quantity; if $Py=0$, then $y=Qy$, and $LQy=\lambda Qy,\ LQ(Qy)=\lambda Qy,\ Qy=y\neq 0$. Thus, λ is again a real quantity.

The following lemma shows that the spectrum $\sigma(L)$ of the operator L consists of two parts; therefore, the operator L, apparently, splits into two parts. Later we will see that this is exactly what happens, and moreover, these parts form a Borg pair under a certain condition.

Lemma 4.2. If L is a linear discrete operator, satisfying the conditions:

1) $PL=L^{+}P$;
2) $LQ=QL^{+}$;
3) $P+Q=I$;

where P,Q are orthogonal projections, and I is identity operator, then

$$\sigma(L)=\sigma(L_1)\cup\sigma(L_2).$$

where $\sigma(L)$ is a spectrum of the operator L, $L_1=PL,\ L_2=LQ$.

Proof.

If $Ly=\lambda y,\ y\neq 0$, then $PLy=\lambda Py,\ L^{+}Py=\lambda Py,\ L^{+}P(Py)=\lambda Py,\ L_1(Py)=\lambda Py$. If $Py\neq 0$, then $\lambda\in\sigma(L_1)$. If $Py=0$, then $y=Qy\neq 0$ and $LQy=\lambda Qy,\ LQ(Qy)=\lambda Qy,\ L_2Qy=\lambda Qy$. Consequently, $\lambda\in\sigma(L_2)$.

Thus $\sigma(L)\subset\sigma(L_1)\cup\sigma(L_2)$, where $\sigma(A)$ means spectrum of the operator A.

Assume that $\lambda\in\sigma(L_1)\cup\sigma(L_2)$ and $\lambda\neq 0$. Then

a) If $\lambda\in\sigma(L_1)$, then $PLy=\lambda y,\ y\neq 0\ \rightarrow\ P^2Ly=\lambda Py, PLy=\lambda Py$, if $Py=0$, then $PLy=0,=>\lambda y=0,\rightarrow y=0$, it is impossible, therefore $Py\neq 0$ and $L^{*}Py=\lambda Py$. Consequently, $\lambda\in\sigma(L^{*})=\sigma(L)$.

b) If $\lambda\in\sigma(L_2)$, then $LQy=\lambda y,\ y\neq 0,\ QL^{*}y=\lambda y,\ Q^2L^{*}y=\lambda Qy,\ QL^{*}y=\lambda Qy,\rightarrow Qy\neq 0$, otherwise $QL^{*}y=0,=>LQy=0,\rightarrow\lambda y=0,\rightarrow y=0$. Consequently, $\lambda Qy=QL^{*}y=LQy,\rightarrow L(Qy)=\lambda Qy$, thus $\lambda\in\sigma(L)$.

c) $0\in\sigma(L_1)\cup\sigma(L_2)$.

If $0 \in \sigma(L_1)$, then $L_1 u = 0,\ PLu = 0,\ u \neq 0$; Operator L_1 maps the subspace $H_1 = PH$ into H_1, thus $u = Pu \neq 0$, then $PLu = L^* Pu = L^* u = 0, \Rightarrow 0 \in \sigma(L^*) = \sigma(L)$.

If $0 \in \sigma(L_2)$, then $L_2 v = 0,\ v \neq 0$; Operator L_2 maps the subspace $H_2 = QH$ into H_2, therefore $v = Qv$ and $L_2 v = LQv = Lv = 0, \Rightarrow 0 \in \sigma(L)$.

Lemma 4.3. If

a) $\Delta_{24} \neq 0$; (4.1)

b) $PL = L^+ P$; (4.2)

where $Pu(x) = \frac{u(x)+u(\pi-x)}{2},\ Qv(x) = \frac{v(x)-v(\pi-x)}{2}$, then for the Sturm - Liouville operator (3.1) – (3.2) the following equalities hold

1) $q(\pi - x) = q(x)$;

2) $\overline{q(x)} = q(x)$;

3) $\Delta_{12} + \Delta_{14} = \Delta_{32} + \Delta_{34}$;

4) $\overline{\left(\frac{\Delta_{12}+\Delta_{14}}{\Delta_{24}}\right)} = \frac{\Delta_{12}+\Delta_{14}}{\Delta_{24}} = \frac{\Delta_{32}+\Delta_{34}}{\Delta_{24}}$;

Moreover, operators L and L^+ take the following forms:

$Ly = -y'' + q(x)y,\ x \in (0, \pi)$;

$$\begin{cases} \frac{\Delta_{12}+\Delta_{14}}{\Delta_{24}}[y(0) + y(\pi)] + y'(0) - y'(\pi) = 0, \\ \Delta_{12} y(0) + \Delta_{32} y(\pi) - \Delta_{24} y'(\pi) = 0. \end{cases}$$

$L^+ z = -z'' + q(x)z,\ x \in (0, \pi)$;

$$\begin{cases} \frac{\overline{\Delta_{14}}-\overline{\Delta_{34}}}{\overline{\Delta_{24}}}[z(0) + z(\pi)] + z'(0) + z'(\pi) = 0, \\ \overline{\Delta_{14}} z(0) + \overline{\Delta_{24}} z'(0) + \overline{\Delta_{12}} z(\pi) = 0. \end{cases}$$

Proof.

If $PL = L^+ P$, then $z(x) = Py(x) \in D(L^+)$, where $y(x) \in D(L)$, thus

$$\begin{cases} \overline{\Delta_{14}}\frac{y(0)+y(\pi)}{2} + \overline{\Delta_{24}}\frac{y'(0)-y'(\pi)}{2} + \overline{\Delta_{12}}\frac{y(\pi)+y(0)}{2} = 0, \\ \overline{\Delta_{34}}\frac{y(0)+y(\pi)}{2} + \overline{\Delta_{32}}\frac{y(\pi)+y(0)}{2} - \overline{\Delta_{24}}\frac{y'(\pi)-y'(0)}{2} = 0; \end{cases}$$

$$\begin{cases} (\overline{\Delta_{12}} + \overline{\Delta_{14}})[y(0) + y(\pi)] + \overline{\Delta_{24}}[y'(0) - y'(\pi)] = 0, \\ (\overline{\Delta_{32}} + \overline{\Delta_{34}})[y(0) + y(\pi)] + \Delta_{24}[y'(0) - y'(\pi)] = 0. \end{cases}$$

For unknown quantities $y(0), y'(0), y(1), y'(1)$ we obtained the system of equations, therefore

$$\begin{vmatrix} \Delta_{14} & \Delta_{24} & \Delta_{34} & 0 \\ \Delta_{12} & 0 & \Delta_{32} & -\Delta_{24} \\ \overline{\Delta_{12}} + \overline{\Delta_{14}} & \overline{\Delta_{24}} & \overline{\Delta_{12}} + \overline{\Delta_{14}} & -\Delta_{24} \\ \overline{\Delta_{32}} + \overline{\Delta_{34}} & \Delta_{24} & \overline{\Delta_{32}} + \overline{\Delta_{34}} & -\Delta_{24} \end{vmatrix} = 0, \Rightarrow$$

$$\begin{vmatrix} \Delta_{14} & \Delta_{24} & \Delta_{34} & \Delta_{24} \\ \Delta_{12} & 0 & \Delta_{32} & -\Delta_{24} \\ \overline{\Delta_{12}} + \overline{\Delta_{14}} & \overline{\Delta_{24}} & \overline{\Delta_{12}} + \overline{\Delta_{14}} & 0 \\ \overline{\Delta_{32}} + \overline{\Delta_{34}} & \overline{\Delta_{24}} & \overline{\Delta_{32}} + \overline{\Delta_{34}} & 0 \end{vmatrix} \sim \begin{vmatrix} \Delta_{14} & \Delta_{24} & \Delta_{34} & \Delta_{24} \\ \Delta_{12} + \Delta_{14} & \Delta_{24} & \Delta_{32} + \Delta_{34} & 0 \\ \overline{\Delta_{12}} + \overline{\Delta_{14}} & \overline{\Delta_{24}} & \overline{\Delta_{12}} + \overline{\Delta_{14}} & 0 \\ \overline{\Delta_{32}} + \overline{\Delta_{34}} & \overline{\Delta_{24}} & \overline{\Delta_{32}} + \overline{\Delta_{34}} & 0 \end{vmatrix} =$$

$$= (-\Delta_{24})\begin{vmatrix} \Delta_{12}+\Delta_{14} & \Delta_{24} & \Delta_{32}+\Delta_{34} \\ \overline{\Delta_{12}}+\overline{\Delta_{14}} & \overline{\Delta_{24}} & \overline{\Delta_{12}}+\overline{\Delta_{14}} \\ \overline{\Delta_{32}}+\overline{\Delta_{34}} & \overline{\Delta_{24}} & \overline{\Delta_{32}}+\overline{\Delta_{34}} \end{vmatrix} =$$

$$= (-\Delta_{24})\begin{vmatrix} \Delta_{12}+\Delta_{14} & \Delta_{24} & \Delta_{32}+\Delta_{34}-\Delta_{12}-\Delta_{14} \\ \overline{\Delta_{12}}+\overline{\Delta_{14}} & \overline{\Delta_{24}} & 0 \\ \overline{\Delta_{32}}+\overline{\Delta_{34}} & \overline{\Delta_{24}} & 0 \end{vmatrix} =$$

$$= (-\Delta_{24})(\Delta_{32}+\Delta_{34}-\Delta_{12}-\Delta_{14})\overline{\Delta_{24}}(\overline{\Delta_{12}}+\overline{\Delta_{14}}-\overline{\Delta_{32}}-\overline{\Delta_{34}}) =$$

$$= |\Delta_{24}|^2|\Delta_{32}+\Delta_{34}-\Delta_{12}-\Delta_{14}|^2 = 0.$$

Since $\Delta_{24} \neq 0$, then $\Delta_{12}+\Delta_{14} = \Delta_{32}+\Delta_{34}$.

Summing up the boundary conditions (3.3), we have

$$(\Delta_{12}+\Delta_{14})y(0) + (\Delta_{32}+\Delta_{34})y(\pi) + \Delta_{24}[y'(0)-y'(\pi)] = 0,$$

$$(\Delta_{12}+\Delta_{14})[y(0)+y(\pi)] + \Delta_{24}[y'(0)-y'(\pi)] = 0.$$

Combining this equation with the first boundary condition (4.3), we receive

$$\begin{cases} (\Delta_{12}+\Delta_{14})[y(0)+y(\pi)] + \Delta_{24}[y'(0)-y'(\pi)] = 0, \\ (\overline{\Delta_{12}}+\overline{\Delta_{14}})[y(0)+y(\pi)] + \overline{\Delta_{24}}[y'(0)-y'(\pi)] = 0. \end{cases} \tag{4.5}$$

This system of equations (4.5) has a non-trivial solution, therefore

$$\Delta = \begin{vmatrix} \Delta_{12}+\Delta_{14} & \Delta_{24} \\ \overline{\Delta_{12}}+\overline{\Delta_{14}} & \overline{\Delta_{24}} \end{vmatrix} = 0,$$

$$\overline{\Delta_{24}}(\Delta_{12}+\Delta_{14}) - \Delta_{24}(\overline{\Delta_{12}}+\overline{\Delta_{14}}) = 0,$$

$$\frac{\overline{\Delta_{12}}+\overline{\Delta_{14}}}{\overline{\Delta_{24}}} = \frac{\Delta_{12}+\Delta_{14}}{\Delta_{24}}.$$

Hence, the operator L has the following form

$$Ly = -y'' + q(x)y, \qquad x \in (0,\pi);$$

$$\begin{cases} \dfrac{\Delta_{12}+\Delta_{14}}{\Delta_{24}}[y(0)+y(\pi)] + y'(0) - y'(\pi) = 0, \\ \Delta_{12}y(0) + \Delta_{32}y(\pi) - \Delta_{24}y'(\pi) = 0. \end{cases}$$

We specify the boundary conditions of the operator L^+, subtracting the second boundary condition from the first boundary condition $(3.3)^+$, we get

$$(\overline{\Delta_{14}}-\overline{\Delta_{34}})z(0) + (\overline{\Delta_{12}}-\overline{\Delta_{32}})z(\pi) + \overline{\Delta_{24}}[z'(0)+z'(\pi)] = 0.$$

From the formula 4.4 it follows that $\overline{\Delta_{14}}-\overline{\Delta_{34}} = \overline{\Delta_{32}}-\overline{\Delta_{12}}$, thus

$$(\overline{\Delta_{14}}-\overline{\Delta_{34}})[z(0)-z(\pi)] + \overline{\Delta_{24}}[z'(0)+z'(\pi)] = 0,$$

$$\frac{\overline{\Delta_{14}}-\overline{\Delta_{34}}}{\overline{\Delta_{24}}}[z(0)-z(\pi)]+z'(0)+z'(\pi)=0.$$

Consequently, the adjoint operator L^{+} has the following form

$$L^{+}z=-z''+q(x)z,$$
$$\begin{cases}\dfrac{\overline{\Delta_{14}}-\overline{\Delta_{34}}}{\overline{\Delta_{24}}}[z(0)-z(\pi)]+z'(0)+z'(\pi)=0,\\ \overline{\Delta_{14}}z(0)+\overline{\Delta_{24}}z'(0)+\overline{\Delta_{12}}z(\pi)=0;\end{cases}$$

Further, the formula $PL=L^{+}P$ implies

$$PLy=P^{\circ}[-y''+q(x)y]=-P[y''(x)]+P[q(x)y(x)]=$$

$$=-\frac{y''(x)+y''(\pi-x)}{2}+\frac{q(x)y(x)+q(\pi-x)y(\pi-x)}{2};$$

$$L^{+}Py=L^{+}\left[\frac{y(x)+y(\pi-x)}{2}\right]=$$

$$=-\frac{y''(x)+y''(\pi-x)}{2}+\bar{q}(x)\frac{y(x)+y(\pi-x)}{2};$$

$$q(x)y(x)+q(\pi-x)y(\pi-x)=\bar{q}(x)y(x)+\bar{q}(x)y(\pi-x),$$

$$[q(x)-\bar{q}(x)]y(x)+[q(\pi-x)-\bar{q}(x)]y(\pi-x)=0,=> \qquad (4.6)$$

$$[q(\pi-x)-\bar{q}(\pi-x)]y(\pi-x)+[q(x)-\bar{q}(\pi-x)]y(x)=0.$$

It is obvious that the system of equations for $y(x)$ and $y(\pi-x)$ has a non-trivial solution, thus

$$\Delta=\begin{vmatrix}q(x)-\bar{q}(x) & q(\pi-x)-\bar{q}(x)\\ q(x)-\bar{q}(\pi-x) & q(\pi-x)-\bar{q}(\pi-x)\end{vmatrix}=0;$$

$$[q(x)-\bar{q}(x)][q(\pi-x)-\bar{q}(\pi-x)]=[q(\pi-x)-\bar{q}(x)][q(x)-\bar{q}(\pi-x)],$$

$$q(x)q(\pi-x)-q(x)\,\bar{q}(\pi-x)-\bar{q}(x)\,q(\pi-x)+\bar{q}(x)\bar{q}(\pi-x)=$$

$$=q(\pi-x)q(x)-q(\pi-x)\bar{q}(\pi-x)-q(x)\bar{q}(x)-\bar{q}(x)\bar{q}(\pi-x),$$

$$q(x)\bar{q}(\pi-x)+\bar{q}(x)\,q(\pi-x)=q(\pi-x)\bar{q}(\pi-x)+q(x)\bar{q}(x),$$

$$q(x)[\bar{q}(\pi-x)-\bar{q}(x)]+q(\pi-x)[\bar{q}(x)-\bar{q}(\pi-x)]=0,$$

$$[\bar{q}(x)-\bar{q}(\pi-x)][q(\pi-x)-q(x)]=0,$$

$$|q(x)-q(\pi-x)|^{2}=0,=>\ q(x)-q(\pi-x)=0; \qquad (4.7)$$

From the formulas (4.6) and (4.7), we have

$$[q(x)-\bar{q}(x)]y(x)+[q(x)-\bar{q}(x)]y(\pi-x)=0,=>$$

$$[q(x)-\bar{q}(x)][y(x)+y(\pi-x)]=0,=>\ q(x)-\bar{q}(x)=0.$$

Lemma 4.4. If

а) $\Delta_{24} \neq 0$;

б) $LQ = QL^{+}$,

then

1) $q(\pi - x) = q(x)$;
2) $\bar{q}(x) = q(x)$,
3) $\overline{\Delta_{12} + \Delta_{14}} = \Delta_{32} + \Delta_{34}$;
4) $\underbrace{\overline{\left(\frac{\Delta_{14}-\Delta_{34}}{\Delta_{24}}\right)}}_{\frac{\Delta_{32}-\Delta_{12}}{\Delta_{24}}} = \left(\frac{\Delta_{14}-\Delta_{34}}{\Delta_{24}}\right) = \frac{\Delta_{32}-\Delta_{12}}{\Delta_{24}}$,

where $Qz = \frac{z(x)-z(\pi-x)}{2}$.

Moreover, the operators L and L^{+} take the following forms

$$Ly = -y'' + q(x)y, \ x \in (0,\pi);$$

$$\begin{cases} \frac{\Delta_{12}+\Delta_{14}}{\Delta_{24}}[y(0) + y(\pi)] + y'(0) - y'(\pi) = 0, \\ \Delta_{12}y(0) + \Delta_{32}y(\pi) - \Delta_{24}y'(\pi) = 0; \end{cases}$$

$$L^{+}z = -z'' + q(x)z, \ x \in (0,\pi);$$

$$\begin{cases} \frac{\Delta_{14}-\Delta_{34}}{\Delta_{24}}[z(0) - z(\pi)] + z'(0) + z'(\pi) = 0, \\ \overline{\Delta_{14}}z(0) + \overline{\Delta_{24}}z'(0) + \overline{\Delta_{12}}z(\pi) = 0. \end{cases}$$

Proof.

If $LQ = QL^{+}$ and $z \in D(L^{+})$, then $y = Qz \in D(L)$, therefore

$$y(x) = \frac{z(x) - z(\pi - x)}{2}, \qquad y'(x) = \frac{z'(x) + z'(\pi - x)}{2};$$

$$\begin{cases} \Delta_{14}\frac{z(0) - z(\pi)}{2} + \Delta_{24}\frac{z'(\pi) + z'(0)}{2} + \Delta_{34}\frac{z(\pi) - z(0)}{2} = 0, \\ \Delta_{12}\frac{z(0) - z(\pi)}{2} + \Delta_{32}\frac{z(\pi) + z(0)}{2} - \Delta_{24}\frac{z'(\pi) + z'(0)}{2} = 0; \end{cases}$$

$$\begin{cases} (\Delta_{14} - \Delta_{34})\frac{z(0)-z(\pi)}{2} + \Delta_{24}\frac{z'(0)+z'(\pi)}{2} = 0, \\ (\Delta_{12} - \Delta_{32})\frac{z(0)-z(\pi)}{2} - \Delta_{24}\frac{z'(0)+z'(\pi)}{2} = 0; \end{cases} \qquad (4.8)$$

It is obvious that the system has a non-trivial solution, therefore

$$\Delta = \begin{vmatrix} \Delta_{14} - \Delta_{34} & \Delta_{24} \\ \Delta_{12} - \Delta_{32} & -\Delta_{24} \end{vmatrix} = -\Delta_{24}(\Delta_{14} - \Delta_{34} + \Delta_{12} - \Delta_{32}) = 0,$$

since $\Delta_{24}\neq 0$, then $\Delta_{12}+\Delta_{14}=\Delta_{32}+\Delta_{34}$. (4.9)

Subtracting the second boundary condition from the first boundary condition (3.3)[+], we get

$$(\overline{\Delta_{14}}-\overline{\Delta_{34}})z(0)+(\overline{\Delta_{12}}-\overline{\Delta_{32}})z(\pi)+\overline{\Delta_{24}}[z'(0)+z'(\pi)]=0$$

Due to the formula (4.9), this formula takes the form

$$(\overline{\Delta_{14}}-\overline{\Delta_{34}})z(0)-(\overline{\Delta_{14}}-\overline{\Delta_{34}})z(\pi)+\overline{\Delta_{24}}[z'(0)+z'(\pi)]=0,$$

$$\frac{\overline{\Delta_{14}}-\overline{\Delta_{34}}}{\overline{\Delta_{24}}}[z(0)-z(\pi)]+z'(0)+z'(\pi)=0.$$

Combining this boundary condition with the first boundary condition (4.8), we obtain

$$\begin{cases}\dfrac{\Delta_{14}-\Delta_{34}}{\Delta_{24}}[z(0)-z(\pi)]+z'(0)+z'(\pi)=0,\\ \dfrac{\overline{\Delta_{14}}-\overline{\Delta_{34}}}{\overline{\Delta_{24}}}[z(0)-z(\pi)]+z'(0)+z'(\pi)=0.\end{cases}$$

$$\Delta=\begin{vmatrix}\dfrac{\Delta_{14}-\Delta_{34}}{\Delta_{24}} & 1\\ \dfrac{\overline{\Delta_{14}}-\overline{\Delta_{34}}}{\overline{\Delta_{24}}} & 1\end{vmatrix}=0,\qquad \overline{\left(\frac{\Delta_{14}-\Delta_{34}}{\Delta_{24}}\right)}=\frac{\Delta_{14}-\Delta_{34}}{\Delta_{24}}.$$

Hence, the operator L^{+} has the form

$$L^{+}z=-z''+\bar{q}(x)z,\qquad x\in(0,\pi);$$

$$\begin{cases}\dfrac{\Delta_{14}-\Delta_{34}}{\Delta_{24}}[z(0)-z(\pi)]+z'(0)+z'(\pi)=0,\\ \overline{\Delta_{14}}z(0)+\overline{\Delta_{24}}z'(0)+\overline{\Delta_{12}}z(\pi)=0;\end{cases}$$

where $\frac{\Delta_{14}-\Delta_{34}}{\Delta_{24}}$ is a real quantity.

Summing up the boundary conditions (3.3), we get

$$(\Delta_{12}+\Delta_{14})y(0)+(\Delta_{32}+\Delta_{34})y(\pi)+\Delta_{24}[y'(0)-y'(\pi)]=0,$$

$$\frac{\Delta_{12}+\Delta_{14}}{\Delta_{24}}[y(0)+y(\pi)]+y'(0)-y'(\pi)=0.$$

Consequently, the operator L has the form

$$Ly=-y''+q(x)y,\qquad x\in(0,\pi);$$

$$\begin{cases}\dfrac{\Delta_{12}+\Delta_{14}}{\Delta_{24}}[y(0)+y(\pi)]+y'(0)-y'(\pi)=0,\\ \Delta_{12}y(0)+\Delta_{32}y(\pi)-\Delta_{24}y'(\pi)=0.\end{cases}$$

Further, from the formula $LQ=QL^{+}$, we have

$$LQz=L^{\circ}\frac{z(x)-z(\pi-x)}{2}=-\frac{z''(x)-z''(\pi-x)}{2}+q(x)\frac{z(x)-z(\pi-x)}{2};$$

$$QL^{+}z=Q^{\circ}\left[-z''+\overline{q(x)}z\right]=-\frac{z''(x)-z''(\pi-x)}{2}+$$

$$+\frac{\bar{q}(x)z(x)-\bar{q}(\pi-x)z(\pi-x)}{2};$$

$$q(x)z(x)-q(x)z(\pi-x)=\bar{q}(x)z(x)-\bar{q}(\pi-x)z(\pi-x),$$

$$\begin{cases}[q(x)-\bar{q}(x)]z(x)+[\bar{q}(\pi-x)-q(x)]z(\pi-x)=0,\\ [\bar{q}(x)-q(\pi-x)]z(x)+[q(\pi-x)-\bar{q}(\pi-x)]z(\pi-x)=0;\end{cases}\qquad (4.10)$$

$$\Delta=\begin{vmatrix} q(x)-\bar{q}(x) & \bar{q}(\pi-x)-q(x) \\ \bar{q}(x)-q(\pi-x) & q(\pi-x)-\bar{q}(\pi-x) \end{vmatrix}=0;$$

$$[q(x)-\bar{q}(x)]\cdot[q(\pi-x)-\bar{q}(\pi-x)]=[\bar{q}(\pi-x)-q(x)]\cdot[\bar{q}(x)-q(\pi-x)]$$

$$q(x)q(\pi-x)-q(x)\bar{q}(\pi-x)-\bar{q}(x)q(\pi-x)+\bar{q}(x)\bar{q}(\pi-x)=$$

$$=\bar{q}(\pi-x)\bar{q}(x)-\bar{q}(\pi-x)q(\pi-x)+q(x)\bar{q}(x)+q(x)q(\pi-x);$$

$$q(x)\bar{q}(\pi-x)+\bar{q}(x)q(\pi-x)=\bar{q}(\pi-x)q(\pi-x)+q(x)\bar{q}(x),$$

$$q(x)[\bar{q}(\pi-x)-\bar{q}(x)]+q(\pi-x)[\bar{q}(x)-\bar{q}(\pi-x)]=0,$$

$$[\bar{q}(x)-\bar{q}(\pi-x)]\cdot[q(\pi-x)-q(x)]=0,$$

$$|q(x)-q(\pi-x)|^2=0, \ => \ q(x)=q(\pi-x).$$

From (4.10) it follows that

$$[q(x)-\bar{q}(x)]z(x)+[\bar{q}(x)-q(x)]z(\pi-x)=0,=>$$

$$[q(x)-\bar{q}(x)][z(x)-z(\pi-x)]=0,=> \ q(x)=\bar{q}(x).$$

The proved Lemmas 4.3 and 4.4 yields the following theorem.

Theorem 4.1. If $\Delta_{24}\neq 0$ and the following formulas hold

a) $PL=L^{+}P$,

b) $LQ=QL^{+}$;

then the operators L and L^{+} take the following forms:

$$Ly=-y''+q(x)y, \ x\in(0,\pi);$$

$$\begin{cases} \frac{\Delta_{12}+\Delta_{14}}{\Delta_{24}}[y(0)+y(\pi)]+y'(0)-y'(\pi)=0, \\ \Delta_{12}y(0)+\Delta_{32}y(\pi)-\Delta_{24}y'(\pi)=0; \end{cases}$$

$$L^{+}z=-z''+q(x)z, \ x\in(0,\pi);$$

$$\begin{cases} \frac{\Delta_{14}-\Delta_{34}}{\Delta_{24}}[z(0)-z(\pi)]+z'(0)+z'(\pi)=0, \\ \overline{\Delta_{14}}z(0)+\overline{\Delta_{24}}z'(0)+\overline{\Delta_{12}}z(\pi)=0; \end{cases}$$

where

1) $q(\pi-x)=q(x)$;
2) $\overline{q}(x)=q(x)$,
3) $\overline{\left(\frac{\Delta_{12}+\Delta_{14}}{\Delta_{24}}\right)}=\frac{\Delta_{12}+\Delta_{14}}{\Delta_{24}}=\frac{\Delta_{32}+\Delta_{34}}{\Delta_{24}}$;
4) $\overline{\frac{\Delta_{14}-\Delta_{34}}{\Delta_{24}}}=\left(\frac{\Delta_{14}-\Delta_{34}}{\Delta_{24}}\right)=\frac{\Delta_{32}-\Delta_{12}}{\Delta_{24}}$.

Further, from the formula $PL=L^{+}P$ we note that the operator $L_1=PL$ acts in the subspace $H_1=PH$, where $H=L^2(0,\pi)$. Supposing,

$$u(x)=Py(x)=\frac{y(x)+y(\pi-x)}{2},$$

we receive

$$u'(x)=\frac{y'(x)-y'(\pi-x)}{2}.$$

Then Theorem 4.1 implies

$$\begin{cases} u'(0) + \dfrac{\Delta_{12} + \Delta_{14}}{\Delta_{24}} u(0) = 0, \\ u'\left(\dfrac{\pi}{2}\right) = 0; \end{cases}$$

$$L_1 u = -u'' + q(x)u, \qquad x \in \left(0, \frac{\pi}{2}\right),$$

$$\begin{cases} u'(0) + \dfrac{\Delta_{12} + \Delta_{14}}{\Delta_{24}} u(0) = 0, \\ u'\left(\dfrac{\pi}{2}\right) = 0. \end{cases}$$

Similarly, supposing

$$v(x) = \frac{z(x) - z(\pi - x)}{2},$$

we get

$$v'(x) = \frac{z'(x) + z'(\pi - x)}{2}.$$

Then from Theorem 4.1 it follows that

$$\begin{cases} v'(0) + \dfrac{\Delta_{14} - \Delta_{34}}{\Delta_{24}} v(0) = 0, \\ v\left(\dfrac{\pi}{2}\right) = 0; \end{cases}$$

$$L_2 v = -v'' + q(x)v, \qquad x \in \left(0, \frac{\pi}{2}\right),$$

$$\begin{cases} v'(0) + \dfrac{\Delta_{14} - \Delta_{34}}{\Delta_{24}} v(0) = 0, \\ v\left(\dfrac{\pi}{2}\right) = 0; \end{cases}$$

From the condition 3) of the proved Theorem 4.1 it follows the following equality

$$\Delta_{12} + \Delta_{14} = \Delta_{14} - \Delta_{34}$$

Supposing $\alpha = \Delta_{24}$, $\beta = \Delta_{12} + \Delta_{14}$, we rewrite the operators L_1 and L_2 in the form

$$L_1 u = -u'' + q(x)u, \qquad x \in \left(0, \frac{\pi}{2}\right),$$

$$\begin{cases} \alpha u'(0) + \beta u(0) = 0, \\ u'\left(\dfrac{\pi}{2}\right) = 0; \end{cases}$$

$$L_2 v = -v'' + q(x)v, \qquad x \in \left(0, \frac{\pi}{2}\right),$$

$$\begin{cases} \alpha v'(0) + \beta v(0) = 0, \\ v\left(\dfrac{\pi}{2}\right) = 0. \end{cases}$$

If spectrum of the operator L is known, then by Lemma 4.2 spectra of the operators L_1 and L_2 are known. It is obvious that they form the Borg pair in the interval $\left[0, \frac{\pi}{2}\right]$. By the Borg theorem spectra of these two operators uniquely determine the Sturm-Liouville operator on the segment $\left[0, \frac{\pi}{2}\right]$, and due to the formula $q(x) = q(\pi - x)$, on all the segment $[0, \pi]$. Theorem 4.1 is proved.

5. Authors thank the leadership of the International Silkway University and the Regional Social Innovation University of Shymkent for the partial funding of the research.

ӘОЖ 517

А.Ш. Шалданбаев[1], А.А. Шалданбаева[2], Б.А. Шалданбай[3]

[1]Халықаралық Silkway университеті, Шымкент қ., Казақстан;
[2]Аймақтық әлеуметтік-инновациялық университеті, Шымкент қ., Казақстан;
[3]М.О.Ауезов атындағы Оңтүстік Қазақстан мемлекеттік университеті, Шымкент қ., Казақстан

ПОТЕНЦИАЛЫ СИММЕТРИЯЛЫ, АЛ ШЕКАРАЛЫҚ ШАРТТАРЫ АЖЫРАМАЙТЫН ШТУРМ-ЛИУВИЛЛ ОПЕРАТОРЫНЫҢ КЕРІ ЕСЕБІ ТУРАЛЫ

Аннотация. Бұл еңбекте потенциалы симметриялы, нақты әрі үзіксіз, ал шекаралық шарттары ажырамайтын Штурм-Лиувилл операторын бір спектр арқылы анықтауға болатыны көрсетілді. Зерттеу әдісі бұрынғы әдістердің ешбіріне ұқсамайды және ол оператордың ішкі симметриясына негізделген, ал ол өз кезегінде инвариантты кеңістіктердің салдары.

Түйін сөздер: Штурм-Лиувиллдің операторы, спектр, Штурм-Лиувиллдің кері есебі, Боргтың теоремасы, Амбарцумянның теоремасы, Левинсонның теоремасы, ажырамайтын шекаралық шарттар, симметриялы потенциал, инвариантты кеңістіктер.

УДК 517

А.Ш.Шалданбаев[1], А.А.Шалданбаева[2], Б.А.Шалданбай[3]

[1]Международный университет Silkway, г. Шымкент, Казахстан;
[2]Региональный социально-инновационный университет, г. Шымкент, Казахстан;
[3]Южно-Казахстанский Государственный университет им.М.Ауезова, г. Шымкент, Казахстан

ОБРАТНАЯ ЗАДАЧА ОПЕРАТОРА ШТУРМА-ЛИУВИЛЛЯ С НЕ РАЗДЕЛЕННЫМИ КРАЕВЫМИ УСЛОВИЯМИ И СИММЕТРИЧНЫМ ПОТЕНЦИАЛОМ

Аннотация. В данной работе доказана теорема единственности по одному спектру, для оператора Штурма-Лиувилля с не разделенными краевыми условиями и вещественным непрерывным и симметричным потенциалом. Метод исследования отличается от всех известных методов, и основан на внутреннюю симметрию оператора, порожденного инвариантными подпространствами.

Ключевые слова: Оператор Штурма-Лиувилля, спектр, обратная задача Штурма-Лиувилля, теорема Борга, теорема Амбарцумяна, теорема Левинсона, неразделенные краевые условия, симметричный потенциал, инвариантные подпространства.

Information about authors:
Shaldanbayev A.Sh. – doctor of physico-mathematical Sciences, associate Professor, head of the center for mathematical modeling, «Silkway» International University, Shymkent; http://orcid.org/0000-0002-7577-8402;
Shaldanbayeva A.A. - "Regional Social-Innovative University", Shymkent; https://orcid.org/0000-0003-2667-3097;
Shaldanbay B.A. - M.Auezov South Kazakhstan State University, Shymkent; https://orcid.org/0000-0003-2323-0119.

REFERENCES

[1] Ambartsumian V.A. Über eine Frage der Eigenwert-theorie, Zsch.f.Physik, 53(1929), 690-695.
[2] Borg G. Eine Umbehrung der Sturm – Liovillschen Eigenwertaufgabe, Acta Math., 78, №2(1946), 1-96.
[3] Levinson N. The inverse Sturm – Lioville problem, Math.Tidsskr. B., 1949, 25-30.
[4] Levitan B.M. On definition of the Sturm-Liouville operator by two spectra. News of AS USSR, ser. Math., 28 (1964), 63-78.
[5] Levitan B.M. On definition of the Sturm-Liouville operator by one and two spectra. News of AS USSR, ser. Math., 42. №1. 1964.
[6] Barcilon V. Iterative solution of the inverse Sturm-Liouville problem. J. Mathematical Phys., 15 (1974), 287-298.
[7] Zhikov V. V. On inverse Sturm-Liouville problems on a finite segment. Math. USSR--Izv.1 (1967), 923-934.
[8] Gasymov G. M., Levitan B. M., On Sturm-Liouville differential operators with discrete spectra. Amer. Math. Soc. Transl. Series 2, 68 (1968), 21-33.

[9] Gelfand I. M., Levitan B. M. On the determination of a differential equation from its spectral function. Amer. Math. Soe. Transl. Series 2, 1 (1955), 253-304.

[10] Hald O. H. Inverse eigenvalue problems for layered media. Comm. Pure Appl. Math.,30 (1977), 69-94.

[11] Hochstad T.H. The inverse Sturm-Liouville problem. Comm. Pure Appl. Math., 26 (1973), 715-729.

[12] Hochstadt H. Well-posed inverse spectral problems. Proc. Nat. Acad. Sci., 72 (1975), 2496-2497.

[13] Hochstadt. H., On the well-posedness of the inverse Sturm-Liouville problem. J. Differential Equations, 23 (1977), 402-413.

[14] Krein M. G., Solution of the inverse Sturm-Liouville problem. Dokl. Akad. Nauk SSSR (N.S.), 76 (1941), 21-24.

[15] Krein, M. G., On the transfer function of a one-dimensional boundary problem of second order.Dokl. Aka:t. 1Vaulc SSSR (N.S.), 88 (1953), 405-408.

[16] Levitan B. M., On the determination of a Sturm-Liouville equation by two spectra. Amer. Math. Soc. Transl. Series 2, 68 (1968), 1-20.

[17] Levitan B. M., Generalized translation operators, Israel Program for Scientific Translations, Jerusalem,1964.

[18] Marchenko V. A., Concerning the theory of a differential operator of the second order. Dokl. Akad. Nauk SSSR (N.S.), 72 (1950), 457-460.

[19] Marchenko V. A., Expansion into eigenfunctions of non-selfadjoint singular differential operators of second order. Amer. Math. Soc. Transl. Series 2, 25 (1963), 77-130.

[20] Hald O.H. The Inverse Sturm--Liouville Problem with symmetric Potentials, Acta mathematica 1978, 141:1, 263 .

[21] Coddinoton E., Levinson, N., Theory of ordinary differential equations. McGraw-Hill, New York, 1955.

[22] Neumark M. A., Lineare Differential Operatoren. Akademie-Verlag, Berlin, 1963.

[23] Titchmarsh E. C., The theory of functions. Oxford University Press, London, 1939.

[24] Titchmarsh E. C., Eigenfunction expansions associated with second order differential equations. Oxford University Press, London, 1946.

[25] Zygmund A., Trigonometric series, vol. I, 2nd ed. Cambridge University Press, London,

[26] Jörgens K., Spectral theory of second-order ordinary differential operators, Lectmyes delivered at Aarhus Universitet, 1962/63, Aarhus, 1964.

[27] Akylbayev M.I., Beysebayeva A., Shaldanbayev A. Sh., On the Periodic Solution of the Goursat Problem for a Wave Equation of a Special Form with Variable Coefficients. News of the National Academy of Sciences of the republic of Kazakhstan. Volume 1, Number 317 (2018), 34 – 50.

[28] Shaldanbaeva A. A., Akylbayev M.I., Shaldanbaev A. Sh., Beisebaeva A.Zh., The Spectral Decomposition of Cauchy Problem's Solution for Laplace Equation. News of the National Academy of Sciences of the republic of Kazakhstan. Volume 5, Number 321 (2018), 75 – 87. https://doi.org/10.32014/2018.2518-1726.10

N E W S
OF THE NATIONAL ACADEMY OF SCIENCES OF THE REPUBLIC OF KAZAKHSTAN
PHYSICO-MATHEMATICAL SERIES
ISSN 1991-346X **https://doi.org/10.32014/2019.2518-1726.42**
Volume 4, Number 326 (2019), 42 – 49

A. Dasibekov[1], A.A. Yunusov[2], A.A. Yunusova[3],
B.N. Korganbayev[1], N.A. Kuatbekov[2], G.A. Takibayeva[1], D.N. Espembetova [2]

[1]M. Auezov South Kazakhstan State University, Shymkent, Kazakhstan;
[2]Kazakhstan Engineering Pedagogical University of Friendship of Peoples, Shymkent, Kazakhstan;
[3]Eurasian humanitarian Institute, Actana, Kazakhstan
Yunusov1951@mail.ru

SEALING OF A LAYER OF A SOUND WITH EFFECT OF ELASTIC PROPERTIES AND INHOMOGENEOUS BORDER CONDITIONS

Abstract. In engineering practice, the problems of compacting an earth medium of finite thickness possessing an elastic property are of great interest. In this connection, the process of one-dimensional compaction of a three-phase base with a water repulsion at a depth and under the influence of an external load, depending on time and coordinate, is considered. In this case, boundary value problems for the partial differential equation are solved. Moreover, the boundary conditions are not homogeneous. Calculation formulas for calculation of pore pressure values, stresses in the skeleton of the ground and the value of precipitation for any time interval from the start of loading t have been determined. Calculations from these formulas show that the precipitation curves for inhomogeneous boundary conditions are, in their value, less than for homogeneous boundary conditions. In this case, the stresses in the skeleton of the ground for inhomogeneous boundary conditions are smaller in magnitude than for homogeneous boundary conditions and they tend to a certain asymptote

Keywords: Process, compaction, soil, parallelepiped, pressure, foundation, foundation, boundary conditions, continuity of functions, differential equations, hypergeometric equations.

All existing works, except for a few, in the field of consolidation of elastic and elastically creeping soils were solved for homogeneous boundary conditions, although they must be non-homogeneous. In this connection, it is time to solve multidimensional problems of consolidation of soils with heterogeneous boundary conditions and on the basis of the solutions obtained, to establish design formulas that make it possible to ensure the strength of any building or structure.

Prof. N.M. Gersevanov at one time pointed out that static calculations of the bases do not give a real picture of the work of the bases. In this connection, it is necessary to proceed to the study of processes in soils that depend on time. In this case, as noted above, in soils of structures very often there are soils impregnated with water, and the soil itself consists of groundwater filling the void between the soil particles and the soil skeleton, consisting of a set of solid particles and bound water. They can be used for compaction of soil massifs having large dimensions in comparison with the thickness of the layer. If the surface of such a soil is taken as a conditional horizon, then before the load is applied, the head H in the whole ground mass will be zero. At the first moment after application of the load, the head H in this section of the ground surface will increase by an amount equal to, then, depending on the time, it will fall. At all other points on the surface of the soil, the head remains zero. At the same time, at the points of the ground not on the surface, a scalar field of heads is created, i.e. at each point the head rises to the value H, which is a function of the point, and, in the future, also from the time t. If the field of heads is known, it is possible in the future to determine a number of quantities depending on the pressure H. And an instant increase in pressure produces an instantaneous pressure p [1-6].

Thus, the instantaneous application of a load on the surface of the soil is the cause of the appearance of a field of heads accompanying the movement of water from points with a high head to a point with hydrodynamic pressure. It can be calculated at any point in the ground mass, if the head function is known. And with a large load, the hydrodynamic pressure, trying to move the soil from under the bases, can destroy it [7-9].

Below we shall consider the compaction of homogeneous soils having elastic properties with inhomogeneous boundary conditions.

To the base of the building are layers of soil lying lower and toward the basement bottom, affecting the stability of the vertical movement of the building. Depending on the task being investigated, they can be represented as a ground layer of the final compaction power, a ground rectangle and a ground parallelepiped.

In engineering practice, the problems of compacting an earth medium of finite thickness possessing an elastic property are of great interest. In this connection, let us consider the process of compaction of a three-phase base with a water repellent at a depth that is under the influence of an external load, depending on time and coordinate [8,10-14].

The compaction of the soil is mainly determined by its compressibility. The compressibility of the substrate depends on both the type of soil and the nature of the load. Dynamic loads cause considerable compaction in sandy soils and a weak one in clayey soils. Long-acting loads on the contrary strongly compact clay soils and weakly-sandy.

The phenomenon of compressibility of soils is very important in the design of engineering facilities on a consolidated basis. At the same time, the deformation of the soil compression mainly occurs due to the approach of solid particles to each other and is estimated by a change in the porosity coefficient with a change in the compressive stresses in the soil skeleton σ. Determination of the relationship between the coefficient of porosity and compressive stresses in the skeleton of the soil is usually made by laboratory means in compression devices [9,12,15-16].

The equation of the compression curve of K. Terzagi [17] is represented by the logarithmic dependence

$$\varepsilon = -A\ln(\sigma + \sigma_0) + C, \tag{1}$$

where A, σ_0 and C are the parameters of this dependence, determined from the experiments.

In the case of a relatively small change in the stress σ, the curvilinear outlines of the compression curve (1) can be replaced by a straight line, i.e.

$$\varepsilon = -\alpha_0\sigma + A, \tag{2}$$

where a_0 and A are the parameters of the linear dependence.

Moreover, a_0 is called the coefficient of instantaneous compaction, and the larger the value of a_0, the more compacted the soil, therefore this parameter is called the coefficient of compaction. However, the coefficient of compaction or compactability of the soil as the stresses increase gradually decreases. Moreover, the compaction coefficients for weakly compacted clays reach values a_0 = 0.10-0.01 MPa, and for compacted clays decrease to values a_0 = 0.05-0.01 MPa [18-21].

Next, we will use the equation of mechanics of three-phase compacted soils, obtained in [16], which will be written as follows:

$$\frac{\partial \varepsilon}{\partial t} + \beta'(1+\varepsilon_{cp})\frac{\partial p}{\partial t} = \frac{k(1+\varepsilon_{cp})}{\gamma_{в}}\frac{\partial^2 p}{\partial z^2}, \tag{3}$$

where β' – the coefficient of volume compression; k – the filtration coefficient; εcp - average porosity coefficient; γ - the volumetric weight of water; p - the pressure in the pore fluid.

Then the basic equation of compaction of the ground medium (3), which has the elastic property (2), has the form

$$\frac{\partial p}{\partial t} = C_V^{(1)} \cdot \frac{\partial^2 p}{\partial z^2} + A\frac{\partial q}{\partial t}, \tag{4}$$

where

$$C_V^{(1)} = \frac{1+\varepsilon_{cp}}{\gamma \cdot [a+\beta'(1+\varepsilon_{cp})]}; \quad A = \frac{a}{a+\beta'(1+\varepsilon_{cp})} \tag{5}$$

Equation (4) for (5) is solved under the following initial and boundary conditions:

$$p(z,\tau_1) = q(z,\tau_1), \quad z \in [0,h], \quad \tau_1 \in [\tau,T]; \tag{6}$$

$$\left.\begin{aligned} & p(0,t) = q(0,\tau_1)\text{æ(t)}, \quad \text{t} \in [\tau,\text{T}], \\ & \left.\frac{\partial \text{p}}{\partial \text{z}}\right|_{z=h} = 0, \quad 0 \le \text{æ(t)} < 1. \end{aligned}\right\} \tag{7}$$

Conditions (7) are not homogeneous. In order to bring them to homogeneous conditions, we make a change of the form

$$\overline{p}(z,t) = p(z,t) - q(\tau_1)\text{æ(t)} \tag{8}$$

from whence

$$p(z,t) = q(t) \cdot \text{æ(t)} + \overline{p}(z,t) \tag{9}$$

Bearing in mind (8) and (9), conditions (6) and (7) are reduced to the form

$$\overline{p}(z,\tau_1) = q(\tau_1) \cdot [1 - \text{æ}(\tau_1)], \tag{10}$$

$$\left.\begin{aligned} & \overline{p}(0,t) = 0, \\ & \left.\frac{\partial \overline{\text{p}}}{\partial \text{z}}\right|_{z=h} = 0. \end{aligned}\right\} \tag{11}$$

In this case, the basic equation of compaction (4) is reduced to the form:

$$\frac{\partial \overline{p}}{\partial t} = C_V^{(1)} \cdot \frac{\partial^2 \overline{p}}{\partial z^2} + (A+1)\frac{\partial q}{\partial t}, \tag{12}$$

where the constants, $C_V^{(1)}$, (A+1)are found from (5).

Below we define the solution of equation (12) for the initial (10) and boundary (11) conditions. This solution satisfying the boundary conditions (11) can be represented in the form

$$\overline{p} = \sum_{i=0}^{\infty} T_i(t) \cdot \sin\frac{(2i+1)\pi}{2h} z, \tag{13}$$

where $T_i(t)$ – is an unknown function depending only on t.

Expression (13) satisfies the boundary conditions (11). Indeed, from (13) for z=0 we have, $\overline{p}(0,t) = 0$ and for z=*h*

$$\frac{\partial \overline{p}}{\partial z} = \sum_{i=0}^{\infty} \frac{(2i+1)\pi}{2h} T_i(t) \cdot \sin\frac{(2i+1)\pi}{2} z = 0. \tag{14}$$

Consequently, expression (13) is a solution of equation (12), which satisfies boundary conditions (11). Next, we find an unknown function. To this end, we substitute expression (13) in (10), then multiply both sides of the resulting equation by $\sin\frac{(2i+1)\pi}{2}z$, We integrate with respect to the independent variable z from 0 to h. In this case we relatively obtain an ordinary differential equation of the form

$$\frac{\partial T_i(t)}{\partial t}+C_V^{(1)}\lambda_i^2 T_i(t)=Q_i(t), \tag{15}$$

Where

$$Q_i(t)=\frac{4(A+1)}{(2i+1)\pi}\cdot\frac{\partial q}{\partial t}. \tag{16}$$

Equation (15) for (16) is an inhomogeneous differential equation, the particular solution of which can be represented in the form

$$T_{1i}(t)=\int_{\tau_1}^{t}Q_i(\tau)\cdot e^{-C_V^{(1)}\lambda_i^2(t-\tau)}d\tau. \tag{17}$$

The general solution of equation (15) with $Q_i(t)=0$

$$T_{0i}(t)=C\cdot e^{-C_V^{(1)}\lambda_i^2 t}$$

Then expression (13) is reduced to the following form

$$\overline{p}=\sum_{i=0}^{\infty}\left[C_i\cdot e^{-C_V^{(1)}\lambda_i^2 t}+\int_{\tau_1}^{t}Q_i(\tau)\cdot e^{-C_V^{(1)}\lambda_i^2(t-\tau)}d\tau\right]\cdot\sin\frac{(2i+1)\pi}{2h}z, \tag{18}$$

where C_i - an arbitrary constant, which is found from the initial condition (10). And with $t=\tau_1$

$$C_i=\frac{4}{(2i+1)\pi}\cdot e^{C_V^{(1)}\lambda_i^2\tau_1}q(\tau_1)[1-æ].$$

The solution (18) of equation (12) with (10) and (11) has the form

$$\overline{p}=\frac{4}{\pi}\sum_{i=0}^{\infty}\frac{1}{2i+1}\left[q(\tau_1)[1-æ]\cdot e^{C_V^{(1)}\lambda_i^2(t-\tau_1)}+(A+1)\int_{\tau_1}^{t}\frac{\partial q}{\partial\tau}\cdot e^{C_V^{(1)}\lambda_i^2(t-\tau)}d\tau\right]\sin\frac{(2i+1)\pi}{2h}z \tag{19}$$

Expressing (19) in (9), we obtain the calculated formula for the pressure in the pore liquid, when the boundary conditions of the compacted ground mass are non-uniform, i.e.

$$p(z,t)=q(t)æ(t)+\frac{4}{\pi}\sum_{i=0}^{\infty}\frac{1}{2i+1}\left[q(\tau_1)[1-æ]\cdot e^{C_V^{(1)}\lambda_i^2(t-\tau_1)}+(A+1)\int_{\tau_1}^{t}\frac{\partial q}{\partial\tau}\cdot e^{C_V^{(1)}\lambda_i^2(t-\tau)}d\tau\right]\times$$
$$\times\sin\frac{(2i+1)\pi}{2h}z. \tag{20}$$

Then the stress in the skeleton of the soil will be calculated by the formula

$$\sigma(x,t)=q(t)[1-æ(t)]+\frac{4}{\pi}\sum_{i=0}^{\infty}\frac{1}{2i+1}\left[q(\tau_1)[1-æ]\cdot e^{C_V^{(1)}\lambda_i^2(t-\tau_1)}+(A+1)\int_{\tau_1}^{t}\frac{\partial q}{\partial\tau}\cdot e^{C_V^{(1)}\lambda_i^2(t-\tau)}d\tau\right]\times$$
$$\times\sin\frac{(2i+1)\pi}{2h}z \tag{21}$$

It should be noted that from (20), (21) we have that $p\to 0$, $\sigma\to q$ for $t\to\infty$.At the same time, for $t\to\tau_1$ we find that $p(z,\tau_1)\to q(\tau_1)$, $\sigma(z,\tau_1)\to 0$.

If we denote the ratio of the draft S_t of a compacted soil mass that has elastic properties for any time t to its total stabilized sediment S_∞, through

$$U=\frac{S_t}{S_\infty}, \tag{22}$$

Then

$$S_t = U\cdot S_\infty, \tag{23}$$

where the degree of consolidation U is from

$$U=1-\frac{8}{\pi^2}\sum_{i=0}^{\infty}\frac{1}{(2i+1)S_\infty}\left[q(\tau_1)[1-æ]\cdot e^{C_V^{(1)}\lambda_i^2(t-\tau_1)}+(A+1)\int_{\tau_1}^{t}\frac{\partial q}{\partial\tau}\cdot e^{C_V^{(1)}\lambda_i^2(t-\tau)}d\tau\right] \tag{24}$$

S_∞ has the meaning

$$S_\infty=\frac{aq(1-æ)h}{1+\varepsilon_{cp}}. \tag{25}$$

Using formulas (20) - (25) and values for e^{-x}, calculate the pore pressure $p(x,t)$, stresses in the skeleton of the ground $\sigma(x,t)$ and the value S_t of the precipitation for any time interval from the start of loading t, respectively.

Let it be required to determine the draft of a soil base with a size of h=5, if the medium to be condensed is characterized by the above parameters, and the external load varies according to law $q=2e^{-0,14t}$. In this case, the integral in (20) is equal to the following quantity;

$$\int_{\tau_1}^{t}\frac{\partial q}{\partial\tau}\cdot e^{C_V^{(1)}\lambda_i^2(t-\tau)}d\tau=\frac{2e^{C_V^{(1)}\lambda_i^2 t}}{C_V^{(1)}\lambda_i^2-0{,}14}\cdot\left\{e^{-[0{,}14-C_V^{(1)}\lambda_i^2]\cdot t}-e^{-[0{,}14-C_V^{(1)}\lambda_i^2]\cdot\tau_1}\right\}, \tag{26}$$

where $k = 36\cdot10^{-8}$ sm/sec; $\beta' = 0{,}35$ MPa; $\varepsilon_{cp} = 1{,}18$; $\gamma = 0{,}01$ n/sm^3; $a_0 = 0{,}022$ MPa we have that $k(1+\varepsilon_{cp}) = 78{,}48\cdot10^{-8}$ sm/sec; $\beta'(1+\varepsilon_{cp}) = 5{,}4936\cdot10^{-7}$ MPa; $C_V^{(1)} = 0{,}0003923$; A = 0,048.

$$\lambda_i^2=\left[\frac{(2i+1)\pi}{2h}\right]^2;\quad æ = 0{,}75;\quad æ = 0{,}5;\quad æ = 0{,}25;\quad æ = 0.$$

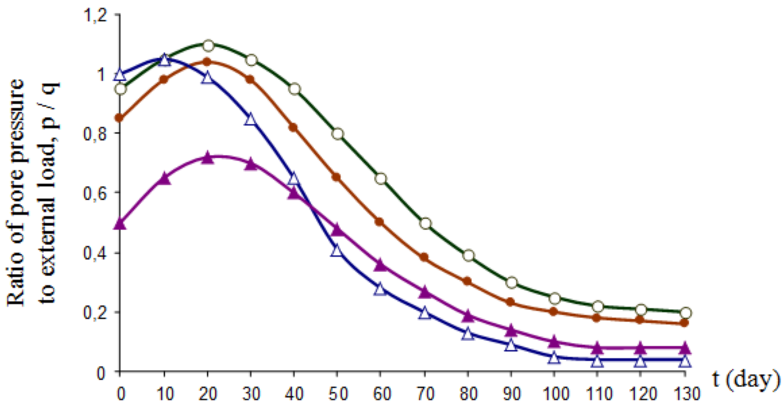

▲ – for homogeneous boundary conditions; ● – for æ = 0,5; ○ – for æ = 0,75; Δ – for a two-phase medium;

Figure 1 - Curves of changes in pore pressure in time

Using the relation (26) and the values $C_V^{(1)}, A, \lambda_i^2$, æ,of the quantities, æ, we obtain the numerical values of the pressure in the pore fluid, the stresses in the skeleton of the soil and the sediment of the compacted soil mass, the diagrams of which are given in Figures 1, 2, and 3.

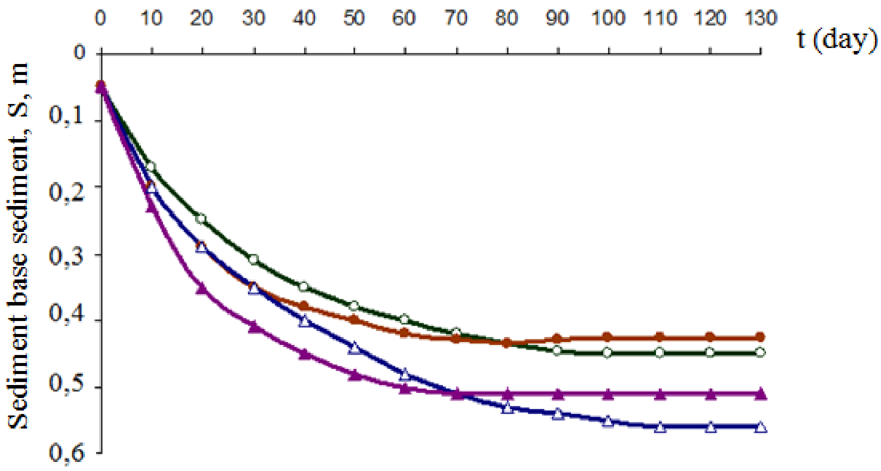

▲ – for homogeneous boundary conditions;
● – for æ = 0,5; ○ – for æ = 0,75; Δ – for a two-phase medium;

Figure 2 - Curves of the changes in the sediment of the condensed massif in time

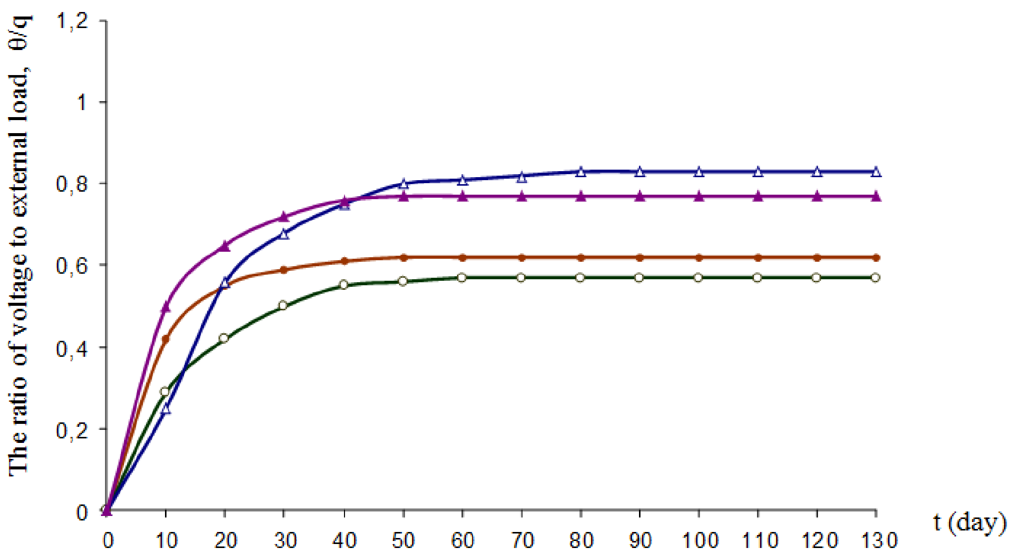

▲ – for homogeneous boundary conditions;
● – for æ = 0,5; ○ – for æ = 0,75; Δ – for a two-phase medium;

Figure 3 - Curves of stress changes in the skeleton of the soil

The precipitation curves for inhomogeneous boundary conditions show that for this case the vertical displacements of any points of the condensed array are smaller in value than in the case of homogeneous boundary conditions. In this case, the stresses in the skeleton of the ground for inhomogeneous boundary conditions are smaller in magnitude than for homogeneous boundary conditions and they tend to a certain asymptote.

It should be noted that recent work has been devoted to these questions [2-6,9].

ӘОЖ 624.131+539.215

А. Дасибеков [1], А.А. Юнусов[2], А.А. Юнусова[3],
Б.Н. Корганбаев[1], Н.А. Куатбеков [2], Г.А. Такибаева [1], Д.Н. Еспембетова [2]

[1] М.Әуезов атындағы Оңтүстік Қазақстан мемлекеттік университеті, Шымкент, Қазақстан;
[2] Қазақстан инженерлі-педагогикалық Халықтар достығы университеті, Шымкент, Қазақстан;
[3]Евразиялық гуманитарлық институты, Астана, Қазақстан

СЕРПІМДІЛІК ҚАСИЕТТЕРІ БАР ЖӘНЕ ШЕКТЕСТІК ЖАҒДАЙЛАРЫ ӘРТЕКТІ ТОПРАҚ ҚАБАТЫҢ ТЫҒЫЗДАУ

Аннотация. Серпімділік қасиеттері баржер қабатының соңғы қалыңдығын тығыздау есептері инженерлік тәжірибе саласында көп қызығушылық туғызады. Осыған орай, суға төзімді тереңдікте жәнеуақыт пен кооржинаттарға тәуелді сыртқы салмақ болған кезде үш фазалы негіздеменің біртекті тығыздалу үрдісі қарастырылды. Бұл жағдайда, дербес туындылар үшін шеттік есептер шығарылады. *t енгізілген кезден бастап кез-келген уақыт аралығы үшін* межелік қысым $p(x,t)$, топырақ қаңқасындағы (құрылымы ?) кернеу көрсеткіштері *о (x,t)* және шөгінді мәнін S_t есептеп шығару үшін есептеу формулалары анықталды. Осы формулалар негізінде табылған мәндер бойынша әртекті шектес жағдайлар үшін қисық шөгінділердің өзінтік көрсеткіштері біртекті шектес жағдайлар үшін көрсеткіштеріне қарағанда аз. Сонымен бірге, әртекті шектес жағдайлар үшін топырақ қаңқасындағы кернеу көрсеткіштері үлкендігі бойынша біртекті шектес жағдайла үшін кернеу көрсеткіштеріне қарағанда төмен және олар белігілі бір асимптотқа талпынады.

Түйін сөздер: үдеріс, топырақ, параллелепипед, қысым, негіздер, негіздеме, шектес жағдайлар, функциялардың үздікссіздігі, дифференциалды теңдеу, гипергеометриалы теңдеу

УДК 624.131+539.215

А. Дасибеков[1], А.А. Юнусов[2], А.А. Юнусова[3],
Б.Н. Корганбаев[1], Н.А. Куатбеков[2], Г.А. Такибаева [1], Д.Н. Еспембетова[2]

[1]Южно-Казахстанский государственный университет им.М.Ауэзова, Шымкент, Казахстан;
[2]Казахстанский инженерно-педагогический университет Дружбы народов, Шымкент, Казахстан;
[3]Евразийский гуманитарный институт, Астана, Казахстан

УПЛОТНЕНИЕ СЛОЯ ГРУНТА, ОБЛАДАЮЩЕГО УПРУГИМ СВОЙСТВОМ И НЕОДНОРОДНОСТЬЮ ГРАНИЧНЫХ УСЛОВИЙ

Аннотация. В инженерной практике большой интерес представляют задачи уплотнения земляной среды конечной толщины, обладающей упругим свойством. В связи с этим рассмотрен процесс одномерного уплотнения трехфазного основания с водоупором на глубине и находящегося под действием внешней нагрузки, зависящей от времени и координаты. При этом решается краевые задачи для уравнении в частных производных. Причем граничные условия неоднородны.

Определены расчетные формулы для вычисления значений порового давления $p(x,t)$, напряжения в скелете грунта $\sigma(x,t)$ и значения осадки S_t для любого промежутка времени от начала загружения t.

Вычисления по этим формулам показывают, что кривые осадки для неоднородных граничных условий по своему значению меньше, чем для однородных граничных условий. При этом значения напряжений в скелете грунта для неоднородных граничных условий по величине меньше, чем для однородных граничных условий и они стремятся к определенной асимптоте

Ключевые слов: Процесс, уплотнения, грунт, параллелипед, давления, основания, фундамент, граничные условия, непрерывность функций, дифференциалные уравнения, гипергеометрические уравнения.

Information about authors:

Dasibekov Azhibek - Doctor of Technical Sciences, Professor, M.Auezov South Kazakhstan State University, Shymkent, Kazakhstan, e-mail: dosibekov-ukgu@gmail.com, ORCID: https://orcid.org/0000-0002-7148-5506;

Yunusov Anarbay Aulbekovich - Candidate of Physical and Mathematical Sciences, assistant professor, Kazakhstan Engineering and Pedagogical University of Peoples’ Friendship, Shymkent, Kazakhstan, e-mail: yunusov1951@mail.ru, ORCID: https://orcid.org/0000-0002-0647-6558;

Yunusova Altynai Anarbaevna - Candidate of Technical Sciences, assistant professor, The Eurasian Humanities Institute, Astana, Kazakhstan, e-mail: altyn_79@mail.ru, ORCID: https://orcid.org/0000-0002-4215-4062;

Korganbayev Baurzhan Nogaybayevich - Doctor of Technical Sciences, Professor, M.Auezov South Kazakhstan State University, Shymkent, Kazakhstan, e-mail: mr.baurs@mail.ru, ORCID: https://orcid.org/0000-0001-9428-2536;

Kuatbekov Nurlan Abdumusayevich - assistant professor, Kazakhstan Engineering and Pedagogical University of Peoples' Friendship, Shymkent, Kazakhstan, e-mail: N.kuatbekov@gmail.com, ORCID: https://orcid.org/0000-0002-9122-8072;

Takibayeva Gulchekhra - Candidate of Technical Sciences, assistant professor, M.Auezov South Kazakhstan State University, Shymkent, Kazakhstan, e-mail: Takibayeva@gmail.com, ORCID: https://orcid.org/0000-0003-2663-0281;

Espembetova Damira Nurmoldaevna – master, Kazakhstan Engineering and Pedagogical University of Peoples' Friendship, Shymkent, Kazakhstan, e-mail: damira-777@gmail.com, ORCID: https://orcid.org/0000-0003-3562-6962

REFERENCS

[1] Gersevanov N. Mmm. Polshin D. E. Theoretical foundations of soil mechanics and their practical application.- Moscow: Stroyizdat, 1948. 247 p.

[2] Tasibekov A. D., Takibaev G. A. plane problem of mechanics of soils in provodolzhala galleriesasian their filtration coefficient and the variability of the modulus of deformation in time // Mechanics and modeling of technological processes.- Taraz, 2006, №1. P. 49-56.

[3] Tasibekov A. , Yunusov A. A., Arapov B. R., Kuatbekov N. A. Yunusova A. A., Taganova G. D., Nurmaganbetova G. K. Consolidation of elastic soil modulus of deformation which varies in time //international journal of applied and fundamentalnyh research-Moscow,2017, No. 9 with 8-13.

[4] Tasibekov A. Yunusov A. A. Imanov J. T. Yunusov A. A. Nurmukhanbetova J. A. solution of the one-dimensional problem of sealing aging hereditary soils//international journal of applied and fundamentalnyh research-Moscow,2014, №12-2 with 192-198.

[5] Tasibekov A. Yunusov A. A. Imanov J. T. Yunusov A. A. problems of the theory of compaction, which is solved in hypergeometric functions, Kummer, Journal "advances in current natural Sciences"Moscow,2014, No. 4-s 96-101.

[6] Tasibekov, A. A., Yunusov A. A., Yunusova A. A. Madjarov N. To. One method of investigating the problem of consolidation provodolzhala heterogeneous soil foundations// Journal "Fundamentalnye studies"Moscow, 2017, No. 9 with 521-528.

[7] Tasibekov A. D., Alibekova A., makasheva G., G. A. Takibaev Seal provodolzhala the earth when galleriesasian the filtration coefficient // Proc.intl.scientific.method. Conf. of the University of Friendship of peoples.- Shymkent, 2006. Part 1. P. 398-404.

[8] Tasibekov A., Yunusov A. A., Saidullaeva N.. Yunusova A. A. Consolidation of inhomogeneous elastic and provodolzhala soils. // International journal of experimental education, Moscow, 2012, №8-p. 67-72,

[9] Tasibekov And, Yunusov A. A., Yunusova A. A., A. Yalova Seal aging hereditary heterogeneous soil bases. // Scientific journal "Fundamental researches", Moscow, 2013, No. 8: pp. 323 to 331, impact factor RISC (2011) – 0,144, contributors:

[10] Tasibekov And, Yunusov A. A., Yunusova A. A., two-Dimensional, uplotnenie provodolzhala heterogeneous soil foundations // Scientific-theoretical magazine "Successes of modern natural Sciences", Moscow, 2013, No. 10: pp. 234-239,

[11] Tasibekov A., Yunusov A. A., Yunusova A. A.. Calculation of inhomogeneous elastic and elastic-creeping soil bases at sand cushion arrangement, Modern problems of science and education, Moscow, 2013, №8. p. 139-144,

[12] Tasibekov A. D., Yunusov A. A., Kambarova O. B., Surganova M. J., G. A. Takibaev Equation of consolidation provodolzhala soils. // Proceedings of the international scientific-methodical conference: Actual problems of education, science and production – 2008 Kazakhstan University of friendship of peoples. - Shymkent, 2008. Vol.1. P. 133-138.

[13] Klein G. K. calculation of sediment structures on the theory of inhomogeneous linear-deformable half-space //Hydrotechnical construction. 1948, №2. P. 7-14.

[14] A. Seitmuratov, S. Tileubay, S. Toxanova, N. Ibragimova, B. Doszhanov, M.Zh. Aitimov. Well-posedness of a nonlocal problem with integral conditions for third order system of the partial differential equations / News Of The National Academy Of Sciences Of The Republic Of Kazakhstan. Series Physico-Mathematical. 2018, No.5, P. 33-41. https://doi.org/10.32014/2018.2518-1726.5

[15] Carillo N. Simple two tree Diemention cases in the Theory of consolidasion of Souls. J. Math. Phis. 1942. V. 21. P. 46-58.

[16] G. A. Takibaev three-Dimensional problem of mechanics of compactable earthen masses in the pressure-dependent filtration coefficient, Izv. OF NAS RK. Series "Physics And Mathematics".- 2006, №1. P. 54-57.

[17] K. Terzaghi structural mechanics soil. M.: Gosstroiizdat, 1933. 510 C.

[18] G. S. Khankhodjaev - Calculations of the consolidation of the elastic-creeping water-saturated soil bases taking into account the structural strength and the initial gradient of the pressure:abstract.dis ... candidate. tech. Sciences'. Shymkent 2010-20s.

[19] Florin, V. A., fundamentals of soil mechanics.–M.: Gosstroiizdat, 1959. Vol. 1, 2. 357 p.; 1961. 543 S.

[20] Shirinkulov T. S., Tasibekov A. D., M. J. two-Dimensional Berdybaeva seal provodolzhala soils in their heterogeneous boundary conditions //Mechanics and modeling of technological processes. Taraz, 2006, №1. P. 61-66.

[21] Shirinkulov T. S., Tasibekov A. D., Berdybaeva M. J. three-dimensional seal provodolzhala heterogeneous soils with their heterogeneous boundary conditions //Mechanics and modeling of technological processes. Taraz, 2006, № 1.P. 30–35.

N E W S
OF THE NATIONAL ACADEMY OF SCIENCES OF THE REPUBLIC OF KAZAKHSTAN
PHYSICO-MATHEMATICAL SERIES
ISSN 1991-346X **https://doi.org/10.32014/2019.2518-1726.43**
Volume 4, Number 326 (2019), 50 – 58

O. Zh. Mamyrbayev [1,2], A.S. Shayakhmetova[1,2], P.B. Seisenbekova[2]

[1]Institute of Information and Computational Technologies, Almaty, Kazakhstan;
[2]Al-Farabi Kazakh National University, Almaty, Kazakhstan
morkenj@mail.ru, asemshayakhmetova@mail.ru, ms.perizat@mail.ru

THE METHODOLOGY OF CREATING AN INTELLECTUAL ENVIRONMENT OF INCREASING THE COMPETENCE OF STUDENTS BASED ON A BAYESIAN APPROACH

Abstract. Artificial intelligence is widely used in solving various problems in various fields of science. The actual use of artificial intelligence methods to create an intellectual environment to improve the competence of the student. Recently, research into the most popular use of artificial intelligence has been the use of Bayesian network apparatus. When creating an intellectual environment for improving the competence of a student, the Bayesian approach is promising. At present, the theory of Bayesian networks is used in various fields of science and production in solving various applied problems. There is a fairly large number of software products for working with Bayesian networks. These products are divided into commercial and free. To implement the mathematical ideas of the Bayesian network, the BayesiaLab application software package is well applied and is one of the high-quality software products that specializes in artificial intelligence technologies. With the help of the package BayesiaLab, you can explore, edit, analyze and determine the model of the Bayesian network. This article provides definitions of various scientists to the term "competence" and explores the possibilities of using Bayesian networks in the formation of students' competence in the direction of information technology. For the formation of students' competencies in the field of information technology, a generalized algorithm and a general architecture of the intellectual environment have been developed. In order to improve professional competence in education, it leads to an increase in the competitiveness of specialists, an improvement in the content, methodology, and updating of the corresponding educational environment. In the formation of competence, a number of technologies are applied: cognitive-oriented, activity-oriented, personality-oriented. The approach used in the formation of competencies is used to simulate the quality of student knowledge. The level of competence depends on the method chosen.

Keywords. Bayesian network, student competencies, knowledge mobility, method flexibility, critical thinking, BayesiaLab software package.

1 Introduction

The development of modern information technologies allows to determine the competence of students in the educational system through information means. This includes the creation of an intellectual environment for the formation of students' competence.

VM Shepel introduces knowledge, skills, theoretical training to competence [1]. Definitions for other competences (V.Landscheer, P.Simonov, M.A.Choshanov) do not contradict this. For example, Landshereer understood the competence as a combination of in-depth knowledge and ability to fulfill the task [2]. P.V. Simonov's commitment to the task, M.A.Choshanov pays attention to the content (knowledge) and procedural components of competence [3].

It is necessary to take into account the following criteria for competence development: mobility, flexibility and critical thinking. Finding the right information and explaining the information creates mobility of knowledge. Flexibility is the organization of the use of information in different ways. Transforming information, finding evidence, and making decisions form critical thinking. By building these skills into the trainee, we will reach the required competence.

Table 1 - An example of a set of questions for competence assessment and competency assessment is given to the students.

Levels of competence determination	To be competent	Sample questions for the assessment
Mobility of knowledge	Being able to find the information you need and to be able to explain the information. This allows the student to be knowledgeable and to explain, to be able to convey his knowledge.	(... who, ... what, ... when, ... what is the meaning, ... what is the main idea, ... the keyword, ... define, define the formulas ... write, type ... description, find dictionary ...), 1 - 10 questions.
Flexible method	It should be able to use information in various situations. That is, the student's flexibility, the ability to adapt quickly to any situation increases.	(... how, why, what, what, what, what, how, ... what differences are there ... give examples, ... solve different ways, ... make a root brief), 11 - 20 questions.
Critical Thinking	They should be able to convert information, find arguments, interact with the game, and make decisions. Through these qualities, the student's confidence in himself, his courage, and his ability to be courageous increases.	(... find the error, because ... what are the criteria, what are the advantages and disadvantages, ... hypothesis, support arguments, or counter arguments), 21 - 30 questions.

Currently, Bayes' approach is a promising aspect in solving applied problems in various research areas as well as deep neural networks [4,5]. Mathematical methods and computer technologies are widely used in biology, technology and medicine. The technique of a monotheist gives precise solutions and theoretical development of these sciences [6].

The method of monotheism is not only rapidly developing in the field of science and technology, but also in the field of education rapidly. The method of education is used to determine the quality of education of students in education, testing systems and competence of students.

The following structure of the article is proposed: the second chapter provides a literary review of the application of the Bayesian approach in various fields of study. The third chapter defines the problem statement. The fourth chapter describes the architecture of the intellectual environment of improving the competence of the student in the field of IT based on the Bayesian approach. The fifth chapter describes the methods and results of the study. The sixth chapter is devoted to the discussion of the findings. At the end of the article, a conclusion is given and a list of references is given.

2 Literature Review

The actual use of artificial intelligence methods in various fields of research [7]. The only way to define competence is to build a student model. The student model can be based on different approaches (neural networks, neuro-fuzzy logic, fuzzy logic, Bayes Networks). The student model is one of the basic components of intelligent computer learning systems. It contains fairly complete information about the student: his level of knowledge, skills and abilities, ability to learn, ability to perform tasks, personal characteristics and other parameters. The student model is dynamic, i.e. changes during the course, in the course of working with the system [8].

The first models of students were described in the works of P.L.Brusilovsky [9], V.A. Petrushina [10] and others. In these works, it was shown that knowledge support is needed to support learning, about learning strategies and methods, and learning about learners. A large number of approaches, specific models and formalisms were proposed for the model representations that are used in organizing the learning process. In [11], it is noted that measuring the level of students' competence with the help of their answers to test tasks is a typical problem of probabilistic reasoning. The two most frequent cases, in view of which uncertainty arises, are called in the foreign literature the terms miss and otgadka. Students may randomly answer the wrong question, the answer to which they know - this situation is called a miss. Also, students may randomly guess the correct answer or write off a task. Such a case is called a clue.

The article [12] describes the general scheme of work with a list of competencies that are formulated in the standard of training. Examples of assessing the level of competence formation are considered.

Bayesian networks are a handy tool for describing fairly complex processes and events with uncertainties. The basic idea of building a network is the decomposition of a complex system into simple elements. To integrate individual elements into a system, the mathematical apparatus of probability theory is used. This approach provides the ability to build models with many interacting variables for the subsequent development of efficient data processing and decision-making algorithms. From a mathematical point of view, the Bayesian network is a model for representing probabilistic dependencies, as well as the absence of these dependencies [13].

To describe the Bayesian network, it is necessary to determine the structure of the graph and the parameters of each node [14]. This information can be obtained directly from the data or from expert assessments. Such a procedure is called learning the Bayesian network [15].

As noted in [16], the Bayesian network is a common choice of researchers for describing the fuzzy connection between student achievements and their competences in many research projects. Since the late 90s of the last century, models based on Bayesian networks have been actively used in the development of computer-aided learning tools [17].

The structure of the Bayesian network reflects the structure of students' knowledge, and is a tool with which you can make judgments and assessments regarding the level of student readiness, as well as make decisions [16].

In [18], Bayesian approaches to building student models were classified into three types. The first type of models in which experts determine the network structure, as well as initial and conditional probabilities. The second type is models aimed at maximizing efficiency by limiting the structure of the network. The third type is data-based models that use data from previous experiments to generate a network structure and probability values.

The attractiveness of Bayesian models lies in their high performance, as well as in an intuitive representation in the form of a graph [19].

In [20], the problem of knowledge modeling with adaptive testing of students in a given discipline is considered. The structure of the training course involves the division of discipline into chapters, and each of the chapters, in turn, corresponds to a set of concepts. Testing includes a set of test items, each of which may require ownership of one or more concepts. In turn, the possession of each of the concepts may be necessary to perform one or several test tasks. This work uses a Bayesian network with binary variables, associated disciplines, topics, concepts, and questions (assignments). Conditional probabilities for variables are set by the teacher.

In article [21], the Bayesian network was used to describe the fuzzy connection between the student’s achievements and their competences. The structure of the Bayesian network reflects the structure of students' knowledge and is a tool with which you can make judgments and assessments regarding the level of student readiness.

In the study [22], the relationship between test problem sets and the rules for solving them is modeled on the basis of the Bayesian network. [21] described methods and algorithms for learning the structure of a Bayesian network with hidden nodes based on the available training data.

3. Task setting

The task definition is formed as follows; it is necessary to form the competence of the student in the direction of IT using the Bayesian approach.

When solving such problems, which require the consideration of uncertainty, the Bayesian approach is promising.

The Bayesian approach is based on the Bayes theorem, which is described as follows [23]:

$$P(A \mid B) = \frac{P(B \mid A)P(A)}{P(B)}$$

where, P (A) is the a priori probability of hypothesis A; $P(A|B)$ - the probability of hypothesis A when an event B occurs; $P(B|A)$ - probability of occurrence of event B with the validity of hypothesis A; $P(B)$ - the total probability of an event B.

Using the Bayes formula, you can more accurately recalculate the probability, based on previously known information and new observations.

To form the competence of the students, it is necessary to consider the following: mobility, flexibility and critical thinking factors. Finding the right information and explaining the information creates mobility of knowledge. Flexible method organization of information usage in different situations. Transforming information, finding evidence, and making decisions form critical thinking[24].

4 Architecture of the intellectual environment for improving the competence of the student in the directionof IT basedon the Bayesianapproach

The overall architecture of the Intelligent Environment is shown in Figure 1 below. Our main goal in creating such an environment is to educate IT students about the course and bring them to some competence. We used a bundle to determine competence. We have designed competencies based on three criteria and developed a system of questions on each criterion. We determine the competence of the student through this system of questions. These criteria are closely interconnected.

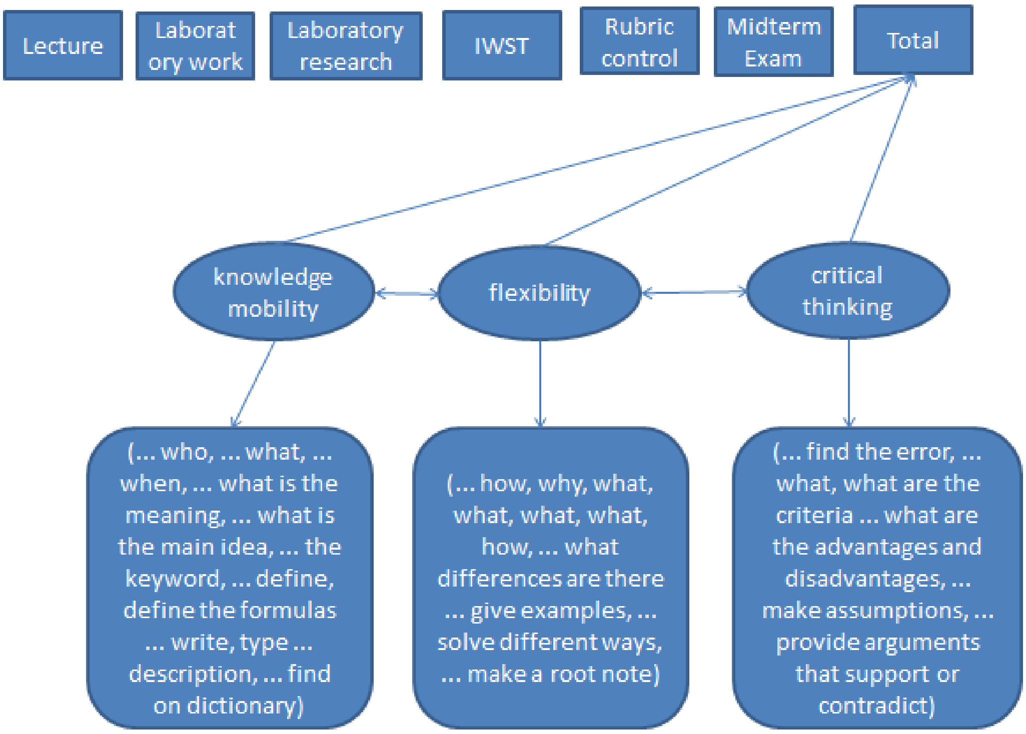

Figure 1 - Intellectual environment architecture

Advantages of the Intellectual Environment:
- It helps to define the competence of students.
- Many visual aids for teachers are offered in English.
- Allows you to study at any convenient location and at any time.
- Efficiently combines learning and new technologies.
- Makes everyone equal opportunities for quality education.

5 Research methods and results

For the solution of the report, we build a network of partners within the framework of the report. For variables and probability links, we will use experts for individual points.

BayesiaLab [25] A very powerful system has been working for about 20 years. Today BayesiaLab'sBayesia is the software market leader for working with Bayes networks. You can work with the Bayesia Engine API (Java Application Library). The disadvantage of this complex is very expensive, but you can download a 30-day free version (you can not save a network).

The accounting net is shown below.

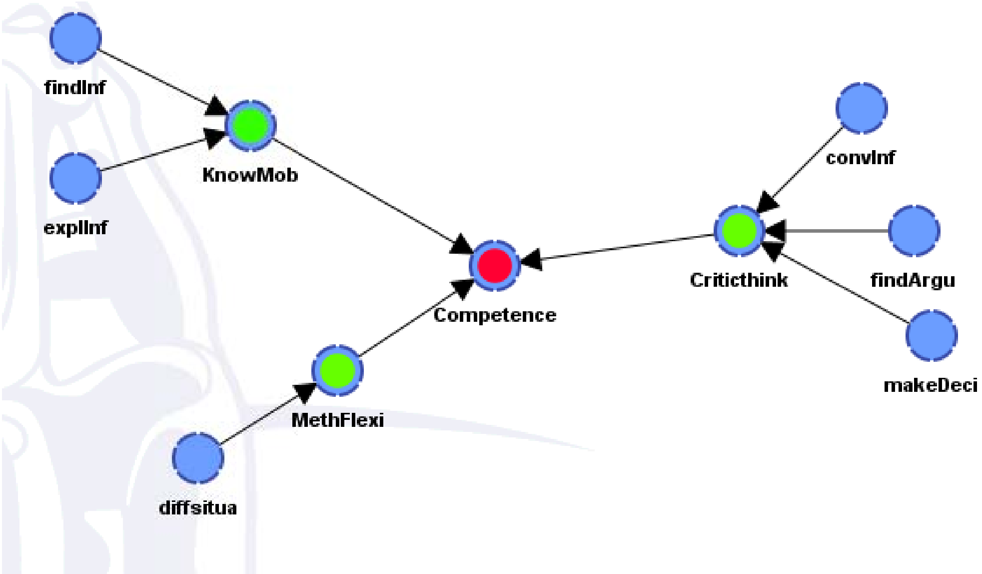

Figure 2 - Bayesian network

Bayesian networks are one type of probabilistic graphical models. A graphical probabilistic model is a probabilistic model, in which the graphs show the dependencies between random variables [26].

The Bayesian Faith Line is a probabilistic-graphic model (that is, not directed to cycles without directed cycles), which is a cyclically oriented graph, the vertices of which are random elements, and the boundary between the edges is the conditional dependence. Each random element is characterized by the probability distribution function, random elements of binary, can be multidimensional and continuous [27].

The mathematical apparatus of Bayesian networks was proposed in the mid-1980s by the American scientist J. Pearl. Methods for computing, learning Bayesian trust networks are developed in the works [21,24,28-31].

From a mathematical point of view, the Bayesian network is a model for the representation of probabilistic dependencies, as well as the absence of these dependencies [31].

We define competencies based on three criteria. They include knowledge mobility, flexibility, and critical thinking. These 3 criteria are closely interconnected.

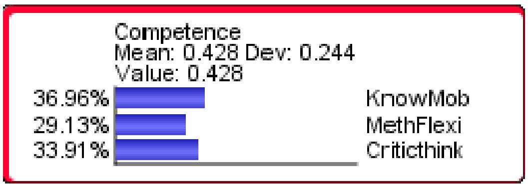

Figure 3 - Determination of competencies by 3 criteria

Let's define the competence of random students to the subjects of information technology. We do not know that this student has the ability to study information technology, and in many cases have the ability to use information and explain information. In this case, high probability - 3%.

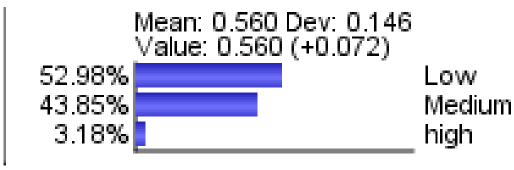

Figure 4 - Determination of competence of random student to discipline

We are aware that the student has the ability to study information technology, to have the ability to access information and explain information in various situations, and to have the ability to transform information, find evidence and make decisions. In this case, we see that high probability - 63%.

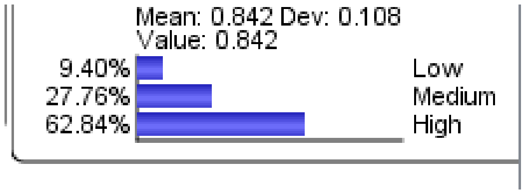

Figure 5 - Definition of competence of the special student for discipline

When determining the competence of the mobility, we pay attention to the ability to find the necessary information and to explain the information.

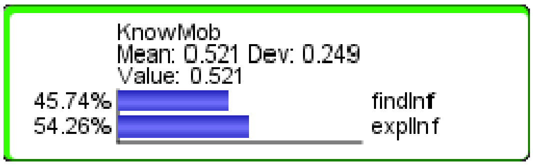

Figure 6 - Definition of mobility competence of knowledge

When considering the competence through flexibility, we consider the ability to use information in different ways.

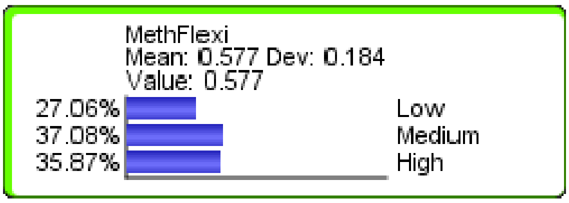

Figure 7 - Determine the competence by using a flexible method

When determining competence by critical thinking, we pay close attention to modifying information, finding arguments, and making decisions.

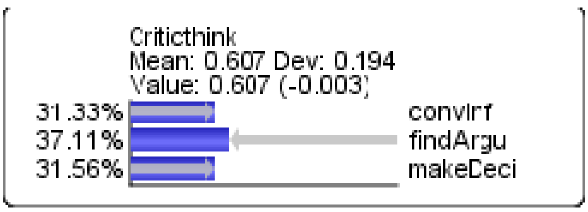

Figure 8 - Determination of Critical Thinking Competence

The following enlarged algorithm of forming the competence of a teacher in the direction of IT has been developed.

Step 1. We define the criteria for the competence of students.

Step 2. Build up the 3 criteria for competence build up.

Step 3. We build a network of 3 by the criteria. We use the BayesiaLab package to build bayes network. Variables and Probability We use experts for individual relationships. (Fig.1)

Step 4. We define individual competencies on each criterion. That is, knowledge mobility, flexibility, critical thinking. (Fig.5-7)

Step 5. Total 3 criteria and their items are interconnected. Under these 3 criteria, we determine the overall competence of IT-trainees. (Fig.2)

6. Discussions

Conducted research and numerous publications on this topic prove the relevance of applying the Bayesian approach in the formation of students' competence.

The competence of the trainee in the intellectual system is based on three main criteria: mobility of knowledge, flexibility of the method and critical thinking boyish zhetiledi. Proceeding from this, one can come to the conclusion that, first, knowledge, not just information, is rapidly changing, dynamic, varied, which needs to be able to be found, separated from unnecessary, translated into the experience of one's own activity. Secondly, the ability to use this knowledge in a particular situation; understanding how to get this knowledge. Thirdly, an adequate assessment of oneself, the world, one's place in the world, specific knowledge, their necessity or uselessness for their activities, as well as their method of obtaining or use. This competence is determined on the basis of one of the methods of the artificial intelligence of the Bayesian approach. The results of this approach contributes to the effective selection of educational resources, choose an individual learning path.

7.Conclusions

Thus, a methodology has been developed for creating an intellectual environment for improving the competence of a student in the field of IT based on the Bayesian approach. As a result of the study: a literature review was conducted on this issue, an architecture of the intellectual environment was created, and an integrated algorithm was developed to form the competence of a teacher in IT.

Acknowledgement

The work was performed under the grant of the Committee of Science of the Ministry of Education and Science of the Republic of Kazakhstan (2018-2020), on the theme "Development and software implementation of an application package for solving applied problems on Bayesian networks.

ӘОЖ 378
МРНТИ 20.01.07

Ө.Ж. Мамырбаев[1,2], Ә.С. Шаяхметова[1,2], П.Б. Сейсенбекова[2]

[1] Ақпараттық және есептеуіш технологиялар институты,Алматы, Қазақстан;
[2]Әл-Фараби атындағы Қазақ ұлттық университеті, Алматы, Қазақстан

БАЙЕС ТӘСІЛІНЕ НЕГІЗДЕЛГЕН АҚПАРАТТЫҚ ТЕХНОЛОГИЯЛАР БАҒЫТЫНДА БІЛІМ АЛУШЫЛАРДЫҢ ҚҰЗЫРЕТТІЛІГІН АРТТЫРУ ҮШІН ЗИЯТКЕРЛІК ОРТАНЫ ҚҰРУ ӘДІСТЕМЕСІ

Аннотация. Жасанды интеллект ғылымның түрлі салаларында әртүрлі мәселелерді шешуде кеңінен қолданылады. Студенттің құзыреттілігін арттыру үшін зияткерлік ортаны құру үшін жасанды интеллект әдістерін пайдалану өзекті. Соңғы уақыттарда жасанды интеллекте ең танымал қолданудың зерттеулері Байес желілік аппаратын пайдалану болып табылады. Студенттің құзыреттілігін арттыру үшін интеллектуалды ортаны құруда Байес тәсілінің келешегі зор. Қазіргі уақытта Байес желілерінің теориясы түрлі қолданбалы мәселелерді шешуде ғылым мен өндірістің әр түрлі салаларында қолданылады. Байес желілерімен жұмыс істеуге арналған бағдарламалық өнімдердің жеткілікті саны бар. Бұл өнімдер коммерциялық және тегін бөлінеді. Байес желісінің математикалық идеяларын жүзеге асыру үшін BayesiaLab қосымшасының бағдарламалық пакеті жақсы қолданылған және жасанды интеллект технологияларына маманданған жоғары сапалы бағдарламалық өнімдердің бірі болып табылады. BayesiaLab пакетінің көмегімен Байес желісінің моделін зерттеу, өңдеу, талдау және анықтауға болады. Бұл мақалада «құзыреттілік» терминіне әртүрлі ғалымдардың анықтамалары берілген және ақпараттық технологиялар

бағытында студенттердің құзыреттілігін қалыптастыруда Байестік желілерді пайдалану мүмкіндіктері зерттелді. Ақпараттық технологиялар саласында студенттердің құзыреттілігін қалыптастыру үшін интеллектуалды орта ортақ алгоритмі және жалпы архитектурасы жасалды. Білім берудегі кәсіби құзыреттілігін арттыру үшін мамандардың бәсекеге қабілеттілігін арттыру, жақсартылған мазмұн, әдіснамасын жетілдіруге және тиісті білім беру ортасын жаңартуға алып келеді. Құзыреттілікті қалыптастыру кезінде бірқатар технологиялар қолданылады: когнитивтік-бағдарланған, қызметке бағытталған, тұлғалық-бағдарланған. Құзыреттілікті қалыптастыруда қолданылатын тәсіл студенттердің білім сапасын модельдеу үшін қолданылады. Құзыреттілік деңгейі таңдалған әдіске байланысты.

Түйін сөздер: Байестік желілер, білім алушылардың құзыреттілігі, білімнің ұтқырлығы, икемділік әдісі, сын тұрғысынан ойлау, BayesiaLab қолданбалы бағдарлама пакеті.

УДК 378
МРНТИ 20.01.07

О.Ж. Мамырбаев[1,2], А.С.Шаяхметова[1,2], П.Б.Сейсенбекова[2]

[1] Институт информационных и вычислительных технологий, Алматы, Қазақстан;
[2]Казахский национальный университет имени аль-Фараби, Алматы, Қазақстан

МЕТОДОЛОГИЯ СОЗДАНИЯ ИНТЕЛЛЕКТУАЛЬНОЙ СРЕДЫ ПОВЫШЕНИЯ КОМПЕТЕНТНОСТИ ОБУЧАЮЩЕГОСЯ ПО НАПРАВЛЕНИЮ IT НА ОСНОВЕ БАЙЕСОВСКОГО ПОДХОДА

Аннотация. Искусственный интеллект широко используется при решении различных проблем в различных областях науки. Актуально применение методов искусственного интеллекта для создания интеллектуальной среды повышения компетентности обучающегося. Последнее время в исследованиях наиболее популярным направлением использования искусственного интеллекта стало применение аппарата байесовских сетей. При создании интеллектуальной среды повышения компетентности обучающегося перспективно применение байесовского подхода. В настоящее время теория байесовских сетей используется в различных областях науки и производства при решении различных прикладных задач. Существует достаточно большое количество программных продуктов для работы с байесовскими сетями. Данные продукты деляться на коммерческие и бесплатные. Для реализации математические идеи байесовской сети хорошо применяется пакет прикладных программ BayesiaLab и является одним из высококачественных программных продуктов, который специализируется на технологиях искусственного интеллекта. С помощью пакета BayesiaLab можно исследовать, редактировать, анализировать и определить модель байесовской сети. В данной статье даны определения различных ученых термину «компетенция» и исследованы возможности использования байесовских сетей при формировании компетенции обучающихся по направлению информационных технологий. Для формирования компетенций обучающихся по направлению информационных технологий разработан обобщенный алгоритм и общая архитектура интеллектуальной среды. Для совершенствования профессиональной компетентности в образовании приводит к повышению конкурентоспособности специалистов, улучшению содержания, методологию и обновлению соответствующей образовательной среды. При формировании компетентности применяются ряд технологий: когнитивно-ориентированная, деятельностно-ориентированная, личностно-ориентированная. Подход используемый при формирований компетенций используется для моделирования качества знаний студента. Уровенькомпетентности зависит от выбранного метода.

Ключевые слова: Байесовские сети, компетентность обучающегося, мобильность знаний, гибкость метода, критичность мышления, пакет прикладных программ BayesiaLab.

Information about authors:

Mamyrbayev O. Zh. - Institute of Information and Computational Technologies, Deputy General Director for Science, PhD Doctor, e-mail: morkenj@mail.ru.

Shayakhmetova A.S. - Institute of Information and Computational Technologies, Senior Researcher, PhD Doctor, e-mail: asemshayakhmetova@mail.ru.

Seisenbekova P.B. - Al-Farabi Kazakh National University, PhD doctoral student, e-mail: ms.perizat@mail.ru.

REFERENCES

[1] Shepel V.M. Management anthropology. Human competence manager. M.
[2] Landsheer V. The concept of "minimal competence" / V. Landsheer // Perspectives. Issues of education. 1988.

[3] Choshanov M.A. Flexible technology of problem-modular learning: a manual / M.A. Choshanov. M .: Public education, 1996. 160 p.

[4] Mamyrbayev O., Turdalyuly M., Mekebayev N., Alimhan K.,Kydyrbekova A., Turdalykyzy T. Automatic Recognition of Kazakh Speech Using Deep Neural Networks // Lecture Notes in Computer Science,2019. Vol. 11432 LNAI, 2019, P. 465-474.

[5] 5.MamyrbayevO.Zh.,Kunanbayeva M.M.,Sadybekov K.S.,Kalyzhanova A.U. One of the methods of segmentation of speech signal on syllables // Bulletin of the National Academy of Sciences of the Republic of Kazakhstan, 2015. Vol. 2. P. 286-290.

[6] V.M. Trembach. Intellectual information system of formation of competencies for the implementation of the model of continuous education. Open Education, 2010 (4), C. 79-91.

[7] Kalimoldayev M. N., Pak I. T., Baipakbayeva S. T., Mun G. A., Shaltykova D. B., Suleimenov I. E. Methodological basis for the development strategy of artificial intelligence systems in the Republic of Kazakhstan in the message of the president of the Republic of Kazakhstan dated October // N E W S OF THE NATIONAL ACADEMY OF SCIENCES OF THE REPUBLIC OF KAZAKHSTAN SERIES OF GEOLOGY AND TECHNICAL SCIENCES, 2018. Vol. 6(432). P. 47–54. https://doi.org/10.32014/2018.2518-170X.34

[8] Bul' E.E. Obzor modelej studenta dlja komp'juternyh system obuchenija // Obrazovatel'nye tehnologii i obshhestvo (Educational Technology & Society). 2003. Tom. 6, № 4. S. 245-250. Rezhimdostupa: http://ifets.ieee.org/russian/depository/v6_i4/html/G.html (data obrashhenija 01.07.2014)

[9] Brusilovskij P.L. Intellektual'nye obuchajushhie sistemy // Informatika. Informacionnye tehnologii. Sredstvaisistemy. 1990. №2. S.3-22.

[10] Petrushin V.A. Jekspertno-obuchajushhiesistemy. K.: Naukovadumka, 1992. 196 s.

[11] Bidjuk P.I., Terent'ev A.N. Postroenie i metody obuchenija bajesovskih setej // Tavrijs'kij visnik informatiki i matematiki, №2/2004. s. 139-154.

[12] Neapolitan RE. Learning Bayesian Networks. NJ: Prentice Hall, 2004. 704 p.

[13] Liu, C. A simulation-based experience in learning structures of Bayesian networks to represent how students learn composite concepts / C. Liu // International Journal of Artificial Intelligence in Education. 2008. V. 8, N. 3. P. 237–285.

[14] Litvinenko A.,MamyrbayevO., Litvinenko N., Shayakhmetova A.,Kotyra A.Application of bayesian networks for estimation of individual psychological characteristics // PRZEGLAD ELEKTROTECHNICZNY, 2019. Vol. 5 (95). P. 92-97.

[15] Villano, M. (1992) Probabilistic student models: Bayesian belief networks and knowledge space theory. In C.Frasson, C. Gauthier, & G. McCalla (Eds.) Intelligent Tutoring Systems, Proceeding of the Second International Conference, ITS'92, Montreal, Canada (pp. 491-498). Berlin: Springer-Verlag.

[16] Mayo, M., &Mitrovic, A. (2001). Optimising ITS behavior with Bayesian networks and decision theory. International Journal of Artificial Intelligence in Education, 12, 124–153.

[17] Desmarais, M. C., & Baker, R. S. (2012). A review of recent advances in learner and skill modeling in intelligent learning environments. User Modeling and User-Adapted Interaction, 22(1–2), 9–38.

[18] Millán E. A Bayesian Diagnostic Algorithm for Student Modeling and its Evaluation / E. Millán, J. L. Pérez-de-la-Cruz // User Modeling and User-Adapted Interaction. 2002. N. 12. P. 281–330.

[19] VanLehn, K. Student modeling from conventional test data: a Bayesian approach without priors / K. VanLehn, Z. Niu, S. Siler, A. Gertner // Proc. of 4th Int. Conf. ITS'96. 1996. P. 29–47.

[20] Reye, J. Student Modelling based on Belief Networks / J. Reye // International Journal of Artificial Intelligence in Education. 2004. N. 14. P. 1–33.

[21] Jensen F. V. Bayesian Networks and Decision Graphs. NY: Springer-Verlag, 2001. 268 p.

[22] VanLehn K., Niu Z., Siler S., Gertner A. Student modeling from conventional test data: a Bayesian approach without priors // Intelligent Tutoring Systems, Proceedings of 4th International Conference ITS'96. 1996. pp. 29–47.

[23] Neapolitan R.E. Learning Bayesian Networks. NJ: Prentice Hall, 2004. 704 p.

[24] Sologub, G. B. Development of mathematical methods and complex software simulation of knowledge based on semantic models: Dis. Cand. f.-m. Sciences: 05.13.18, 05.13.11 / G.B.Sologub. Moscow, 2013. 134 p.

[25] Koller D., Friedman N. Probabilistic Graphical Models. Massachusetts: MIT Press, 2009. 1208 p.

[26] Khlopotov M.V. The use of the Bayesian network in building models of students to assess the level of formation of competencies. Internet journal "SCIENCE" http://naukovedenie.ru Issue 5 (24), 2014.

[27] Pearl J. Probabilistic Reasoning in Expert Systems: Networks of Plausible Inference. San Francisco: Morgan Kaufmann, 1988. 552 p.

[28] Heckerman D. A tutorial on learning with Bayesian networks / M.I. Jordan (ed.). Dordrecht: Kluwer Academic, 1998. 57 p.

[29] Tulupyev, AL, Nikolenko, S.I., Sirotkin, AV Bayesian trust networks: logical-probabilistic inference in acyclic directed graphs. - SPb .: Publishing house of S.-Petersburg. University, 2009. 400 p.

[30] Darwiche A. Modeling and Reasoning with Bayesian Networks. Cambridge University Press, 2009. 526 p.

[31] Bidyuk P.I., Terentyev A.N. Construction and teaching methods of Bayesian networks // Tavreysky Informatics i Mathematics, №2. 2004. p. 139-154.

N E W S
OF THE NATIONAL ACADEMY OF SCIENCES OF THE REPUBLIC OF KAZAKHSTAN
PHYSICO-MATHEMATICAL SERIES
ISSN 1991-346X **https://doi.org/10.32014/2019.2518-1726.44**
Volume 4, Number 326 (2019), 59 – 67

M. Kalimoldayev, M. Akhmetzhanov, M. Kunelbayev

Institute Information and Computational Technologies CS MES RK, Almaty, Republic of Kazakhstan
maks714@mail.ru, murat7508@yandex.ru

DETERMINATION OF THE POWER INTERACTION OF THE HYDRO TURBINE GRID WITH A FLUID FLOW FOR A DOUBLE-ROTOR MICRO HYDRO POWER PLANT

Abstract. The problem in given article consists in definition of power interaction of a lattice of the turbine with a liquid stream. The moment on the driving wheel is equal to change of the moment of quantity of movement of a proceeding liquid. To find the moment and capacity on a driving wheel shaft, it is necessary to define kinematic parameters of the stream which is flowing round a lattice of a wheel. At calculation new the blade systems the return problem of the theory of lattices is used. The return problem consists in definition of the form of a profile under the set law of distribution of speed (pressure) on a profile contour, and as in definition of power interaction of a stream and a lattice profile. For durability calculations of water-wheels it is necessary to know the hydrodynamic forces operating on the blade of the driving wheel. Analysis and study of the peculiarities of electromagnetic calculation disk generator in static mode does not allow to evaluate the work make full disk generator. This regard, studies have been conducted dynamic mode disk generator. Studies and calculations were carried out by computer simulation using the program «Ansoft Maxwell».Us essentially new design of micro hydroelectric power station with double-rotor the hydro generator is offered.
Keywords: water, method, calculation, spiral chamber, micro hydro power station.

1. Introduction

Renewable energy resources are gaining global attention due to depleting fossil fuels and harmful environmental effects associated with their usage. Hydro, wind, solar, biomass and geothermal energies form the bulk of renewable energy sources; among which hydro power offers one of the most exciting and sustainable proposition. Traditionally, hydropower has accounted for the bulk of the renewable energy production in the United States. The primary energy use in the U.S. in 2011 was 28,516 TWh/yr of which only 9% came from renewable [1]. Traditional hydroelectric or micro-hydro facilities contributed 35% of total renewable energy production [1]. However, growth of conventional hydropower plants are limited due to limitations on the number of available natural sites, large capital (initial) investment, pay-back time and environmental concerns. In lieu of this, marine and hydrokinetic (MHK) systems offer many advantages: these are portable systems with small initial cost, no large infrastructure and easy and quick deployment [2-5]. A study conducted by Electric Power Research Institute (EPRI) for US rivers estimated hydrokinetic power potential of 12,500 MW [6, 7]. This study was based on conservative assumption of turbine array deployment for rivers with discharge rates greater than 113 m3/s and flow velocities greater than 1.3 m/s. A study conducted by EPRI evaluated many, but not all tidal energy sites in U.S. and estimated 115 TWh/yr of tidal energy[6, 7]. These estimates show potential of MHK systems.

Hydrokinetic turbines (HKT) are a class of low head energy conversion devices which convert kinetic energy of flowing water into mechanical work [8, 9]. Tidal and marine current turbines also fall into similar category of (lift-drag) devices which utilize hydrodynamic blade shapes to derive power from flowing fluid. Depending on the flow direction of water relative to the axis of rotation, HKT can be classified as horizontal axis and vertical axis turbines. The performance of these turbines is governed by the three non-dimensional parameters defined below: (a) tip-speed ratio (TSR) that is defined as the ratio of blade tip speed to fluid speed; (b) solidity (σ) that is defined as the ratio of blade chord length times the number of blades to turbine circumference; and, (c) Reynolds number.

Over the last decade, the hydrodynamics of HKT has been investigated using computational fluid dynamics (CFD) [10-12] and laboratory scale experiments [13-15]. Blade-element-momentum (BEM) analysis which forms the backbone of wind turbine rotor design can be used for HKT design [16]. Apart from BEM, a series of inexpensive CFD tools based on the solution of the Euler or Navier-Stokes equations like panel method and vortex lattice method can be used for aerodynamic/hydrodynamic analysis of these devices [17]. In addition, computationally expensive techniques that involve solving Reynolds-averaged-Navier-Stokes equations (RANS) with turbulence models has been successfully used for hydrodynamic analysis of HKT [10, 12, 18]. Consul *et al* .[10] performed a two dimensional CFD analysis to understand the influence of number of blades on performance of cross flow turbines and found improved performance with higher number of blades. Higher solidity turbine performed better at low tip speed ratios and low angles of attack [10]. Duquette and co-workers [12] performed experiments and 2-D numerical analysis to study the effect of number of blades and solidity on the performance of horizontal axis wind turbine. The numerical analysis was performed using BEM and lifting line based wake theory [12]. The knowledge base derived from aerodynamic/hydrodynamic analysis of wind/hydrokinetic turbines can be used for further design optimization study. Most of the optimization studies for wind turbines [19- 21] were focused on maximizing coefficient of performance and annual energy production (AEP). Selig and Coverstone-Carroll [19] used a genetic algorithm (GA) for optimizing AEP and cost of energy of low-lift airfoils for stall regulated wind turbines (wind turbines that have their blades designed so that when fluid speeds are high, the rotational speed or the torque, and thus the power production, decreases with increasing fluid speed above a certain value that is usually not the same as the rated speed). Belesis[20] presented GA for constrained optimization of stall regulated wind turbine and found it to be superior to classical optimization methods. Researches were conducted in the given work and optimization cone a sucking away pipe. Transformation of kinetic energy to energy of pressure to a sucking away pipe occurs to losses of some part of energy. On length of a pipe they can be divided into losses on a friction and expansion. The more diffuser pipes, the there is less than loss of kinetic energy, however with increase diffuser increase as hydraulic losses in tap. Losses in a sucking away pipe reduce effect of restoration of energy. Calculations show that losses on a friction make insignificant size, and the cores are losses on the expansion, increasing with corner increase cone, and losses on an exit which size decreases with corner increase cone as the area of target section thus increases [21].

This paper explores the rotor core and pole double-rotor hydro generator for micro hydropower plants. To assemble the rotor core double-rotor hydro generator used forged multifaceted steel sheets thickness of 1-2 mm without insulation coating, where the number of faces of the core will match to the number of poles double-rotor hydro generator. Investigated the creation of EMF double-rotor hydro generator in one conductor. When calculating, EMF double-rotor hydro generator. Guides phase-shifted by the same angle a, and describe a circle. The induced EMF in them is equal in value but opposite in direction. Therefore, the EMF coiled twice EMF one conductor. Hydro generator designed with different number of poles, sometimes quite large. We studied double-rotor hydro pole is clearly synchronous generator with two poles. All along the bore north and south poles of the stator pole 2p double-rotor hydro generator has a p-wave magnetic field. Therefore, we can distinguish two pole divisions as one period of the magnetic field and treat them as some elementary machine -one period. Circle real model double-rotor hydro generator attributed the electrical angle of 360 (electrical degrees) or 2p.Each geometric degrees double-rotor hydro generator corresponds to p electrical degrees elementary machine. For double-rotor hydro generator which is a low-power not exceeding 1,000 V and a capacity of less than 100 kW is used in designing a single-layer winding, which is to operate in a safe and cost-effective [22].

2. Experimental investigation

2.1. Apparatus

The major factor defining structure of a stream in the driving wheel, power interaction between the moving blade and a liquid which creates the driving wheel moment is.

If we will consider flows of a separate profile the infinite established stream on infinity from a profile not indignant stream which is characterized in the constant speed V_{∞} drawing 1 is had. As approaching a profile its influence on a current all becomes stronger that is shown in a curvature of lines of a current and change of distances between them. Over a streamline profile of a line of a current are condensed, and under it to be rarefied. As the expense between two lines of a current is constant, over a profile of speed increase in comparison with V $_{\infty,}$ and under a profile decrease. According to the equation of Bernoulli at the expense of change of speed of a current pressure over a profile should go down, and under a profile to rise. It creates power influence of a stream on a profile.

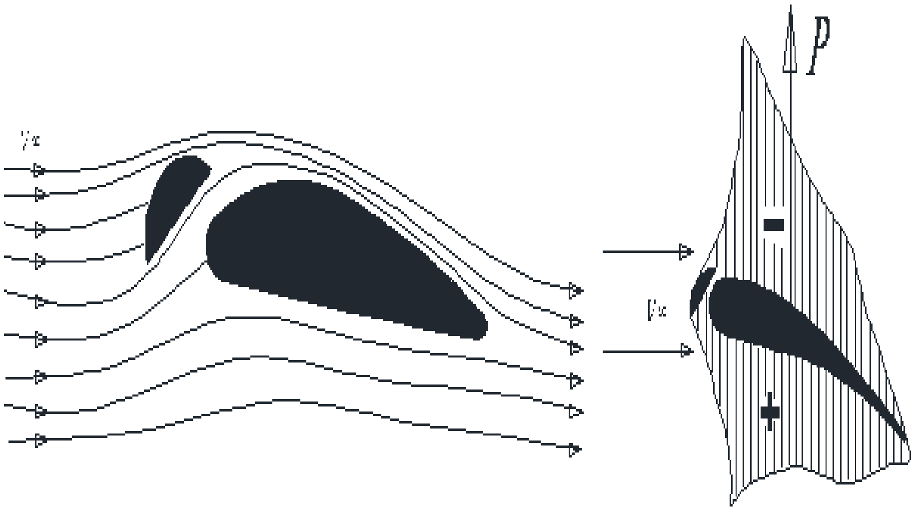

Figure 1 - A profile Flow

The driving wheel has a number of identical blades in regular intervals located on a circle under the form, limited to concentric surfaces of rotation or planes. A problem of the hydrodynamic theory of lattices is current definition in a rotating lattice of any form.

The problem decision in a general view for a lattice of any form difficultly, therefore we will present a current in the schematized and simplified kind fig.2.

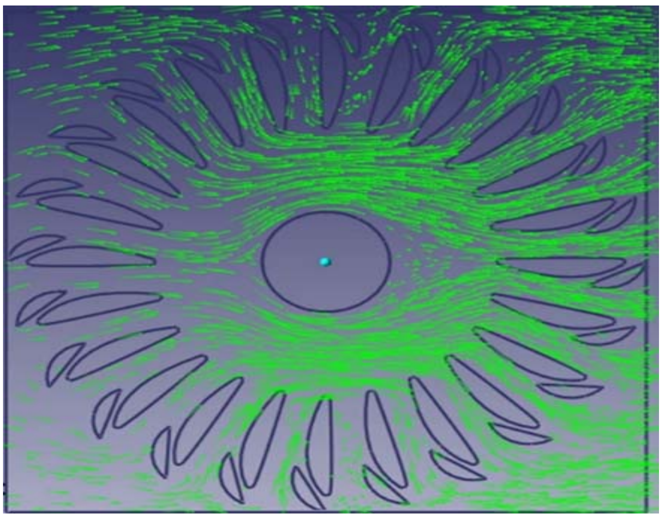

Figure 2 - A driving wheel General view

For the water-wheel of a surface of a current represent planes, perpendicular axes of rotation, and a current on different surfaces the identical. On various flat surfaces of a current there is a flow of identical lattices under the form. The difficult spatial current is approximately led to a flat current. For the decision of a problem of a flow of such kind of spatial lattices it is necessary to find the decision of a flat problem. The section of a lattice a plane, a perpendicular axis of the turbine, gives a flat circular lattice.

The problem consists in definition of power interaction of a lattice of the turbine with a liquid stream. The moment on the driving wheel is equal to change of the moment of quantity of movement of a proceeding liquid. To find the moment and capacity on a driving wheel shaft, it is necessary to define kinematic parameters of the stream which is flowing round a lattice of a wheel. At calculation new лопастных systems the return problem of the theory of lattices is used. The return problem consists in definition of the form of a profile under the set law of distribution of speed (pressure) on a profile contour, and as in definition of power interaction of a stream and a lattice profile. For прочностных calculations of water-wheels it is necessary to know the hydrodynamic forces operating on the blade of the driving wheel.

In a general view for a viscous liquid it is necessary to search for the decision of problems from the equation of Nave - Stokes of movement of a viscous incompressible liquid

$$\frac{\overrightarrow{dv}}{dt} = \vec{F} - \frac{1}{\rho} grad\ p + v\nabla^2\vec{\vartheta} \tag{1}$$

Where $\frac{\overrightarrow{dv}}{dt}$ - full acceleration of a particle of a liquid; $\vec{F}$ - acceleration from mass forces; $-\frac{1}{\rho} grad\ p$ - acceleration from pressure forces; $v\nabla^2\vec{\vartheta}$- acceleration from forces of viscosity.

For a flat problem in projections on axes of co-ordinates (1) will register in a kind

$$\left.\begin{aligned} \frac{dv_x}{dt} &= F_x - \frac{1}{\rho}\frac{\partial\rho}{\partial x} + v\left(\frac{\partial^2\vartheta_x}{\partial x^2} + \frac{\partial^2\vartheta_x}{\partial y^2}\right) \\ \frac{dv_y}{dt} &= F_y - \frac{1}{\rho}\frac{\partial\rho}{\partial y} + v\left(\frac{\partial^2\vartheta_y}{\partial y^2} + \frac{\partial^2\vartheta_y}{\partial x^2}\right) \end{aligned}\right\} \tag{2}$$

Euler's equation of movement of an ideal incompressible liquid

$$\frac{\overrightarrow{dv}}{dt} = \vec{F} - \frac{1}{\rho} grad\ p \tag{3}$$

Differs from the equation of Naveir - Stocks absence of the third member in the right part, caused by viscosity presence. Use of the equation of Euler it is possible only when the member including acceleration from forces of viscosity, is small in comparison with other members of the equation. It is possible if a liquid a little viscous, having small factor of kinematic viscosity and size $\frac{\partial^2\vartheta_x}{\partial x^2} \cdot \frac{\partial^2\vartheta_x}{\partial y^2}$ etc. in (2) were insignificant.

At a flow of a body a liquid on a surface a tangent speed is equal to zero, i.e. a liquid, sticks to a surface. At removal from a body speed rather quickly increases within an interface. Outside of an interface change of speed from a point to a point the insignificant. Therefore, outside of an interface it is possible to neglect influence of viscosity and to consider that liquid movement submits to the equation (3) received for an ideal liquid.

Us essentially new design of micro hydroelectric power station with double-rotor the hydro generator is offered. The principle of work of micro hydroelectric power station with double-rotor the hydro generator essentially does not differ from микро HYDROELECTRIC POWER STATION, only in one hydraulic stream two driving wheels which are located vertically on work one axis one after another and rotating, thus every which way rather to each other fig. 3.

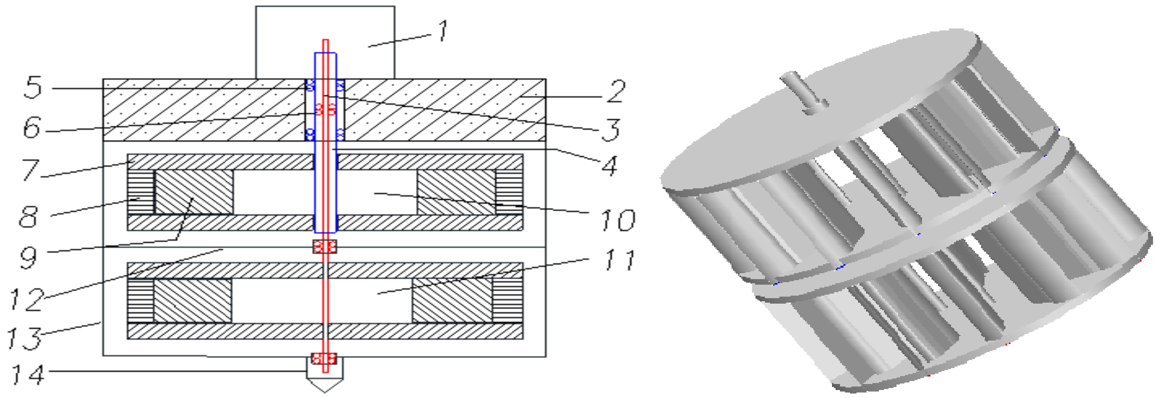

Figure 3 -The Circuit diagrammed double-rotor micro hydroelectric power station
and model double-rotor turbines

Installation as follows works. Installation consists of two independent vertical driving wheels 10 and 11, located one over another. Each driving wheel has the shaft of rotation 3 and 4. On external a floor to a shaft 4 with the help radials - the basic bearing 5 the tank - a float 2 fastens. It is not placed double-rotor the generator 1. In the middle of a hollow external shaft 4 it is established radials - the basic bearing 6 on which internal ring takes place an internal integral shaft 3 bottom driving wheels. Each driving wheel consists from: the top and bottom rim 7, blades 9 and before a wing 8. Two turbines are divided among themselves by a dividing plane 12 and protected by a metal grid 13. At installation immersing on water installation work is carried out as follows: the water stream arrives on turbines and they start to rotate every which way at the expense of various installations of blades and before a wing. The bottom driving wheel it is connected to a rotor of the generator by means of an internal shaft and rotates clockwise. The top driving wheel it is connected with stator the generator by means of an external shaft and rotates counter-clockwise. Thus rotation of a rotor and stator is carried out rather each other in the opposite sides that provides increase in frequency of crossing with a magnetic field of an electric winding of the hydro generator.

Such technical decision allows to avoid presence of the animator for increase in frequency of rotation of a rotor as in the classical generator. Moreover there is a possibility to simplify a design such double-rotor the hydro generator and to lower it mass dimensions the sizes.

The blade looks like an asymmetrical aviation wing with предкрылком which back form has the roundish form. The profile before a wing has the segment form. At a flow of a firm body the stream is exposed to deformation that leads to change of speed, pressure, temperatures and density in stream streams. In drawing 4 the settlement model of interaction of a water stream with the turbine blade is resulted. P - full hydrodynamic force, a resultant of all pressure forces and viscosity of a water stream; Y - hydrodynamic force is a projection of full hydrodynamic force to a perpendicular to a vector of speed of a running water stream; Q - front resistance - a projection of full hydrodynamic force to a vector of speed of a running water stream; P', Y', Q', similar hydrodynamic forces that operate on fixed предкрылки. Apparently from settlement model, about a surface of a streamline body the area of variable speeds and pressure is created. Presence of various pressure on size at a surface of a firm body leads to occurrence of hydrodynamic forces (Y, P, Q) and the moments. Distribution of these forces depends on character of a flow of a body, its position in a stream and a body configuration. On the top surface of a body, in a place of the greatest поджатия streams, according to the law of indissolubility of streams will observe local increase in speed of a stream (V) and, hence, pressure reduction. On the bottom surface stream deformation will be less and, hence, less change of speed and pressure.

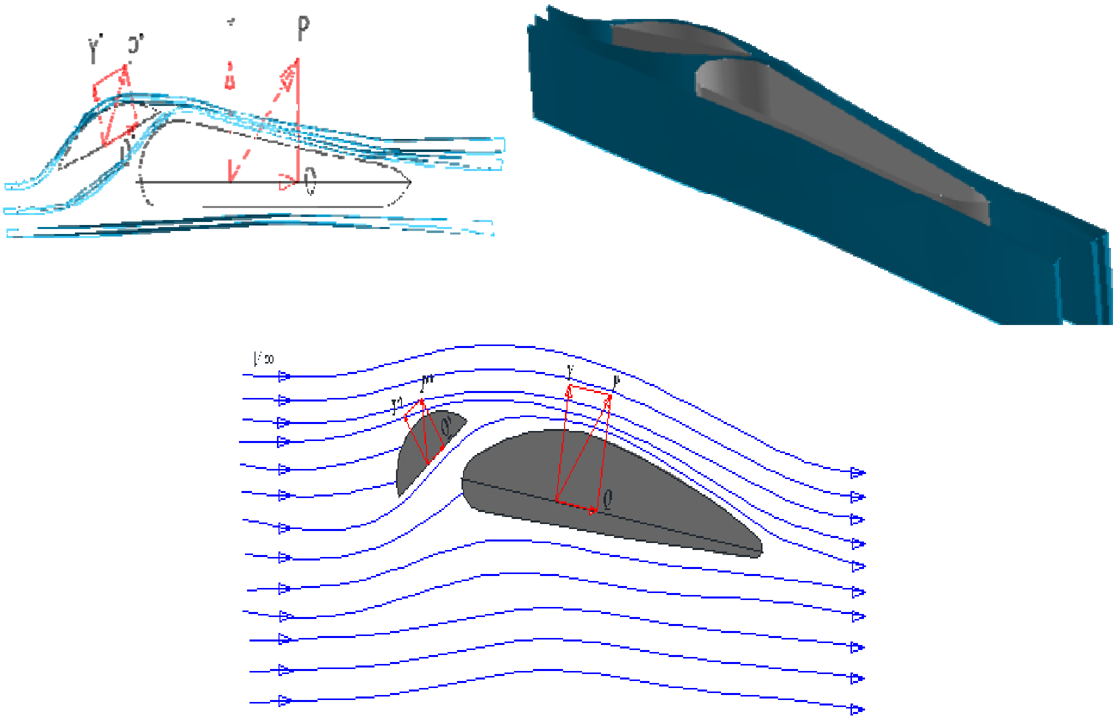

Figure 4 - The Hydrodynamic forces operating on the blade with предкрылком

Knowing a spectrum of a flow of a body, it is possible to count up size of pressure for its each point and thus to judge sizes and character of action of hydrodynamic forces. As on various points of a surface of a streamline body pressure forces different in size operate, their resultant will be distinct from zero. This distinction of pressure in different points of a surface of the moving blade is a major factor causing occurrence of hydro dynamic forces.

2.Results

The most important characteristic is the synchronous hydro generator rotor speed, which allows you to get the necessary speed standard values. As can be seen from the formula 1, an increase in hydro-generator rotor speed n reduces the number of pole pairs p.

$$p=60\cdot f/n \qquad (8)$$

To increase the hydro-generator rotor speed must increase flow or pressure hydraulic flow in the supply of the micro hydro generator. However, increasing the hydraulic parameters of micro hydro generator is not always possible and expedient.

In the case of hydro-generator, as seen from (1), requires fewer pairs of poles than the conventional hydroelectric generators because at a certain value of rotor speed can be obtained by hydro-generator stator speed in the opposite direction with the same values (Fig. 4) . In this case the rotation of the rotor and stator of hydraulic, as already indicated above, is carried out with respect to each other in the opposite side. This leads to an increase in the frequency of crossing the magnetic field of electric generator windings. This principle of doubling the speed will hydro generator.

Produced analysis and study of electromagnetic calculation hydro generator including a selection of the main dimensions of the stator and rotor hydro generator show that the number of winding turns w_0, the inner diameter of the stator core hydro generator D_ (0) is almost two times less than traditional hydro generator W_1, D_1. These results can be achieved only in the case of the hydroelectric principle, which generally leads to a reduction in the geometric and mass-dimensions hydro generator.

$$w_0 = \frac{N_{п1} \cdot p \cdot q_1}{a_1} = 180 \quad (9)$$

$$D_0 = 6 + 0.69 \cdot D_{H1} = 90.18 \text{ mm} \quad (10)$$

$$w_1 = \frac{N_{п1} \cdot p \cdot q_1}{a_1} = 594 \quad (11)$$

$$D_1 = 6 + 0.69 \cdot D_{H1} = 126.75 \text{ mm} \quad (12)$$

where - w_0 - the number of windings hydro generator; p = 1 - number of pole pairs hydro generator; $N_{п1}$ = 60, the number of effective-conductors in the slot hydro generator; q_1= 3, the number of slots hydro generator; a_1 = 1, the number of parallel branches in the stator winding hydro generator; D_0-inner diameter of the stator core hydro generator; D_{H1} = 122 mm -the outer diameter of the stator core hydro generator; w_1 the number of windings of traditional hydro-generator; p = 2, the number of pole pairs of the traditional hydro-generator; $N_{п1}$-99-effective amount of conductors in the groove of traditional hydro-generator; q_1 = 3, the number-hydro generator traditional slots; D_1 - inner diameter of the stator core of traditional hydro-generator; D_{H1} = 175mm,-the outer diameter of the stator core of traditional hydro-generator.

Analysis and study of the peculiarities of electromagnetic calculation disk generator in static mode does not allow to evaluate the work make full disk generator. This regard, studies have been conducted dynamic mode disk generator. Studies and calculations were carried out by computer simulation using the program «Ansoft Maxwell». During the simulation studied the characteristics induced EMF in the stator winding disk generator. On Fig.8.shows a fragment of the moment and the magnetic induction field lines at time t = 0.2sec.

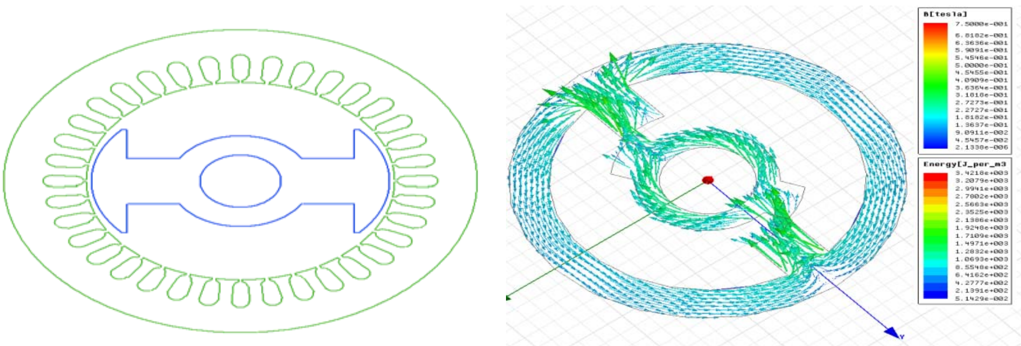

Figure 8 -Unit of magnetic induction and field lines at time t = 0.2sec

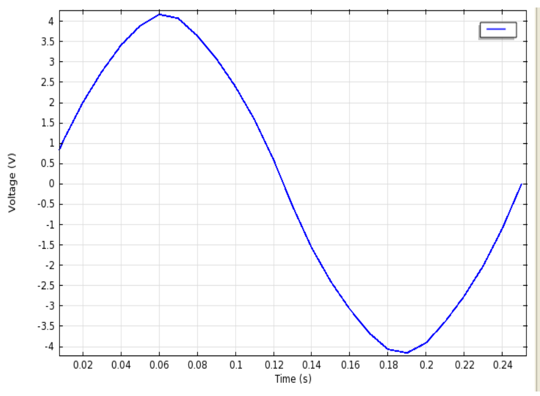

Figure 9 - Voltage waveform disk generator

3.Conclusion

Thus, in the first proposed new scheme for micro hydro disk generator with new technical solution and its structure. The analysis and study of electromagnetic processes by modeling disk generator shows that the creation of hydro-generator for micro hydro gives doubling speed hydro-generator, which allows to reduce the number of pole pairs, the number of windings, as well as to reduce the inner diameter of the stator core. This generally leads to a reduction of geometric and mass-dimensions of hydro-generator and as a result reduce the cost of micro hydro. In addition to these calculations, the computer simulation shows a complete dynamic stability of hydro-generator, which is characterized by forms of voltage and the induced emf (Fig. 9).

As a result of calculations the greatest influence on power indicators of the generator renders: width of a groove and size of an air backlash. From drawing 8 it is visible that at increase in number of grooves at a pole, the factor of dispersion of a pole that is an effective indicator for electric cars decreases. From this it follows that with reduction the width of a groove, increases its number of grooves on magnet of wires stator, the number of grooves thereby increases by one pole.

М. Калимолдаев, М. Ахметжанов, М. Кунелбаев

ЕКІ РОТОРЛЫҚ ШАҒЫН ГИДРОЭЛЕКТРОСТАНЦИЯ ҮШІН СҰЙЫҚТЫҚ АҒЫНЫМЕН ГИДРО ТУРБИНАЛЫ ТОРДЫҢ ЭНЕРГЕТИКАЛЫҚ ӨЗАРА ӘРЕКЕТТЕСУІН АНЫҚТАУ

Аннотация. Берілген мақалада сұйықтық ағынымен турбиналық тордың энергетикалық өзара әрекет-тесуін анықтау табылады. Қозғалтқыш дөңгелегіндегі сәтте жүретін сұйықтықтың қозғалыс санының өзгеруіне тең. Қозғалтқыш дөңгелегі білігінің сәті мен қуатын табу үшін дөңгелек тордың айналасында ағып жатқан ағынның кинематикалық параметрлерін анықтау қажет. Жаңа жүзгіш жүйелерді есептеу кезінде торлар теориясының қайтару мәселесі қолданылады. Қайтару мәселесі бейінді контурға жылдамдықты (қысым) бөлу заңымен және ағынның және торлы профильдің өзара әрекеттесуін анықтау сияқты профиль-дің формасын анықтаудан тұрады. Су дөңгелектерінің беріктігін есептеу үшін жетекші дөңгелек жүзінде жұмыс істейтін гидродинамикалық күштерді білу қажет. Диск генераторының электромагниттік генератор-дың статикалық режимде ерекшеліктерін зерттеу және талдау жұмыстың толық диск генераторын жасауына мүмкіндік бермейді. Осыған байланысты, зерттеулер динамикалық режим диск генераторы жүргізілді. Зерттеулер мен есептер «Ansoft Maxwell» бағдарламасын қолдана отырып компьютерлік модельдеу арқылы жүргізілді. Екі роторлы гидроэлектростанциямен бірге микроэлектростанцияның жаңа дизайны ұсынылған.

Түйін сөздер: су, әдіс, есептеу, спиралды камера, микроэлектростанция.

М. Калимолдаев, М. Ахметжанов, М. Кунелбаев

Институт информационных и вычислительных технологий КН МОН РК

ОПРЕДЕЛЕНИЕ СИЛОВОГО ВЗАИМОДЕЙСТВИЯ ГИДРОТУРБИННОЙ СЕТКИ С ПОТОКОМ ЖИДКОСТИ ДЛЯ ДВУХРОТОРНОЙ МИКРО ГЭС

Аннотация. Задача в данной статье состоит в определении силового взаимодействия решетки турбины с потоком жидкости. Момент на рабочем колесе равен изменению момента количества движения протекающей жидкости. Чтобы найти момент и мощность на валу рабочего колеса, необходимо определить кинематические параметры потока, обтекающего решетку колеса. При расчете новых блейд-систем используется обратная задача теории решеток. Обратная задача заключается в определении формы профиля по заданному закону распределения скорости (давления) по контуру профиля, а так же в определении силового взаимодействия потока и профиля решетки. Для расчета долговечности водяных колес необходимо знать гидродинамические силы, действующие на лопасти рабочего колеса. Анализ и изучение особенностей электромагнитного расчета дискового генератора в статическом режиме не позволяет оценить работу полного дискового генератора. В связи с этим были проведены исследования динамического режима работы дискового генератора. Исследования и расчеты проводились путем компьютерного моделирования с использованием программы «Ansoft Maxwell». Предложена принципиально новая конструкция микро ГЭС с двухроторным гидрогенератором.

Ключевые слова: вода, метод, расчет, спиральная камера, микро ГЭС.

REFERENCE

[1] Annual Energy Review, in Office of Energy Statistics, U.S. Energy Information. Administration Washington, DC 20585 (2011).

[2] Hall, D.G., et al., Water Energy Resources of the United States with Emphasis on Low Head/Low Power Resources, I.N.E. Laboratory and Environmental, Editors. U.S. Department of Energy (2004).

[3] Hall, D.G., et al., Wind and Hydropower Technologies, Feasibility Assessment of the Water Energy Resources of the United States for New Low Power and Small Hydro Classes of Hydroelectric plants, Tech report-DOE-ID-11263, in U.S. Department of Energy, Energy Efficiency and Renewable Energy. Idaho National Laboratory (2006).

[4] Date, A. and A. Akbarzadeh, Design and Cost Analysis of Low Head Simple Reaction Hydro Turbine for Remote Area Power Supply. Renewable Energy (34), 409-415(2009).

[5] Guney, M.S. and K. Kaygusuz, Hydrokinetic Energy Conversion Systems: A Technology Status Review. Renewable and Sustainable Energy Reviews 14(9), 2996-3004 (2010).

[6] Bedard, R., Overview of U.S. Ocean Wave and Current Energy: Resource, Technology, Environmental and Business Issues and Barriers. Electric Power Research Institute (2007)

[7] Bedard, R., Prioritized Research, Development, Deployment and Demonstration Needs: Marine and Other Hydrokinetic Renewable Energy.Electric Power Research Institute (2008).

[8] Khan, M.J., M.T. Iqbal, and J.E. Quaicoe, River Current Energy Conversion Systems: Progress, Prospects and Challenges. Renewable and Sustainable Energy Reviews (12), 2177-2193. (2008).

[9] Schwartz, S.S., Proceedings of the Hydrokinetic and Wave Energy Technologies Technical and Environmental Issues Workshop, ed. I. 10 Prepared by Resolve, Washington, D.C.: Office of Energy Efficiency and Renewable Energy, U.S. Department of Energy (2006).

[10] Consul, C.A., et al. Influence of Solidity on the Performance of a Cross-flow Turbine. In\ Proceedings of the 8th European Wave and Tidal Energy Conference.pp.484-493. (2009).

[11] Duquette, M.M. and J. Swanson, Solidity and Blade Number Effects on a Fixed Pitch, 50W Horizontal Axis Wind Turbine. Wind Engineering 27(4),299-316 (2003).

[12] Duquette, M.M. and K.D. Visser, Numerical Implications of Solidity and Blade Number on Rotor Performance of Horizontal Axis Wind Turbines. Journal of Solar Energy Engineering (125),425-432 (2003).

[13] Myers, L. and A.S. Bahaj, Wake Studies of a 1/30th Scale Horizontal Axis Marine Current Turbine. Ocean Engineering (34), 758- 762 (2007).

[14] Myers, L. and A.S. Bahaj, Power Output Performance Characteristics of a Horizontal Axis Marine Current Turbine. Renewable Energy (31), 197-208 (2006).

[15] Myers, L.E. and A.S. Bahaj, Experimental Analysis of the Flow Field around Horizontal Axis Tidal Turbines by use of Scale Mesh Disk Rotor Simulators. Ocean Engineering 37(2–3), 218-227 (2010).

[16] Glauert, H., Airplane Propellers, in Aerodynamic Theory W.F. Durand, Editor., Berlin:Springer Verlag.(1935)

[17] Sørensen, J.N., Aerodynamic Aspects of Wind Energy Conversion. Annual Review of Fluid Mechanics,. 43(1), 427-448 (2011)

[18] Mukherji, S.S., et al., Numerical Investigation and Evaluation of Optimum Hydrodynamic Performance of a Horizontal Axis Hydrokinetic Turbine. Journal of Renewable and Sustainable Energy (3), 063105-063118 (2011).

[19] Selig, M.S. and V.L. Coverstone-Carroll, Application of a Genetic Algorithm to Wind Turbine Design. Journal of Energy Resources Technology 118(1),22-28 (1996).

[20] Belessis, M.A., D.G. Stamos, and S.G. Voutsinas. Investigation of the Capabilities of a Genetic Optimization Algorithm in Designing Wind Turbine Rotors. in Proc. European Union Wind Energy Conf. and Exhibition. Proceedings of European Union Wind Energy Conference and Exhibition, Goteborg, Sweden,124-7, (1996).

[21] Zhamalov A.Zh, Kunelbayev M. Research and optimization a cone of a sucking away pipe in micro hydroelectric power station. 14th International Multidisciplinary Scientific GeoConference SGEM 2014_Conference Proceedings, Book 3, Vol. 1, pp.603-610 (2014)

[22] Zhamalov A.Zh, Kunelbayev M. Investigation of the rotor core and poles double-rotor hydro generator for micro hydro power plants. Journal of Engineering Science and Technology Review. Volume 11, Issue 2, 2018, Pages 13-18.

[23] Islamgozhayev, T., Kalimoldayev, M., Eleusinov, A., Mazhitov, S., Mamyrbayev, O. First results in the development of a mobile robot with trajectory planning and object recognition capabilities (2016) Open Engineering, 6 (1), pp. 347-352.

[24] Yeshmukhametov, A., Kalimoldayev, M., Mamyrbayev, O., Amirgaliev, Y. Design and kinematics of serial/parallel hybrid robot (2017) 2017 3rd International Conference on Control, Automation and Robotics, ICCAR 2017, статья № 7942679, pp. 162-165.

[25] Kalimoldayev, M.N., Abdildayeva, A.A., Mamyrbayev, O.Z., Akhmetzhanov, M. Information system based on the mathematical model of the EPS. Open Engineering 6(1), pp. 464-469.

N E W S
OF THE NATIONAL ACADEMY OF SCIENCES OF THE REPUBLIC OF KAZAKHSTAN
PHYSICO-MATHEMATICAL SERIES
ISSN 1991-346X **https://doi.org/10.32014/2019.2518-1726.45**
Volume 4, Number 326 (2019), 68 – 75

UDC 519.63; 53.03
IRSTI27.35.21; 27.35.47

A.A. Issakhov, A. Abay, P.T. Omarova, Zh.E. Bekzhigitova

Department of mechanics and mathematics, Al-farabi Kazakh National University, Almaty 050040, Kazakhstan
alibek.issakhov@gmail.com

NUMERICAL MODELING OF CONTAMINATING SUBSTANCES DISTRIBUTION IN RESIDENTIAL AREAS

Abstract. In this study, a numerical simulation of the contaminants distribution in a street canyon and the effect of barriers on this process were carried out. To solve this problem, a Reynolds-averaged Navier-Stokes equation was used. To solve this problem, a turbulent DES model was used, which showed good results for the test problem. To test the mathematical model and the numerical algorithm, the test problem was solved. The obtained numerical results were compared with experimental data and the results of modeling by other authors. After checking the mathematical model and the numerical algorithm, the main problem was described considering the process of pollutant emission between houses using different barrier heights. As a computational area, a model of a street canyon was taken with a ratio of sides that ranged from 0.05 m to 0.2 m. As shown by numerical modeling, the presence of barriers leads to the appearance of an additional vortex in the space between objects, which increase as their height increases. As a result, it can be observed that most of the contaminants are trapped between them. In the course of various studies it was revealed that the presence of barriers along the roads reduces the concentration of harmful substances in the air. So when using a grass barrier height of 0.1 m, the concentration value falls into the section x=0.05 m more than 1.5 times as compared without using barriers. Thus, it can be said that barriers provide good filtration of polluted air, which has a detrimental effect on the environment and human health.

Keywords:air pollution; pollutantsdispersion; concentration fluctuations; high concentration; transport; urban street canyon.

1. INTRODUCTION

Today, statistically, it can be observed the high level of an urbanization that led to the fact that people began to move more often to the large cities with rich infrastructure. All this caused rapid growth of urban population around the world which only amplified with development of science and technology. If in the middle of the last century the rural population were twice more than urban, then in 1990 43% of world's population lived in the cities, and these are 2.3 billion people. By 2015 this number grew to 54% or 4 billion people, and, according to forecasts, by 2030 about 60% of world's population will live in the cities [1]. Big cities involve the high level of pollution to the environment as in the large cities, the main source of air pollution (70-80%) are exhaust gases of cars, with growth of urban population the number of harmful emissions in the atmosphere sharply increases. High air pollution considerably increases incidence of the population. In this regard, the purpose of this work is studying of pollutants distribution in the cities and influence of acoustic barriers on this process.

A large number of researches were conducted to study this problem. For example, in research influence of stability conditions of the atmosphere on pollutants distribution of city canyons [2] which showed that at emergence of an air pollution source it was observed instability of air flow, the involving emergence of a whirlwind between buildings on site of collision of two flows. In other paper [3] was estimated influence of different conditions to temperature stratification on pollutants distribution near the uninsulated multi-storey building. From all numerical models, according to results, the LES model gives more exact forecasts of speed for neutral conditions, than for others. Also influence of billboards on pollutants distribution on streets with a different party'sratio of H/W where W – width of a canyon, H –

height of a canyon was estimated [4]. The case with H/W=2 shows smaller concentration of pollutants, than a case with H/W=1. With a versatile source vertical and two-layer billboards result in larger concentration, than side and single-layer.

In paper [5] was applied k-ε turbulent model to an influence research at presence of the buildings located against wind on pollutants distribution in the multi-storey building. According to results, existence of buildings above on a current has a significant positive effect on ventilation of the building at the oblique winddirection, than at normal impact of wind as they have an insignificant impact. In other similar research [6] authors applied the LES model to studying of the air pollution impact caused by cars on air quality in rooms of buildings with natural ventilation in close proximity to the carriageway. In this work influence of such factors as distance from the carriageway to the building, the wind speed, particle size, arrangement and the size of a window were studied.

In paper [7] dispersion of the pollutants which are thrown out from a source on the bottom of a city canyon caused only by thermal buoyancy force created by the heated outside surfaces of the building and a bottom of a street canyon was investigated. They also considered how the different horizons (skylines) will influence deduction of pollutants in city canyons. In paper [8] was carried out computational modeling of pollutants dispersion in canyons with different ratios of the parties with using DES. This research shows that for street canyons with W/H=1 and W/H=2 the upper corner of a leeward wall will be a zone of the contaminating impurityaccumulation, and in case of W/H=2 such zone can arise in the middle of the lower part of a canyon. In paper [9] was applied LES to define whether it is possible to classify flow models on some identified modes in a three-dimensional canopy of the city building and to define the main features of distribution of pollutants in the different modes of a flow.

Also influence of chemical reactions, chemically active pollutants on structure of a flow and dispersion of pollutants was investigated. In paper [10] was conducted a research to study influence of bimolecular reactions and city configurations on concentration and transfer of pollutants of air at the city microlevel. The LES model in combination with second ordered speed constant model was used for computer simulation. In the paper [11] developed and implemented a computational model of hydrodynamics in combination with the mechanism of carbon communications of IV (CBM-IV) for studying of chemically active pollutants dispersion in urbanareas. With use of this model dispersion of reactive pollutants in a street canyon above with a ratio of the parties of equal 1 m is investigated.

In paper [12] the research for definition influence of computing parameters, such as permission of a grid, step size on time, on characteristics of Navier-Stokes's (RANS) equations with Reynolds-averaged stability model, a method of large vortex method (LES) and model with the deferred vortex simulation (DES) was conducted. According to results, the LES model gives the most exact forecast of pollutants distribution in comparison with results of an experiment in the wind tunnel. In the paper [13] used the system of modeling Quick Urbanand Industrial Complex (QUIC) for a research of influence of buildings presence on dispersion of exhaust gases in the city. In point comparison concentration of vehicles emission was usually higher for a case with buildings because ofthe increased holding time of pollutants in street canyons. However, it is possible to observe the return when concentration in all area was on average lower for a case with buildings.

Influence of trees presence on distribution of pollutants was investigated in paper [14]. Authors developed new structure (framework) of modeling, the connecting LES and Lagrangian stochastic model (LSM) for this purpose. Results of this research showed that trees which are higher than building height, have the most considerable impact on distribution of pollutants and on air flow in general.

There were many experiments on a research of flow structure in city street canyons. In paper [15] made an experiment to investigate interaction between inertially managed flow caused by surrounding winds, and the flow caused by force of buoyancy and uneven walls heating of a canyon.

2. Mathematical model

Computer simulation was carried out with use of the DES model which represents a combination of the LES and RANS models. The LES method is used for modeling of certain areas of a flow, and RANS for an interface. The new parameter determinedas $d = \min(d, C_{des}\Delta)$ where $\Delta = \max(\Delta x, \Delta y, \Delta z)$ is the large scale of a cell of a grid, and C_{des} - empirical values, in our case equal 0.61, guarantees the correct switching of the modes between LES and RANS.

Main equations of the LES model:

$$\frac{\partial \overline{u_I}}{\partial x_i} = 0$$

$$\frac{\partial(\rho \overline{u_I})}{\partial t} + \frac{\partial(\rho \overline{u_i u_J})}{\partial x_j} = -\frac{\partial \overline{p}}{\partial x_j} + \vartheta \frac{\partial^2 \overline{u_I}}{\partial x_i^2} - \frac{\partial \tau_{ij}}{\partial x_j}$$

$$\frac{\partial(\rho \overline{c})}{\partial t} + \frac{\partial(\rho \overline{u_J c})}{\partial x_j} = -\frac{\partial J_j}{\partial x_j}$$

where u_i and u_j components of speed, ρ – pressure, ρ – density, with – concentration of the contaminating impurity and ϑ – viscosity. RANS was used in an interface for increase in accuracy of modeling near a wall. It was used the Realizable $k-\varepsilon$ model which is improvement of the Standard $k-\varepsilon$ model. Kinetic energy of turbulence is defined as:

$$\frac{\partial}{\partial t}(\rho k) + \frac{\partial}{\partial x_j}(\rho k u_j) = \frac{\partial}{\partial x_j}\left[\left(\mu + \frac{\mu_t}{\sigma_k}\right)\frac{\partial k}{\partial x_j}\right] + \mathrm{P}_k + \mathrm{P}_b - \rho\varepsilon - Y_M + S_k$$

$$\frac{\partial}{\partial t}(\rho\varepsilon) + \frac{\partial}{\partial x_j}(\rho a u_j) = \frac{\partial}{\partial x_j}\left[\left(\mu + \frac{\mu_t}{\sigma_\varepsilon}\right)\frac{\partial \varepsilon}{\partial x_j}\right] + \rho C_1 S_\varepsilon - \rho C_2 \frac{\varepsilon^2}{k + \sqrt{\nu\varepsilon}} + C_{1\varepsilon}\frac{\varepsilon}{k} C_{3\varepsilon} P_b + S_\varepsilon$$

where

$$C_1 = \max\left[0.43, \frac{\eta}{\eta + 5}\right], \eta = S\frac{k}{\varepsilon}, S = \sqrt{2S_{ij}S_{ij}}$$

Turbulent viscosity:

$$\mu_t = \rho C_\mu \frac{k^2}{\varepsilon}$$

where

$$C_\mu = \frac{1}{\mathrm{A}_0 + \mathrm{A}_S U * \frac{k}{\varepsilon}}$$

$$U^* = \sqrt{S_{ij}S_{ij} + \widetilde{\Omega}_{ij}\widetilde{\Omega}_{ij}}, \widetilde{\Omega}_{ij} = \Omega_{ij} - 2\varepsilon_{ijk}\omega_k, \Omega_{ij} = \overline{\Omega_{IJ}} - \varepsilon_{ijk}\omega_k$$

Where (Ω_{ij}) the tensor of average speed of rotation observed in the frame of reference rotating with angular speed ω_k. A_0 and A_s is defined as:

$$\mathrm{A}_0 = 4.04, \mathrm{A}_S = \sqrt{6}\cos\phi$$

$$\phi = \frac{1}{3}\cos^{-1}\left(\sqrt{6W}\right), W = \frac{S_{ij}S_{jk}S_{ki}}{\widetilde{S}^3}, \widetilde{S} = \sqrt{S_{ij}S_{ij}}, S_{ij} = \frac{1}{2}\left(\frac{\partial u_j}{\partial x_i} + \frac{\partial u_i}{\partial x_j}\right)$$

Model constants:

$$C_{1\varepsilon} = 1.44, C_2 = 1.9, \sigma_k = 1.0, \sigma_\varepsilon = 1.2$$

3. METHOD OF SOLUTION

It was used a semi-implicit method for the equations connected with pressure, or SIMPLE [16-19] for correction of pressure. The SIMPLE method was developed and presented by Spalding and Patankar [16].

4. DESCRIPTION OF AN EXPERIMENT

It is supposed that the direction of wind is perpendicular to a street canyon. Circulation in a canyon is caused by a flow over a canyon. In the lower part of the camera center the line of a source of pollutants as in figure 1 was placed.

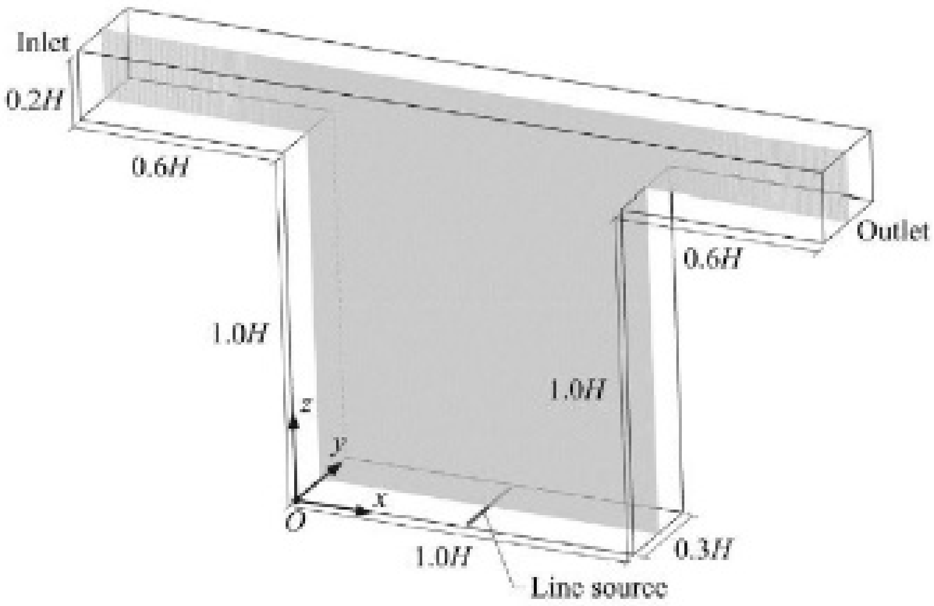

Figure 1– Geometry of a test problem

A mixture of air and ethylene C_2H_4 with a concentration of 1.2% was used as pollutants. The speed of the air flow over the canyon was equal to 1 m/s, the speed from the linear source was equal to 0.1923 m/s.

5. COMPUTATIONAL MODELING

As estimated area the model of a street canyon with the ratio of the parties equal to 1 was used. As in this research it wants to estimate influence of barriers presence on distribution of pollutants, it was needed to add a wall for their modeling. Such walls are located as on the right, and to the left of the line of a source. Modeling was carried out for 3 different heights of barriers: 0.05 m, 0.1 m and 0.2 m.

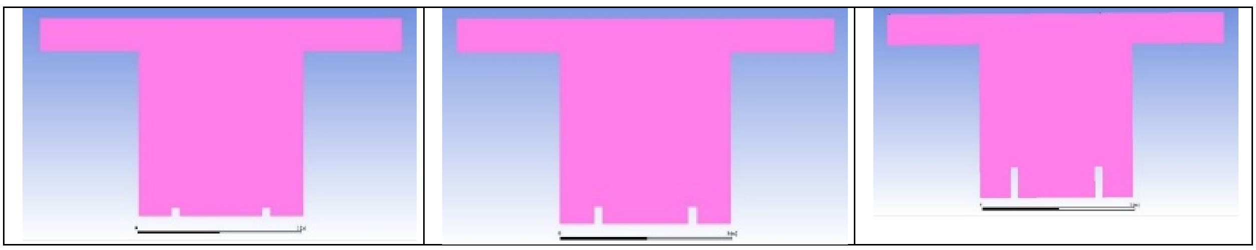

Figure 2 – Task geometry with different type of a barrier with height

Computer simulation was carried out on Ansys 18.0 on a heterogeneous grid with a scale which will increase from a bottom up to top of geometryfield. The space near the line of a source has the smallest slot pitch equal to 1 m, and the space over a canyon has slot pitch of 5 m. Thus, grids for these three geometries have 3706717, 3921432 and 4357700 elements for height of a barrier of 0.05 m, 0.1 m and 0.2 m respectively, as in figure 2.

6. RESULTS AND DISCUSSION

In figure 3 mean values of velocity components on for all the time of calculation is represented.

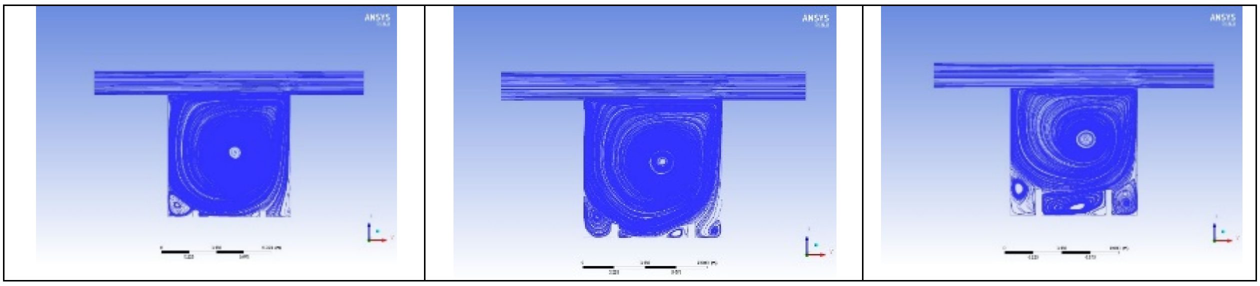

Figure 3 – Mean value of components of speed

In figure 4 lines of current for different heights of barriers are represented. It is possible to notice how in process of increase in height of barriers new whirlwinds appear and amplify. Thus for h=0.2 m flow direction near a source of the contaminating impurity changes on opposite.

In figure 5 distribution of concentration of the contaminating impurity in a street canyon where it is visible that with a barriers height of 0.2 meters concentration of pollutant between barriers considerably increases in space is represented.

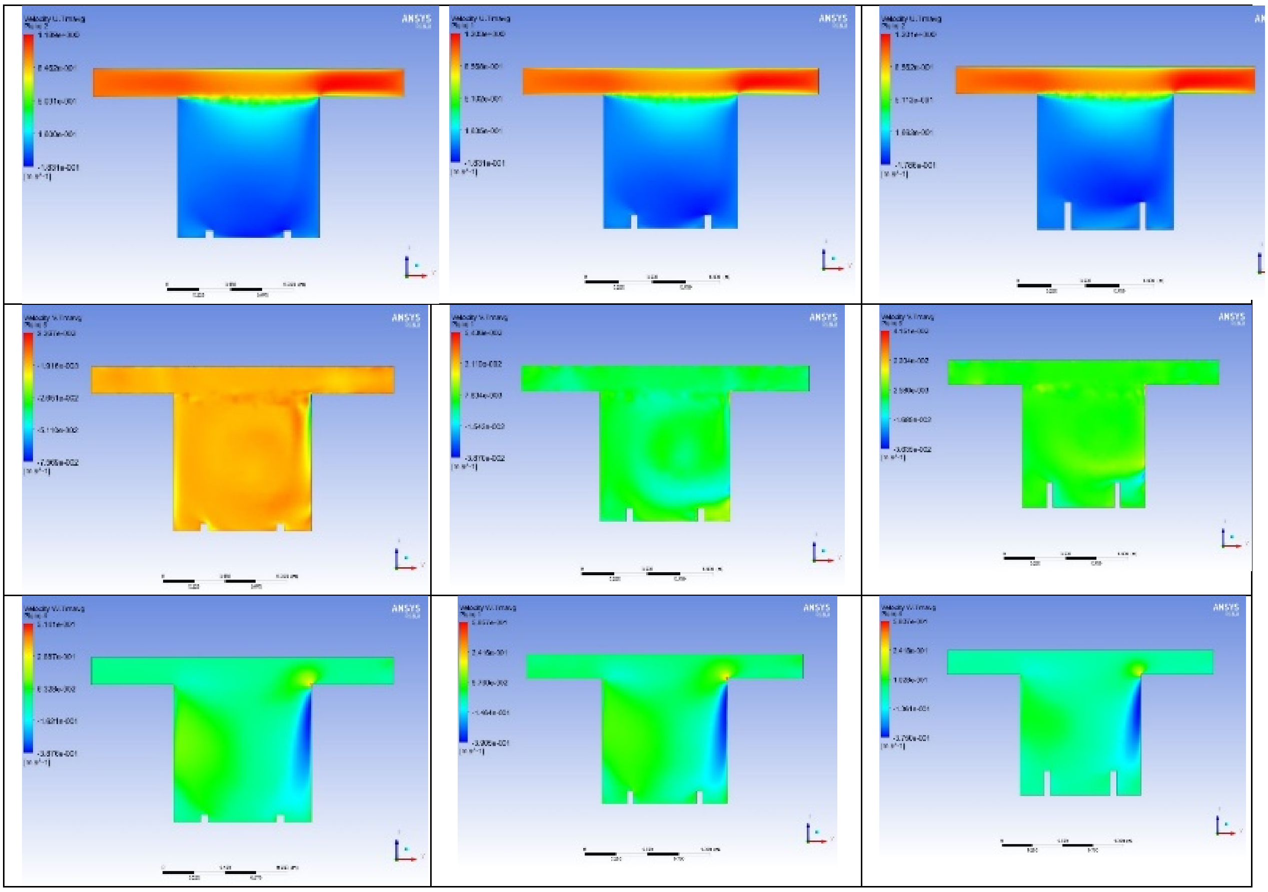

Figure 4 – Lines of current for different heights of barriers

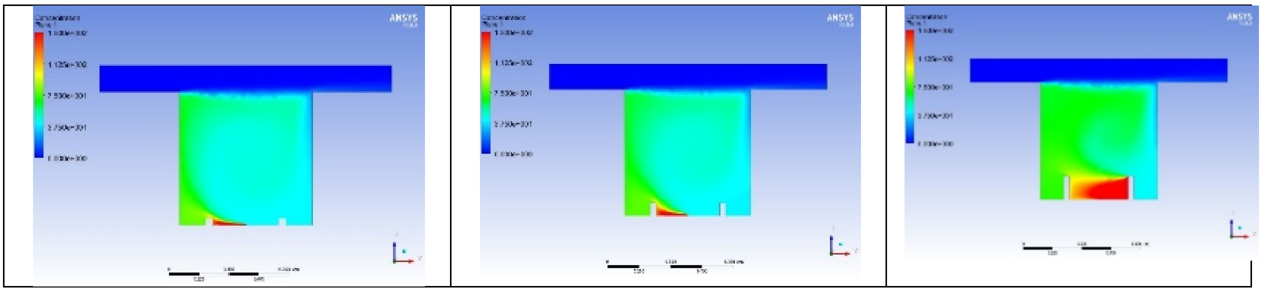

Figure 5 – Distribution of concentration of the contaminating impurity

In figure 6 it is shown a velocity profile. In figure 7 the concentration profile is represented. Apparently, from drawings barriers reduce concentration of the contaminating impurity approximately twice at X=0.05 m, and leads to insignificant increase in concentration at X=0.95 m. At the same time whenbarrier height of 0.2 m the most part of pollutant remains in space between barriers and in general reduces concentration near houses.

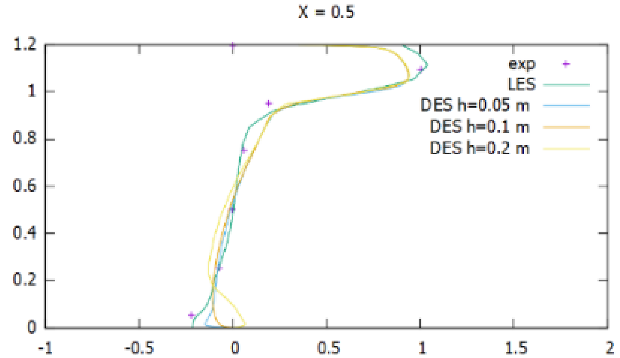

Figure 6 – Speed profile

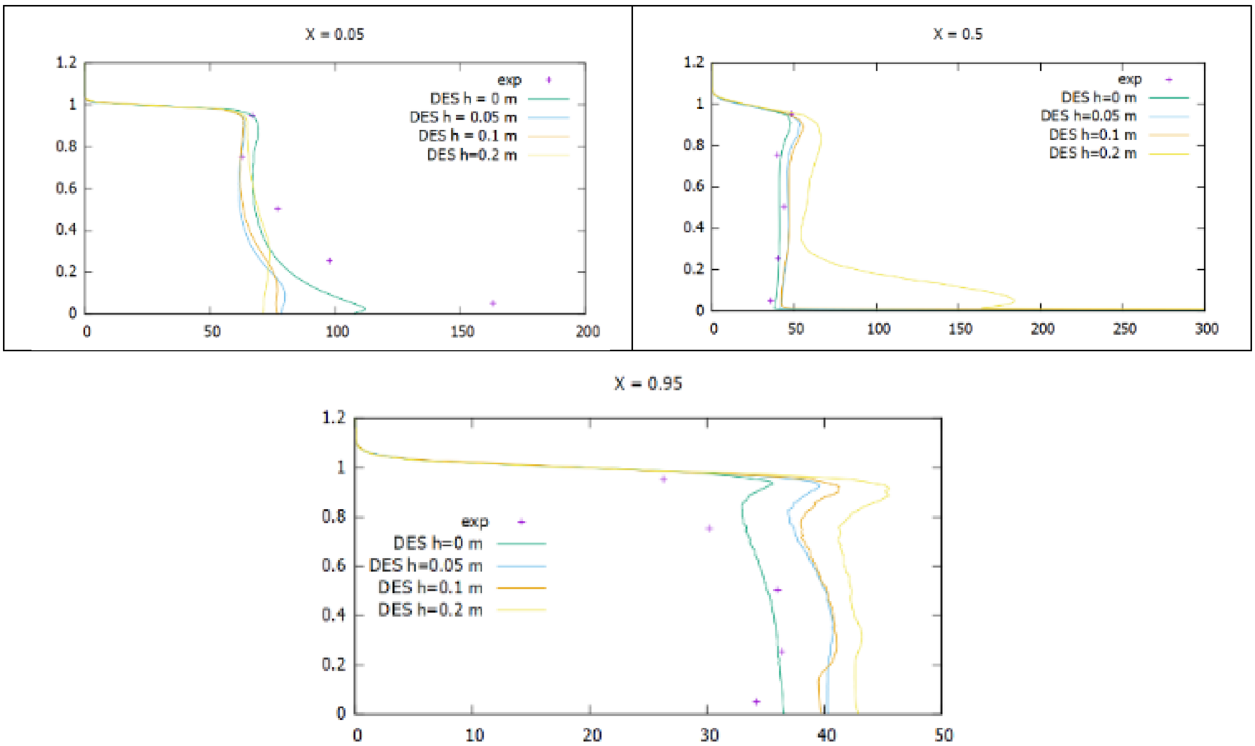

Figure 7 – Concentration profile for different sections

7. CONCLUSION

Computational modeling of the contaminating impurity distribution in a street canyon with barriers to different heights was carried out. For computational modeling the DetachedEddySimulations (DES) model which showed good accuracy at a solution of a test problem was selected. To check model the test problem, results which showed that the selected model is suitable for computational modeling was solved.

As show results of modeling, existence of barriers has significant effect on distribution of the contaminating impurity. Concentration of impurity on leeward of a canyon decreases approximately twice, and from less windy party slightly increases though apparently from the received diagrams it is still twice lower, than on leeward. At the same time concentration of pollutant between barriers considerably increases in space. Proceeding from it is possible to tell that barriers provide protection of houses not only against noise, but also against the contaminating impurity which are thrown out air vehicles.

Acknowledgements

This work is supported by grant from the Ministry of education and science of the Republic of Kazakhstan.

А.А. Исахов, А. Абай, П.Т. Омарова, Ж.Е. Бекжигитова

Механика-математика факультеті, Әл-Фараби атындағы ҚазҰУ, 050040, Қазақстан

ТҰРҒЫН ҮЙ АУМАҒЫНДАҒЫ ЛАСТАУШЫ ЗАТТАРДЫҢ ТАРАЛУЫНЫҢ САНДЫҚ МОДЕЛДЕУІ

Аннотация. Бұл зерттеуде көше каньонындағы ластаушы заттардың таралуын сандық моделдеу және осы үдеріске кедергілердің әсері жүргізілді. Бұл мәселені шешу үшін Рейнольдс орташаланғаны бойынша Навье-Стокс теңдеуі қолданылды. Бұл мәселені шешу үшін DES турбуленттік моделі қолданылды,ол тест тапсырмасы үшін жақсы нәтижелер көрсетті. Математикалық модельді және сандық алгоритмді тексеру үшін тест тапсырмасы шешілді. Алынған сандық нәтижелер эксперименталдық деректермен және басқа авторлардың үлгілеу нәтижелерімен салыстырылды. Математикалық модельді және сандық алгоритмді тексергеннен кейін үйлер арасындағы ластаушы заттардың эмиссия процесін есепке ала отырып, кедергілердің әр түрлі биіктіктерін пайдалануда негізгі міндеттері сипатталған.0,05 м-ден 0,2 м-ге дейінгі диапазондағы аралығында арақатынасы бар көше каньонының моделі есептік аймақ ретінде алынды. Сандық үлгілеу көрсеткендей, кедергінің биіктігінің өзгеруіне байланысты, кедергілердің болуы объектілер арасындағы кеңістікте қосымша құйынды пайда болуына алып келеді. Нәтижесінде ластаушы заттардың көпшілігі олардың арасындағы тұзаққа түсетінін байқауға болады. Әр түрлі зерттеулер барысында жол бойындағы кедергілердің болуы ауадағы зиянды заттардың концентрациясын төмендететіні анықталды. Сондықтан биіктігі 0,1 м шөп кедергісін пайдаланған кезде шоғырлану мәні x=0,05 м қимасында тура келеді, кедергілерді пайдаланбай-ақ салыстырғанда 1,5 еседен азаяды. Осылайша, қоршаған орта мен адам денсаулығына зиянды заттардың әсер етуін алдын алуға және кедергілер ластанған ауаны жақсы сүзуді қамтамасыз ететінін айтуға болады.

Түйін сөздер: ауаның ластануы; ластаушы заттардың дисперсиясы; концентрацияның ауытқуы; жоғары концентрациялар; тасымалдау; қалалық көше каньоны.

А.А. Исахов, А. Абай, П.Т. Омарова, Ж.Е. Бекжигитова

Механико-математический факультет, КазНУ Аль-Фараби им., 050040, Казахстан

ЧИСЛЕННОЕ МОДЕЛИРОВАНИЕ РАСПРОСТРАНЕНИЕ ЗАГРЯЗНЯЮЩИХ ВЕЩЕСТВ В ЖИЛЫХ РАЙОНАХ

Аннотация. В данном исследовании проведено численное моделирование распределения загрязняющих веществ в уличном каньоне и влияния барьеров на этот процесс. Для решения этой задачи было использовано усредненное по Рейнольдсу уравнение Навье-Стокса. Для решения этой задачи была использована турбулентная модель DES, которая показала хорошие результаты для тестовой задачи. Для проверки математической модели и численного алгоритма была решена тестовая задача. Полученные численные результаты сравнивались с экспериментальными данными и результатами моделирования других авторов. После проверки математической модели и численного алгоритма была описана основная задача с

учетом процесса эмиссии загрязняющих веществ между домами, использующими различные высоты барьера. В качестве вычислительной площади была взята модель уличного каньона с соотношением сторон, которое колебалось от 0,05 м до 0,2 м. Как показывает численное моделирование, наличие барьеров приводит к появлению дополнительного вихря в пространстве между объектами, который увеличивается по мере увеличения их высоты. В результате можно наблюдать, что большинство загрязняющих веществ попадает в ловушку между ними. В ходе различных исследований было выявлено, что наличие барьеров вдоль дорог снижает концентрацию вредных веществ в воздухе. Поэтому при использовании травяного барьера высотой 0,1 м значение концентрации попадает в сечение x=0,05 м более чем в 1,5 раза по сравнению с без использования барьеров. Таким образом, можно сказать, что барьеры обеспечивают хорошую фильтрацию загрязненного воздуха, что пагубно сказывается на окружающей среде и здоровье человека.

Ключевые слова:загрязнение воздуха; дисперсия загрязняющих веществ; колебания концентрации; высокие концентрации; транспорт; городской уличный каньон.

REFERENCES

[1] UN-Habitat. Urbanization and development: emergingfutures. World cities report 2016.Nairobi: United Nations Human Settlements Programme (UN-Habitat); 2016.

[2] Sang JinJeong, A Ra Kim., CFD Study on the Influence of Atmospheric Stability on Near-field Pollutant Dispersion from Rooftop Emissions. *Asian Journal of Atmospheric Environment - Vol. 12 No. 1.* 2017.

[3] Bazdidi-Tehrani, F., Gholamalipour, P., Kiamansouri, M., &Jadidi, M., Large eddy simulation of thermal stratification effect on convective and turbulent diffusion fluxes concerning gaseous pollutant dispersion around a high-rise model building. *Journal of Building Performance Simulation*, 1–20. 2018.

[4] Lin, Y., Chen, G., Chen, T., Luo, Z., Yuan, C., Gao, P., & Hang, J., The influence of advertisement boards, street and source layouts on CO dispersion and building intake fraction in three-dimensional urban-like models. *Building and Environment*, 2019.

[5] Dai, Y. W., Mak, C. M., & Ai, Z. T. Computational fluid dynamics simulation of wind-driven inter-unit dispersion around multi-storey buildings: Upstream building effect. *Indoor and Built Environment*, 2017.

[6] Tong, Z., Chen, Y., Malkawi, A., Adamkiewicz, G., & Spengler, J. D., Quantifying the impact of traffic-related air pollution on the indoor air quality of a naturally ventilated building. *Environment International*, 89-90, 138–146. 2016.

[7] Mei, S.-J., Hu, J.-T., Liu, D., Zhao, F.-Y., Li, Y., & Wang, H.-Q., Airborne pollutant dilution inside the deep street canyons subjecting to thermal buoyancy driven flows: Effects of representative urban skylines. *Building and Environment*, 149, 592–606. 2019.

[8] Scungio, M., Arpino, F., Cortellessa, G., &Buonanno, G., Detached eddy simulation of turbulent flow in isolated street canyons of different aspect ratios. *Atmospheric Pollution Research,* 6(2), 351–364. 2015.

[9] Shen, Z., Wang, B., Cui, G., & Zhang, Z., Flow pattern and pollutant dispersion over three dimensional building arrays. *Atmospheric Environment,* 116, 202–215. 2015.

[10] Kikumoto, H., &Ooka, R., A study on air pollutant dispersion with bimolecular reactions in urban street canyons using large-eddy simulations. *Journal of Wind Engineering and Industrial Aerodynamics,* 104-106, 516–522. 2012.

[11] Kwak, K.-H., &Baik, J.-J., A CFD modeling study of the impacts of NOx and VOC emissions on reactive pollutant dispersion in and above a street canyon. *Atmospheric Environment*, 46, 71–80. 2012.

[12] Dai, Y., Mak, C. M., Ai, Z., & Hang, J., Evaluation of computational and physical parameters influencing CFD simulations of pollutant dispersion in building arrays. *Building and Environment,* 137, 90–107. 2018.

[13] Brown, M. J., Williams, M. D., Nelson, M. A., &Werley, K. A., QUIC Transport and Dispersion Modeling of Vehicle Emissions in Cities for Better Public Health Assessments. *Environmental Health Insights,* 9(S1), EHI.S15662.2015.

[14] Wang, C., Li, Q., & Wang, Z.-H.,Quantifying the impact of urban trees on passive pollutant dispersion using a coupled large-eddy simulation–Lagrangian stochastic model. *Building and Environment.*2018.

[15] Dallman, A., Magnusson, S., Britter, R., Norford, L., Entekhabi, D., & Fernando, H. J. S., Conditions for thermal circulation in urban street canyons. *Building and Environment,* 80, 184–191.2014.

[16] Patankar, S.V., Numerical Heat Transfer and Fluid Flow. *Taylor & Francis.*ISBN 978-0-89116-522-4.1980.

[17] Issakhov A., Zhandaulet Y., Nogaeva A., Numerical simulation of dam break flow for various forms of the obstacle by VOF method. International Journal of Multiphase Flow, 109 (2018) 191–206.

[18] Issakhov A., Imanberdiyeva M., Numerical simulation of the movement of water surface of dam break flow by VOF methods for various obstacles. International Journal of Heat and Mass Transfer, 2019136, 1030-1051.

[19] Issakhov A. Mathematical modeling of the discharged heat water effect on the aquatic environment from thermal power plant under various operational capacities.Applied Mathematical Modelling, 40(2), 2016, 1082-1096.

N E W S
OF THE NATIONAL ACADEMY OF SCIENCES OF THE REPUBLIC OF KAZAKHSTAN
PHYSICO-MATHEMATICAL SERIES
ISSN 1991-346X **https://doi.org/10.32014/2019.2518-1726.46**
Volume 4, Number 326 (2019), 76 – 82

UDK 517.958

B. Bekbolat[1], B. Kanguzhin[2], N. Tokmagambetov[3]

[1,2,3]Al-Farabi Kazakh National University, Almaty, Kazakhstan;
[3]Ghent University, Ghent, Belgium;
[1,2,3]Institute of Mathematics and Mathematical Modeling,Almaty, Kazakhstan
bekbolat@math.kz, kanbalta@mail.ru, niyaz.tokmagambetov@gmail.com

TO THE QUESTION OF A MULTIPOINT MIXED BOUNDARY VALUE PROBLEM FOR A WAVE EQUATION

Abstract. It is well known that some problems in mechanics and physics lead to partial differential equations of the hyperbolic type. A classical example of the hyperbolic type is wave equation. When posed, the task sometimes lacks the classical boundary condition and the need arises to have a nonlocal boundary condition. Aim our work is get D'Alembert formula for mixed boundary value problem generated by a wave equation. In the classical case, given D'Alembert formula for boundary value problem generated by a wave equation. In our case, we must give D'Alembert formula for mixed boundary value problem. For this, we consider ordinary differential operator $\mathcal{L}$ withnon–local boundary conditions. We search the solution of the wave equation like a sum with eigenfunction of the operator $\mathcal{L}$. There are we use that fact, that eigenfunction of the operator $\mathcal{L}$ is Riesz basis in $L^2(0,l)$. Through this method and calculation we get D'Alembert formula.

Key words: D'Alembert formula, wave equation, mixed boundary value problem, nonlocal boundary condition.

1 Introduction

It is well known that some problems in mechanics and physics lead to partial differential equations of the hyperbolic type. When posed, the task sometimes lacks the classical boundary condition and the need arises to have a nonlocal boundary condition (see, [2, 3, 4, 5]). A simple example of such nonlocal conditions are multipoint conditions relating the value of the solution at the boundary points with the values at some interior points. For example, we refer the reader to [6, 7, 8, 9, 10].

2 Main result

Let us consider mixed boundary value problem generated by the homogeneous wave equation

$$\frac{\partial^2 U}{\partial t^2} - \frac{\partial^2 U}{\partial x^2} = 0, (x,t) \in \mathrm{S} \tag{1}$$

with inhomogeneous initial data

$$U(x,0) = f(x), U_t(x,0) = F(x), x \in [0,l], \tag{2}$$

and with non–local conditions

$$U(0,t) = 0, \sum_{j=0}^{N} \alpha_j U_x{}'(x_j,t) = 0, \tag{3}$$

where $\mathrm{S} = \{(x,t): 0 < x < l, t > 0\}$,

$$0 = x_0 < x_1 <\ldots< x_N = l, \alpha_0 \neq 0, \alpha_N \neq 0, \sum_{j=0}^{N} \alpha_j = 1,\ l < \infty,$$

the system of point $\{x_j\}_{j=0}^{N}$ on the segment $[0, l]$ is chosen such that the relation $\frac{x_j}{x_{j+1}}$ is a rational number for all $j \geq 0$.

Also consider an ordinary differential operator $\mathcal{L}$ with the expression

$$\mathcal{L}(y) \equiv -y''(x), 0 < x < b, \tag{4}$$

with non–local boundary conditions

$$y(0) = 0, \sum_{j=0}^{N} \alpha_j y'(x_j) = 0. \tag{5}$$

By $\{\lambda_k\}_{k=1}^{\infty}$ denote eigenvalues of $\mathcal{L}$, which are zeros of the characteristic function

$$\Phi(\lambda) = \sum_{j=0}^{N} \alpha_j cos\sqrt{\lambda}x_j.$$

Theorem 1 *A solution of the boundary value problem (1)–(3) has the form*

$$U(x,t) = \frac{\tilde{f}(x+t) + \tilde{f}(x-t)}{2} + \frac{1}{2}\int_{x-t}^{x+t} \tilde{F}(\tau)d\tau.$$

Proof. The system of eigen- and associated functions has the form

$$\{X_{kn}(x) = \frac{1}{k!}\frac{\partial^k}{\partial\lambda^k}(\frac{sin\sqrt{\lambda}x}{\sqrt{\lambda}})|_{\lambda=\lambda_n}, k = 0,1,\ldots,m_n - 1\}_{n=1}^{\infty}, \tag{6}$$

which is the Riesz basis in $L^2(0, l)$ (see [1]). Here m_n is a multiplicity of the corresponding eigenvalue λ_n for all $n \in \mathbb{N}$.

Using this fact, let us prove solvability of the problem (1)-(3). The solution of the problem (1)-(3) we will seek in the view

$$U(x,t) = \sum_{n=1}^{\infty} \sum_{k=0}^{m_n-1} d_{kn}(t)X_{kn}(x), \tag{7}$$

where d_{kn} is a coefficient of the Fourier decomposition of U, depends on second argument.

By differentiating twice respect to x (7), we get

$$\frac{\partial^2 U}{\partial x^2} = \sum_{n=1}^{\infty} \sum_{k=0}^{m_n-1} d_{kn}(t)\left[-\lambda_n X_{kn}(x) - X_{k-1,n}(x)\right] =$$

$$\sum_{n=1}^{\infty} \sum_{k=0}^{m_n-1} [-\lambda_n d_{kn}(t) - d_{k+1,n}(t)]X_{kn}(x), \tag{8}$$

where $d_{m_n,n} = 0$.

By differentiating twice respect to t (7), we have

$$\frac{\partial^2 U}{\partial t^2} = \sum_{n=1}^{\infty} \sum_{k=0}^{m_n-1} d_{kn}''(t)X_{kn}(x), \tag{9}$$

By using the condition $U(0, t) = 0$, from (8)-(9) we take

$$d_{kn}''(t) = -\lambda_n d_{kn}(t) - d_{k+1,n}(t), k < m, where d_{m_n,n} = 0. \tag{10}$$

Use initial conditions (2):

$$U(x,0) = \sum_{n=1}^{\infty} \sum_{k=0}^{m_n-1} d_{kn}(0) X_{kn}(x) = f(x),$$

$$U_t(x,0) = \sum_{n=1}^{\infty} \sum_{k=0}^{m_n-1} d_{kn}'(0) X_{kn}(x) = F(x).$$

We calculate Fourier coefficients using the biorthogonal system of $\{X_{kn}(x)\}$ by formulas

$$d_{kn}(0) = d_{kn}^{f} = \int_0^b f(x)\overline{h_{kn}(x)}dx,$$
$$d_{kn}'(0) = d_{kn}^{F} = \int_0^b F(x)\overline{h_{kn}(x)}dx. \quad (11)$$

Indeed, (10) – (11) is a Cauchy problem, and it's solution has the form

$$d_{kn}(t) = d_{kn}^{f} cos\sqrt{\lambda_n}t + d_{kn}^{F}\frac{sin\sqrt{\lambda_n}t}{\sqrt{\lambda_n}} - \int_0^t \frac{sin\sqrt{\lambda_n}(t-\xi)}{\sqrt{\lambda_n}} d_{k+1,n} d\xi. \quad (12)$$

Taking into account $d_{m_n,n} = 0$, for $k = m_n - 1$ we have

$$d_{m_n-1,n}(t) = d_{m_n-1,n}^{f} cos\sqrt{\lambda_n}t + d_{m_n-1,n}^{F}\frac{sin\sqrt{\lambda_n}t}{\sqrt{\lambda_n}}.$$

And for $k = m_n - 2$ we have

$$d_{m_n-2,n}(t) = d_{m_n-2,n}^{f} cos\sqrt{\lambda_n}t +$$

$$d_{m_n-2,n}^{F}\frac{sin\sqrt{\lambda_n}t}{\sqrt{\lambda_n}} - \int_0^t \frac{sin\sqrt{\lambda}(t-\zeta)}{\sqrt{\lambda}} d_{m_n-1,n}(t) d\zeta$$

$$= d_{m_n-2,n}^{f} cos\sqrt{\lambda_n}t - \int_0^t \frac{sin\sqrt{\lambda}(t-\zeta)}{\sqrt{\lambda_n}} d_{m_n-1,n}^{f} cos\sqrt{\lambda_n}t d\zeta$$

$$+ d_{m_n-2,n}^{F}\frac{sin\sqrt{\lambda_n}t}{\sqrt{\lambda_n}} - \int_0^t \frac{sin\sqrt{\lambda}(t-\zeta)}{\sqrt{\lambda_n}} d_{m_n-1,n}^{F}\frac{sin\sqrt{\lambda_n}t}{\sqrt{\lambda_n}} d\zeta.$$

We denote

$$C_{0n}(t) = cos\sqrt{\lambda_n}t, S_{0n}(t) = \frac{sin\sqrt{\lambda_n}t}{\sqrt{\lambda_n}},$$

$$C_{kn}(t) = -\int_0^t \frac{sin\sqrt{\lambda_n}(t-\zeta)}{\sqrt{\lambda_n}} cos\sqrt{\lambda_n}\zeta d\zeta,$$

$$S_{kn}(t) = -\int_0^t \frac{sin\sqrt{\lambda_n}(t-\zeta)}{\sqrt{\lambda_n}} \frac{sin\sqrt{\lambda_n}\zeta}{\sqrt{\lambda_n}} d\zeta,$$

and

$$C_{k+1,n}(t) = \frac{1}{k!}\frac{\partial^{k+1}}{\partial\lambda^{k+1}} C_{0n}(t),$$
$$S_{k+1,n}(t) = \frac{1}{k!}\frac{\partial^{k+1}}{\partial\lambda^{k+1}} S_{0n}(t). \quad (13)$$

Therefore

$$d_{m_n-2,n}(t) = d^f_{m_n-2,n} cos\sqrt{\lambda_n}t + d^F_{m_n-2,n}\frac{sin\sqrt{\lambda_n}t}{\sqrt{\lambda_n}} -$$

$$d^f_{m_n-1,n}C_{1,n}(t) - d^F_{m_n-1,n}S_{1,n}(t).$$

Analogically for another k the function $d_{kn}(t)$ can be written as

$$d_{kn}(t) = \sum_{j=k}^{m_n-1} [d^f_{jn}C_{j-k,n}(t) + d^F_{jn}S_{j-k,n}(t)]. \tag{14}$$

By substituting found $d_{kn}(t)$ in (7), we get

$$U(x,t) = \sum_{n=1}^{\infty}\sum_{k=0}^{m_n-1}\sum_{j=k}^{m_n-1} [d^f_{jn}C_{j-k,n}(t) + d^F_{jn}S_{j-k,n}(t)]X_{kn}(x)$$

$$= \sum_{n=1}^{\infty}\sum_{j=0}^{m_n-1} \{d^f_{jn}\sum_{k=0}^{j} C_{j-k,n}(t)X_{kn}(x) + d^F_{jn}\sum_{k=0}^{j} S_{j-k,n}(t)X_{kn}(x)\}.$$

By virtue of (6) and (13), we have a new presentation

$$U(x,t) = \sum_{n=1}^{\infty}\sum_{j=0}^{m_n-1} \{d^f_{jn}\sum_{k=0}^{j}\frac{1}{(j-k)!}\frac{\partial^{j-k}}{\partial\lambda_n^{j-k}}(cos\sqrt{\lambda_n}t)\frac{1}{k!}\frac{\partial^k}{\partial\lambda_n^k}(\frac{sin\sqrt{\lambda_n}t}{\sqrt{\lambda_n}})$$

$$+d^F_{jn}\sum_{k=0}^{j}\frac{1}{(j-k)!}\frac{\partial^{j-k}}{\partial\lambda_n^{j-k}}(\frac{sin\sqrt{\lambda_n}t}{\sqrt{\lambda_n}})\frac{1}{k!}\frac{\partial^k}{\partial\lambda_n^k}(\frac{sin\sqrt{\lambda_n}x}{\sqrt{\lambda_n}})\}.$$

Syne $\frac{sin\sqrt{\lambda_n}t}{\sqrt{\lambda_n}} = \int_0^t cos\sqrt{\lambda_n}\tau d\tau$, then

$$U(x,t) = \sum_{n=1}^{\infty}\sum_{j=0}^{m_n-1} d^f_{jn}\frac{1}{j!}\sum_{k=0}^{j}\frac{j!}{k!\,(j-k)!}\frac{\partial^{j-k}}{\partial\lambda_n^{j-k}}(cos\sqrt{\lambda_n}t)\frac{\partial^k}{\partial\lambda_n^k}(\frac{sin\sqrt{\lambda_n}x}{\sqrt{\lambda_n}})$$

$$+\int_0^t d\tau\sum_{n=1}^{\infty}\sum_{j=0}^{m_n-1} d^F_{jn}\frac{1}{j!}\sum_{k=0}^{j}\frac{j!}{k!\,(j-k)!}\frac{\partial^{j-k}}{\partial\lambda_n^{j-k}}(cos\sqrt{\lambda_n}\tau)\frac{\partial^k}{\partial\lambda_n^k}(\frac{sin\sqrt{\lambda_n}x}{\sqrt{\lambda_n}}).$$

And using $\sum_{k=0}^{j} C_k^j U^{(k)}(x)V^{(j-k)}(x) = (UV)^{(j)}$, we take

$$U(x,t) = \sum_{n=1}^{\infty}\sum_{j=0}^{m_n-1} d^f_{jn}\frac{1}{j!}\frac{\partial^j}{\partial\lambda_n^j}(cos\sqrt{\lambda_n}t\frac{sin\sqrt{\lambda_n}x}{\sqrt{\lambda_n}})$$

$$+\int_0^t d\tau\sum_{n=1}^{\infty}\sum_{j=0}^{m_n-1} d^F_{jn}\frac{1}{j!}\frac{\partial^j}{\partial\lambda_n^j}(cos\sqrt{\lambda_n}\tau\frac{sin\sqrt{\lambda_n}x}{\sqrt{\lambda_n}})$$

$$= \frac{1}{2}\sum_{n=1}^{\infty} \sum_{j=0}^{m_n-1} d_{jn}^{f} \frac{1}{j!}\frac{\partial^j}{\partial\lambda_n^j}\left(\frac{sin\sqrt{\lambda_n}(x+t)}{\sqrt{\lambda_n}}\right)$$

$$+\frac{1}{2}\sum_{n=1}^{\infty} \sum_{j=0}^{m_n-1} d_{jn}^{f} \frac{1}{j!}\frac{\partial^j}{\partial\lambda_n^j}\left(\frac{sin\sqrt{\lambda_n}(x-t)}{\sqrt{\lambda_n}}\right)$$

$$+\frac{1}{2}\int_0^t d\tau \sum_{n=1}^{\infty} \sum_{j=0}^{m_n-1} d_{jn}^{F} \frac{1}{j!}\frac{\partial^j}{\partial\lambda_n^j}\left(\frac{sin\sqrt{\lambda_n}(x+\tau)}{\sqrt{\lambda_n}}\right)$$

$$+\frac{1}{2}\int_0^t d\tau \sum_{n=1}^{\infty} \sum_{j=0}^{m_n-1} d_{jn}^{F} \frac{1}{j!}\frac{\partial^j}{\partial\lambda_n^j}\left(\frac{sin\sqrt{\lambda_n}(x-\tau)}{\sqrt{\lambda_n}}\right).$$

So,

$$\begin{aligned} U(x,t) &= \frac{1}{2}\sum_{n=1}^{\infty} \sum_{j=0}^{m_n-1} d_{jn}^{f} X_{jn}(x+t) + \frac{1}{2}\sum_{n=1}^{\infty} \sum_{j=0}^{m_n-1} d_{jn}^{f} X_{jn}(x-t) \\ &+ \frac{1}{2}\int_x^{x+t} \sum_{n=1}^{\infty} \sum_{j=0}^{m_n-1} d_{jn}^{F} X_{jn}(\tau)d\tau + \frac{1}{2}\int_{x-t}^{x} \sum_{n=1}^{\infty} \sum_{j=0}^{m_n-1} d_{jn}^{F} X_{jn}(\tau)d\tau. \end{aligned} \quad (15)$$

When $0 \le x - t \le x + t \le b$, then sums of series are coincides with the initial data

$$\sum_{n=1}^{\infty} \sum_{j=0}^{m_n-1} d_{jn}^{f} X_{jn}(x+t) = f(x+t),$$

$$\sum_{n=1}^{\infty} \sum_{j=0}^{m_n-1} d_{jn}^{f} X_{jn}(x-t) = f(x-t),$$

$$\sum_{n=1}^{\infty} \sum_{j=0}^{m_n-1} d_{jn}^{F} X_{jn}(\tau) = F(\tau).$$

For $0 \le x - t \le x + t \le b$ the solution is well–known D'Alembert formula

$$U(x,t) = \frac{f(x+t)+f(x-t)}{2} + \frac{1}{2}\int_{x-t}^{x+t} F(\tau)d\tau.$$

Thus, the formula (15) can be interpreted as a generalization of the D'Alembert formula for arbitrary $0 \le x \le b, t \ge 0$.

As a result, we conclude

$$U(x,t) = \frac{\tilde{f}(x+t)+\tilde{f}(x-t)}{2} + \frac{1}{2}\int_{x-t}^{x+t} \tilde{F}(\tau)d\tau,$$

where $\tilde{f}(x)$ and $\tilde{F}(x)$ extended from the segment $[0, l]$ to the whole real axis by the analytical continuation of the basis system

$$\{X_{kn}(x) = \frac{1}{k!}\frac{\partial^k}{\partial\lambda^k}\frac{sin\sqrt{\lambda_n}x}{\sqrt{\lambda_n}}\}.$$

Since $\{X_{kn}(x)\}$ is defined on $(-\infty, +\infty)$, then we can always to continue functions $f(x)$ and $F(x)$ outside of the segment $[0, l]$. From [1] follows that the system $\{X_{kn}(x)\}$ is Riesz basis in $L_2(-\infty, +\infty)$.

ACKNOWLEDGEMENTS

The authors were supported by the Ministry of Education and Science of the Republic of Kazakhstan (MESRK) Grant AP05130994. No new data was collected or generated during the course of research.

Б. Бекболат[1], Б. Кангужин[2], Н. Токмагамбетов[3],

[1,2,3]Әл-Фараби атындағы ҚазҰУ, Алматы, Қазақстан;
[3]Гент университеті, Гент, Белгия;
[1,2,3]Математика және математикалық модельдеу институты, Алматы, Қазақстан

ТОЛҚЫН ТЕҢДЕУІ ҮШІН КӨП НҮКТЕЛІ АРАЛАС ШЕКАРАЛЫҚ ЕСЕП

Аннотация.Механика мен физиканың кейбір есептері дербес туындылы дифференциалдық теңдеулердің гиперболалық түріне алып келетіні белгілі. Гиперболалық теңдеудің классикалық өкіліне толқын теңдеуі жатады. Кейде есеп шығару барысында тек шекаралық шарт жеткіліксіз болады, сондықтан қосымша локалды емес шекаралық шартта қолданылады. Біздің жұмыстың мақсаты толқын теңдеуі арқылы туындаған аралас шекаралық есептің Даламбер формуласын табу. Классикада толқын теңдеуі арқылы туындаған шекаралық есеп үшін Даламбер формуласы берілген. Біз аралас шекаралық есеп үшін Даламбер формуласын табу керекпіз. Ол үшін біз қосымша $\mathcal{L}$дифференциалдық операторын қарастырамыз. Себебі біз шешімді $\mathcal{L}$ операторының меншікті функциялары арқылы құрылған қатар арқылы іздейміз. Біз бұл жерде $\mathcal{L}$ операторының меншікті функциялары $L^2(0,l)$кеңістігінде Рисс базисы болатынын пайдаланамз. Біз осы әдіс және есептеулер арқылы Даламбер формуласын аламыз.

Түйін сөздер:Даламбер формуласы, толқын теңдеуі, аралас шекаралық есеп, локалды емес шекаралық шарт.

Б. Бекболат[1], Б. Кангужин[2], Н. Токмагамбетов[3]

[1,2,3]КазНУ им. Аль-Фараби, Алматы, Казахстан;
[3]Гентский университет, Гент, Белгия;
[1,2,3]Институт математики и математического моделирования, Алматы, Казахстан

О МНОГОТОЧЕЧНОЙ ЗАДАЧЕ СМЕШАННОЙ ГРАНИЦЫ ДЛЯ ВОЛНОВОГО УРАВНЕНИЯ

Аннотация.Хорошо известно, что некоторые проблемы механики и физики приводят к уравнениям в частных производных гиперболического типа. Классическим примером гиперболического типа является волновое уравнение. При постановке задачи иногда не хватает классического граничного условия, и возникает необходимость иметь нелокальное граничное условие. Цель нашей работы - получить формулу Даламбера для смешанной краевой задачи, порожденной волновым уравнением. В классическом случае дана формула Даламбера для краевой задачи, порожденная волновым уравнением. В нашем случае мы должны дать формулу Даламбера для смешанной краевой задачи. Для этого рассмотрим обыкновенный дифференциальный оператор $\mathcal{L}$ с нелокальными граничными условиями. Мы ищем решение волнового уравнения как сумму с собственной функцией оператора $\mathcal{L}$. Мы используем тот факт, что собственная функция оператора $\mathcal{L}$ является базисом Рисса в $L^2(0,l)$. С помощью этого метода и расчета мы получаем формулу Даламбера.

Ключевые слова:Формула Даламбера, волновое уравнение, смешанная краевая задача, нелокальные краевые условия.

Information about authors:

Kanguzhin Baltabek – Doctor of Physical and Mathematical Sciences, Professor,Al–Farabi Kazakh National University, Almaty, Kazakhstan;

Tokmagambetov Niyaz – PhD doctor, Department of Mathematics: Analysis, Logic and Discrete Mathematics, Ghent University, Ghent, Belgium;

Bekbolat Bayan – Doctorate, al-Farabi Kazakh National University, Almaty, Kazakhstan.

REFERENCES

[1] Gubreev G. M., *Spectral analysis of biorthogonal expansions of functions, and exponential series*, Izv. Akad. Nauk SSSR Ser. Mat.,Vol.53, №6. 1989. P.1236–1268.

[2] Kanguzhin B. E., Anijarov A. A., *Well-Posed Problems for the Laplace Operator in a Punctured Disk*, Mathematical Notes.Vol.89, №6. 2011. P.819–829.

[3] Kanguzhin B. E., Tokmagambetov N. E., *On Regularized Trace Formulas for a Well-Posed Perturbation of the m-Laplace Operator.* Differential Equations. **51**:1583-1588 (2015).

[4] Kanguzhin B. E., Tokmagambetov N. E., *Resolvents of well-posed problems for finite-rank perturbations of the polyharmonic operator in a punctured domain.* Siberian Mathematical Journal. **57**:265-273 (2016)

[5] Kanguzhin B. E., Tokmagambetov N. E., *A regularized trace formula for a well-perturbed Laplace operator*, Doklady Mathematics.Vol.91, №1. 2015.P.1–4.

[6] Bastys A., Ivanauskas F., Sapagovas M., *An explicit solution of a parabolic equation with nonlocal boundary conditions*, Lithuanian Mathematical Journal. –Vol.45, №3. 2005. P.257–271.

[7] Zhanbing Bai, *On positive solutions of a nonlocal fractional boundary value problem*, Nonlinear analysis-theory methods and applications. Vol.72, №2. 2005. P.916–924.

[8] Webb J. R. L., Gennaro I., *Positive solutions of nonlocal boundary value problems: A unified approach*, Jornal of the London Mathematical society series. Vol.74, №3. 2006. P.973–693.

[9] Webb J. R. L., Gennaro I., *Positive solutions of nonlocal boundary value problems involving integral conditions*, Node-nonlinear differential equations and applications. Vol. 15, №1-2. 2008. P.45–67.

[10] Goodrich, Christopher S., *Existence and uniqueness of solutions to a fractional difference equation with nonlocal conditions*, Computers and mathematics with applications. Vol.61, №2. 2011. P.191–202.

[11] Seitmuratov A., Zharmenova B., Dauitbayeva A., Bekmuratova A. K., Tulegenova E., Ussenova G.,*Numerical analysis of the solution of some oscillation problems by the decomposition method*,News of the national academy of sciences of the republic of Kazakhstan,Series physic-mathematical. Vol.323, №1.2019. P.28–37.ISSN 1991-346X https://doi.org/10.32014/2019.2518-1726.4

N E W S
OF THE NATIONAL ACADEMY OF SCIENCES OF THE REPUBLIC OF KAZAKHSTAN
PHYSICO-MATHEMATICAL SERIES
ISSN 1991-346X **https://doi.org/10.32014/2019.2518-1726.47**
Volume 4, Number 326 (2019), 83 – 91

UDC 517.946:517.588
IRSTI 27.29.21; 27.23.25

Zh.N. Tasmambetov[1], N. Rajabov[2], Zh.K.Ubayeva[3]

[1]Aqtobe Regional Zhybanov State University;
[2]Tajic National University;
[3]Aqtobe Regional Zhybanov State University
tasmam@rambler.ru, nusrat38@mail.ru, zhanar_ubaeva@mail.ru

THE COORDINATED SOLUTION OF TWO DIFFERENTIAL EQUATIONS IN PRIVATE DERIVATIVES OF THE THIRD ORDER

Abstract. In the study the possibility of constructing a solution near a variety of special features of the system consisting of two differential equations in partial derivatives of the third order was investigated. There definitive aspects of such systems in comparison with systems consisting of two differential equations in partial derivatives of second order were established. The classification of regular and irregular singularities was carried out, the relevant solutions are constructed. A specific example shows that the application of the Frobenius - Latysheva method to the construction of a solution of a degenerate hypergeometric system consisting of two third-order partial differential equations. A variety of properties of system solution were considered, which shows that these solutions have the properties of generalized hypergeometric functions.

Key words: solution, constructed, system, features, regular, irregular, generalized, third order.

Introduction. The solutions of particular cases of systems of differential equations of second order type

$$\left.\begin{aligned} G^{(0)}\cdot Z_{xx}+G^{(1)}\cdot Z_{xy}+G^{(2)}\cdot Z_x+G^{(3)}\cdot Z_y+G^{(4)}\cdot Z=0\\ Q^{(0)}\cdot Z_{yy}+Q^{(1)}\cdot Z_{xy}+Q^{(2)}\cdot Z_x+Q^{(3)}\cdot Z_y+Q^{(4)}\cdot Z=0\end{aligned}\right\} \tag{1}$$

where $G^{(i)}=G^{(i)}(x,y), Q^{(i)}=Q^{(i)}(x,y), (i=\overline{0,4})$ analytic functions or polynomials of two variables, $Z=Z(x,y)$ – total unknown, are the generalized hypergeometric functions of two variables. The general theory of systems type (1) was established by American mathematician E. Wilczynski [1] - [2] using it to support special cases of projective differential geometry. He proved compatibility and integrability conditions

$$1-\frac{G^{(1)}}{G^{(0)}}\cdot\frac{Q^{(1)}}{Q^{(0)}}\neq 0 \tag{2}$$

of system type (1) [1].

In carrying out these important conditions the following statement is fair.

Theorem 1. Suppose that the conditions of compatibility and integrability are fulfilled (2). Then, system (1) has four linearly independent particular solutions of the form

$$Z_j(x,y)=\sum_{m,n=0}^{\infty}A_{m,n}\cdot x^m\cdot y^n,\ (A_{0,0}\neq 0),\ \ (j=1,2,3,4) \tag{3}$$

The overall solution of system (1) is represented as the sum

$$Z_k(x,y)=\sum_{k=1}^{4} G_j\cdot Z_k(x,y),\ \ k=1,2,3,4 \tag{4}$$

where G_j- is arbitrary constant, that is, the general solution of a system of partial differential equations depends on arbitrary constants, and not on an arbitrary constant.

Theorem 2. If the compatibility conditions are satisfied, and the integrability condition is not satisfied, that is,

$$1-\frac{G^{(1)}}{G^{(0)}}\cdot\frac{Q^{(1)}}{Q^{(0)}}=0 \tag{5}$$

then system (1) has no more than three linearly independent solutions, or the number of them will be countless.

Further development of the study was obtained in the works of J. Horn [3] - [4], P. Appell, J. Kampe de Feriet [5], W. Sternberg [6], A. Erdelyi [7] - [8], P. Humbert [9], E. Ince [10], L. Borngesser [11] and others, in connection with the study of the theory of generalized hypergeometric series of two variables [12] - [13] - [14]. Using the concepts of rank $p=1+k$ ($k-$subrank) and antiranga $m=-1-\lambda$ ($\lambda-$ antipodrang). Zh.N. Tasmambetov developed [15] efficient algorithms for constructing normal, subnormal series, and normal-regular and final solutions of systems of the form (1) consisting of two second-order partial differential equations.

The aim of this work is to study a special system consisting of two differential equations in partial derivatives of the third order; to establish the distinctive features of such systems; to classify regular and irregular features and construct the corresponding solutions; to show the application of the Frobenius-Latysheva method to constructing a solution of a degenerate hypergeometric system consisting of two third-order partial differential equations by using a specific example.

THE COORDINATED SOLUTION OF TWO DIFFERENTIAL EQUATIONS IN PRIVATE DERIVATIVES OF THE THIRD ORDER

Statement. Studying the possibility of coordinated solving a homogeneous system of third-order partial differential equations consisting of two equations of the form

$$\begin{aligned} &x^3g^{(0)}p_{30}+x^2yg^{(1)}p_{21}+x^2g^{(2)}p_{20}+xyg^{(3)}p_{11}+xg^{(4)}p_{10}+yg^{(5)}p_{01}+g^{(6)}p_{0,0}=0,\\ &y^3g^{(0)}p_{03}+xy^2g^{(1)}p_{12}+y^2g^{(2)}p_{02}+xyg^{(3)}p_{11}+xg^{(4)}p_{10}+yg^{(5)}p_{01}+g^{(6)}p_{0,0}=0, \end{aligned} \tag{6}$$

where

$$\begin{aligned} &p_{30}=Z_{xxx}, p_{03}=Z_{yyy}, p_{21}=Z_{xxy}, p_{12}=Z_{xyy}, p_{20}=Z_{xx}, p_{02}=Z_{yy},\\ &p_{11}=Z_{xy}, p_{10}=Z_x, p_{01}=Z_y, p_{0,0}=Z(x,y) \end{aligned} \tag{7}$$

– total unknown, and the coefficients

$$\begin{aligned} &g^{(i)}=g^{(i)}(x,y)=a_{00}^{(i)}+a_{10}^{(i)}\cdot x,\\ &q^{(i)}=q^{(i)}(x,y)=b_{00}^{(i)}+b_{01}^{(i)}\cdot y,(i=\overline{0,6}). \end{aligned} \tag{8}$$

It is required to classify regular and irregular singularities and establish the type of solution near each singularity; to determine the number of linearly independent solutions near these features; to examine the relationship of the original system with systems solutions that are generalized hypergeometric functionы of two variables and properties of such functions.

Solution of a system of differential equations.

To construct solutions of the system of equations (6), it is required to carry out a number of conditions, let us discuss the major of them

1. It must be carried out the compatibility conditions. However, the general compatibility condition, as for system (1), is difficult to control. Usually, such checking is carried out for specific systems solutions which are generalized hypergeometric functions of two variables. The Kampe de Feriet method can be applied [5, p.155], [16, p.21] - [17].
2. Integrability condition

$$1-\frac{g^{(1)}}{g^{(0)}}\cdot\frac{q^{(1)}}{q^{(0)}}\neq 0. \tag{9}$$

3. Unknown function $p_{0,0}=Z(x,y)$ depends on two variables, therefore, as before, depending on the regularity and irregularity of the singular curves, solutions should be sought in the form of generalized, normal and normal-regular series of two variables [15, p.159].

4. If in (6) the coefficients at higher derivatives p_{30} and p_{03}: $x^3\cdot g^{(0)}(x,y)\equiv 1$ and $y^3\cdot g^{(0)}(x,y)\equiv 1$ then solution can be sought as a simple series of two variables (3) since there are no singularities. Then, in order to formulate Theorems 1 and 2 for this case, it is necessary to establish the number of linearly independent particular solutions of system (6), which we will do next.

5. The special curves of the system (6) are established by equating to zero the coefficients of the highest derivatives. $p_{30}=Z_{xxx}$ и $p_{03}=Z_{yyy}$:

$$x^3\cdot(a_{00}^{(0)}+a_{10}^{(0)}\cdot x)=0,\ \ x_1=0,\ \ x_2=-\frac{a_{00}^{(0)}}{a_{10}^{(0)}},$$

$$y^3\cdot(b_{00}^{(0)}+b_{01}^{(0)}\cdot y)=0,\ \ y_1=0,\ \ y_2=-\frac{b_{00}^{(0)}}{b_{01}^{(0)}}.$$

Composed from them pairs $(0,0),(0,-\frac{b_{00}^{(0)}}{b_{01}^{(0)}}),(-\frac{a_{00}^{(0)}}{a_{01}^{(0)}},0),(-\frac{a_{00}^{(0)}}{a_{01}^{(0)}},-\frac{b_{00}^{(0)}}{b_{01}^{(0)}})$ - represent the final features, $(0,\infty),(\infty,0),(\infty,-\frac{b_{00}^{(0)}}{b_{01}^{(0)}}),(-\frac{a_{00}^{(0)}}{a_{01}^{(0)}},\infty)$ and (∞,∞) - features at infinity. Normally, when building solutions two pairs of features identified (0,0) and (∞,∞). Classification for regularity and irregularity will be carried out using simple rules [15].

Rule I. If in (6) coefficient $a_{00}^{(0)}\neq 0, b_{00}^{(0)}\neq 0,$ then the feature (0,0) is special regular. When $a_{00}^{(0)}=0, b_{00}^{(0)}=0,$ then (0,0) is a special irregular.

Rule II. If in (6) coefficient $a_{10}^{(0)}\neq 0$ and $b_{01}^{(0)}\neq 0,$ then the feature (∞,∞) – special regular, and when $a_{10}^{(0)}=0, b_{01}^{(0)}=0$ – special irregular.

Features of constructing a solution by the Frobenius-Latyshev method.

The Frobenius-Latyshev method allows determining directly the structure and construct solutions of the system near particular curves. So, when the feature (0,0) is regular, the desired solution is represented as a generalized power series of two variables

$$Z(x,y)=x^{\rho}\cdot y^{\sigma}\cdot\sum_{m,n=0}^{\infty}A_{m,n}\cdot x^m\cdot y^n, \tag{10}$$

where ρ,σ and $A_{m,n}$ $(m,n=0,1,2,3,...)$ – unknown constants to be determined. If the feature (0,0) is irregular, then the desired solution is represented as

$$Z(x,y)=\exp Q(x,y)\cdot x^{\rho}\cdot y^{\sigma}\cdot\sum_{m,n=0}^{\infty}A_{m,n}\cdot x^m\cdot y^n,\quad A_{0,0}\neq 0 \tag{11}$$

$Q(x,y)$ – polynomial of two variables

$$Q(x,y)=\frac{\alpha_{p1}\cdot x^p}{p}+\frac{y^p\cdot\alpha_{0p}}{p}+...+\alpha_{11}\cdot x\cdot y+\alpha_{10}\cdot x+\alpha_{01}\cdot y, \tag{12}$$

with uncertain parameters $\alpha_{p,0},\alpha_{0,p},...,\alpha_{11},\alpha_{10},\alpha_{01.}$

Similarly, near the regular singularity (∞,∞) the solution is constructed in the form

$$Z(x,y) = x^{\rho}\cdot y^{\sigma}\cdot \sum_{m,n=0}^{\infty} B_{m,n}\cdot x^{-m}\cdot y^{-n}, \quad B_{0,0}\neq 0 \tag{13}$$

and near irregular features in the form

$$Z(x,y) = \exp(x,y)\cdot x^{\rho}\cdot y^{\sigma}\cdot \sum_{m,n=0}^{\infty} B_{m,n}\cdot x^{-m}\cdot y^{-n}, \; B_{0,0}\neq 0 \tag{14}$$

where ρ,σ and $B_{m,n}$ $(m,n=0,1,2,3,...)$ – unknown constant.

Polynomial $Q(x,y)$ is common to the type (11) and (14). Its degree is determined by the rank value

$$p = 1+k, \; k = \max_{(1\le s\le n)} \frac{\beta_s - \beta_0}{s} \tag{15}$$

introduced by A. Poincare to study ordinary differential equations, and β_0, β_s - the greatest degrees of the coefficients of the equation [18].

MAIN RESULTS

We will start the application of the Frobenius-Latysheva method with drawing up a system of Frobenius characteristic functions [15].

Definition 1. The system of characteristic functions of Frobenius is called the system

$$\begin{aligned} L_1\left[x^{\rho}\cdot y^{\sigma}\right] &\equiv x^{\rho}\cdot y^{\sigma}\cdot\left[f_{00}^{(1)}(\rho,\sigma) + f_{11}^{(1)}(\rho,\sigma)\cdot x\right],\\ L_2\left[x^{\rho}\cdot y^{\sigma}\right] &\equiv x^{\rho}\cdot y^{\sigma}\cdot\left[f_{00}^{(2)}(\rho,\sigma) + f_{11}^{(1)}(\rho,\sigma)\cdot y\right], \end{aligned} \tag{16}$$

where

$$f_{00}^{(1)}(\rho,\sigma) = a_{00}^{(0)}\rho(\rho-1)(\rho-2) + a_{00}^{(1)}\rho(\rho-1)\sigma + a_{00}^{(2)}\rho(\rho-1) + a_{00}^{(3)}\rho\sigma + a_{00}^{(4)}\rho + a_{00}^{(5)}\sigma + a_{00}^{(6)} \quad 16.1)$$

$$f_{00}^{(2)}(\rho,\sigma) = b_{00}^{(0)}\sigma(\sigma-1)(\sigma-2) + b_{00}^{(1)}\rho\sigma(\sigma-1) + b_{00}^{(2)}\sigma(\sigma-1) + b_{00}^{(3)}\rho\sigma + b_{00}^{(4)}\rho + b_{00}^{(5)}\sigma + b_{00}^{(6)} \quad (16.2)$$

$$f_{10}^{(1)}(\rho,\sigma) = a_{10}^{(0)}\rho(\rho-1)(\rho-2) + a_{10}^{(1)}\rho(\rho-1)\sigma + a_{10}^{(2)}\rho(\rho-1) + a_{10}^{(3)}\rho\sigma + a_{10}^{(4)}\rho + a_{10}^{(5)}\sigma + a_{10}^{(6)} \quad (16.3)$$

$$f_{01}^{(2)}(\rho,\sigma) = b_{01}^{(0)}\sigma(\sigma-1)(\sigma-2) + b_{01}^{(1)}\rho\sigma(\sigma-1) + b_{01}^{(2)}\sigma(\sigma-1) + b_{01}^{(3)}\rho\sigma + b_{01}^{(4)}\rho + b_{01}^{(5)}\sigma + b_{01}^{(6)} \quad (16.4)$$

obtained by substituting into system (6) with coefficients of the form (8) instead of $Z = x^{\rho}\cdot y^{\sigma}$. Define the system of determining equations for features (0,0) and (∞,∞) from (16).

Definition 2. The system of defining equations for the feature (0,0) is called the system

$$f_{00}^{j}(\rho,\sigma) = 0 \quad (j=1,2) \tag{17}$$

from which the indicators of series (10) and (11) are determined in the form of pairs (ρ_t,σ_t).

Definition 3. A system of defining equations for a feature (∞,∞) is called a system

$$\begin{aligned} f_{10}(\rho,\sigma) &= 0,\\ f_{01}(\rho,\sigma) &= 0 \end{aligned} \tag{18}$$

from which the indicators of series (13) and (14) are determined in the form of pairs (ρ_t,σ_t).

In this pairs (ρ_t,σ_t) it is important to determine the index t, since the number of such pairs allows determining the number of linearly independent solutions of the original system (6) near the specified features.

Theorem 3. For the existence the solutions of the form (10) in the system (6) with coefficients (8) near the singularity (0.0) requires the equality (17).**Theorem 4.** For the existence of solutions of the form (13) in the system (6) with coefficients (8) near the singularity (∞,∞) equality is necessary (18).

Let's determine how many roots have the systems of constitutive equations (17) and (18). In view of this, the system (17) can be written in expanded form, using (16.1) and (16.2). From $f_{0,0}^{(1)}(\rho,\sigma)=0$ we will find out

$$\sigma=\frac{a_{00}^{(0)}\rho(\rho-1)(\rho-2)+a_{00}^{(2)}\rho(\rho-1)+a_{00}^{4}\rho+a_{10}^{(6)}}{a_{00}^{(1)}\rho(\rho-1)+a_{00}^{(3)}\rho+a_{00}^{(5)}}$$

and substituting in the second equation $f_{00}^{(2)}(\rho,\sigma)=0$ of the system (17), after exclusion ρ, we obtain the ninth degree equation for σ. If there are only simple roots, then from here we define nine roots σ_t $(t=\overline{1,9})$. Similarly, you can define nine simple roots ρ_t $(t=\overline{1,9})$. Of these, make nine pairs of roots (ρ_t,σ_t) $(t=\overline{1,9})$ of system (17), which allows us to construct nine linearly independent particular solutions of system (17) near the singularity (0,0).

Theorem 5. Suppose the system (6) with coefficients of the form (8), where $a_{00}^{(0)}\neq 0, b_{00}^{(0)}\neq 0$ conditions of compatibility and integrability are satisfied (9). Then system (6) has nine linearly independent regular particular solutions of the form

$$Z_t(x,y)=x^{\rho_t}\cdot y^{\sigma_t}\cdot\sum_{m,n=0}^{\infty}A_{m,n}^{(t)}\cdot x^m\cdot y^n,\quad A_{0,0}^{(t)}\neq 0,\ (t=\overline{1,9}),\tag{19}$$

near feature (0,0), where ρ_t,σ_t $(t=\overline{1,9})$, $A_{m,n}^{(t)}$ $(m,n=0,1,2,...)$.

A similar argument can be sure that the system (6) also has nine linear - independent particular solutions near the singularity (∞,∞).

Theorem 6. Suppose the system (6) with coefficients of the form (8), where $a_{10}^{(0)}\neq 0, b_{01}^{(0)}\neq 0$ conditions of compatibility and integrability are satisfied (9). Then the system (6) has nine linearly independent regular particular solutions of the form

$$Z_t(\rho,\sigma)=x^{\rho_t}\cdot y^{\sigma_t}\cdot\sum_{m,n=0}^{\infty}B_{m,n}^{(t)}\cdot x^m\cdot y^n,\quad B_{0,0}^{(t)}\neq 0,\ (t=\overline{1,9}),\tag{20}$$

near feature (∞,∞), where $\rho_t,\sigma_t,(t=\overline{1,9}),B_{m,n}^{(t)}$ $(m,n=0,1,2,...)$ - unknown constant.

In the theorem 5 and 6, conditions $a_{00}^{(0)}\neq 0, b_{00}^{(0)}\neq 0$ and $a_{10}^{(0)}\neq 0, b_{01}^{(0)}\neq 0$ essential since, ninth degree equations are relatively ρ and σ it turns out only when they are non-zero. Therefore, near regular singular curves (0,0) and (∞,∞) there are nine regular linearly independent particular solutions. Then, the overall solution is represented as the following sum

$$Z(x,y)=\sum_{t=1}^{9}C_t\cdot Z_t(x,y),\ (t=\overline{1,9}).\tag{21}$$

Unknown row coefficients (19) $A_{m,n}^{(t)}$ $(m,n=0,1,2,...)$ are determined from systems of recurrent sequences

$$\sum_{m,n=0}^{\infty}A_{\mu-m,\nu-n}^{(t)}\cdot f_{m,n}^{(j)}(\rho+\mu-m,\sigma+\nu-n)=0\tag{22}$$

$(\mu,\nu=0,1,2,...,;j=1,2;t=\overline{1,9})$(obtained by substituting series (19) into system (6) with coefficients (8).

Application to the construction of a specific system solutions.

All hypergeometric functions of two variables satisfy a system consisting of two partial differential equations of second order. The coefficient of such systems are polynomials x and y. These coefficients can be calculated if in the hypergeometric functions defined by double series

$$F(x,y)=\sum_{m,n} a_{m,n}\cdot x^m\cdot y^n, \tag{23}$$

the coefficients satisfy the following relations

$$\frac{a_{m+1,n}}{a_{m,n}}=\frac{P(m,n)}{R(m,n)},\ \frac{a_{m,n+1}}{am,n}=\frac{Q(m,n)}{S(m,n)}, \tag{24}$$

where P, R, Q, S are known polynomials.

The use of such an approach enabled the intensification of the study of relations between systems consisting of two second-order equations and generalized hypergeometric series of two variables.

However, the relationship between systems consisting of two equations of the third and fourth orders and generalized hypergeometric series has not been studied at the proper level. Here, it should be noted the work of Kampe de Feriet [5], [16] - [17], which provides a method for constructing a series of third and fourth order systems, while ensuring the compatibility of such systems. In this paper we will also proceed from the studies of J. Kampe de Feriet [5, p.155-169].

Theorem 7. The system of partial differential equations consisting of two equations of third order

$$\begin{aligned} x^2\cdot p_{30}+(\delta_1+\delta_2+1)\cdot x\cdot p_{20}+(\delta_1\cdot\delta_2-x)\cdot p_{10}-y\cdot p_{01}-\alpha\cdot p_{0,0}=0,\\ y^2\cdot p_{30}+(\delta_1^{'}+\delta_2^{'}+1)\cdot y\cdot p_{02}+(\delta_1\cdot\delta_2-y)\cdot p_{01}-x\cdot p_{10}-\alpha\cdot p_{0,0}=0, \end{aligned} \tag{25}$$

where $p_{30}=Z_{xxx}, p_{03}=Z_{yyy}, p_{20}=Z_{xx}, p_{02}=Z_{yy}, p_{10}=Z_x, p_{01}=Z_y, p_{0,0}=Z(x,y)$ – common unknown, has nine linearly independent regular particular solutions, and the general solution is represented as the sum (21).

Argument. We will carry out the proof by the Frobenius-Latyshev method, while revealing the additional properties of system (25) can be obtained from the original system (6) with coefficients of the form (8) using the Kampe de Feriet method [5, p.155-164]. As we noted above, this ensures the compatibility of the two equations of the system (25). The integrability condition (9) is also satisfied, since $g^{(1)}=q^{(1)}\equiv 0$.

Coefficients $a_{00}^{(0)}\neq 0$ и $b_{00}^{(0)}\neq 0$, so the feature (0,0) is regular based on the Rule I, a $a_{10}^{(0)}=0, b_{01}^{(0)}=0$, therefore, on the basis of the Rule II feature (∞,∞) – irregular. Let us build regular solutions in the form (10) near feature (0,0).

To this end, we compose a system of Frobenius characteristic functions (15) - (16) and define systems of defining equations (17) with respect to the singularity (0,0), in a transformed expanded form

$$\left.\begin{aligned} f_{00}^{(1)}(\rho,\sigma)=\rho\cdot(\rho-1+\delta_1)\cdot(\rho-1+\delta_2)=0,\\ f_{00}^{(2)}(\rho,\sigma)=\sigma\cdot(\sigma-1+\delta_1)\cdot(\sigma-1+\delta_2)=0.\end{aligned}\right\} \tag{26}$$

It has nine pairs of roots $(\rho_t,\sigma_t, t=\overline{1,9})$:

1. $(\rho_1=0,\sigma_1=0)$, 2. $(\rho_2=1-\delta_{,1}\ \sigma_1=0)$, 3. $(\rho_1=0,\sigma_2=1-\delta_1^{'})$, 4. $(\rho_3=1-\delta_2,\sigma_1=0)$,
5. $(\rho_1=0,\sigma_3=1-\delta_2^{'})$, 6. $(\rho_2=1-\delta_1,\sigma_2=1-\delta_1^{'})$, 7. $(\rho_2=1-\delta_1,\sigma_3=1-\delta_2^{'})$,
8. $(\rho_3=1-\delta_2,\sigma_2=1-\delta_1^{'})$, 9. $(\rho_3=1-\delta_2,\sigma_3=1-\delta_2^{'})$.

Then, on the basis of Theorem 5, the system (25) near the singularity (0,0) has nine linearly - independent regular partial solutions, corresponding to these indicators.:

$$
\begin{aligned}
&Z_1 = \Phi(\alpha, \delta_{1,} \delta_1^{'}, \delta_2, \delta_2^{'}; x, y),\\
&Z_2 = x^{1-\delta_1} \cdot \Phi(\alpha + 1 - \delta_{1,}; 2 - \delta_1^{'}, \delta_1^{'}, \delta_2 + 1 - \delta_1, \delta_2^{'}; x, y),\\
&Z_3 = y^{1-\delta_1^{'}} \cdot \Phi(\alpha + 1 - \delta_{1,}^{'}, \delta_1; 2 - \delta_1^{'}, \delta_2, \delta_2^{'} + 1 - \delta_1^{'}; x, y),\\
&Z_4 = x^{1-\delta_2} \cdot \Phi(\alpha + 1 - \delta_2; \delta_1 + 1 - \delta\ , \delta_1^{'}, 2 - \delta_2^{'}; x, y),\\
&Z_5 = y^{1-\delta_2^{'}} \cdot \Phi(\alpha + 1 - \delta_2^{'}, \delta_1; \delta_1^{'} + 1 - \delta_2^{'}, 2 - \delta_2^{'}; x, y), \qquad (27)\\
&Z_6 = x^{1-\delta_1} \cdot y^{1-\delta_1^{'}} \cdot \Phi(\alpha + 2 - \delta_1, \delta_1^{'}; 2 - \delta_1, 2 - \delta_1^{'}, \delta_1^{'}, \delta_2 + 1 - \delta_1, \delta_2^{'} + 1 - \delta_1^{'}; x, y),\\
&Z_7 = x^{1-\delta_1} \cdot y^{1-\delta_2^{'}} \cdot \Phi(\alpha + 2 - \delta_1 - \delta_2^{'}; 2 - \delta_1, 2 - \delta_1 \cdot \delta_1^{'}, \delta_1^{'} + 1 - \delta_2^{'}, \delta_2 + 1 - \delta_1, 2 - \delta_1^{'}; x, y),\\
&Z_8 = x^{1-\delta_2} \cdot y^{1-\delta_2^{'}} \cdot \Phi(\alpha + 2 - \delta_2 - \delta_1, \delta_1 + 1 - \delta_2, 2 - \delta_1^{'} 2 - \delta_2, \delta_2^{'} + 1 - \delta_1^{'}; x, y),\\
&Z_9 = x^{1-\delta_2} \cdot y^{1-\delta_2^{'}} \cdot \Phi(\alpha + 2 - \delta_2 - \delta_2^{'}, \delta_1 + 1 - \delta_2, \delta_1 + 1 - \delta_2 . \delta_1^{'} + 1 - \delta_2^{'}, 2 - \delta_2, 2 - \delta_2^{'}; x, y).
\end{aligned}
$$

All the solutions obtained coincide exactly with the solutions in the monograph. [5, p.166].

Conclusions: We note some properties of the studied system and its solution.

Properties 1. The monograph [5] does not classify the regular and irregular features of the system (25). In system (25) $a_{10}^{(0)} = 0$ and $b_{01}^{(0)} = 0$. Therefore, on the basis of Rule II, we conclude that the peculiarity (∞, ∞) irregular and system (25) must have a solution in the form of a normal Tome series (14). However, in this case, the system of defining equations will be written as

$$f_{10}(\rho, \sigma) = -(\rho + \sigma + 2) = 0,$$
$$f_{01}(\rho, \sigma) = -(\rho + \sigma + 2) = 0$$

that is, it boils down to one equation and defines an infinite number of solutions. Then, due to the uncertainty of the indicators (ρ_t, σ_t) there is no solution in the form of a normal Tome series (14)

Properties 2. It is also not difficult to make sure that the solutions of system (25) presented in the form of (27) possess many properties of generalized hypergeometric series [5],[14]. Thus, the first derivatives (27) are represented as

$$
\begin{aligned}
&\frac{\partial Z_1}{\partial x} = \frac{\partial \Phi[\alpha, \delta_1, \delta_1^{'}, \delta_2, \delta_2^{'}; x, y]}{\partial x} = \frac{\alpha}{\delta_1 \cdot \delta_2} \cdot \Phi[\alpha + 1, \delta_1 + 1, \delta_1^{'}; 1 + \delta_2, \delta_2^{'}; x, y]\\
&\frac{\partial Z_1}{\partial y} = \frac{\partial \Phi[\alpha, \delta_1, \delta_1^{'}, \delta_2, \delta_2^{'}; x, y]}{\partial y} = \frac{\alpha}{\delta_1^{'} \cdot \delta_2^{'}} \cdot \Phi[\alpha + 1, \delta_1, \delta_1^{'} + 1, \delta_2, \delta_2^{'} + 1; x, y] \qquad (28)\\
&\frac{\partial Z_1}{\partial x \partial y} = \frac{\partial \Phi[\alpha, \delta_1, \delta_1^{'}, \delta_2, \delta_2^{'}; x, y]}{\partial x \partial y} = \frac{\alpha(\alpha + 1)}{\delta_1 \cdot \delta_2 \cdot \delta_1^{'} \cdot \delta_2^{'}} \cdot \Phi[\alpha + 2, \delta_1 + 1, \delta_1^{'} + 1, \delta_2 + 1, \delta_2^{'} + 1; x, y]
\end{aligned}
$$

Properties 3. The first solution $Z_1(x, y)$ represents a double row depending on five parameters $\alpha, \delta_1, \delta_2, \delta_1^{'}, \delta_2^{'}$ [14]:

$$Z_1(x, y) = {}_1\Phi_4 \begin{bmatrix} \alpha \\ \delta_1, \delta_1^{'}, \delta_2, \delta_2^{'} \end{bmatrix}; x, y = \sum_{m,n=0}^{\infty} \frac{(\alpha)_{m+n}}{(\delta_1)_m, (\delta_1^{'})_n (\delta_2)_m (\delta_2^{'})_n} \cdot \frac{x^m}{m!} \cdot \frac{x^n}{n!} \qquad (29)$$

In the same way, it can be verified that the remaining solutions (27) have similar properties, that is, all the functions listed in (27) are generalized hypergeometric functions [14], [19]. The question of the computational application of special functions of several variables, as in monographs, remains topical [20]. The development [21] of a numerical method for calculating the values of the degenerate hypergeometric Humbert functions is also required $\Psi_2(\alpha,\gamma,\gamma';x,y)$ through the products of Laguerre polynomials [22].

Ж.Н. Тасмамбетов[1], Н. Раджабов[2], Ж.К. Убаева[3]

[1]Қ.Жұбанов атындағы АӨМУ, Ақтөбе, Қазақстан;
[2]Тәжік ұлттық университеті, Душанбе, Тәжікстан;
[3]Қ.Жұбанов атындағы АӨМУ, Ақтөбе, Қазақстан

ҮШІНШІ РЕТТІ ДЕРБЕС ТУЫНДЫЛЫ ЕКІ ДИФФЕРЕНЦИАЛДЫҚ ТЕҢДЕУЛЕРДІҢ БІРЛЕСКЕН ШЕШІМІ

Аннотация. Мақалада үшінші ретті дербес туындылы екі дифференциалдық теңдеулерден тұратын арнайы жүйенің ерекше нүктелерінің маңайындағы шешімдерін тұрғызу мүмкіндіктері зерттелді. Мұндай жүйелердің айрықша ерекше нүктелері екінші ретті дербес туындылы екі дифференциалдық теңдеулерден тұратын жүйелермен салыстыру арқылы алынды. Регулярлы және иррегулярлы ерекшеліктеріне жіктеу жүргізіліп, олардың сәйкес шешімдері тұрғызылды. Нақты мысал арқылы үшінші ретті дербес туындылы екі дифференциалдық теңдеулерден тұратын туындалған гипергеометриялық жүйенің шешімін табуда Фробениус-Латышева әдісінің қолдануы келтірілген. Жүйе шешімдерінің бірқатар қасиеттері келтіріліп, бұл шешімдердің өзі жалпыланған гипергеометриялық функциялардың да қасиеттеріне ие екені көрсетілген.
Түйін сөздер: шешім, тұрғызылған, жүйе, ерекше нүктелер, регулярлы, иррегулярлы, жалпыланған, үшінші ретті.

УДК 517.946:517.588

Ж.Н. Тасмамбетов[1], Н. Раджабов[2], Ж.К. Убаева[3]

[1]АРГУ им. К.Жубанова, Актобе, Казахстан;
[2]Таджикский национальный университет, Таджикистан, Душанбе;
[3]АРГУ им. К.Жубанова, Актобе, Казахстан

СОВМЕСТНОЕ РЕШЕНИЕ ДВУХ ДИФФЕРЕНЦИАЛЬНЫХ УРАВНЕНИЙ В ЧАСТНЫХ ПРОИЗВОДНЫХ ТРЕТЬЕГО ПОРЯДКА

Аннотация. В работе изучена возможности построения решения вблизи различных особенностей специальной системы состоящим из двух дифференциальных уравнений в частных производных третьего порядка. Установлены отличительные особенности таких систем по сравнению с системами состоящих из двух дифференциальных уравнений в частных производных второго порядка. Проведена классификация регулярных и иррегулярных особенностей, построены соответствующие им решения. На конкретном примере показано применение метода Фробениуса-Латышевой к построению решения вырожденной гипергеометрической системы состоящих из двух дифференциальных уравнении в частных производных третьего порядка. Рассмотрены ряд свойств решения системы, которое показывает, что эти решения обладают свойствами обобщенных гипергеометрических функций.
Ключевые слова: решение, построены, система, особенности, регулярные, иррегулярные, обобщенная, третьего порядка.

Information about authors:

Tasmambetov Zhaksylyk Nuradinovych – Aqtobe Regional Zhubanov State University, Doctor of physical and mathematical sciences, Professor Chair of Mathematics, tasmam@rambler.ru;

Rajabov Nusrat – Tajik National University, Professor Chair Mathematical Analysis and Function Theory Tajik National University, Academician Academy of Science the Republic of Tajikistan, nusrat38@mail.ru;

Ubayeva Zhanar Kartbaevna– Phd Student of Aqtobe Regional Zhubanov State University, Zhanar_ubaeva@mail.ru.

REFERENCES

[1] Wilczynski E.J. Projective differential geometry of Curves and Ruled surfaces. Leipzig: Leubner , 1966-120pp.

[2] Wilczynski E.J. On a Certain Completery Integrable system of Linear. Partial Differential Equations // Amer. Journal of Math., 36, №3, 1994, p.180-194.

[3] Horn J. Uber die Convergenz der hypergeometrischen Reihen Zweierund drieier Veranderliechen //Math. Ann, 1889,v.34, p.544-600.

[4] Horn J. Uber das verhalten der Integrale Lineere Differenzen und Differentialgleichungen fur gobe der veranderliechen // Journal fur Math, 1910, v.138, p. 159-191.

[5] Appell P., Kampe de Feriet M.J. Fonctions hypergeometriques et hypersperiques. Paris: Gauthier Villars. 1926. -434 pp.

[6] Sternberg W. Uber dis asymptotiche Integration von Differential gleichungen. Marh. Ann., 1920, Bd.81, 119-186 pp.

[7] Erdelyi A. Same confluent Hypergeometric Functions of two variables. Proc. Roy. Sos Edinburgh, 1940, v.60, p.344-361.

[8] Erdelyi A. Same confluent Hypergeometric Functions of two variables. Acta. Math, 1950, v.83, p.130-163.

[9] Humbert P. The confluent Hypergeometric Functions of two variables. Proc. Roy. Sos. Edin., 1920, v.10, p.73-96.

[10] Ince E.L. Proc. Roy. Sos. Edinburgh, A61,1942, p.195-209.

[11] Borngusser L. Uber hypergeometrishe Functionen zweier Verander Lichen, Dissertation. Darmstsdt , 1933, 236 p.

[12] Bateman G., Erdelyi A. Higher Transcendental Functions. Part I. Hypergeometric functions. The functions of the Lezhanders. M.: Science, 1965, -294 pp. (In Russian).

[13] Slater L.J., Lit D., PH. D. Confluent hypergeometric series. Cambridge At the university Press, 1960.-249 pp.

[14] Slater L.J., Lit D., PH. D. Generalized Hypergeometric functions. Cambridge At the university Press, 1966.-292 pp.

[15] Tasmambetov Zh.N. Construction of normal and normally-regular solutions of special systems of partial equations of second order. IP Zhanadilov S.T., Actobe, 2015, 463pp. (In Russian).

[16] Kampe de Feriet J. Fonctions de la physique Mathematique. Fascicule IX, M.: 1963, 102 pp. (In Russian).

[17] Kampe de Feriet J. Quelques proprietis des fonctions hypergeometriques dordre superieur a deux variables. Comptes rendus, t. CLXXIII, 1921, p.489

[18] Latysheva K.Ya., Tereschenko N.I., Orel N.S. Normal-regular solutions and their applications. Kiev, v.sh., 1974, p.136. (In Russian).

[19] Bailey WN. Generalized hypergeometric series. Cambridge Mathematical Tract. 1935, №32 (Second edition 1964). Cambridge University Press.

[20] Luke Yedell L. Mathematical funktions and their approximations. Academic Rpess.Jue. New York- San Francisco - London. 1975.608 p.

[21] Dzhumabaev D.S., Bakirova EA., Kadirbayeva ZhM. (2018) An algorithm for solving a control problem for a differential Equation with a parameter. News of the National Academy of Sciences of the Republic of Kazakhstan. Series of physic-mathematical sciences. Volume 5, Number 321(2018), pp. 25-32. https://doi.org/10.32014/2018.2518-1726.4 ISSN 1991-346X. ISSN 2518-1726 (Online), ISSN 1991-346X (Print).

[22] Tasmambetov Zh.N., Rajabov N., Issenova A.A. (2019) The construction of a solution of a related system of the laguerre type. New of the National Academy of Sciences of the Republic of Kazakhstan. Series of physic-mathematical sciences. Volume 1, Number 323(2019), pp. 38-45. https://doi.org/10.32014/2019.2518-1726.5

ISSN 1991- 346X. ISSN 2518-1726 (Online), ISSN 1991-346X (Print).

N E W S
OF THE NATIONAL ACADEMY OF SCIENCES OF THE REPUBLIC OF KAZAKHSTAN
PHYSICO-MATHEMATICAL SERIES
ISSN 1991-346X **https://doi.org/10.32014/2019.2518-1726.48**
Volume 4, Number 326 (2019), 92 – 109

UDK 517.958

B. Bekbolat[1], D. B. Nurakhmetov[2], N. Tokmagambetov[3], G. H. Aimal Rasa[4]

[1,3,4]Al–Farabi Kazakh National University, Almaty, Kazakhstan
[2]S.Seifullin Kazakh Agro Technical University, Astana, Kazakhstan
[3]Ghent University, Ghent, Belgium
[1,3]Institute of Mathematics and Mathematical Modeling, Almaty, Kazakhstan
bekbolat@math.kz, dauletkaznu@gmail.com,
niyaz.tokmagambetov@gmail.com, aimal.rasa14@gmail.ru

ON THE MINIMALITY OF SYSTEMS OF ROOT FUNCTIONS OF THE LAPLACE OPERATOR IN THE PUNCTURED DOMAIN

Abstract. In this paper, we consider the Laplace operator in a punctured domain, which generates a class of "new" correctly solvable boundary value problems. And for this class of problems the resolvent formula is obtained. Also described are meromorphic functions that generate the root functions of the class of problems studied. The main goal is to study the minimality of root function systems. The paper is a continuation of [8], where a description is given of correctly solvable boundary value problems for the Laplace operator in punctured domains. The Laplace operator in the punctured domain, which generates the class of "new" correctly solvable boundary value problems, is considered, and the resolvent formula is obtained for the generated problems, and meromorphic functions are described that induce systems of functions. One of these systems is a system of eigenfunctions and associated functions. The last section is devoted to the study of the minimality of the system of root functions.

Key words: Laplace operator, punctured domain, resolvent, meromorphic function, correctly solvable boundary value problems, root functions system, minimal system.

1 Introduction

Operators of the form $L+K$, where $L=\Delta$ is the Laplace operator, and K is the operator of multiplication by a generalized function, appeared in the physical works of the 30s in connection with the problem of scattering neutral particles on the nucleus, when the interaction is strong at small distances and negligibly small to medium to large [1]. The model potential of such an interaction is the Dirac δ-function. A mathematical study of the operator $-\Delta+\mu\delta(x)$ was undertaken by Berezin and Fadeev [2], Minlos and Fadeev [3], Berezin [4]. In [2, 3], the operator $-\Delta+\mu\delta(x)$ was understood as an extension of the operator $L_0=-\Delta$ with the definition domain $D(L_0)=C_0^\infty(\mathbb{R}^3\backslash\{0\})$. Interesting are the works [5, 6], where the following important question was studied: if the operator $-\Delta+q$ with a singular potential q is already defined, can it be approximated in some sense by operators with smooth potentials so that the corresponding operators approximate the original in the sense of resolvent convergence. The paper [7] investigated the spectral properties of the Schrödinger operator with point interactions using positive definite functions. For complete review, see marked work and links to them.

The paper is a continuation of [8], where a description is given of correctly solvable boundary value problems for the Laplace operator in punctured domains. The Laplace operator in the punctured domain, which generates the class of "new" correctly solvable boundary value problems, is considered, and the resolvent formula is obtained for the generated problems, and meromorphic functions are described that induce systems of functions. One of these systems is a system of eigenfunctions and associated functions. The last section is devoted to the study of the minimality of the system of root functions.

Consider a differential expression

$$\Delta W(x,y) := \frac{\partial^2 W(x,y)}{\partial x^2} + \frac{\partial^2 W(x,y)}{\partial y^2}$$

in the punctured area $\Omega_0 = \Omega \backslash \{(x_0, y_0)\}$, here $\Omega = \{x^2 + y^2 < 1\}$ and (x_0, y_0) is internal fixed point of area Ω. We Turn from the expression $\Delta W(x,y)$ to the operator L_{σ_1} in the space $\mathbb{L}_2(\Omega)$.

Denote by $\mathcal{D}$ the set of all functions

$$h(x,y) = h_1(x,y) + \alpha\, G(x,y,x_0,y_0), (x,y) \in \Omega_0,$$

where $\alpha \in \mathbb{R}$, $h_1 \in \mathbb{D} = \{h_1 \in \mathbb{W}_2^2(\Omega), h_1|_{\partial\Omega} = 0\}$. Here and after $G(x,y,x_0,y_0)$ is Green function of the Dirichlet problem for the Laplace operator in Ω [9].

For $h(x,y) \in \mathcal{D}$ we introduce functionals

$$\alpha(h) = \frac{1}{2}\lim_{\delta\to+0}\left\{\int_{y_0-\delta}^{y_0+\delta}\left[\frac{\partial h(x_0+\delta,y)}{\partial x} - \frac{\partial h(x_0-\delta,y)}{\partial x}\right]dy + \right.$$

$$\left.\int_{x_0-\delta}^{x_0+\delta}\left[\frac{\partial h(x,y_0+\delta)}{\partial y} - \frac{\partial h(x,y_0-\delta)}{\partial y}\right]dx\right\},$$

$$\beta(h) = \lim_{\delta\to+0}\int_{y_0-\delta}^{y_0+\delta}[h(x_0-\delta,y) - h(x_0+\delta,y)]dy,$$

$$\gamma(h) = \lim_{\delta\to+0}\int_{x_0-\delta}^{x_0+\delta}[h(x,y_0-\delta) - h(x,y_0+\delta)]dx.$$

Note that, the introduced functionals were first obtained in [8] to describe correctly solvable boundary value problems for the Laplace operator in the punctured domain Ω_0.

Consider in the space $\mathbb{L}_2(\Omega)$ the operator L_{σ_1} generated by the differential equation

(1.1) $$W(x,y) = f(x,y),\ (x,y) \in \Omega_0,$$

with external boundary condition

(1.2) $$W(x,y)|_{\partial\Omega} = 0,$$

and "internal boundary conditions"

(1.3) $$\frac{1}{2}\lim_{\delta\to+0}\int_{y_0-\delta}^{y_0+\delta}\left[\frac{\partial W(x_0+\delta,y)}{\partial x} - \frac{\partial W(x_0-\delta,y)}{\partial x}\right]dy +$$

$$+\frac{1}{2}\lim_{\delta\to+0}\int_{x_0-\delta}^{x_0+\delta}\left[\frac{\partial W(x,y_0+\delta)}{\partial y} - \frac{\partial W(x,y_0-\delta)}{\partial y}\right]dx - < \Delta W(x,y), \sigma_1(x,y) >= 0,$$

(1.4) $$\lim_{\delta\to+0}\int_{y_0-\delta}^{y_0+\delta}[W(x_0-\delta,y) - W(x_0+\delta,y)]dy = 0,$$

(1.5) $$\lim_{\delta\to+0}\int_{x_0-\delta}^{x_0+\delta}[W(x,y_0-\delta) - W(x,y_0+\delta)]dx = 0,$$

where $f(x,y), \sigma_1(x,y) \in \mathbb{L}_2(\Omega)$, $< f(x,y), \sigma_1(x,y) >$ mean inner product in $\mathbb{L}_2(\Omega)$.

2 Auxiliary statements

In the sequel, we will need a well-known statement from [10].

Theorem A. *Let $h(x,y) \in \mathcal{D}$ and there exists functional $\alpha(h)$. Then function*

$$W(x,y) = \iint\limits_{\Omega} G(x,y,\xi,\eta) f(\xi,\eta) d\xi d\eta + \int_{\partial\Omega} \frac{\partial G(x,y,\xi,\eta)}{\partial \overline{n}_{\xi\eta}} h(\xi,\eta) ds_{\xi,\eta} -$$

$$-\alpha(h) G(x,y,x_0,y_0) - \beta(h) \frac{\partial G(x,y,x_0,y_0)}{\partial \xi} - \gamma(h) \frac{\partial G(x,y,x_0,y_0)}{\partial \eta}$$

is uniqueness solution of the problem

(2.1) $$\Delta W(x,y) = f(x,y), (x,y) \in \Omega_0,$$

(2.2) $$W(x,y)|_{\partial\Omega} = h(x,y)|_{\partial\Omega},$$

(2.3) $$\frac{1}{2} \lim_{\delta \to +0} \int_{y_0-\delta}^{y_0+\delta} \left[\frac{\partial W(x_0+\delta,y)}{\partial x} - \frac{\partial W(x_0-\delta,y)}{\partial x} \right] dy +$$

$$+\frac{1}{2} \lim_{\delta \to +0} \int_{x_0-\delta}^{x_0+\delta} \left[\frac{\partial W(x,y_0+\delta)}{\partial y} - \frac{\partial W(x,y_0-\delta)}{\partial y} \right] dx = \alpha(h).$$

(2.4) $$\lim_{\delta \to +0} \int_{y_0-\delta}^{y_0+\delta} [W(x_0-\delta,y) - W(x_0+\delta,y)] dy = \beta(h),$$

(2.5) $$\lim_{\delta \to +0} \int_{x_0-\delta}^{x_0+\delta} [W(x,y_0-\delta) - W(x,y_0+\delta)] dx = \gamma(h).$$

Here $G(x,y,\xi,\eta)$ is Green function of the Dirichlet problem in Ω [9].

If we assume that $h(x,y) \in \mathcal{D}$ in a continuous manner in Ω_0 in the norm of $\mathbb{L}_2$ depends on the right side $f(x,y) \in \mathbb{L}_2(\Omega)$, then the outer boundary condition (2.2) takes the form

(2.6) $$W(x,y)|_{\partial\Omega} =< \Delta W(x,y), \sigma_0(x,y) >,$$

and the internal boundary conditions (2.3)-(2.5) will take the following types

(2.7) $$\frac{1}{2} \lim_{\delta \to +0} \int_{y_0-\delta}^{y_0+\delta} \left[\frac{\partial W(x_0+\delta,y)}{\partial x} - \frac{\partial W(x_0-\delta,y)}{\partial x} \right] dy +$$

$$+\frac{1}{2} \lim_{\delta \to +0} \int_{x_0-\delta}^{x_0+\delta} \left[\frac{\partial W(\xi,y_0+\delta)}{\partial y} - \frac{\partial W(\xi,y_0-\delta)}{\partial y} \right] dx =< \Delta W(x,y), \sigma_1(x,y) >.$$

(2.8) $$\lim_{\delta \to +0} \int_{y_0-\delta}^{y_0+\delta} [W(x_0-\delta,y) - W(x_0+\delta,y)] dy =< \Delta W(x,y), \sigma_2(x,y) >,$$

(2.8) $$\lim_{\delta \to +0} \int_{x_0-\delta}^{x_0+\delta} [W(x,y_0-\delta) - W(x,y_0+\delta)] dx =< \Delta W(x,y), \sigma_3(x,y) >,$$

where $\sigma_j(x,y) \in \mathbb{L}_2(\Omega), j = \overline{0,3}$.

For clarity of results, we assume that $\sigma_j(x,y) \equiv 0, j = 0,2,3$. For the operator L_{σ_1} the following theorem is true.

Theorem 1. Function

(2.10) $W(x,y) = \iint_{\Omega} G(x,y,\xi,\eta)f(\xi,\eta)d\xi d\eta + < f(\xi,\eta), \sigma_1(\xi,\eta) > G(x,y,x_0,y_0)$

represents the only solution for all right-hand sides $f(x,y) \in \mathbb{L}_2(\Omega)$ of problem (1.1)-(1.5).
For prove theorem 1 we will use well known lemmas from [11]:

Lemma A. For any continuously differentiable function $g(x,y)$ the following equalities are true:

$$\lim_{\delta\to+0} \int_{y_0-\delta}^{y_0+\delta} \left[\frac{\partial g(x_0+\delta,y)}{\partial x} - \frac{\partial g(x_0-\delta,y)}{\partial x}\right] dy +$$

$$\lim_{\delta\to+0} \int_{x_0-\delta}^{x_0+\delta} \left[\frac{\partial g(x,y_0+\delta)}{\partial y} - \frac{\partial g(x,y_0-\delta)}{\partial y}\right] dx = 0,$$

$$\lim_{\delta\to+0} \int_{y_0-\delta}^{y_0+\delta} [g(x_0-\delta,y) - g(x_0+\delta,y)]dy = 0,$$

$$\lim_{\delta\to+0} \int_{x_0-\delta}^{x_0+\delta} [g(x,y_0-\delta) - g(x,y_0+\delta)]dx = 0.$$

Lemma B. For function $G(x,y,x_0,y_0)$ the following equalities are true:

$$\alpha(G) = \frac{1}{2}\lim_{\delta\to+0} \int_{y_0-\delta}^{y_0+\delta} \left[\frac{\partial G(x_0+\delta,y,x_0,y_0)}{\partial x} - \frac{\partial G(x_0-\delta,y,x_0,y_0)}{\partial x}\right] dy +$$

$$+\frac{1}{2}\lim_{\delta\to+0} \int_{x_0-\delta}^{x_0+\delta} \left[\frac{\partial G(x,y_0+\delta,x_0,y_0)}{\partial y} - \frac{\partial G(x,y_0-\delta,x_0,y_0)}{\partial y}\right] dx = 1,$$

$$\beta(G) = \lim_{\delta\to+0} \int_{x_0-\delta}^{x_0+\delta} \left[\frac{\partial G(x,y_0+\delta,x_0,y_0)}{\partial y} - \frac{\partial G(x,y_0-\delta,x_0,y_0)}{\partial y}\right] dx = 0,$$

$$\gamma(G) = \lim_{\delta\to+0} \int_{x_0-\delta}^{x_0+\delta} [G(x,y_0-\delta,x_0,y_0) - G(x,y_0+\delta,x_0,y_0)]dx = 0.$$

Now, we proof the theorem 1.

Proof. Let us show that equation (1.1) holds for $W(x,y)$. Operate the operator Laplace to the (2.10):

$$\Delta W(x,y) = \Delta\left(\iint\limits_{\Omega} G(x,y,\xi,\eta)f(\xi,\eta)d\xi d\eta\right) +$$

$$\langle f(\xi,\eta), \sigma_1(\xi,\eta)\rangle \Delta(G(x,y,x_0,y_0)) = f(x,y)$$

when $(x,y) \in \Omega_0$, as by the Green function property $\Delta\left(\iint_{\Omega} G(x,y,\xi,\eta)f(\xi,\eta)d\xi d\eta\right) = f(x,y)$ and $\Delta(G(x,y,x_0,y_0)) = 0$.

The validity of the first condition follows from the properties of the Green function.
Check the second condition

$$\alpha(W) - < \Delta W(x,y), \sigma_1(x,y) > =$$

$$\alpha\left(\iint_{\Omega} G(x,y,\xi,\eta)f(\xi,\eta)d\xi d\eta\right) - < \Delta\left(\iint_{\Omega} G(x,y,\xi,\eta)f(\xi,\eta)d\xi d\eta\right), \sigma_1(x,y) >$$

$$+ < f(\xi,\eta), \sigma(\xi,\eta) > \alpha\big(G(x,y,x_0,y_0)\big) - < f(\xi,\eta), \sigma_1(\xi,\eta) >$$

$$< \Delta G(x,y,x_0,y_0), \sigma_1(\xi,\eta) > = 0,$$

as by the Green function property $\Delta\big(\iint_{\Omega} G(x,y,\xi,\eta)f(\xi,\eta)d\xi d\eta\big) = f(x,y)$ and $\Delta(G(x,y,x_0,y_0)) = 0$. And also by Lemma B $\alpha(G) = 1$. By Lemma B $\alpha\big(\iint_{\Omega} G(x,y,\xi,\eta)f(\xi,\eta)d\xi d\eta\big) = 0$, as a function $u(x,y) = \alpha\big(\iint_{\Omega} G(x,y,\xi,\eta)f(\xi,\eta)d\xi d\eta\big)$ is a twice differentiable function.

Check the third condition

$$\beta(W) = \beta\left(\iint_{\Omega} G(x,y,\xi,\eta)f(\xi,\eta)d\xi d\eta\right) +$$

$$< f(\xi,\eta), \sigma_1(\xi,\eta) > \beta\big(G(x,y,x_0,y_0)\big) = 0.$$

By Lemma A $\beta\big(\iint_{\Omega} G(x,y,\xi,\eta)f(\xi,\eta)d\xi d\eta\big) = 0$, as a function $u(x,y) = \alpha\big(\iint_{\Omega} G(x,y,\xi,\eta)f(\xi,\eta)d\xi d\eta\big)$ is a twice differentiable function. And also by Lemma B $\beta(G(x,y,x_0,y_0)) = 0$.

Check the fourth condition

$$\gamma(W) = \gamma\left(\iint_{\Omega} G(x,y,\xi,\eta)f(\xi,\eta)d\xi d\eta\right) +$$

$$< f(\xi,\eta), \sigma_1(\xi,\eta) > \gamma\big(G(x,y,x_0,y_0)\big) = 0.$$

By Lemma A $\gamma(G(x,y,x_0,y_0)) = 0$, as a function $u(x,y) = \alpha\big(\iint_{\Omega} G(x,y,\xi,\eta)f(\xi,\eta)d\xi d\eta\big)$ is a twice differentiable function. By Lemma B $\gamma\big(\iint_{\Omega} G(x,y,\xi,\eta)f(\xi,\eta)d\xi d\eta\big) = 0$.

Theorem 1 is completely proved.

3 The resolvent of correct internal boundary value problems for the Laplace operator in a punctured domain

In this section in the functional space $\mathbb{W}_2^2(\Omega_0) \cap \mathbb{C}(\Omega)$, we calculate the explicit form of the resolvent for a wider class of operators $L_{\sigma_1\sigma_2\sigma_3} =: L$, generated by the differential equation (2.1) and internal boundary conditions (2.6)-(2.9) with $\sigma_0(\cdot,\cdot) \equiv 0$. The explicit form of the resolvent plays an essential role in studies of the spectral properties of the operator L. For convenience, we introduce the notation

$$T_1(x,y) := G(x,y,x_0,y_0), T_2(x,y) := \frac{\partial G(x,y,x_0,y_0)}{\partial \xi}, T_3(x,y) := \frac{\partial G(x,y,x_0,y_0)}{\partial \eta},$$

$$\kappa_j(x,y,\lambda) = L_0(L_0 - \lambda I)^{-1}T_j, j = 1,2,3.$$

We formulate the main result of this section.

Theorem 2. The resolvent of the operator L represents an operator-valued function of the spectral parameter λ and has the following representation:

$$(L - \lambda I)^{-1}f(x,y) = -\frac{H(f)}{d(\lambda)}, \quad (3.1)$$

$$H(f) = \begin{vmatrix} \kappa_1(x,y,\lambda) & \kappa_2(x,y,\lambda) & \kappa_3(x,y,\lambda) & (L_0-\lambda I)^{-1}f(x,y) \\ 1-\lambda\tilde{\alpha}(\kappa_1(x,y,\lambda)) & -\lambda\tilde{\alpha}(\kappa_2(x,y,\lambda)) & -\lambda\tilde{\alpha}\big(\kappa_3(x,y,\lambda)\big) & -\tilde{\alpha}(L_0(L_0-\lambda I)^{-1}f(x,y)) \\ -\lambda\tilde{\beta}(\kappa_1(x,y,\lambda)) & 1-\lambda\tilde{\beta}(\kappa_2(x,y,\lambda)) & -\lambda\tilde{\beta}(\kappa_3(x,y,\lambda)) & -\tilde{\beta}(L_0(L_0-\lambda I)^{-1}f(x,y)) \\ -\lambda\tilde{\gamma}(\kappa_1(x,y,\lambda)) & -\lambda\tilde{\gamma}(\kappa_2(x,y,\lambda)) & 1-\lambda\tilde{\gamma}(\kappa_3(x,y,\lambda)) & -\tilde{\gamma}(L_0(L_0-\lambda I)^{-1}f(x,y)) \end{vmatrix},$$

$$d(\lambda) = \begin{vmatrix} 1-\lambda\tilde{\alpha}(\kappa_1(x,y,\lambda)) & -\lambda\tilde{\alpha}(\kappa_2(x,y,\lambda)) & -\lambda\tilde{\alpha}(\kappa_3(x,y,\lambda)) \\ -\lambda\tilde{\beta}(\kappa_1(x,y,\lambda)) & 1-\lambda\tilde{\beta}(\kappa_2(x,y,\lambda)) & -\lambda\tilde{\beta}(\kappa_3(x,y,\lambda)) \\ -\lambda\tilde{\gamma}(\kappa_1(x,y,\lambda)) & -\lambda\tilde{\gamma}(\kappa_2(x,y,\lambda)) & 1-\lambda\tilde{\gamma}(\kappa_3(x,y,\lambda)) \end{vmatrix},$$

where

$$\kappa_j(x,y,\lambda) := L_0(L_0-\lambda I)^{-1}T_j(x,y),\ j=1,2,3,$$

$$\tilde{\alpha}\left(\kappa_j(x,y,\lambda)\right) = < \kappa_j(x,y,\lambda), \sigma_1(x,y) >, \tilde{\beta}\left(\kappa_j(x,y,\lambda)\right) =$$
$$< \kappa_j(x,y,\lambda), \sigma_2(x,y) >,$$
$$\tilde{\gamma}\left(\kappa_j(x,y,\lambda)\right) = < \kappa_j(x,y,\lambda), \sigma_3(x,y) >, \tilde{\alpha}(L_0(L_0-\lambda I)^{-1}f(x,y)) =$$
$$< L_0(L_0-\lambda I)^{-1}f(x,y), \sigma_1(x,y) >,$$
$$\tilde{\beta}(L_0(L_0-\lambda I)^{-1}f(x,y)) = < L_0(L_0-\lambda I)^{-1}f(x,y), \sigma_2(x,y) >,$$
$$\tilde{\gamma}(L_0(L_0-\lambda I)^{-1}f(x,y)) = < L_0(L_0-\lambda I)^{-1}f(x,y), \sigma_3(x,y) >.$$

Here L_0 is discred operator, corresponding to the Dirichlet problem.
Proof. In paper [12] the following relation was proved for the resolvent of the operator L:

(3.2)
$$(L-\lambda I)^{-1}f(x,y) = (L_0-\lambda I)^{-1}f(x,y) +$$
$$\sum_{j=1}^{3} < L_0(L_0-\lambda I)^{-1}f(x,y), \sigma_j(x,y) > L(L-\lambda I)^{-1}T_j(x,y).$$

Set $f(x,y) = T_1(x,y)$. Then we have

$$(L-\lambda I)^{-1}T_1(x,y) = (L_0-\lambda I)^{-1}T_1(x,y) +$$
$$\sum_{j=1}^{3} < L_0(L_0-\lambda I)^{-1}T_1(x,y), \sigma_j(x,y) > L(L-\lambda I)^{-1}T_j(x,y).$$

We act on the obtained relation with the operator Δ. Recall that
1) when $u \in D(L)$ we have $\Delta u = Lu$;
2) when $u \in D(L_0)$ we obtain $\Delta u = L_0 u$. As a result, we get

(3.3)
$$(1-\lambda < \kappa_1(x,y,\lambda), \sigma_1(x,y) >)L(L-\lambda I)^{-1}T_1(x,y) =$$
$$L_0(L_0-\lambda I)^{-1}T_1(x,y) + \sum_{j=2}^{3} \lambda < \kappa_1(x,y), \sigma_j(x,y) > L(L-\lambda I)^{-1}T_j(x,y).$$

Here it is taken into account that $(L_0-\lambda I)^{-1}T_1(x,y) \in D(L_0)$ and $(L-\lambda I)^{-1}T_j(x,y) \in D(L)$ when $j = 1,2,3$.

Now, assume $f(x,y) = T_2(x,y)$. Then from similar reasoning we have

$$(L-\lambda I)^{-1}T_2(x,y) = (L_0-\lambda I)^{-1}T_2(x,y) +$$

$$\sum_{j=1}^{3} < L_0(L_0-\lambda I)^{-1}T_2(x,y), \sigma_j(x,y) > L(L-\lambda I)^{-1}T_j(x,y).$$

We act on the obtained relation by the Laplace operator. As a result, we get that

(3.4) $$(1-\lambda < \kappa_2(x,y,\lambda), \sigma_2(x,y) >)L(L-\lambda I)^{-1}T_2(x,y) =$$

$$L_0(L_0-\lambda I)^{-1}T_2(x,y) + \lambda < \kappa_2(x,y), \sigma_1(x,y) > L(L-\lambda I)^{-1}T_1(x,y)$$

$$+\lambda < \kappa_2(x,y), \sigma_3(x,y) > L(L-\lambda I)^{-1}T_3(x,y).$$

When $f(x,y) = T_3(x,y)$, we have

$$(L-\lambda I)^{-1}T_3(x,y) = (L_0-\lambda I)^{-1}T_3(x,y) +$$

$$\sum_{j=1}^{3} < L_0(L_0-\lambda I)^{-1}T_3(x,y), \sigma_j(x,y) > L(L-\lambda I)^{-1}T_j(x,y).$$

We act on the obtained relation by the Laplace operator. As a result, we get that

(3.5) $$(1-\lambda < \kappa_3(x,y,\lambda), \sigma_1(x,y) >)L(L-\lambda I)^{-1}T_3(x,y) =$$

$$L_0(L_0-\lambda I)^{-1}T_3(x,y) + + \sum_{j=1}^{2} \lambda < \kappa_3(x,y), \sigma_j(x,y) > L(L-\lambda I)^{-1}T_j(x,y).$$

Relations (3.2)-(3.5) constitute a homogeneous system of algebraic equations, which takes the matrix form

$$\begin{bmatrix} 0 & 0 & 0 & 0 \end{bmatrix} =$$

$$= \begin{bmatrix} 1 & -L(L-\lambda I)^{-1}T_1(x,y) & -L(L-\lambda I)^{-1}T_2(x,y) & -L(L-\lambda I)^{-1}T_3(x,y) \end{bmatrix}.$$

.

$$\begin{bmatrix} \kappa_1(x,y,\lambda) & \kappa_2(x,y,\lambda) & \kappa_3(x,y,\lambda) & (L_0-\lambda I)^{-1}f(x,y) - (L-\lambda I)^{-1}f(x,y) \\ 1-\lambda\tilde{\alpha}(\kappa_1(x,y,\lambda)) & -\lambda\tilde{\alpha}(\kappa_2(x,y,\lambda)) & -\lambda\tilde{\alpha}(\kappa_3(x,y,\lambda)) & -\tilde{\alpha}(L_0(L_0-\lambda I)^{-1}f(x,y)) \\ -\lambda\tilde{\beta}(\kappa_1(x,y,\lambda)) & 1-\lambda\tilde{\beta}(\kappa_2(x,y,\lambda)) & -\lambda\tilde{\beta}(\kappa_3(x,y,\lambda)) & -\tilde{\beta}(L_0(L_0-\lambda I)^{-1}f(x,y)) \\ -\lambda\tilde{\gamma}(\kappa_1(x,y,\lambda)) & -\lambda\tilde{\gamma}(\kappa_2(x,y,\lambda)) & 1-\lambda\tilde{\gamma}(\kappa_3(x,y,\lambda)) & -\tilde{\gamma}(L_0(L_0-\lambda I)^{-1}f(x,y)) \end{bmatrix}$$

It is known from the course of linear algebra that a homogeneous system of equations has a non-trivial solution for

$$\begin{vmatrix} \kappa_1(x,y,\lambda) & \kappa_2(x,y,\lambda) & \kappa_3(x,y,\lambda) & (L_0-\lambda I)^{-1}f(x,y)-(L-\lambda I)^{-1}f(x,y) \\ 1-\lambda\tilde{\alpha}(\kappa_1(x,y,\lambda)) & -\lambda\tilde{\alpha}(\kappa_2(x,y,\lambda)) & -\lambda\tilde{\alpha}(\kappa_3(x,y,\lambda)) & -\tilde{\alpha}(L_0(L_0-\lambda I)^{-1}f(x,y)) \\ -\lambda\tilde{\beta}(\kappa_1(x,y,\lambda)) & 1-\lambda\tilde{\beta}(\kappa_2(x,y,\lambda)) & -\lambda\tilde{\beta}(\kappa_3(x,y,\lambda)) & -\tilde{\beta}(L_0(L_0-\lambda I)^{-1}f(x,y)) \\ -\lambda\tilde{\gamma}(\kappa_1(x,y,\lambda)) & -\lambda\tilde{\gamma}(\kappa_2(x,y,\lambda)) & 1-\lambda\tilde{\gamma}(\kappa_3(x,y,\lambda)) & -\tilde{\gamma}(L_0(L_0-\lambda I)^{-1}f(x,y)) \end{vmatrix} = 0.$$

According to the standard properties of the determinants, we can write the equality

$$\begin{vmatrix} \kappa_1(x,y,\lambda) & \kappa_2(x,y,\lambda) & \kappa_3(x,y,\lambda) & (L-\lambda I)^{-1}f(x,y) \\ 1-\lambda\tilde{\alpha}(\kappa_1(x,y,\lambda)) & -\lambda\tilde{\alpha}(\kappa_2(x,y,\lambda)) & -\lambda\tilde{\alpha}(\kappa_3(x,y,\lambda)) & 0 \\ -\lambda\tilde{\beta}(\kappa_1(x,y,\lambda)) & 1-\lambda\tilde{\beta}(\kappa_2(x,y,\lambda)) & -\lambda\tilde{\beta}(\kappa_3(x,y,\lambda)) & 0 \\ -\lambda\tilde{\gamma}(\kappa_1(x,y,\lambda)) & -\lambda\tilde{\gamma}(\kappa_2(x,y,\lambda)) & 1-\lambda\tilde{\gamma}(\kappa_3(x,y,\lambda)) & 0 \end{vmatrix} =$$

$$= \begin{vmatrix} \kappa_1(x,y,\lambda) & \kappa_2(x,y,\lambda) & \kappa_3(x,y,\lambda) & (L_0-\lambda I)^{-1}f(x,y) \\ 1-\lambda\tilde{\alpha}(\kappa_1(x,y,\lambda)) & -\lambda\tilde{\alpha}(\kappa_2(x,y,\lambda)) & -\lambda\tilde{\alpha}(\kappa_3(x,y,\lambda)) & -\tilde{\alpha}(L_0(L_0-\lambda I)^{-1}f(x,y)) \\ -\lambda\tilde{\beta}(\kappa_1(x,y,\lambda)) & 1-\lambda\tilde{\beta}(\kappa_2(x,y,\lambda)) & -\lambda\tilde{\beta}(\kappa_3(x,y,\lambda)) & -\tilde{\beta}(L_0(L_0-\lambda I)^{-1}f(x,y)) \\ -\lambda\tilde{\gamma}(\kappa_1(x,y,\lambda)) & -\lambda\tilde{\gamma}(\kappa_2(x,y,\lambda)) & 1-\lambda\tilde{\gamma}(\kappa_3(x,y,\lambda)) & -\tilde{\gamma}(L_0(L_0-\lambda I)^{-1}f(x,y)) \end{vmatrix}$$

This implies the assertion of Theorem 2.

From the explicit resolvent formula for the operator L, it is not difficult to see that the resolvent is a meromorphic operator-valued function, since the characteristic determinant $d(\lambda)$ may have poles in the spectrum of the operator L_0. Since the spectrum of the Dirichlet problem for the Laplace equation is canonical restricted domains can be explicitly computed, then these poles are written out explicitly.

Corollary 1. The resolvent of the operator L can also be represented as

(3.6) $$(L-\lambda I)^{-1}f(x,y) = (L_0-\lambda I)^{-1}f(x,y) - \frac{\widetilde{H}(f)}{d(\lambda)}$$

where

$$\widetilde{H}(f) = \begin{bmatrix} \kappa_1(x,y,\lambda) & \kappa_2(x,y,\lambda) & \kappa_3(x,y,\lambda) & 0 \\ 1-\lambda\tilde{\alpha}(\kappa_1(x,y,\lambda)) & -\lambda\tilde{\alpha}(\kappa_2(x,y,\lambda)) & -\lambda\tilde{\alpha}(\kappa_3(x,y,\lambda)) & -\tilde{\alpha}(L_0(L_0-\lambda I)^{-1}f(x,y)) \\ -\lambda\tilde{\beta}(\kappa_1(x,y,\lambda)) & 1-\lambda\tilde{\beta}(\kappa_2(x,y,\lambda)) & -\lambda\tilde{\beta}(\kappa_3(x,y,\lambda)) & -\tilde{\beta}(L_0(L_0-\lambda I)^{-1}f(x,y)) \\ -\lambda\tilde{\gamma}(\kappa_1(x,y,\lambda)) & -\lambda\tilde{\gamma}(\kappa_2(x,y,\lambda)) & 1-\lambda\tilde{\gamma}(\kappa_3(x,y,\lambda)) & -\tilde{\gamma}(L_0(L_0-\lambda I)^{-1}f(x,y)) \end{bmatrix}$$

Corollary 2. In particular, if $\sigma_j(x,y) \equiv 0, j = 2,3$, then the operator's resolution L_{σ_1} take the form

(3.7) $$(L_{\sigma_1}-\lambda I)^{-1}f(x,y) = (L_0-\lambda I)^{-1}f(x,y) + \frac{\tilde{\alpha}(\kappa_1(x,y,\lambda))}{d(\lambda)}\kappa_1(x,y,\lambda),$$

where

(3.8) $$d(\lambda) = 1-\lambda\tilde{\alpha}(\kappa_1(x,y,\lambda)) = 1-\lambda < \kappa_1(x,y,\lambda), \sigma(x,y) >.$$

4 Meromorphic function generating root functions operator L_{σ_1}

In further research we will need some properties $\kappa_1(x,y,\lambda)$.

Lemma 1. Meromorphic function $\kappa_1(x,y,\lambda)$ is the main solution of the homogeneous equation

$$\Delta(\kappa_1(x,y,\lambda)) = \lambda\kappa_1(x,y,\lambda),$$

satisfying linear conditions

$$\kappa_1(x,y,\lambda)|_{\partial\Omega} = 0,$$

$$\alpha(\kappa_1(x,y,\lambda)) - < \Delta(\kappa_1(x,y,\lambda)), \sigma_1(x,y) >= d(\lambda),$$

$$\beta(\kappa_1(x,y,\lambda)) = 0,$$

$$\gamma(\kappa_1(x,y,\lambda)) = 0,$$

where $d(\lambda)$ is define by (3.8).

Proof. Check that the function $\kappa_1(x,y,\lambda)$ is a solution of the homogeneous equation

$$\Delta(\kappa_1(x,y,\lambda)) = \Delta(T_1(x,y)) + \lambda L_0(L_0 - \lambda I)^{-1}T_1(x,y) = \lambda\kappa_1(x,y,\lambda).$$

Here it is taken into account that $\Delta(T_1(x,y)) = 0$ и $(L_0 - \lambda I)^{-1}T_1(x,y) \in D(L_0)$.
The validity of the first condition follows from the properties of the Green function.
Let us prove the validity of the second condition.

$$\alpha(\kappa_1(x,y,\lambda)) - < \Delta(\kappa_1(x,y,\lambda)), \sigma_1(x,y) >= \alpha(T_1(x,y)) +$$

$$\lambda\alpha((L_0 - \lambda I)^{-1}T_1(x,y)) - < \Delta(T_1(x,y)), \sigma_1(x,y) > -$$

$$\lambda < L_0(L_0 - \lambda I)^{-1}T_1(x,y), \sigma_1(x,y) >= d(\lambda),$$

so by Lemma B $\alpha(T_1(x,y)) = 1$. From Lemma A it follows that $\alpha((L_0 - \lambda I)^{-1}T_1(x,y)) = 0$. It is also taken into account that $\Delta(T_1(x,y)) = 0$ and $(L_0 - \lambda I)^{-1}T_1(x,y) \in D(L_0)$.
Check the third condition

$$\beta(\kappa_1(x,y,\lambda)) = \beta(T_1(x,y)) + \lambda\beta((L_0 - \lambda I)^{-1}T_1(x,y)) = 0,$$

as by Lemma B $\beta(T_1(x,y)) = 0$. From Lemma A it follows that $\beta((L_0 - \lambda I)^{-1}T_1(x,y)) = 0$.
Check the fourth condition

$$\gamma(\kappa_1(x,y,\lambda)) = \gamma(T_1(x,y)) + \lambda\gamma((L_0 - \lambda I)^{-1}T_1(x,y)) = 0,$$

as by Lemma B $\gamma(T_1(x,y)) = 0$. From Lemma A it follows that $\gamma((L_0 - \lambda I)^{-1}T_1(x,y)) = 0$.
Lemma 1 is proved.
For convenience, we introduce the notation

(4.1) $$\varphi_1(x,y,\lambda) = \frac{\kappa_1(x,y,\lambda)}{d(\lambda)}.$$

If relation (4.1) is taken into account, then formula (3.7) for the resolvent of the operator L_{σ_1} can be written in the following form

(4.2) $$(L_{\sigma_1} - \lambda I)^{-1}f(x,y) = (L_0 - \lambda I)^{-1}f(x,y) + \tilde{\alpha}(\kappa_1(x,y,\lambda))\varphi(x,y,\lambda).$$

This implies that the poles of $\varphi_1(x,y,\lambda)$, and at the same time, the poles of the resolvent $(L_{\sigma_1} - \lambda I)^{-1}$ coincide with the zeros of the meromorphic function $d(\lambda)$. We show that the introduced solution $\kappa_1(x,y,\lambda)$ as a function of λ on the spectrum of the operator L_{σ_1} generates all its root functions.

Theorem 3. Let λ_k be an arbitrary zero of the characteristic determinant $d(\lambda)$ of multiplicity m_k. Then the functions from the following line:

(4.3) $$\kappa_1(x,y,\lambda_k), \frac{1}{1!}\frac{\partial \kappa_1(x,y,\lambda_k)}{\partial \lambda}, \dots, \frac{1}{(m_k-1)!}\frac{\partial^{m_k-1}\kappa_1(x,y,\lambda_k)}{\partial \lambda^{m_k-1}},$$

have a spectral interpretation: the first nonzero zero function is a proper one, and the subsequent ones are attached, generated by the indicated eigenfunction, corresponding to the eigenvalue λ_k of the operator L_{σ_1}.

Proof. The proof of Theorem 3 is that it is necessary to check for $p = 0, \dots, m_k - 1$ relations

(4.4) $$\frac{1}{p!}\frac{\partial^p \kappa_1(x,y,\lambda_k)}{\partial \lambda^p} \in D(L_{\sigma_1}),$$

(4.5) $$L_{\sigma_1}\left(\frac{1}{p!}\frac{\partial^p \kappa_1(x,y,\lambda_k)}{\partial \lambda^p}\right) = \lambda_k\left(\frac{1}{p!}\frac{\partial^p \kappa_1(x,y,\lambda_k)}{\partial \lambda^p}\right) + \frac{\epsilon}{(p-1)!}\frac{\partial^{p-1}\kappa_1(x,y,\lambda_k)}{\partial \lambda^{p-1}},$$

where $\epsilon = 0$ when $p = 0$, $\epsilon = 1$ when $p > 0$. From what $d(\lambda_k) = 0$ and follows from Lemma 1 $\kappa_1(x,y,\lambda_k) \in D(L_{\sigma_1})$. Therefore, the operator relation $L_{\sigma_1}(\kappa_1(x,y,\lambda_k)) = \lambda_k \kappa_1(x,y,\lambda_k)$ coincides with a homogeneous differential equation $\Delta(\kappa_1(x,y,\lambda_k)) = \lambda_k\kappa_1(x,y,\lambda_k)$, which by definition $\kappa(x,y,\lambda)$ holds when $\lambda = \lambda_k$. Thus, if $\kappa(x,y,\lambda_k)$ is not identically zero functions, then $\kappa(x,y,\lambda_k)$ is eigenfunction of the operator L_{σ_1}.

Now let $p = 1 < m_k$. Notice, that $d(\lambda_k) = 0$, $d'(\lambda_k) = 0$ and

$$\frac{\partial \kappa_1(x,y,\lambda)}{\partial \lambda} = (L_0 - \lambda I)^{-1}T_1(x,y) + \lambda\frac{\partial}{\partial \lambda}(L_0 - \lambda I)^{-1}T_1(x,y),$$

$$d'(\lambda) = -< \kappa_1(x,y,\lambda), \sigma_1(x,y) > -\lambda < \frac{\partial}{\partial \lambda}\kappa_1(x,y,\lambda), \sigma(x,y) >.$$

Calculate

$$\Delta\left(\frac{\partial \kappa_1(x,y,\lambda)}{\partial \lambda}\right) = L_0(L_0 - \lambda I)^{-1}T_1(x,y) + \lambda\frac{\partial}{\partial \lambda}L_0(L_0 - \lambda I)^{-1}T_1(x,y) =$$

$$= \lambda\frac{\partial}{\partial \lambda}\kappa_1(x,y,\lambda) + \kappa_1(x,y,\lambda).$$

The validity of the first condition follows from the properties of the Green function.

Let us prove the validity of the second condition.

$$\alpha\left(\frac{\partial \kappa_1(x,y,\lambda)}{\partial \lambda}\right) -< \Delta\left(\frac{\partial \kappa_1(x,y,\lambda)}{\partial \lambda}\right), \sigma_1(x,y) >= \alpha((L_0 - \lambda_k)^{-1}T_1(x,y)) +$$

$$\lambda_k\frac{\partial}{\partial \lambda}\alpha((L_0 - \lambda_k)^{-1}T_1(x,y)) -< \Delta\big((L_0 - \lambda_k)^{-1}T_1(x,y)\big), \sigma_1(x,y) >$$

$$-\lambda_k\frac{\partial}{\partial \lambda} < \Delta((L_0 - \lambda_k)^{-1}T_1(x,y)), \sigma_1(x,y) >= d'(\lambda_k) = 0,$$

so by Lemma A $\alpha((L_0 - \lambda_k I)^{-1}T_1(x,y)) = 0$. It is also taken into account that $(L_0 - \lambda_k I)^{-1}T_1(x,y) \in D(L_0)$.

Check the third condition

$$\beta\left(\frac{\partial \kappa_1(x,y,\lambda)}{\partial \lambda}\right) = \beta((L_0 - \lambda_k)^{-1}T_1(x,y)) + \lambda_k\frac{\partial}{\partial \lambda}\beta((L_0 - \lambda_k)^{-1}T_1(x,y)) = 0,$$

so by Lemma A $\beta((L_0 - \lambda I)^{-1}T_1(x,y)) = 0$.

Check the fourth condition

$$\gamma(\kappa_1(x,y,\lambda)) = \gamma((L_0 - \lambda_k)^{-1}T_1(x,y)) + \lambda_k\frac{\partial}{\partial \lambda}\gamma((L_0 - \lambda_k)^{-1}T_1(x,y)) = 0,$$

so by Lemma A $\gamma((L_0 - \lambda I)^{-1}T_1(x,y)) = 0$.

Continuing the arguments for other admissible p, we obtain a complete proof of Theorem 3.

5 Projectors on rood supspace

In the monograph ([13], стр. 445) the decomposition theorem is given, from which it follows that the projector $P_k: \mathbb{L}_2(\Omega_0) \to (L_{\sigma_1} - \lambda_k I)^{m_k}$ represents the residue of the resolvent at the singular point λ_k:

$$(P_k f)(x,y) = -\frac{1}{2\pi i} \oint\limits_{|\lambda-\lambda_k|=\delta} (L_{\sigma_1} - \lambda I)^{-1} f(x,y)\, d\lambda$$

with some $\delta > 0$. Since the resolvent of the Dirichlet operator has poles, for completeness of information we consider two cases.

First, we consider the case when the eigenvalue λ_k of the operator L_{σ_1} does not coincide with any eigenvalue λ_j^0 of the operator L_0. Recalling the representation of the resolvent (3.7) from Corollary 2 and considering that the resolvent $(L_0 - \lambda I)^{-1}$ of the Dirichlet operator represents a holomorphic function of λ, projector type P_k can be specified:

(5.1) $$(P_k f)(x,y) = -\frac{1}{2\pi i} \oint_{|\lambda-\lambda_k|=\delta} \frac{\kappa_1(x,y,\lambda)}{d(\lambda)}$$

$$< f(\xi,\eta), L_0^*(L_0^* - \bar{\lambda} I)^{-1} \sigma_1(\xi,\eta) > d\lambda = \underset{\lambda_k}{\operatorname{res}} \frac{\kappa_1(x,y,\lambda)}{d(\lambda)} < f(\xi,\eta), M_1(\xi,\eta,\bar{\lambda}) >,$$

where $M_1(\xi,\eta,\bar{\lambda}) = \overline{L_0^*(L_0^* - \bar{\lambda} I)^{-1} \sigma_1(\xi,\eta)}$.

Apply the Cauchy residue theorem to the relation (5.1), we obtain

(5.2) $$(P_k f)(x,y) = -\frac{1}{(m_k-1)!} \lim_{\lambda\to\lambda_k} \frac{\partial^{m_k-1}}{\partial\lambda^{m_k-1}} \left(\frac{(\lambda-\lambda_k)^{m_k} < f(\xi,\eta), M_1(\xi,\eta,\bar{\lambda}) >}{d(\lambda)} \kappa_1(x,y,\lambda) \right) =$$

$$-\sum_{p=0}^{m_k-1} \frac{1}{(m_k-1-p)!} \lim_{\lambda\to\lambda_k} \frac{\partial^{m_k-1-p}}{\partial\lambda^{m_k-1-p}} \left(\frac{(\lambda-\lambda_k)^{m_k} < f(\xi,\eta), M_1(\xi,\eta,\bar{\lambda}) >}{d(\lambda)} \right) \frac{1}{p!} \frac{\partial^p \kappa_1(x,y,\lambda)}{\partial\lambda^p} \bigg|_{\lambda=\lambda_k} =$$

$$\sum_{p=0}^{m_k-1} < f(\xi,\eta), -\frac{1}{(m_k-1-p)!} \lim_{\bar{\lambda}\to\bar{\lambda}_k} \frac{\partial^{m_k-1-p}}{\partial\bar{\lambda}^{m_k-1-p}} \left(\frac{(\bar{\lambda}-\bar{\lambda}_k)^{m_k} M_1(\xi,\eta,\bar{\lambda})}{\overline{d(\lambda)}} \right) >$$

$$\frac{1}{p!} \frac{\partial^p \kappa_1(x,y,\lambda)}{\partial\lambda^p} \bigg|_{\lambda=\lambda_k}$$

Analysis of formula (5.2) leads to the following notation.

(5.3) $$E_k' = \{h_{k,0}(\xi,\eta), h_{k,1}(\xi,\eta), \dots, h_{k,m_k-1}(\xi,\eta)\},$$

where

(5.4) $$h_{k,m_k-1-p}(\xi,\eta) = -\frac{1}{(m_k-1-p)!} \lim_{\bar{\lambda}\to\bar{\lambda}_k} \frac{\partial^{m_k-1-p}}{\partial\bar{\lambda}^{m_k-1-p}} \left(\frac{(\bar{\lambda}-\bar{\lambda}_k)^{m_k} M_1(\xi,\eta,\bar{\lambda})}{\overline{d(\lambda)}} \right),$$

$$p = \overline{0, m_k - 1}.$$

We introduce the following family of functions

(5.5) $$E' = \{E_k': \lambda_k \text{ is arbitrary eigenvalue of the operator } L_{\sigma_1}\}.$$

Thus, we need to study the decomposition of arbitrary elements from the functional space $\mathbb{L}_2(\Omega_0)$ in the system of root functions of the operator L_{σ_1}.

(5.6) $$E=\{E_k\colon \lambda_k \text{ is arbitrary eigenvalue of the operator } \mathrm{L}_{\sigma_1}\}.$$

(5.7) $$E_k=\{W_{k,0}(x,y),W_{k,1}(x,y),\dots,W_{k,m_k-1}(x,y)\},$$

where

$$W_{k,p}(x,y)=\frac{\partial^p\kappa_1(x,y,\lambda)}{\partial\lambda^p}\Big|_{\lambda=\lambda_k}$$

Now, we consider the case $\lambda_k=\lambda_k^0$.

$$(P_kf)(x,y)=-\frac{1}{2\pi i}\oint_{|\lambda-\lambda_k|=\delta}(L_{\sigma_1}-\lambda I)^{-1}f(x,y)\,d\lambda=$$

$$=\underset{\lambda_k=\lambda_k^0}{res}((L_0-\lambda I)^{-1}f(x,y))+$$

$$\underset{\lambda_k=\lambda_k^0}{res}\left(\tilde{\alpha}(L_0(L_0-\lambda I)^{-1}f(x,y))\frac{\kappa_1(x,y,\lambda)}{1-\lambda\tilde{\alpha}(\kappa_1(x,y,\lambda))}\right).$$

First, we calculate the first addend. Given the representation for the resolvent of the Dirichlet problem as an expansion in eigenfunctions

(5.8) $$(L_0-\lambda I)^{-1}f(x,y)=\sum_{m=1}^{\infty}\frac{1}{\lambda_m^0-\lambda}f_m\omega_m^0(x,y),$$

we calculate the first addend

$$V_1:=\underset{\lambda_k=\lambda_k^0}{res}((L_0-\lambda I)^{-1}f(x,y))=$$

$$\underset{\lambda_k=\lambda_k^0}{res}\left(\sum_{m=1}^{\infty}\frac{1}{\lambda_m^0-\lambda}f_m\omega_m^0(x,y)\right)=-f_k\omega_k^0(x,y).$$

Calculate the second addend. Here we use the standard transform.

$$L_0(L_0-\lambda I)^{-1}T_1(x,y)=T_1(x,y)+\lambda(L_0-\lambda I)^{-1}T_1(x,y).$$

Then

$$V_2:=\underset{\lambda_k=\lambda_k^0}{res}\left(\left[\tilde{\alpha}(f)+\sum_{m=1}^{\infty}\frac{\lambda}{\lambda_m^0-\lambda}f_m\tilde{\alpha}\big(\omega_m^0(x,y)\big)\right]\right.$$

$$\left.\frac{T_1(x,y)+\sum_{m=1}^{\infty}\frac{\lambda}{\lambda_m^0-\lambda}T_{1m}\omega_m^0(x,y)}{1-\lambda\tilde{\alpha}(T_1(x,y))-\sum_{m=1}^{\infty}\frac{\lambda^2}{\lambda_m^0}T_{1m}\tilde{\alpha}(\omega_m^0(x,y))}\right).$$

Multiply the denominator and numerator in the last relation by $\lambda_k-\lambda$. As a result, the deduction will be equal to

$$V_2 = \lambda_k^0 f_k \tilde{\alpha}(\omega_k^0(x,y)) \cdot \frac{\lambda_k^0 T_{1k}\omega_k^0(x,y)}{(\lambda_k^0)^2 T_{1k}\tilde{\alpha}(\omega_k^0(x,y))} = f_k \omega_k^0(x,y).$$

So in the case of $\lambda_k = \lambda_k^0$ the projector

$$(P_k f)(x,y) = V_1 + V_2 = -f_k\omega_k^0(x,y) + f_k\omega_k^0(x,y) = 0.$$

The main result of this section is formulated as a theorem.

Theorem 4. Let λ_k is eigenvalue of the multiplicity m_k of the operator L_{σ_1}. P_k operator on root the subspace of the operator L_{σ_1} corresponding to λ_k is determined by formula (5.2).

6 Minimality of the root function system

In this section we prove the minimality of the system of root functions of the operator L_{σ_1} in the functional space $\mathbb{L}_2(\Omega_0)$. Generally speaking, choosing one or another basis in the root subspaces $P_k\mathbb{L}_2(\Omega_0)$, it is possible to study different systems of root functions. We investigate the minimality of a concrete system (5.6). System (5.6) is generated by solutions of the differential equation (4.5), generating operator L_{σ_1}. In particular, the Green's function associated with the operator L_{σ_1} is written through them. To prove the minimality of (5.6) in the functional space $\mathbb{L}_2(\Omega_0)$, it suffices to construct a biorthogonal system of functions in this space. In the previous paragraph 5 such a system has already been built. It remains to verify that system (5.6) lies in $\mathbb{L}_2(\Omega_0)$ and satisfies the biorthogonality relation.

To begin with, we verify that the functions in (5.6) are elements of the space $\mathbb{L}_2(\Omega_0)$. Since, according to (5.4), each $h_{k,t}(\xi,\eta)$ represents a linear combination of functions $M_1(\xi,\eta,\overline{\lambda})$ and its derivatives for $\lambda = \lambda_k$ $(k = 1,2,\dots,n)$, it suffices to check that these functions $M_1(\xi,\eta,\overline{\lambda_k})$, $(k = 1,2,\dots,n)$ belong to $\mathbb{L}_2(\Omega_0)$. The latter fact is obvious, since $M_1(\xi,\eta,\overline{\lambda}) = L_0^*(L_0^* - \overline{\lambda}I)^{-1}\sigma_1(\xi,\eta)$ and $\sigma_1(\xi,\eta)$ are an element of $\mathbb{L}_2(\Omega)$.

To establish the biorthogonality relations, we need the following lemma.

Lemma 2. For arbitrary complex numbers λ,μ the identity is correct

$$< \kappa_1(x,y,\lambda), M_1(x,y,\overline{\mu}) >= -\frac{d(\lambda)-d(\mu)}{\lambda-\mu}.$$

Proof. For arbitrary λ,μ we calculate the following inner product

$$\lambda < \kappa_1(x,y,\lambda), M_1(x,y,\overline{\mu}) >_{\mathbb{L}_2(\Omega_0)} = \lambda < \kappa_1(x,y,\lambda), \sigma_1(x,y) +$$

$$\mu(L_0^* - \overline{\mu}I)^{-1}\sigma_1(x,y) \ge < \Delta\kappa_1(x,y,\lambda), \sigma_1(x,y) > +$$

$$\mu < \Delta\kappa_1(x,y,\lambda), (L_0^* - \overline{\mu}I)^{-1}\sigma_1(x,y) >$$

$$= 1 - d(\lambda) + \mu < \Delta\kappa_1(x,y,\lambda), \widetilde{M_1}(x,y,\overline{\mu}) >,$$

where $\widetilde{M_1}(x,y,\overline{\mu}) = (L_0^* - \overline{\mu}I)^{-1}\sigma_1(x,y)$. Here, took into account the formula (3.8) for the characteristic determinant operator L_{σ_1}. We calculate separately the scalar product

$$< \Delta\kappa_1(x,y,\lambda), \widetilde{M_1}(x,y,\overline{\mu}) >=< \kappa_1(x,y,\lambda), \Delta\widetilde{M_1}(x,y,\overline{\mu}) > +$$

$$+\lim_{\delta\to+0}\int_{\partial\Omega}\left(\frac{\partial\kappa_1(x,y,\lambda)}{\partial\overline{n}}\widetilde{M_1}(x,y,\overline{\mu}) - \kappa_1(x,y,\lambda)\frac{\partial\widetilde{M_1}(x,y,\overline{\mu})}{\partial\overline{n}}\right)ds -$$

$$-\lim_{\delta\to+0}\int_{\partial\prod_\delta^0}\left(\frac{\partial\kappa_1(x,y,\lambda)}{\partial\overline{n}}\widetilde{M_1}(x,y,\overline{\mu})-\kappa_1(x,y,\lambda)\frac{\partial\widetilde{M_1}(x,y,\overline{\mu})}{\partial\overline{n}}\right)ds=$$

$$=<\kappa_1(x,y,\lambda),\Delta\widetilde{M_1}(x,y,\overline{\mu})>-$$

$$\lim_{\delta\to+0}\int_{\partial\prod_\delta^0}\left(\frac{\partial\kappa_1(x,y,\lambda)}{\partial\overline{n}}-\kappa_1(x,y,\lambda)\frac{\partial\widetilde{M_1}(x,y,\overline{\mu})}{\partial\overline{n}}\right)ds,$$

in that $\kappa_1(x,y,\lambda),\widetilde{M_1}(x,y,\overline{\mu})\in\mathbb{W}_2^2(\Omega)$, then

$$\lim_{\delta\to+0}\int_{\partial\Omega}\left(\frac{\partial\kappa_1(x,y,\lambda)}{\partial\overline{n}}\widetilde{M_1}(x,y,\overline{\mu})-\kappa_1(x,y,\lambda)\frac{\partial\widetilde{M_1}(x,y,\overline{\mu})}{\partial\overline{n}}\right)ds=0.$$

Here $\prod_\delta^0=\{(x,y):-\delta\le x-x_0\le\delta,-\delta\le y-y_0\le\delta\}$. Then

$$(\lambda-\mu)<\kappa_1(x,y,\lambda),M_1(x,y,\overline{\mu})>=1-d(\lambda)-$$

$$-\mu\lim_{\delta\to+0}\int_{\partial\prod_\delta^0}\left(\frac{\partial\kappa_1(x,y,\lambda)}{\partial\overline{n}}\widetilde{M_1}(x,y,\overline{\mu})-\kappa_1(x,y,\lambda)\frac{\partial\widetilde{M_1}(x,y,\overline{\mu})}{\partial\overline{n}}\right)ds.$$

Notice, that $\Delta\widetilde{M_1}(x,y,\overline{\mu})=M_1(x,y,\overline{\mu})$, because $(L_0^*-\overline{\mu}I)^{-1}\sigma_1(x,y)\in D(L_0^*)$. Hence, when $\lambda=\mu$, we have

$$\mu\lim_{\delta\to+0}\int_{\partial\prod_\delta^0}\left(\frac{\partial\kappa_1(x,y,\mu)}{\partial\overline{n}}\widetilde{M_1}(x,y,\overline{\mu})-\kappa_1(x,y,\mu)\frac{\partial\widetilde{M_1}(x,y,\overline{\mu})}{\partial\overline{n}}\right)ds=1-d(\mu).$$

Considering the last relation, we transform the previous equality

$$(\lambda-\mu)<\kappa_1(x,y,\lambda),M_1(x,y,\overline{\mu})>=1-d(\lambda)-1+d(\mu)-$$

$$\mu\lim_{\delta\to+0}\int_{\partial\prod_\delta^0}\left[\left(\frac{\partial\kappa_1(x,y,\lambda)}{\partial\overline{n}}-\frac{\partial\kappa_1(x,y,\mu)}{\partial\overline{n}}\right)\widetilde{M_1}(x,y,\overline{\mu})-\right.$$

$$\left.(\kappa_1(x,y,\lambda)-\kappa_1(x,y,\mu))\frac{\partial\widetilde{M_1}(x,y,\overline{\mu})}{\partial\overline{n}}\right]ds=-d(\lambda)+d(\mu)-$$

$$-(\lambda-\mu)\mu\lim_{\delta\to+0}\int_{\partial\prod_\delta^0}\frac{\partial}{\partial\overline{n}}(L_0-\lambda I)^{-1}T_1(x,y)\cdot(L_0^*-\overline{\mu}I)^{-1}\sigma_1(x,y)ds+$$

$$+(\lambda-\mu)\mu\lim_{\delta\to+0}\int_{\partial\prod_\delta^0}(L_0-\lambda I)^{-1}T_1(x,y)\cdot\frac{\partial}{\partial\overline{n}}(L_0^*-\overline{\mu}I)^{-1}\sigma_1(x,y)ds$$

Recall the representation for the Dirichlet problem as an expansion in eigenfunctions

$$(L_0-\lambda I)^{-1}T_1(x,y)=\sum_{m=1}^{\infty}\frac{<T_1(x,y),\omega_m^0(x,y)>}{\lambda_m^0-\lambda}\omega_m^0(x,y)=$$

$$\sum_{m=1}^{\infty}\frac{T_{1m}}{\lambda_m^0-\lambda}\omega_m^0(x,y),$$

$$(L_0^*-\overline{\mu}I)^{-1}\sigma_1(x,y)=\sum_{n=1}^{\infty}\frac{<\sigma_1(x,y),\omega_n^0(x,y)>}{\lambda_n^0-\overline{\mu}}\omega_n^0(x,y)=\sum_{n=1}^{\infty}\frac{\sigma_{1n}}{\lambda_n^0-\overline{\mu}}\omega_n^0(x,y).$$

As a result, we have

$$(\lambda-\mu) < \kappa_1(x,y,\lambda), M_1(x,y,\overline{\mu}) >= -d(\lambda)+d(\mu)-$$

$$-(\lambda-\mu)\mu\sum_{m=1}^{\infty}\sum_{n=1}^{\infty}\frac{T_{1m}\sigma_{1n}}{(\lambda_m^0-\lambda)(\lambda_n^0-\mu)}$$

$$\lim_{\delta\to+0}\int\limits_{\partial\Pi_\delta^0}\left[\frac{\partial}{\partial\overline{n}}\omega_m^0\omega_n^0(x,y)-\omega_m^0(x,y)\frac{\partial}{\partial\overline{n}}\omega_n^0(x,y)\right]ds=-d(\lambda)+d(\mu)-$$

$$(\lambda-\mu)\mu\sum_{m=1}^{\infty}\sum_{n=1}^{\infty}\frac{T_{1m}\sigma_{1n}}{(\lambda_m^0-\lambda)(\lambda_n^0-\mu)}$$

$$\lim_{\delta\to+0}\int\limits_{\partial\Pi_\delta^0}[\Delta\omega_m^0\omega_n^0(x,y)-\omega_m^0(x,y)\Delta\omega_n^0(x,y)]ds=-d(\lambda)+d(\mu)-$$

$$(\lambda-\mu)\mu\sum_{m=1}^{\infty}\sum_{n=1}^{\infty}\frac{T_{1m}\sigma_{1n}}{(\lambda_m^0-\lambda)(\lambda_n^0-\mu)}(\lambda_m^0-\lambda_n^0)$$

$$\lim_{\delta\to+0}\int\limits_{\Pi_\delta^0}\omega_m^0\omega_n^0(x,y)ds=-d(\lambda)+d(\mu)$$

as if $m=n$, то $\lambda_m^0-\lambda_n^0=0$. If $m\neq n$, then the integral is equal to zero due to the orthogonality of the eigenfunctions of the operator L_0.

Lemma 2 is proved.

To establish the biorthogonality relations, we check the

$$< W_{n,s}(x,y), h_{k,m_k-1-p}(x,y) >= \begin{cases}1, & \text{если } (n,s)=(k,p);\\ 0, & \text{если } (n,s)\neq(k,p).\end{cases}$$

We consider two eigenvalue λ_s and λ_k. They match pairs (s,t) and (k,p), where $t=0,1,\dots,m_s-1$ and $p=0,1,\dots,m_k-1$. Note that the inner product

$$< W_{n,s}(x,y), h_{k,m_k-1-p}(x,y) >=$$

$$=-\lim_{\lambda\to\lambda_s}\lim_{\mu\to\lambda_k}\frac{1}{n!}\frac{\partial^n}{\partial\lambda^n}\frac{1}{(m_k-1-p)!}\frac{\partial^{m_k-1-p}}{\partial\mu^{m_k-1-p}}\left(< \kappa_1(x,y,\lambda), M_1(x,y,\overline{\mu}) > \frac{(\mu-\lambda_k)^{m_k}}{d(\mu)}\right).$$

Recalling Lemma 2, we get equality

$$< W_{n,s}(x,y), h_{k,m_k-1-p}(x,y) >= \tag{6.1}$$

$$=\lim_{\lambda\to\lambda_s}\lim_{\mu\to\lambda_k}\frac{1}{n!}\frac{\partial^n}{\partial\lambda^n}\frac{1}{(m_k-1-p)!}\frac{\partial^{m_k-1-p}}{\partial\mu^{m_k-1-p}}\left(\frac{d(\lambda)-d(\mu)}{\lambda-\mu}\frac{(\mu-\lambda_k)^{m_k}}{d(\mu)}\right).$$

We introduce the notation

$$H_{k,t}(\lambda)=\lim_{\mu\to\lambda_k}\frac{1}{t!}\frac{\partial^t}{\partial\mu^t}\left(\frac{d(\lambda)-d(\mu)}{\lambda-\mu}\frac{(\mu-\lambda_k)^{m_k}}{d(\mu)}\right) \tag{6.2}$$

We consider the function

$$F(\mu)=\frac{d(\lambda)-d(\mu)}{\lambda-\mu}\frac{(\mu-\lambda_k)^{m_k}}{d(\mu)}$$

and expand it in a neighborhood of the point $\mu=\lambda_k$ into a Taylor series. Then

$$F(\mu)=H_{k,0}(\lambda)+H_{k,1}(\lambda)(\mu-\lambda_k)+\dots+H_{k,m_k-1}(\lambda)(\mu-\lambda_k)^{m_k-1}+\cdots,$$

that is, $H_{k,t}(\lambda)$ is the k-th Taylor coefficient, with a corresponding expansion, in a neighborhood of $\mu = \lambda_k$. The direct calculation of the coefficient of the Taylor series of the function $F(\mu)$ leads to the following formula for $t = 0,1,\dots,m_k - 1$:

$$H_{k,t}(\lambda) = d(\lambda)\Big(A_{k,m_k-1}\frac{1}{(\lambda-\lambda_k)^{t+1}} + A_{k,m_k-2}\frac{1}{(\lambda-\lambda_k)^{t}} + \cdots + A_{k,m_k-t-1}\frac{1}{\lambda-\lambda_k}\Big), \tag{6.3}$$

where number $A_{k,m_k-1},\dots,A_{k,0}$ define by identity

$$\frac{1}{d(\mu)} = \frac{A_{k,m_k-1}}{(\mu-\lambda_k)^{m_k}} + \frac{A_{k,m_k-2}}{(\mu-\lambda_k)^{m_k-1}} + \cdots + \frac{A_{k,0}}{\mu-\lambda_k} + \sum_{q=0}^{\infty} B_{k,q}(\mu-\lambda_k)^q.$$

If $\lambda_s \neq \lambda_k$, that of (6.1), (6.2) and (6.3) when $n = 0,1,\dots,m_k - 1$

$$< W_{n,s}(x,y), h_{k,m_k-1-p}(x,y) >= \lim_{\lambda\to\lambda_s}\frac{1}{n!}\frac{\partial^n}{\partial\lambda^n}H_{k,t}(\lambda) =$$

$$= \lim_{\lambda\to\lambda_s}\frac{1}{n!}\frac{\partial^n}{\partial\lambda^n}d(\lambda)\sum_{i=1}^{t+1}\frac{A_{k,m_k-t+i-2}}{(\lambda-\lambda_k)^i} = \frac{1}{n!}d^{(n)}(\lambda_s)\sum_{i=1}^{t+1}\frac{A_{k,m_k-t+i-2}}{(\lambda_s-\lambda_k)^i} = 0,$$

in that $d^{(n)}(\lambda_s) = 0$.

Now consider the case $\lambda_s = \lambda_k$. Transform the right side of the relation (6.3)

$$H_{k,t}(\lambda) = d(\lambda)\sum_{i=1}^{t+1}\frac{A_{k,m_k-t+i-2}}{(\lambda_s-\lambda_n)^i} = \tag{6.4}$$

$$= d(\lambda)(\lambda-\lambda_k)^{m_k-t-1}\Big(A_{k,m_k-1}\frac{1}{(\lambda-\lambda_k)^{m_k}} + A_{k,m_k-2}\frac{1}{(\lambda-\lambda_k)^{m_k-1}} + \cdots$$

$$+A_{k,m_k-1-t}\frac{1}{(\lambda-\lambda_k)^{m_k-t}}\Big) = d(\lambda)(\lambda-\lambda_k)^{m_k-t-1}$$

$$\Big(\frac{1}{d(\lambda)} - A_{k,m_k-2}\frac{1}{(\lambda-\lambda_k)^{m_k-1-t}} - \cdots - A_{k,0}\frac{1}{\lambda-\lambda_k} - \sum_{q=m_k}^{\infty} B_{k,q}(\lambda-\lambda_k)^q\Big) =$$

$$(\lambda-\lambda_k)^{m_k-1-t} + \sum_{q=m_k}^{\infty} c_{kq}^t(\lambda-\lambda_k)^q, k = 0,1,\dots,m_k-1.$$

From relation (6.1), (6.2) and (6.3) we obtain

$$< W_{n,s}(x,y), h_{k,m_k-1-p}(x,y) >= \frac{1}{n!}\lim_{\lambda\to\lambda_k}\frac{\partial^n}{\partial\lambda^n}H_{k,m_k-1-p}(\lambda) =$$

$$\frac{1}{n!}\lim_{\lambda\to\lambda_k}\frac{\partial^n}{\partial\lambda^n}\Big((\lambda-\lambda_k)^{m_k-1-t} + \sum_{q=m_k}^{\infty} c_{kq}^t(\lambda-\lambda_k)^q\Big).$$

This implies the required assertion for $\lambda_s = \lambda_k$. Q.E.D.

Note the works of the authors [14, 15], where obtained the formulas of the first regularized traces for Laplace operator and double differentiation in the punctured areas.

ACKNOWLEDGEMENTS

The authors were supported by the Ministry of Education and Science of the Republic of Kazakhstan (MESRK) Grant AP05130994. No new data was collected or generated during the course of research.

Б. Бекболат[1], Д. Б. Нурахметов[2], Н. Токмагамбетов[3], Г. Х. Аймал Раса[4]

[1,3,4]Әл-Фараби атындағы ҚазҰУ, Алматы, Қазақстан;
[2]Сәкен Сейфуллин атындағы Қазақ ұлттық аграрлық университеті, Астана, Казахстан;
[3]Гент университеті, Гент, Белгия;
[1,3]Математика және математикалық модельдеу институты, Алматы, Казахстан

ОЙЫЛҒАН АЙМАҚТАҒЫ ЛАПЛАС ОПЕРАТОРЫНЫҢ ТҮБІР ФУНКЦИЯЛАР ЖҮЙЕСІНІҢ МИНИМАЛДЫЛЫҒЫ

Аннотация. Біз осы мақаламызда, қисынды шешілетін шеттік есептердің «жаңа» классын туындататын, ойылған аймақтағы Лаплас операторын қарастырамыз. Осы есеп үшін резольвента формуласы алынған. Сонымен қатар, зерттелген есептің түбір функцияларын туындататын мероморфты функциялар сипатталған. Негізгі мақсатымзы түбір функциялар жүйесінің минималдылығын қарастыру. Біздің жұмыс ойылған аймақтағы Лаплас операторы үшін шеттік есептің шешімділігі сипатталған [8] жұмысының жалғасы болып табылады. Мақалада қисынды шешілетін шеттік есептердің «жаңа» классын туындататын, ойылған аймақтағы Лаплас операторы қарастырылып, туындаған есеп үшін резольвента формуласы алынған, сонымен қатар, функциялар жүйесін құратын мероморфты функциялар сипатталған. Меншікті және қосалқы функциялардың жүйесі осындай жүйенің бірі болып табылады. Соңғы бөлім түбір функциялардың минималдылығын зерттеуге арналған.

Түйін сөздер: Лаплас операторы, ойылған аймақ, резольвента, мероморфты функция, шеттік есептің қисынды шешімділігі, түбір функциялар жүйесі, минимал жүйе.

Б. Бекболат[1], Д. Б. Нурахметов[2], Н. Токмагамбетов[3], Г. Х. Аймал Раса[4]

[1,3,4]КазНУ им. Аль-Фараби, Алматы, Казахстан;
[2]Казахский агротехнический университет имени Сакена Сейфуллина, Астана, Казахстан;
[3]Гентский университет, Гент, Белгия;
[1,3]Институт математики и математического моделирования, Алматы, Казахстан;

О МИНИМАЛЬНОСТИ СИСТЕМ КОРНЕВЫХ ФУНКЦИЙ ОПЕРАТОРА ЛАПЛАСА В ПРОКОЛОТОЙ ОБЛАСТИ

Аннотация. В данной работе рассмотрен оператор Лапласа в проколотой области, который порождает класс "новых" , корректно разрешимых краевых задач. И для этого класса задач получена формула резольвенты. Также описаны мероморфные функции, порождающие корневых функций класса исследуемых задач. Основная цель – изучение минимальности систем корневых функций. Статья является продолжением работы [8], где дано описание корректно разрешимых краевых задач для оператора Лапласа в проколотых областях. Рассмотрен оператор Лапласа в проколотой области, который порождает класс "новых" , корректно разрешимых краевых задач, и для порожденных задач получена формула резольвенты, а также описаны мероморфные функции, которые индуцируют системы функций. Одна из этих систем, как раз, и является системой собственных и присоединенных функций. Последний раздел посвящен исследованию минимальности системы корневых функций.

Ключевые слова: Оператор Лапласа, проколотая область, резольвента, мероморфная функция, корректно разрешимая краевая задача, система корневых функций, минимальная система.

Information about authors:

Nurakhmetov Daulet – PhD doctor, S.Seifullin Kazakh Agro Technical University, Astana, Kazakhstan;

Tokmagambetov Niyaz – PhD doctor, Department of Mathematics: Analysis, Logic and Discrete Mathematics, Ghent University, Ghent, Belgium;

Bekbolat Bayan – Doctorate, Al–Farabi Kazakh National University, Almaty, Kazakhstan;

Aimal Rasa Ghulam Hazrat – Doctorate, Al–Farabi Kazakh National University, Almaty, Kazakhstan

REFERENCES

[1] Landau L. D., Lifschitz E. M., *Course of theoretical physics*. M.: Nauka, 1989.

[2] Berezin F. A., Faddeev L. D, Remark on the Scrodinger equation with singular potential, Soviet Phys. Dokl., №2. 1961. P. 372–375.

[3] Minlos R. A., Faddeev L. D, *Point interaction for a three-particle system in quantum mechanics*, Docl. Akad. Nauk SSSR. Vol. 141, №6. 1961. P. 1335–1338.

[4] Berezin F. A., *About Lee 's model*, Matematicheskii Sbornic. Vol. 60, №4. 1963. P. 425–446.

[5] M. I. Neiman-Zade, A. A. Shkalikov, Schrödinger operators with singular potentials from spaces of multipliers, Mathematical notes. Vol. 66, №5. 1999. P. 599–607.

[6] Neiman-Zade M. I., Savchuk A. M., *Schrodinger Operators with Singular Potentials*, Tr. Mat. Inst. Steklova, Vol. 236. 2002. P. 262–371.

[7] Goloschapova N. I., Zastavnyi V. P., Malamud M. M., *Positive definite functions and spectral properties of the Schrodinger operator with point interactions*, Mathematical notes, Vol. 90, №1. 2011. P. 149–154.

[8] Kanguzhin B. E., Anijarov A. A., *Well-Posed Problem for the Laplace Operator in a Punctured Disk*, Mat. Zametki, Vol. 89, №6. 2011. P. 856–867.

[9] Bitsadze A. V., *Equations of Mathematical Physics*, M.: Nauka, 1976.

[10] Kanguzhin B. E., Tokmagambetov N. E., *On Regularized Trace Formulas for a Well-Posed Perturbation of the m-Laplace Operator.* Differential Equations. **51**:1583-1588 (2015).

[11] Kanguzhin B. E., Tokmagambetov N. E., *Resolvents of well-posed problems for finite-rank perturbations of the polyharmonic operator in a punctured domain.* Siberian Mathematical Journal. **57**:265-273 (2016)

[12] Anijarov A. A, *Resolutions of finite-dimensional perturbations of well-posed problems for the Laplace operator*, Almaty, 2010. C. 102.

[13] Riesz F., Sz-Nagy B. *Lecons D'analyse fonctionnelle*. Sixiete edition, Academiai kiado, Budapest 1972.

[14] Kanguzhin B. E., Tokmagambetov N. E., *Regularized trace formula for a well-perturbed Laplace operator*, Doklady mathematics, Vol. 460, №1. 2015. – P. 7–10.

[15] Akhymbek M. E., Nurakhmetov D. B., *The first regularized trace for the two-fold differentiation operator in a punctured segment*, Siberian mathematical journal, Vol. 11. 2014. P. 626–633.

[16] Seitmuratov A., Zharmenova B., Dauitbayeva A., Bekmuratova A. K., Tulegenova E., Ussenova G., *Numerical analysis of the solution of some oscillation problems by the decomposition method*, News of the national academy of sciences of the republic of Kazakhstan,Series physic-mathematical. Vol. 323, №1. 2019. P.28–37. ISSN 1991-346X https://doi.org/10.32014/2019.2518-1726.4

N E W S
OF THE NATIONAL ACADEMY OF SCIENCES OF THE REPUBLIC OF KAZAKHSTAN
PHYSICO-MATHEMATICAL SERIES
ISSN 1991-346X **https://doi.org/10.32014/2019.2518-1726.49**
Volume 4, Number 326 (2019), 110 – 121

УДК: 517.958:531.72

Marat Nurtas[1], Zh.D.Baishemirov[2,3]

[1]International Information Technology University, 050040 Almaty, Kazakhstan;
[2]Abai Kazakh National Pedagogical University, 050010 Almaty, Kazakhstan;
[3]Institute of Information and Computational Technology, 050010 Almaty, Kazakhstan
marat_nurtasj@mail.ru, zbai.kz@gmail.com

INVESTIGATION OF THE TEMPERATURE REGIME OF THE TERRITORY OF THE SEMIPALATINSK POLYGON AND DESCRIPTION OF THE MATHEMATICAL MODEL AND ITS NUMERICAL SOLUTION

Abstract. After the collapse of the Soviet Union, Kazakhstan inherited a very unpleasant legacy - the Semipalatinsk test site, where 456 nuclear explosions were made for 45 years [1]. Nuclear explosions formed on the ground long-term radioactive contamination in the form of long strips, the so-called "radioactive traces" that go far beyond the site [2]. Explosive mixtures especially led to numerous changes, including fire. The Relevance of the article is that despite the fact that the Semipalatinsk test site is closed, the heat distribution around the source of nuclear waste is preserved hence there is the need to study the temperature variation around the waste. This article reflects the change in the ambient temperature of nuclear waste that has been affected by nuclear explosions. As a basis for the article, we examined the effect of a small iron piece exposed to radiation and its effect on the temperature of the environment itself. The problem considers a mathematical model of a two-dimensional heat parabolic type equation and the value of initial and boundary conditions, as well as its numerical solution and a graphical representation of the same numerical solution.

The result of this article is to demonstrate how accurately the environment exposed to radiation can be used for production or otherwise, and how to calculate a digital solution in the form of mathematical models and graphically illustrate a numerical solution.

Key words: Mathematical modeling, Numerical methods, radioactive waste, heat equations.

1. INTRODUCTION

At the time of the USSR atomic bombs were tested on the territory of Kazakhstan. 18 million hectares of land were allocated for this purpose and the Semipalatinsk nuclear test site was opened [1]. The Semipalatinsk nuclear test site was established by decision of the USSR Council of Ministers of August 21, 1947 [2].

On August 29, 1949 in Abai and Abyralinsky districts the first explosion was made with a capacity of 30 kilotons without prior notice of the population. Here was a uranium bomb on October 18, 1951, and on August 12, 1953, a world-class hydrogen 500 kilotons bomb was first tested. At the Semipalatinsk nuclear test site in 1961-1962, about 50 nuclear bombs were tested on the air, and in the period from 1963 to 1988, 14-18 tests were conducted each year and 343 nuclear explosions were underground. Under the influence of these explosions, radioactive sediments spread through the epicenter from the explosive clouds and wind. At the test site, the radiation level reached 448 Rem (roentgen equivalent man). The total number of nuclear charges tested at the Semipalatinsk nuclear test site in the air and on Earth has exceeded 2.5 thousand times the bomb placed in Hiroshima [3].

Nuclear testing in air directly affected people, animals and nature. Then they began to conduct underground nuclear explosions [1]. After the collapse of the Soviet Union, Kazakhstan inherited a very unpleasant legacy - the Semipalatinsk test site, where 456 nuclear explosions were made for 45 years [4].

Nuclear explosions formed on the ground long-term radioactive contamination in the form of long strips, the so-called "radioactive traces" that go far beyond the site [5]. Explosive mixtures especially led to numerous changes, including fire.

The Relevance of the topic of the graduation project is that despite the fact that the Semipalatinsk test site is closed, the heat distribution around the source of nuclear waste is preserved hence there is the need to study the temperature variation around the waste.

In the spring of 1997, in the process of monitoring the snow cover of the territory of Kazakhstan, temperature anomalies were detected in the Semipalatinsk test site (STS) - snow-free zones characterized by elevated temperature of the underlying surface were clearly distinguished in satellite images of the NOAA AVHRR series. The main interest was the question of the possible causes of the anomaly. Two hypotheses of the origin of the temperature anomaly were mainly discussed - natural tectonic processes and the consequences of nuclear explosions [6].

The maxima of the incipient and expanding thermal anomalies are located both in the territory of the landfill and beyond. They are also preserved during the period of the greatest development of the thermal anomaly and have a constant local association with certain areas of the earth surface. Such sites are both natural geological formations with high contents of natural radioactive elements (uranium, thorium, potassium), and areas of the earth surface with high density of technogenic contamination with radioactive elements associated with conducted nuclear explosions.

From the northeastern and eastern sides of the Murzhik mountains, in the area of the Saryuzen site where underground nuclear explosions were conducted in large-diameter battle wells, the Institute of Radiation Safety and Ecology of NNC RK revealed quite intense halos Pu239. The source of the appearance of these halos throughout the southern trail, apparently, is still the aerial nuclear explosions produced at the Experimental Field. When the LANDSAT image obtained during the period of maximum development of the regional thermal anomaly is enlarged, a local source of heat radiation in the form of a thermal halo around the Atomic Lake inside the intense halo of radioactive contamination Cs137 is clearly visible in the Balapan section near the Chagan River [7].

2.STATEMENT OF THE PROBLEM

In this model, we consider the temperature changes of nuclear sticks (buried), which produce heat due to radioactive decomposition.

$$\frac{1}{K}\frac{\partial T}{\partial t}(r,t) - \nabla^2 T(r,t) = Source(r,t) \tag{1.1}$$

$$Source(r,t) = \begin{cases} T_{rod}\dfrac{e^{\frac{-t}{\tau_0}}}{a^2}, for\ r \leq a\ else\ where \\ 0 \end{cases}$$

Where: $a = 25cm,\ K = 2 \times 10^7\ cm^2/year,\ T_{rod} = 1K,\ \tau_0 = 100year, r_c = 100cm, T_E = 300K$, $0 < r < 100cm$ and $0 < t < 100year$. If the initial $T(r, t = 0) = 300K$

Since this question is round symmetric (independent of φ), the 2-D (two-dimensional) Problem becomes a 1-D (one- dimensional) problem. Obviously, the value $\nabla^2 T = T_{xx} + T_{yy}$ is a two-dimensional problem in the system of rectangular coordinates.However, if we choose to use polar coordinates, then $T(r,t)$ is a function of r and t , since the wand is round symmetric and there is no dependence on φ . This reduces the initial two-dimensional problem to a one-dimensional problem. Thus, task 2-D goes to 1-D.

Tasks:

- to collect information about the landfill;
- to study materials for creating a mathematical model;
- build a mathematical model;
- consider methods for solving this problem;
- write an algorithm for implementing a numerical solution;
- check on test versions of the adequacy of the software implementation;
- process and analyze the data, summarize results.

According to the SRI (Space Research Institute) MES (Ministry of Education and Science) RK, during periods of maximum development of this anomaly, the temperature drop in the epicenter relative to the background reaches 10–12 or more degrees, and the dimensions cover an area of up to 250,500 km.

At the same time, under the place of demolition or scattering of accumulations of thermal gases (Figure 1.1, red color) snow is again visible. In the example shown in Figure 1, which covers an area of 180170 km, the Degelen mountain massif is visible in the lower part of the image after band-spreading. All of the above can speak of the gaseous essence of the thermal anomaly. The maxima of the incipient and expanding thermal anomalies are located both in the territory of the landfill and beyond. They are also preserved during the period of the greatest development of the thermal anomaly and have a constant local association with certain areas of the earth surface. Such sites are both natural geological formations with high contents of natural radioactive elements (uranium, thorium, potassium), and areas of the earth surface with a high density of technogenic contamination with radioactive elements associated with conducted nuclear explosions. In Figure 1.2 it can be seen that within the STS such areas with a high content of technogenic radionuclides (or traces of radioactive contamination) are marked by extended halos Cs137 of the south-east and south directions.

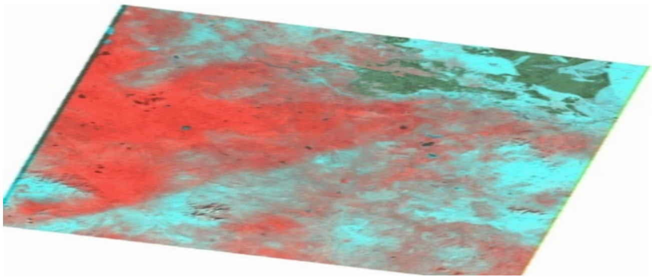

Figure 1.1 – Example of partial strip drift and gas dispersion of a regional thermal anomaly (red color) in the area of STS. LANDSAT image on January 27, 2002. (RGB combination of spectral channels 5, 4, 3 [20]

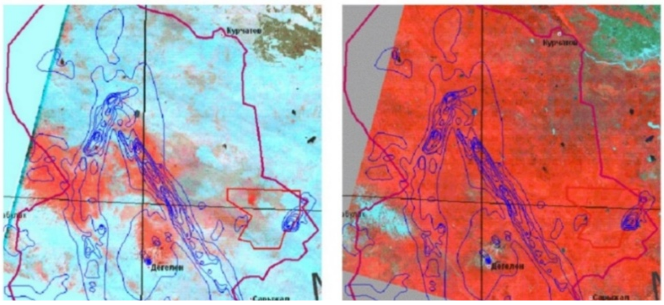

a - February 15, 2003 (spectral channels 5, 4, 3) b - February 28, 2002 (spectral channels 5, 4, 3)[20].

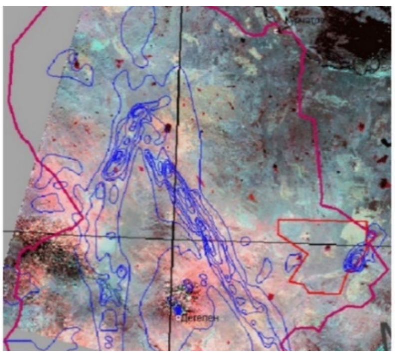

c- February 28, 2002 (combination of infrared channels 6, 7, 5)

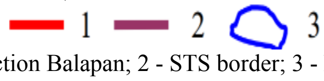

1 - contour section Balapan; 2 - STS border; 3 - halos Cs 137

Figure 1.2 – The territory of the STS. Comparison of areas of origin of thermal gases (red color) in the initial period and sources, heat radiation on the earth surface (reddish-pink color) in the period of maximum development of the gaseous thermal anomaly with traces of radioactive contamination. LANDSAT Snapshots [20]

From the northeastern and eastern sides of the Murzhik mountains, in the area of the Saryuzen site where underground nuclear explosions were conducted in large-diameter battle wells, the Institute of Radiation Safety and Environment NNC RK revealed quite intense halos Pu239. The source of the appearance of these halos throughout the southern wake, apparently, is still the aerial nuclear explosions produced at the Experimental Field. When the LANDSAT image obtained during the period of maximum development of the regional thermal anomaly is enlarged, a local source of heat radiation in the form of a thermal halo around the Atomic Lake inside the intense radioactive contamination halo Cs137 (Figure 1.3) is clearly visible in the Balapan section near the Chagan River in infrared channels. Nearby in the Karazhira coal pit, there is also a local heat source associated with the degassing of coal seams. Red color - sources of heat radiation on the earth surface; pink color - moist non-freezing salt marshes.

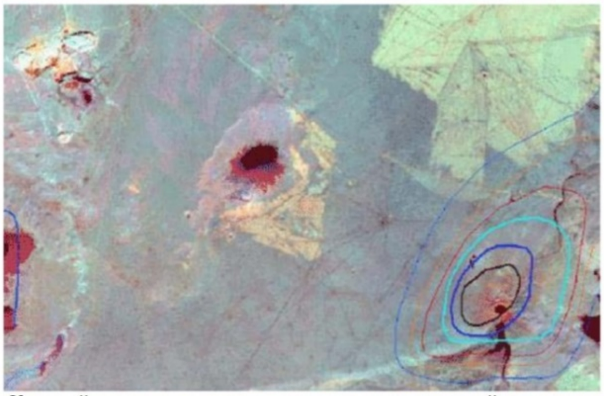

Figure1.3 – Local sources of heat radiation around an atomic lake inside the Cs137 halo and in the area of the Karazhira coal pit during the period of maximum development of the gaseous thermal anomaly. Snapshot LANDSAT for 02.28.2002 (RGB combination of infrared channels 6, 7, 5) [20]

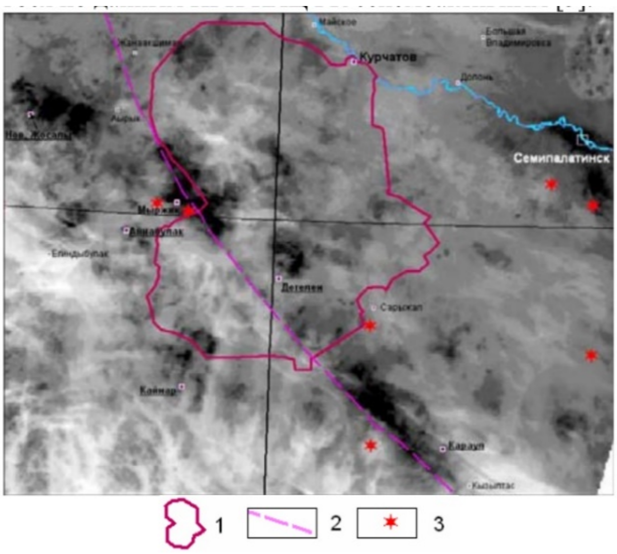

1 - STS contour; 2 - Main Chingiz fault; 3 - epicenters of seismic events. Black color - smog in the area of the city of Semey and areas of the origin of thermal gases on the earth surface in the initial period of development of the gaseous thermal anomaly.
Figure 1.4 – Inversion image of LST (Land Surfase Temperature) temperature data of the Terra / MODIS meteorological satellite for February 15, 2003 [20].

Areas of natural geological formations with a high content of natural radioactive elements in the STS region are most often mountains of effusive rocks of medium-acidic composition of increased alkalinity, less often - river valleys with alluvial demolition of fragments of the same bedrock (Paleozoic trachiliparite and trahiandesite composition with bodies subvolcanic intrusions of trachiliparite and syenite composition). The content of uranium (by radium) in these rocks exceeds 10-15 10-4%, thorium - 20-40 10-4% (more than background ones 5-10 or more times). In addition, they contain elevated levels of niobium, beryllium, yttrium, molybdenum and lead. The most intense manifestation of high concentrations of natural radioactive elements in geological formations, which coincides with the sites of origin of thermal gases, is observed (Figure 1.4) in the eastern part of the Kyzyltau mountains near the village of New Zhosaly; in the near mountains of Dos and Irgiz near the village. Ainabulak (Abay); in the mountains of Abraila, near the village Kaynar; in the eastern part of the Degelen Mountains and in the northeastern part of the Kanchingiz Range, near the village of Guard. In general, the thermal anomaly is elongated in the NW direction. The same direction within the anomaly have the main Chingiz and a number of secondary tectonic faults. At the stage of nucleation, the elongated sections of the thermal anomaly are located in the location of the Main Chingiz Fault, which is seismic-active according to the data of the NNC RK.

3. MATHEMATICAL MODEL TO DETERMINE THE TEMPERATURE AROUND NUCLEAR WASTE

Since this question (1.1) is round symmetric (independent of φ), the 2-D (two-dimensional) Problem becomes a 1-D (one- dimensional) problem. Obviously, the value $\nabla^2 T = T_{xx} + T_{yy}$ is a two-dimensional problem in the system of rectangular coordinates.However, if we choose to use polar coordinates, then $T(r,t)$ is a function of r and t , since the damaged iron piece is round symmetric and there is no dependence on φ . This reduces the initial two-dimensional problem to a one-dimensional problem. Thus, task 2-D goes to change 1-D.

We are going to replace the polar coordinate system: for this we need the following formula. If the nuclear residue is struck out like this

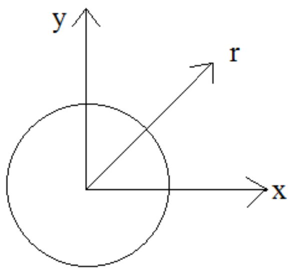

Figure 2.1r = a

We suppose that there is buried nuclear waste (iron fracture)

2-D polar coordinate(2.1)

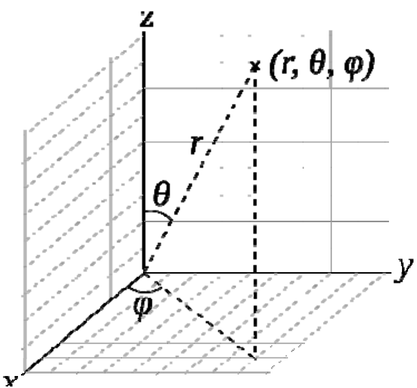

Figure 2.3 – The polar coordinate system measuring 3-D.

$$T_x = T_r r_x + T_\phi \phi_x \tag{2.2}$$

$$\frac{\partial T}{\partial x} = \frac{\partial r}{\partial x}\frac{\partial T}{\partial r} + \frac{\partial \varphi}{\partial x}\frac{\partial T}{\partial \varphi} + \frac{2x}{2\sqrt{x^2+y^2}}\frac{\partial T}{\partial r} + \frac{1}{1+\frac{y^2}{x^2}}\cdot\left(-\frac{y}{x^2}\right)\frac{\partial T}{\partial \varphi} = \cos\varphi\frac{\partial T}{\partial r} - \frac{\sin\varphi}{r}\frac{\partial T}{\partial \varphi}$$

$$T_y = T_r r_y + T_\varphi \varphi_y \quad (2.3)$$

$$\frac{\partial r}{\partial y}\frac{\partial T}{\partial r} + \frac{\partial \varphi}{\partial y}\frac{\partial T}{\partial \varphi} = \frac{2y}{2\sqrt{x^2+y^2}}\frac{\partial T}{\partial r} + \frac{1}{1+\frac{y^2}{x^2}}\cdot\left(\frac{1}{x}\right)\frac{\partial T}{\partial \varphi} = \sin\varphi\frac{\partial T}{\partial r} + \frac{\cos\varphi}{r}\frac{\partial T}{\partial \varphi}$$

that,

$$T_{xx} = T_{rr}(r_x)^2 + 2T_{r\varphi}r_x\phi_x + T_{\phi\phi}(\phi_x)^2 + T_r r_{xx} + T_\phi \phi_{xx} \quad (2.4)$$

$$\mathrm{T_x} = \frac{\mathrm{x}}{\sqrt{\mathrm{x^2+y^2}}}\frac{\partial \mathrm{T}}{\partial \mathrm{r}} - \frac{\mathrm{y}}{\mathrm{x^2+y^2}}\frac{\partial \mathrm{T}}{\partial \varphi}$$

$$T_{xx} = \frac{\partial^2 T}{\partial x^2} = \frac{x^2}{x^2+y^2}\frac{\partial^2 T}{\partial r^2} - \frac{2xy}{\sqrt{(x^2+y^2)^3}}\frac{\partial^2 T}{\partial r\partial\varphi} + \frac{y^2}{(x^2+y^2)^2}\frac{\partial^2 T}{\partial \varphi^2} + \frac{\sqrt{x^2+y^2} - \frac{1}{2}\frac{2x^2}{\sqrt{x^2+y^2}}}{(x^2+y^2)}\frac{\partial T}{\partial r} +$$

$$+\frac{2xy}{(x^2+y^2)^2}\frac{\partial T}{\partial\varphi} = \frac{x^2}{x^2+y^2}\frac{\partial^2 T}{\partial r^2} - \frac{2xy}{\sqrt{(x^2+y^2)^3}}\frac{\partial^2 T}{\partial r\,\partial\varphi} + \frac{y^2}{(x^2+y^2)^2}\frac{\partial^2 T}{\partial\varphi^2} + \frac{y^2}{\sqrt{(x^2+y^2)^3}}\frac{\partial T}{\partial r} +$$

$$+\frac{2xy}{(x^2+y^2)^2}\frac{\partial T}{\partial\varphi} = \frac{r^2\cos^2\varphi}{r^2(\cos^2\varphi+\sin^2\varphi)}\frac{\partial^2 T}{\partial r^2} - \frac{2r^2\cos\varphi\sin\varphi}{\sqrt{\left(r^2(\cos^2\varphi+\sin^2\varphi)\right)^3}}\frac{\partial^2 T}{\partial r\,\partial\varphi} +$$

$$+\frac{r^2\sin^2\varphi}{\left(r^2(\cos^2\varphi+\sin^2\varphi)\right)^2}\frac{\partial^2 T}{\partial\varphi^2} + \frac{r^2\sin^2\varphi}{\sqrt{\left(r^2(\cos^2\varphi+\sin^2\varphi)\right)^3}}\frac{\partial T}{\partial r} + \frac{2r^2\cos\varphi\sin\varphi}{\left(r^2(\cos^2\varphi+\sin^2\varphi)\right)^2}\frac{\partial T}{\partial\varphi} =$$

$$= \cos^2\varphi\frac{\partial^2 T}{\partial r^2} - \frac{2\cos\varphi\sin\varphi}{r}\frac{\partial^2 T}{\partial r\,\partial\varphi} + \frac{\sin^2\varphi}{r^2}\frac{\partial^2 T}{\partial\varphi^2} + \frac{\sin^2\varphi}{r}\frac{\partial T}{\partial r} + \frac{2\cos\varphi\sin\varphi}{r^2}\frac{\partial T}{\partial\varphi}$$

$$T_{yy} = T_{rr}(r_y)^2 + 2T_{r\varphi}r_y\phi_y + T_{\phi\phi}(\phi_y)^2 + T_r r_{yy} + T_\phi\phi_{yy} \quad (2.5)$$

$$T_y = \frac{y}{\sqrt{x^2+y^2}}\frac{\partial T}{\partial r} + \frac{x}{x^2+y^2}\frac{\partial T}{\partial\varphi}$$

$$T_{yy} = \sin^2\varphi\frac{\partial^2 T}{\partial r^2} + \frac{2\cos\varphi\sin\varphi}{r}\frac{\partial^2 T}{\partial r\partial\varphi} + \frac{\cos^2\varphi}{r^2}\frac{\partial^2 T}{\partial\varphi^2} + \frac{\cos^2\varphi}{r}\frac{\partial T}{\partial r} - \frac{2\cos\varphi\sin\varphi}{r^2}\frac{\partial T}{\partial\varphi}$$

$$T_{xx} + T_{yy} = \cos^2\phi\frac{\partial^2 T}{\partial r^2} - \frac{2\cos\phi\sin\phi}{r}\frac{\partial^2 T}{\partial r\partial\phi} + \frac{\sin^2\phi}{r^2}\frac{\partial^2 T}{\partial\phi^2} + \frac{\sin^2\phi}{r}\frac{\partial T}{\partial r} + \frac{2\cos\phi\sin\phi}{r^2}\frac{\partial T}{\partial\phi} +$$

$$+\sin^2\phi\frac{\partial^2 T}{\partial r^2} + \frac{2\cos\phi\sin\phi}{r}\frac{\partial^2 T}{\partial r\partial\phi} + \frac{\cos^2\phi}{r^2}\frac{\partial^2 T}{\partial\phi^2} + \frac{\cos^2\phi}{r}\frac{\partial T}{\partial r} - \frac{2\cos\phi\sin\phi}{r^2}\frac{\partial T}{\partial\phi} =$$

$$= \frac{\partial^2 T}{\partial r^2} + \frac{1}{r}\frac{\partial T}{\partial r} + \frac{1}{r^2}\frac{\partial^2 T}{\partial\phi^2}$$

If $T_{xx}+T_{yy}$, the total result is displayed as:

$$\frac{\partial^2 T}{\partial x^2}+\frac{\partial^2 T}{\partial y^2}=\frac{\partial^2 T}{\partial r^2}+\frac{1}{r}\frac{\partial T}{\partial r}+\frac{1}{r^2}\frac{\partial^2 T}{\partial \phi^2} \qquad (2.6)$$

But due to the fact that the temperature $T(r,t)$ here does not depend on , we can take it like this $\frac{\partial^2 T}{\partial \varphi^2}=0$.

Then we obtain one-dimensional heat equation can be written as follows:

$$\frac{1}{K}\frac{\partial T}{\partial t}-\frac{\partial^2 T}{\partial r^2}-\frac{1}{r}\frac{\partial T}{\partial r}=Source(r,t) \qquad (2.7)$$

2.2 Numerical solution and algorithm of the ambient temperature change under the influence of nuclear waste

If we consider the solution of the problem in stationary conditions, the nuclear residue for a long time will not be in a radioactive state, then stops the emission of heat, ie.: $Source(r,t)\to 0 \text{if} t\to\infty$, and we can consider it as the temperature of the environment, because in the territory remote from the nuclear residue, there is no radioactive impact on the temperature.It means $T(r=r_c,t)=300K$.Thus, the solution of the problem assumes that when the ambient temperature$T(r,t=0)=300K$ is reached, the radioactive residue ceases to have an effect.

We solve equation (1.1) using a finite difference scheme. If we consider the equation (1.1) in the case $r=0$, then its quantitative solution is stable. We set the initial condition$T(r,t=0)=300K$, and the boundary condition$r=0$of the Neumann type (the temperature in the region does not change)$\frac{\partial T}{\partial r}(r=0,t)=0$ And in the boundary condition$r=r_c$ the Dirichlettype$T(r=r_c,t)=300K$.

If we proceed to the numerical calculation with the given conditions of the problem (1.1), then

$$\Delta r=\frac{r_c}{(n+1)},\Delta t=\frac{\tau}{m},\ r_j=j\cdot\Delta r 0\le j\le n+1,\ t_k=k\cdot\Delta t 0\le k\le m$$

Denote $T(r_j,t_k)=T_j^k$and $Source(r_j,t_k)=Source_j^k$

For$r=0$, the Neumann boundary condition can be written as follows:

$$\frac{\partial T_j^k}{\partial t}(r=0,t)=\frac{\partial T_0^k}{\partial t}=0\approx\frac{T_1^k-T_0^k}{\Delta t}\Rightarrow T_0^k\approx T_1^k \qquad (2.8)$$

When the Dirichlet boundary condition $r=r_c$:

$$T_j^k(r=r_c,t)=T_{n+1}^k=300$$

In this problem we use the undefined Euler scheme [24]. This means special derivatives of $r$write by time t_{k+1}. So:

$$T_t(t_{k+1},r_j)=\frac{T_j^{k=1}-T_j^k}{\Delta t} \qquad (2.9)$$

$$T_{rr}(t_{k+1},r_j)=\frac{T_{j+1}^{k+1}-2T_j^{k+1}T_{j-1}^{k+1}}{\Delta r^2} \qquad (2.10)$$

$$T_r(t_{k+1},r_j)=\frac{T_{j+1}^{k+1}-T_{-1-j}^{k+1}}{2\Delta r}\text{(leap-frog in space)} \qquad (2.11)$$

Using $r_j = j \cdot \Delta r$we write (2.1) in this form of scheme.

So we write this$\frac{1}{K}T_t - T_{rr} - \frac{1}{r}T_r = Source(r,t)$in the following form:

$$\frac{1}{K \cdot \Delta t}\left[T_j^{k+1} - T_j^k\right] - \left[\frac{T_{j+1}^{k+1} + 2T_j^{k+1} + T_{j-1}^{k+1}}{\Delta r^2}\right] - \frac{1}{j \cdot \Delta r}\left[\frac{T_{j+1}^{k+1} - T_{j-1}^{k+1}}{2 \Delta r}\right] = Soirse_j^k \tag{2.12}$$

Denote S as $S = \frac{K \cdot \Delta t}{r^2}$, then the expression above we write in the following form.

$$T_{j+1}^{k+1}\left[-S - \frac{S}{2j}\right] + T_{j-1}^{k+1}\left[-S + \frac{S}{2j}\right] + T_j^{k+1}[1 + 2S] = T_j^k + Soirse_j^k \cdot K \cdot \Delta t \tag{2.13}$$

The above formula can be written as a tridiagonalmatrix for$1 \le j \le n$when n =3:

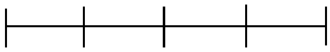

$r_0 = 0 r_1 r_2\, r_3\, r_{n+1} = r_c = r_4$

From the boundary condition $T_0^k \approx T_1^k$ and$\left(\frac{\partial T}{\partial r}(r = 0, t) = 0\right)$,$T_4^k = 300Kand(T(r = r_c, t) = 300)$and the initial condition$T_j^0 = 300K$.

$$T_j^k = T_j^{k+1} - S\left[T_{j+1}^{k+1} - 2T_j^{k+1} + T_{j-1}^{k+1}\right] - S\left[\frac{T_{j+1}^{k+1} - T_{j-1}^{k+1}}{2j}\right] - Source_j^k \cdot K \cdot \Delta t$$

$$j = 1, T_1^k = T_1^{k+1} - S\left[T_2^{k+1} - 2T_1^{k+1} + T_0^{k+1}\right] - S\left[\frac{T_2^{k+1} - T_0^{k+1}}{2}\right] - Source_1^k \cdot K \cdot \Delta t$$

$$T_1^k = (1 + 2S)T_1^{k+1} + \left(-S - \frac{S}{2j}\right)T_2^{k+1} + \left(-S + \frac{S}{2j}\right)T_0^{k+1} - Source_1^k \cdot K \cdot \Delta t$$

$$j = 2, T_2^k = T_2^{k+1} - S\left[T_3^{k+1} - 2T_2^{k+1} + T_1^{k+1}\right] - S\left[\frac{T_3^{k+1} - T_1^{k+1}}{4}\right] - Source_2^k \cdot K \cdot \Delta t$$

$$T_2^k = (1 + 2S)T_2^{k+1} + \left(-S - \frac{S}{2j}\right)T_3^{k+1} + \left(-S + \frac{S}{2j}\right)T_1^{k+1} - Source_2^k \cdot K \cdot \Delta t$$

$$j = 3, \ldots$$

Then from the (1.1) – equation we write forT_1^k,T_2^k,$T_3^k$and solve at every(t_k):

$$\begin{pmatrix} 1 + 2S & \left(-S - \frac{S}{2j}\right) & 0 \\ \left(-S + \frac{S}{2j}\right) & 1 + 2S & \left(-S - \frac{S}{2j}\right) \\ 0 & \left(-S + \frac{S}{2j}\right) & (1 + 2S) \end{pmatrix} \cdot \begin{pmatrix} T_1^{k+1} \\ T_2^{k+1} \\ T_3^{k+1} \end{pmatrix} + \begin{pmatrix} \left(-S + \frac{S}{2j}\right)T_0^{k+1} \\ 0 \\ \left(-S - \frac{S}{2j}\right)T_4^{k+1} \end{pmatrix} = \begin{pmatrix} T_1^k \\ T_2^k \\ T_3^k \end{pmatrix} + K\Delta t \begin{pmatrix} Source_1^k \\ Source_2^k \\ Source_3^k \end{pmatrix}$$

When we use the Neumann boundary condition for$r = 0$

$$\frac{\partial T_j^k}{\partial t}(r = 0, t) = \frac{\partial T_0^k}{\partial t} = 0 \approx \frac{T_1^k - T_0^k}{\Delta t} \Longrightarrow T_0^k \approx T_1^k \tag{2.14}$$

When the Dirichlet boundary condition $r = r_c$:

$$T_j^k(r = r_c, t) = T_{n+1}^k = 300 \tag{2.15}$$

Check for

$$j = 1: T_1^k = T_1^{k+1} - S\left[T_2^{k+1} - 2T_1^{k+1} + T_1^{k+1}\right] - S\left[\frac{T_2^{k+1} - T_1^{k+1}}{2}\right] - Source\ {}_1^k \cdot K \cdot \Delta t$$
$$\Rightarrow T_1^k = \left(1 + S + \frac{S}{2}\right) \cdot T_1^{k+1} + \left(-S - \frac{S}{2}\right) \cdot T_2^{k+1} - Source\ {}_1^k \cdot K \cdot \Delta t \quad (2.16)$$

$$\begin{pmatrix} \left(1+S+\frac{S}{2}\right) & \left(-S-\frac{S}{2}\right) & 0 \\ \left(-S+\frac{S}{4}\right) & 1+2S & \left(-S-\frac{S}{4}\right) \\ 0 & \left(-S+\frac{S}{6}\right) & (1+2S) \end{pmatrix} \cdot \begin{pmatrix} T_1^{k+1} \\ T_2^{k+1} \\ T_3^{k+1} \end{pmatrix} = \begin{pmatrix} T_1^k \\ T_2^k \\ T_3^k \end{pmatrix} + K\Delta t \begin{pmatrix} Source_1^k \\ Source_2^k \\ Source_3^k \end{pmatrix} - \begin{pmatrix} 0 \\ 0 \\ \left(-S-\frac{S}{6}\right)300 \end{pmatrix}$$

Then for all iteration:

$$\begin{pmatrix} \left(1+S+\frac{S}{2j}\right) & \left(-S-\frac{S}{2j}\right) & 0 \\ \left(-S+\frac{S}{2j}\right) & 1+2S & \left(-S-\frac{S}{2j}\right) \\ 0 & \left(-S+\frac{S}{2j}\right) & (1+2S) \end{pmatrix} \cdot \begin{pmatrix} T_1^{k+1} \\ T_2^{k+1} \\ T_3^{k+1} \end{pmatrix}$$
$$= \begin{pmatrix} T_1^k \\ T_2^k \\ T_3^k \end{pmatrix} + K\Delta t \begin{pmatrix} Source_1^k \\ Source_2^k \\ Source_3^k \end{pmatrix} - \begin{pmatrix} 0 \\ 0 \\ \left(-S-\frac{S}{2j}\right) T_4^{k+1} \end{pmatrix}$$

Thus, if we solve this matrix for an unknown $\overrightarrow{T}^{k+1}$ temperature, we will get the result of the report.

$$A \cdot \vec{T}^{k+1} = \vec{T}^k + (k \cdot \Delta t) \cdot \vec{S}ource\ {}^k + \vec{b}$$
$$\vec{T}^{k+1} = \left(\vec{T}^k + (k \cdot \Delta t) \cdot \vec{S}ource\ {}^k + \vec{b}\right) * inverse\ \ (A)$$

2.3. Analysis of the temperature variation around nuclear waste and numerical solution using the Matlab software package

The air temperature changes in time. Temperature changes also occur depending on the coefficients. An experiment was made by changing the parameters. The analysis was made using the results of the experiment. Modified parameters for thrust - time (T), depth of deposition (a) of radioactive particles. Changed parameters for the experiment - time (T), depth of iron particles exposed to radiation (a).

Initially, the parameters r = 100 cm, T = 100 years, a = 25 cm were chosen. Its results are shown in the table below.

Table 1 - Temperature change at r = 100 cm, T = 100 years, a = 25 cm

№	Temp1year	Temp10year	Temp50year	Temp100year
1	300.9053	300.8273	300.5546	300.3364
10	300.8665	300.7919	300.5308	300.3220
20	300.7478	300.6835	300.4581	300.2779
30	300.5721	300.5229	300.3505	300.2126
40	300.4354	300.3980	300.2668	300.1618
50	300.3294	300.3010	300.2018	300.1224
60	300.2428	300.2219	300.1487	300.0902
70	300.1695	300.1549	300.1038	300.0630
80	300.1060	300.0969	300.0650	300.0394
90	300.0501	300.0458	300.0307	300.0186
99	300.0048	300.0044	300.0029	300.0018

As indicated in the table, the period of time for 100 years is divided into 4 stages, that is, the results for 1, 10, 50, 100-year period. At each stage, temperature results are recorded every 10 cm. According to the results, the temperature is observed in normal decrease, both in time and at a distance.

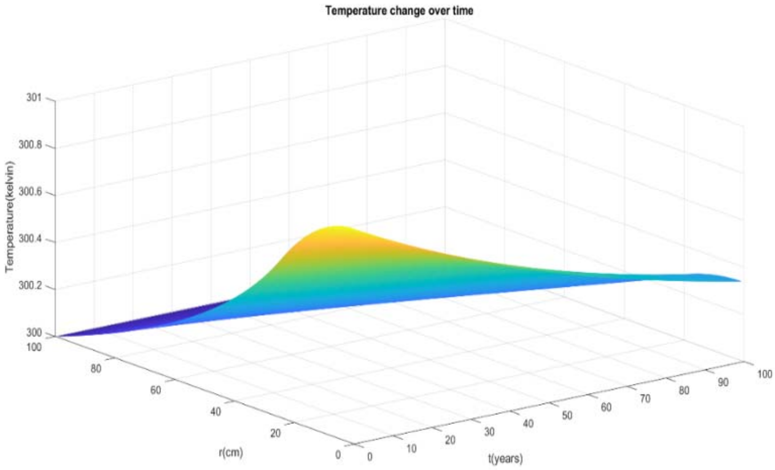

Figure 1 - The measurement of the temperature with respect to time and distance

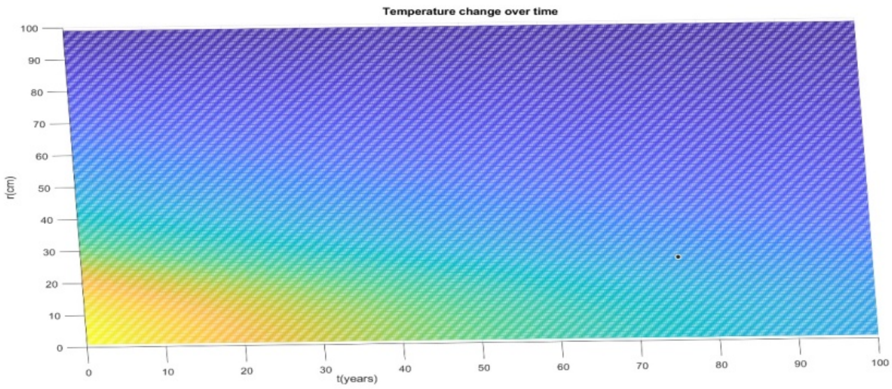

Figure 2 - Temperature distribution during inspection in planar conditions

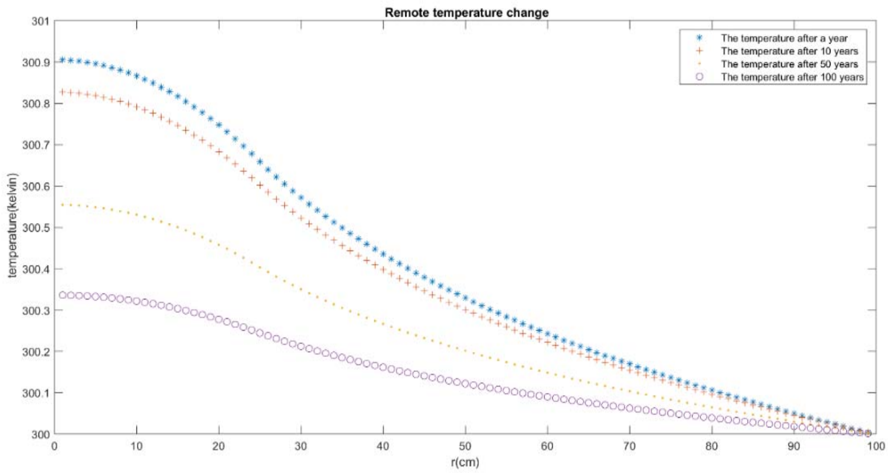

Figure 3 - The impact radionational iron on temperature at a distance of 100 cm
at each moment of the year taken by time up to 100 years

Acknowledgements. This research has been supported from the Science Committee of the Ministry of Education and Science of the Republic of Kazakhstan (Grants № AP05132680).

Марат Нуртас[1], Ж.Д. Байшемиров [2,3]

[1]Международный университет информационных технологий;
[2]Казахский национальный педагогический университет имени Абая;
[3]Институт информационных и вычислительных технологий.

ИССЛЕДОВАНИЕ ТЕМПЕРАТУРНОГО РЕЖИМА ТЕРРИТОРИИ СЕМИПАЛАТИНСКОГО ПОЛИГОНА И ОПИСАНИЕ МАТЕМАТИЧЕСКОЙ МОДЕЛИ И ЕГО ЧИСЛЕННОГО РЕШЕНИЯ

Аннотация. После распада Советского Союза Казахстан унаследовал очень неприятное наследство - Семипалатинский полигон, где за 45 лет было произведено 456 ядерных взрывов [1]. Ядерные взрывы на земле образовались при длительном радиоактивном загрязнении в виде длинных полос, так называемых «радиоактивных следов», которые выходят далеко за пределы площадки [2]. Взрывоопасные смеси особенно приводили к многочисленным изменениям, включая пожар. Актуальность этой работы заключается в том, что, несмотря на то, что Семипалатинский испытательный полигон закрыт, распределение тепла вокруг источника ядерных отходов сохраняется, поэтому необходимо изучать изменение температуры вокруг отходов. Это работа отражает изменение температуры окружающей среды ядерных отходов, которые подверглись воздействию ядерных взрывов. В качестве основы проекта мы изучили влияние небольшого железного куска, подвергшегося воздействию радиации, и его влияние на температуру самой окружающей среды. В задаче рассмотрена математическая модель двумерного уравнения теплового параболического типа и значение начальных и граничных условий, а также приведено ее численное решение и графическое представление того же численного решения.

Результатом данной работы является демонстрация того, насколько точно среда, подверженная воздействию радиации, может использоваться для производства или иным образом, и как рассчитать цифровое решение в форме математических моделей и графически проиллюстрировать численное решение.

Ключевые слова: Математическое моделирование, Численные методы, радиоактивные отходы, уравнения теплопроводности.

Марат Нуртас[1], Байшемиров Ж.Д.[2,3]

[1]Халықаралық ақпараттық технологиялар университеті;
[2] Абай атындағы Қазақ ұлттық педагогикалық университеті;
[3]Ақпараттық және есептеуіш технологиялар институты

СЕМЕЙ ПОЛИГОНЫ АУМАҒЫНЫҢ ТЕМПЕРАТУРАЛЫҚ РЕЖИМІН ЗЕРТТЕУ ЖӘНЕ МАТЕМАТИКАЛЫҚ МОДЕЛЬДІ ЖӘНЕ ОНЫҢ САНДЫҚ ШЕШІМІН СИПАТТАУ

Аннотация. Кеңес Одағы ыдырағаннан кейін Қазақстан 45 жылда 456 ядролық жарылыс болған Семей полигоныны өте залалды мұра қалдырды [1]. Жер бетіндегі ядролық жарылыстар ұзақ мерзімді радиоактивті ластану кезінде сынақ алаңының беткі сыртында көрінетін ұзын жолақтар түрінде пайда болған белгілері «радиоактивті іздер» деп аталды. Жарылғыш қоспалар, әсіресе, өртті қоса алғанда көптеген өзгерістерге әкелді[2]. Бұл жұмыстың өзектілігі Семей сынақ полигонының жабылғанына қарамастан, ядролық қалдықтардың көзі айналасында жылуды тарату болып қалады, сондықтан қалдықтардың айналасындағы температура өзгерісін зерттеу қажет. Бұл жұмыста ядролық полигонда болған жарылыстардың әсерінен жан жағына тараған ядролық қалдықтардың қоршаған ортаның температурасының өзгерісі есептелінген. Есептің негізі ретінде радиацияға ұшыраған кішкентай ғана темір кесегін тәжірибеге ала отырып, оның өзі жатқан ортаның температурасына әсер етуін қарастырдық. Қарастырылып отырған есепте екі өлшемді параболалық типтегі жылу өткізгіштік теңдеуі және оған қатысты алынған бастапқы және шекарылық шарттарының көмегімен математикалық модель құрылып, оның сандық шешімін алу барысы көрсетілген жане сол сандық шешімінің нәтижелері графикалық түрде көрсетілген. Бұл жұмыстың нәтижесінде сол радияциямен залалданған ортаның өндіріске не басқалай жағдайда пайдалануға қаншалықты жарамды екенін нақыты жылдар есебінде анықтау және математикалық модел түрінде берілген сандық шешімін графикалық түрде көрсету.

Түйін сөздер: Математикалық модельдеу, сандық әдістер, радиоактивті қалдықтар, жылу өткізгіштік теңдеулері.

Information about authors:

Marat Nurtas - International Information Technology University, 050040 Almaty, Kazakhstan, marat_nurtasj@mail.ru, https://orcid.org/0000-0003-4351-0185;

Baishemirov Zh.D. - Abai Kazakh National Pedagogical University, 050010 Almaty, Kazakhstan, Institute of Information and Computational Technology, 050010 Almaty, Kazakhstan, e-mail: zbai.kz@gmail.com, https://orcid.org/0000-0002-4812-4104

REFERENCES

[1] Бүгін – Семейполигоныныңжабылғанына 26 жыл, KHABAR.KZ, Aug. 2017. [Online]. Available: https://khabar.kz/kz/news/kogam-kz/item/89212-b-gin-semej-poligonyny-zhabyl-anyna-26-zhyl-toldy [Accessed: 27.08.17]

[2] Мамаш, Е.А., Аюнов, Д.Е., Кихтенко, В.А., Смирнов, В.В., Чубаров, Д.Л.,Исследование температурного режима в территории Семипалатинского полигона с использованием пространственно-временной агрегации длинных рядов спутниковых измерений,ИНТЕРЭКСПО ГЕО-СИБИРЬ, С. 40, 2015

[3] Великанов, А.Е., К вопросу о радиоактивной и газообразной сущности периодически появляющейся региональной тепловой аномалии в районе Семипалатинского испытательного полигона, Журнал ВЕСТНИК НЯЦ РК, Выпуск 2, С. 73-74, Jun. 2007

[4] A. Fichtner, Full Seismic Waveform Modelling and Inversion, Springer- Verlag Berlin Heidelberg. (2011) pp. 113--140.

[5] Miklos, V., The tragic story of the Semipalatinsk nuclear test site, Gizmodo, May. 2013. [Online] Available: https://io9.gizmodo.com/the-tragic-story-of-the-semipalatinsk-nuclear-test-site-5988266 [Accessed: 01.05.13]

[6] Карманов, А.В., Сейтжанов, Р.Ж., Френкель, Е.Э. Последствия испытаний на Семипалатинском ядерном полигоне, [Online]. Available:https://scienceforum.ru/2016/article/2016024352

[7] Лукьяненко С.А., Михайлова И.Ю. Методы моделирования температурного поля при бесконтактной лазерной деформации пластины // Научно-технический вестник информационных технологий, механики и оптики, 2014, №1 (89).

[8] Semipalatinsk Polygon, Atlas Obscura, [Online]. Available: https://www.atlasobscura.com/places/semipalatinsk-polygon

[9] Надёжин, А. Страшное наследие СССР: Семипалатинский полигон сегодня, Рамблер, Sep. 2018. [Online], Available: https://news.rambler.ru/other/40825907-strashnoe-nasledie-sssr-semipalatinskiy-poligon-segodnya/?utm_source=copylink&utm_content=rnews&utm_medium=read_more [Accessed: 18.09.18]

[10] Hermans, S., Semipalatinsk Test Site (Polygon), Kurchatov&Chagan Air Base, Caravanistan, Nov. 2018. [Online]. Available: https://caravanistan.com/kazakhstan/north/semey/kurchatov-polygon/ [Accessed: 12.11.18]

[11] Великанов, А.Е., К вопросу о радиоактивной и газообразной сущности периодически появляющейся региональной тепловой аномалии в районе Семипалатинского испытательного полигона, Журнал ВЕСТНИК НЯЦ РК, Выпуск 2, С. 72-79, Jun. 2007

[12] Coleman, M.P. An introduction to partial differential equation with MatLab, second edition, U.S.: Taylor & Francis Group, 2013.

[13] MeirmanovA.M., Nurtas M. Mathematical models of seismic in composite media: elastic and poroelastic components// Electronic Journal of Differential Equations. №184. 2016. PP.1-22.

[14] R.E. Burns., W.E. Causey, Nuclear waste disposal in space. NASA technical paper 1225.1978.

[15] Todd Young and Martin J. Mohlenkamp, Introduction to Numerical Methods and Matlab Programming for Engineers. Department of Mathematics Ohio University, May 4, 2017.

[16] R.E. Burns., W.E. Causey, Nuclear waste disposal in space. NASA technical paper 1225.1978.

N E W S
OF THE NATIONAL ACADEMY OF SCIENCES OF THE REPUBLIC OF KAZAKHSTAN
PHYSICO-MATHEMATICAL SERIES
ISSN 1991-346X **https://doi.org/10.32014/2019.2518-1726.50**
Volume 4, Number 326 (2019), 122 – 128

UDC 517.951

D.Serikbaev[1], N. Tokmagambetov[2]

[1,2]Al–Farabi Kazakh National University, Almaty, Kazakhstan;
[2]Ghent University, Ghent, Belgium;
[1,2]Institute of Mathematics and Mathematical Modeling,Almaty, Kazakhstan
serykbaev.daurenbek@gmail.com, niyaz.tokmagambetov@gmail.com

AN INVERSE PROBLEM FOR THE PSEUDO-PARABOLIC EQUATION FOR A STURM-LIOUVILLE OPERATOR

Abstract. A class of inverse problems for restoring the right-hand side of the pseudo-parabolic equation for Sturm–Liouville operator is considered. The inverse problem is to be well-posed in the sense of Hadamard whenever an overdetermination condition of the final temperature is given. Mathematical statements involve inverse problems for the pseudo-parabolic equation in which, solving the equation, we have to find the unknown right-hand side depending only on the space variable. We prove the existence and uniqueness of classical solutions to the problem. The proof of the existence and uniqueness results of the solutions is carried out by using L-Fourier analysis. The mentioned results are presented as well as for the fractional time pseudo–parabolic equation.Inverse problem of identifying the right hand side function of pseudo-parabolic equation from the local overdetermination condition, which has important applications in various areas of applied science and engineering, alsosuch problems are modeled using common homogeneous left-invariant hypoelliptic operators on common graded Lie groups.

Key words: Pseudo-parabolic equation, Sturm-Liouville operator, fractional Caputo derivative, inverse problem, well-posedness.

1 Introduction

The study of inverse problems for pseudo-parabolic equations goes back to 1980s. The first result [3] refers to the inverse problems of determining a source function f in the pseudo-parabolic equation

$$(u + \mathcal{L}_1 u)_t + \mathcal{L}_2 u = f, \tag{1}$$

with linear operators $\mathcal{L}_1$ and $\mathcal{L}_1$ of the second order, $\mathcal{L}_1 = \mathcal{L}_2$. Such equations arise in the models of the heat transfer, filtration in the fissured media, quasi-stationary processes in the crystalline semiconductor.

In this paper we consider pseudo–parabolic equation generated by Sturm–Liouville operator with Caputo time-fractional derivative. We study the following equation

$$\mathcal{D}_t^\alpha[u(t,x) + \mathcal{L}u(t,x)] + \mathcal{L}u(t,x) = f(x), \tag{2}$$

for $(t,x) \in \Omega = \{(t,x) | 0 < t \le T < \infty, a \le x \le b\}$, where $\mathcal{D}_t^\alpha$ is the Caputo derivative and $\mathcal{L}$ is the Sturm–Liouville operator which are defined in the next section.

This paper is devoted to the inverse problems of determining a source function in the pseudo-parabolic equation (2) by using the L-Fourier method.

In a series of articles [7, 8, 9, 10, 11, 13, 14, 15, 16, 17, 18, 19] some recent work has been done on inverse problems and spectral problems for the diffusion and anomalous diffusion equations.

2 Preliminaries

2.1 Sturm-Liouville problem

We first describe the setting of the Sturm-Liouville operator. Let $\mathcal{L}$ be an ordinary second order differential operator in $L^2(a,b)$ generated by the differential expression

$$\mathcal{L}(u) = -u_{xx}(x), a < x < b, \tag{3}$$

and boundary conditions

$$A_1 u'(b) + B_1 u(b) = 0, A_2 u'(a) + B_2 u(a) = 0, \tag{4}$$

where $A_1^2 + A_2^2 > 0, B_1^2 + B_2^2 > 0$, and $A_j, B_j, j = 1,2$, are some real numbers.

It is known [2] that the Sturm-Liouville problem for(3) with boundary conditions (4) is self-adjoint in $L^2(a,b)$. It is known that the self-adjoint problem has real eigenvalues and their eigenfunctions form a complete orthonormal basis in $L^2(a,b)$. So we can denote eigenvalues of the operator $\mathcal{L}$ and their eigenfunctions accordingly by λ_ξ and $e_\xi(x)$. That say us for $e_\xi(x) \in L^2(a,b)$ following identity is hold:

$$\mathcal{L}e_\xi(x) = \lambda_\xi e_\xi(x), \lambda_\xi \in \mathbb{R}. \tag{5}$$

Where $\mathcal{I}$ is a countable set and $\forall \xi \in \mathcal{I}$.

2.2 Definitions of the Caputo fractional derivative

Definition 2.1 *[6] The Riemann-Liouville fractional integral I^α of order $\alpha > 0$ for an integrable function is defined by*

$$I^\alpha[f](t) = \frac{1}{\Gamma(\alpha)} \int_c^t (t-s)^{\alpha-1} f(s) ds, t \in [c,d],$$

where Γ denotes the Euler gamma function.

Definition 2.2 *[6] The Riemann-Liouville fractional derivative D^α of order $\alpha \in (0,1)$ of a continuous function is defined by*

$$D^\alpha[f](t) = \frac{d}{dt} I^\alpha[f](t), t \in [c,d].$$

Definition 2.3 *[6] The Caputo fractional derivative of order $0 < \alpha < 1$ of a differentiable function is defined by*

$$\mathcal{D}_*^\alpha[f](t) = D^\alpha[f'(t)], t \in [c,d].$$

3 Formulation of the problem

Problem 3.1 *We aim to find a couple of functions $(u(t,x), f(x))$ satisfying the equation (2) , under the conditions*

$$u(0,x) = \varphi(x), x \in [a,b] \tag{6}$$

$$u(T,x) = \psi(x), x \in [a,b]. \tag{7}$$

and the homogeneous boundary conditions(4).

By using $\mathcal{L}$–Fourier analysis we obtain existence and uniqueness results for this problem.

We say a solution of Problem 3.1 is a pair of functions $(u(t,x), f(x))$ such that they satisfy equation (2) and conditions (6) , (7) and (4) where $u(t,x) \in C^1([0,T]; C^2([a,b]))$ and $f(x) \in C([a,b])$.

4 Main results

For Problem 3.1, the following theorem holds.

Theorem 4.1 *Assume that* $\varphi(x), \psi(x) \in C^2[a,b]$. *Then the solution* $u(t,x) \in C^1([0,T], C^2([a,b])), f(x) \in C([a,b])$ *of the Problem 3.1 exists, is unique, and can be written in the form*

$$u(x,t) = \varphi(x) + \sum_{\xi \in \mathcal{I}} \frac{\left(\psi_\xi^{(2)} - \varphi_\xi^{(2)}\right)\left(1 - E_{\alpha,1}\left(-\frac{\lambda_\xi}{1+\lambda_\xi} t^\alpha\right)\right) e_\xi(x)}{\lambda_\xi \left(1 - E_{\alpha,1}\left(-\frac{\lambda_\xi}{1+\lambda_\xi} T^\alpha\right)\right)},$$

$$f(x) = -\varphi''(x) + \sum_{\xi \in \mathcal{I}} \frac{\left(\psi_\xi^{(2)} - \varphi_\xi^{(2)}\right) e_\xi(x)}{1 - E_{\alpha,1}\left(-\frac{\lambda_\xi}{1+\lambda_\xi} T^\alpha\right)}$$

where $\varphi_\xi^{(2)} = (\varphi'', e_\xi)_{L^2(0,l)}, \psi_\xi^{(2)} = (\psi'', e_\xi)_{L^2(0,l)}$ and $E_{\alpha,\beta}(\lambda t)$ is Mittag-Leffler type function (see [5]):

$$E_{\alpha,\beta}(z) = \sum_{n=0}^{\infty} \frac{z^m}{\Gamma(\alpha m + \beta)}.$$

Proof. First of all, we start by proving an existence result. Let us look for functions $u(t,x)$ and $f(x)$ in the forms:

$$u(t,x) = \sum_{\xi \in \mathcal{I}} u_\xi(t) e_\xi(x), \tag{8}$$

and

$$f(x) = \sum_{\xi \in \mathcal{I}} f_\xi e_\xi(x), \tag{9}$$

where $u_\xi(t)$ and f_ξ are unknown. Substituting (8) and (9) into Problem 3.1 and using(5) we obtain the following problem for the functions $u_\xi(t)$ and for the constants $f_\xi, \xi \in \mathcal{I}$:

$$\begin{cases} \mathcal{D}^\alpha u_\xi(t) + \frac{\lambda_\xi}{1+\lambda_\xi} u_\xi(t) = \frac{f_\xi}{1+\lambda_\xi}, \\ u_\xi(0) = \varphi_\xi, \\ u_\xi(T) = \psi_\xi, \end{cases} \tag{10}$$

where φ_ξ, ψ_ξ are $\mathcal{L}$-Fourier coefficients of $\varphi(x)$ and $\psi(x)$:

$$\varphi_\xi = (\varphi, e_\xi)_{L^2(a,b)},$$

$$\psi_\xi = (\psi, e_\xi)_{L^2(a,b)}.$$

General solution of this problem:

$$u_\xi(t) = \frac{f_\xi}{\lambda_\xi} + C_\xi E_{\alpha,1}\left(-\frac{\lambda_\xi}{1+\lambda_\xi} t^\alpha\right), \tag{11}$$

where the constants C_ξ, f_ξ are unknown. By using initial and additional conditions we can find they. We first find C_ξ:

$$u_\xi(0) = \frac{f_\xi}{\lambda_\xi} + C_\xi = \varphi_\xi,$$

$$u_\xi(T) = \frac{f_\xi}{\lambda_\xi} + C_\xi E_{\alpha,1}\left(-\frac{\lambda_\xi}{1+\lambda_\xi} T^\alpha\right) = \psi_\xi,$$

$$\varphi_\xi - C_\xi + C_\xi E_{\alpha,1}\left(-\frac{\lambda_\xi}{1+\lambda_\xi} T^\alpha\right) = \psi_\xi.$$

Then

$$C_\xi = \frac{\varphi_\xi - \psi_\xi}{1 - E_{\alpha,1}\left(-\frac{\lambda_\xi}{1+\lambda_\xi} T^\alpha\right)}.$$

f_ξ is represented as

$$f_\xi = \lambda_\xi \varphi_\xi - \lambda_\xi C_\xi.$$

Substituting $f_\xi, u_\xi(t)$ into formulas (8) and (9), we find

$$u(x,t) = \varphi(x) + \sum_{\xi \in \mathcal{J}} C_\xi \left(E_{\alpha,1}\left(-\frac{\lambda_\xi}{1+\lambda_\xi} t^\alpha\right) - 1\right) e_\xi(x).$$

Using self-adjoint property of operator $\mathcal{L}$

$$\left(-\varphi'', e_\xi\right)_{L^2(a,b)} = \left(\varphi, -e_{\xi''}\right)_{L^2(a,b)}$$

and in respect that(5) we obtain

$$\left(\varphi, e_\xi\right)_{L^2(a,b)} = \frac{\left(-\varphi'', e_\xi\right)_{L^2(a,b)}}{\lambda_\xi},$$

and for $\psi(x)$ we can write analogously. Substituting these equality into formula of C_ξ we can get that

$$C_\xi = \frac{\psi_\xi^{(2)} - \varphi_\xi^{(2)}}{\lambda_\xi \left(1 - E_{\alpha,1}\left(-\frac{\lambda_\xi}{1+\lambda_\xi} T^\alpha\right)\right)}.$$

Then

$$u(t,x) \quad = \varphi(x) + \sum_{\xi \in \mathcal{J}} \frac{\left(\psi_\xi^{(2)} - \varphi_\xi^{(2)}\right)\left(1 - E_{\alpha,1}\left(-\frac{\lambda_\xi}{1+\lambda_\xi} t^\alpha\right)\right) e_\xi(x)}{\lambda_\xi \left(1 - E_{\alpha,1}\left(-\frac{\lambda_\xi}{1+\lambda_\xi} T^\alpha\right)\right)}, \tag{12}$$

$$f(x)=\mathcal{L}\varphi(x)+\sum_{\xi\in\mathcal{I}}\frac{\left(\psi_\xi^{(2)}-\varphi_\xi^{(2)}\right)e_\xi(x)}{1-E_{\alpha,1}\left(-\frac{\lambda_\xi}{1+\lambda_\xi}T^\alpha\right)}. \tag{13}$$

The following Mittag-Leffler function's estimate is known by [12]:

$$|E_{\alpha,\beta}(z)|\leq\frac{M}{1+|z|}, arg(z)=\pi, |z|\to\infty. \tag{14}$$

Now, we show that $u(t,x)\in C^1([0,T];C^2([a,b]))$, $f(x)\in C([a,b])$, that is

$$\| u \|_{C^1([0,T];C^2([a,b]))}=\max_{t\in[0,T]}\| u(t,\cdot) \|_{C^2([a,b])}+\max_{t\in[0,T]}\| \mathcal{D}_t^\alpha u(t,\cdot) \|_{C^2([a,b])}<\infty,$$

and

$$\| f \|_{C([a,b])}<\infty.$$

By using(14), we get the following estimates

$$\begin{aligned}|u(t,x)| &\lesssim |\varphi(x)|+\sum_{\xi\in\mathcal{I}}\frac{\left|\varphi_\xi^{(2)}\right|+\left|\psi_\xi^{(2)}\right|}{\lambda_\xi\left(1-E_{\alpha,1}\left(-\frac{\lambda_\xi}{1+\lambda_\xi}T^\alpha\right)\right)}\\ &\lesssim |\varphi(x)|+\sum_{\xi\in\mathcal{I}}\frac{\left|\varphi_\xi^{(2)}\right|+\left|\psi_\xi^{(2)}\right|}{\lambda_\xi},\end{aligned} \tag{15}$$

$$\begin{aligned}|f(x)| &\lesssim |\varphi''(x)|+\sum_{\xi\in\mathcal{I}}\frac{\left|\varphi_\xi^{(2)}\right|+\left|\psi_\xi^{(2)}\right|}{1-E_{\alpha,1}\left(-\frac{\lambda_\xi}{1+\lambda_\xi}T^\alpha\right)}\\ &\lesssim |\varphi''(x)|+\sum_{\xi\in\mathcal{I}}\left|\varphi_\xi^{(2)}\right|+\left|\psi_\xi^{(2)}\right|.\end{aligned} \tag{16}$$

Where, $L\lesssim Q$ \$L denotes $L\leq CQ$ for some positive constant C independent of L and Q.

By supposition of the theorem we know $\varphi^{(2)}$ and $\psi^{(2)}$ are continuous on $[a,b]$. Then by the Bessel inequality for the trigonometric series (see [1]) and by the Weierstrass M-test (see [4]), series (15) and (16) converge absolutely and uniformly in the region $\overline{\Omega}$. Now we show

$$\begin{aligned}|u_{xx}(t,x)| &\lesssim |\varphi''(x)|+\sum_{\xi\in\mathcal{I}}\frac{\left|\varphi_\xi^{(2)}\right|+\left|\psi_\xi^{(2)}\right|}{1-E_{\alpha,1}\left(-\frac{\lambda_\xi}{1+\lambda_\xi}T^\alpha\right)}\\ &\lesssim |\varphi''(x)|+\sum_{\xi\in\mathcal{I}}\left|\varphi_\xi^{(2)}\right|+\left|\psi_\xi^{(2)}\right|<\infty,\end{aligned}$$

$$\begin{aligned}|\mathcal{D}_t^\alpha u(t,x)| &\lesssim \sum_{\xi\in\mathcal{I}}\frac{\left|\varphi_\xi^{(2)}\right|+\left|\psi_\xi^{(2)}\right|}{(1+\lambda_\xi)\left(1-E_{\alpha,1}\left(-\frac{\lambda_\xi}{1+\lambda_\xi}T^\alpha\right)\right)}\\ &\lesssim \sum_{\xi\in\mathcal{I}}\frac{\left|\varphi_\xi^{(2)}\right|+\left|\psi_\xi^{(2)}\right|}{1+\lambda_\xi}<\infty,\end{aligned}$$

$$|\mathcal{D}_t^\alpha u_{xx}(t,x)| \lesssim \sum_{\xi\in\mathcal{I}} \frac{\lambda_\xi\left(\left|\varphi_\xi^{(2)}\right|+\left|\psi_\xi^{(2)}\right|\right)}{(1+\lambda_\xi)\left(1-E_{\alpha,1}\left(-\frac{\lambda_\xi}{1+\lambda_\xi}T^\alpha\right)\right)}$$

$$\lesssim \sum_{\xi\in\mathcal{I}} \left|\varphi_\xi^{(2)}\right|+\left|\psi_\xi^{(2)}\right|+\sum_{\xi\in\mathcal{I}}\frac{\left|\varphi_\xi^{(2)}\right|+\left|\psi_\xi^{(2)}\right|}{1+\lambda_\xi}<\infty.$$

Finally, we obtain

$$\parallel u \parallel_{C^1([0,T],C^2[a,b])} \leq C < \infty, C = const,$$

and

$$\parallel f \parallel_{C([a,b])} < \infty.$$

Existence of the solution is proved.

Now, we start proving uniqueness of the solution

Let us suppose that $\{u_1(t,x), f_1(x)\}$ and $\{u_2(t,x), f_2(x)\}$are solution of the Problem 3.1. Then $u(t,x) = u_1(t,x) - u_2(t,x)$ and $f(x) = f_1(x) - f_2(x)$ are solution of following problem:

$$\mathcal{D}_t^\alpha[u(t,x) - u_{xx}(t,x)] - u_{xx}(t,x) = f(x), \tag{17}$$

$$u(0,x) = 0, \tag{18}$$

$$u(T,0) = 0. \tag{19}$$

By using (12) and (13) for (17) - (19) we easily see $u(x,t) \equiv 0, f(x) \equiv 0$. Uniqness of the solution of the Problem 3.1.

ACKNOWLEDGEMENTS

The authors were supported by the Ministry of Education and Science of the Republic of Kazakhstan (MESRK) Grant AP05130994. No new data was collected or generated during the course of research.

Д. Серикбаев[1], Н. Токмагамбетов[2]

[1,2]Әл-ФарабиатындағыҚазҰУ, Алматы, Қазақстан;
[2]Гент университеті, Гент, Белгия;
[1,2]Математикажәнематематикалық модельдеу институты, Алматы, Қазақстан

ШТУРМ-ЛУИВИЛЛ ОПЕРАТОРЛЫ ПСЕВДО-ПАРАБОЛАЛЫҚ ТЕҢДЕУ ҮШІН КЕРІ ЕСЕП

Аннотация.Штурм-Лиувилл операторлы псевдо-параболалық теңдеудің оң жақ бөлігін қалпына келтіру кері есебі қарастылады. Соңғы уақыт моментіндегі температура алдын ала берілген жағдайда кері есеп әр уақытта Адамар мағынасында қисынды болуы керек. Математикалық тұжырымдарға сүйенсек, псевдо-параболалық теңдеу үшін кері есеп қатарына теңдеуді шешу барысында тек кеңістік айнымалыдан тәуелді теңдеудің оң жақ функциясын табу есебі жатады. Теңдеудің классикалық шешімі бар және жалғыз екендігі дәлелденеді, дәлелдеу L-Фурье талдауы арқылы жүргізіледі. Аталған нәтижелер уақыт бойынша бөлшек туындылы псевдо-параболалық теңдеу үшін көрсетілді. Алдын ала берілген локалдық шарт бойынша псевдо-параболалық теңдеудің оң жақ функциясын анықтау есебі, әр түрлі қолданбалы ғылым және де техника саласында маңызды қолданысы бар. Сонымен қатар, мұндай проблемалар жалпы біртекті сол-инвариантты гипоэллиптикалық операторлар арқылы біртекті Ли топтары бойынша модельденеді.

Түйін сөздер: Псевдопараболалық теңдеу, Штурм-Лиувилл операторы, бөлшек Капуто туындысы, кері есеп, есептің қисындылығы.

Д. Серикбаев[1], Н. Токмагамбетов[2]

[1,2]КазНУ им. Аль-Фараби, Алматы, Казахстан; [2]Гентский университет, Гент, Белгия;
[1,2]Институт математики и математического моделирования, Алматы, Казахстан

ОБРАТНАЯ ЗАДАЧА ДЛЯ ПСЕВДО-ПАРАБОЛИЧЕСКОГО УРАВНЕНИЯ ДЛЯ ОПЕРАТОРА ШТУРМА-ЛИУВИЛЯ

Аннотация. Рассматривается класс обратных задач восстановления правой части псевдопараболичес-кого уравнения для оператора Штурма-Лиувилля. Обратная задача должна быть корректной в смысле Адамара всякий раз, когда дается условие переопределения конечной температуры. Математические утверждения включают обратные задачи для псевдопараболического уравнения, в котором, решая уравнение, мы должны найти неизвестную правую часть, зависящую только от пространственной переменной. Доказано существование и единственность классических решений задачи. Доказательство результатов существования и единственности решений проводится с помощью L-анализа Фурье. Упомя-нутые результаты представлены также для псевдопараболического уравнения с дробным временем. Обратная задача идентификации функции правой части псевдопараболического уравнения из условия локального переопределения, имеють важные приложения в различных областях прикладной науки и техники, а так же эти проблемы моделируются на однородных группах Ли с помощью однородных левоинвариантных гипоэллиптических операторов.

Ключевые слова: Псевдопараболическое уравнение, оператор Штурма-Лиувилля, дробная производная Капуто, обратная задача, корректность.

Information about authors:

Tokmagambetov Niyaz – PhD doctor, Department of Mathematics: Analysis, Logic and Discrete Mathematics, Ghent University, Ghent, Belgium;

Serikbaev Daurenbek – Doctorate, Al–Farabi Kazakh National University, Almaty, Kazakhstan.

REFERENCES

[1] Zygmund, A., “Trigonometrical Series”, Cambridge, 1959.

[2] M. A. Naimark. *Linear Differential Operators.* Ungar, New York, 1968.

[3] Rundell W. Determination of an unknown nonhomogeneous term in a linear partial differential equation from overspecified boundary data // Appl. Anal. 1980. V. 10. P. 231-242.

[4] Knopp K. Theory of Functions Parts I and II, Two Volumes Bound as One, Part I. New York: Dover; 1996:73.

[5] Y. Luchko, R. Gorenflo. An operational method for solving fractional differential equations with the Caputo derivatives. Acta Math. Vietnam., 24:207–233, 1999.

[6] Kilbas A.A, Srivastava H.M., Trujillo J.J. Theory and Applications of Fractional Differential Equations, Mathematics studies, vol. 204. North-Holland: Elsevier;2006:vii–x.

[7] Kaliev I.A, Sabitova M.M. Problems of determining the temperature and density of heat sources from the initial and final temperatures. J Appl Ind Math. 2010;4(3):332-339.

[8] M. Kirane, A.S. Malik. Determination of an unknown source term and the temperature distribution for the linear heat equation involving fractional derivative in time. Applied Mathematics and Computation. 218(1):163–170, 2011.

[9] I. Orazov, M.A. Sadybekov. One nonlocal problem of determination of the temperature and density of heat sources. Russian Mathematics. 56(2):60–64, 2012.

[10] I. Orazov, M.A. Sadybekov. On a class of problems of determining the temperature and density of heat sources given initial and final temperature. Siberian Mathematical Journal. 53(1):146–151, 2012.

[11] K.M. Furati, O.S. Iyiola, M. Kirane. An inverse problem for a generalized fractional diffusion. Applied Mathematics and Computation. 249: 24–31, 2014.

[12] Z. Li, Y. Liu, M. Yamamoto. Initial-boundary value problems for multi-term time-fractional diffusion equations with positive constant coefficients. Appl. Math. Comput., 257:381–397, 2015.

[13] M. Kirane, Al-Salti N. Inverse problems for a nonlocal wave equation with an involution perturbation. J Nonlinear Sci Appl. 2016;9(3):1243-1251.

[14] H. T. Nguyen, D. L. Le, V. T. Nguyen. Regularized solution of an inverse source problem for a time fractional diffusion equation. Applied Mathematical Modelling. 40(19): 8244–8264,2016.

[15] M. I. Ismailov, M. Cicek. Inverse source problem for a time-fractional diffusion equation with nonlocal boundary conditions. Applied Mathematical Modelling. 40(7): 4891–4899, 2016.

[16] N. Al-Salti, M. Kirane, B. T. Torebek. On a class of inverse problems for a heat equation with involution perturbation. Hacettepe Journal of Mathematics and Statistics. 2017, Doi: 10.15672/HJMS.2017.538

[17] M. Kirane, B. Samet, B. T. Torebek. Determination of an unknown source term temperature distribution for the sub-diffusion equation at the initial and final data. *Electronic Journal of Differential Equations*. 2017: 1–13, 2017.

[18] B. T. Torebek, R. Tapdigoglu. Some inverse problems for the nonlocal heat equation with Caputo fractional derivative. *Mathematical Methods in the Applied Sciences*. 40(18):6468–6479, 2017.

[19] Shaldanbaeva A. A., Akylbayev M.I., Shaldanbaev A. Sh., Beisebaeva A.Zh. **(2018)**The spectral decomposition of cauchy problem’s solution for Laplace equation. *News of the National Academy of Sciences of the Republic of Kazakhstan. Series of physic-mathematical sciences.* Volume 5, Number 321(2018), pp 75-87. https://doi.org/10.32014/2018.2518-1726.10 ISSN 1991-346X.

N E W S
OF THE NATIONAL ACADEMY OF SCIENCES OF THE REPUBLIC OF KAZAKHSTAN
PHYSICO-MATHEMATICAL SERIES
ISSN 1991-346X **https://doi.org/10.32014/2019.2518-1726.51**
Volume 4, Number 326 (2019), 129 – 134

A.F. Yakovets[1], A. Jahanshir[2], G.I. Gordienko[1], B.T. Zhumabayev[1], Yu.G. Litvinov[1], N. Abdrakhmanov[3]

[1]«Institute of Ionosphere» JSC «NCSRT», Almaty, Kazakhstan;
[2]Buein Zahra Technical University, Iran;
[3]Korkyt ata's Kysylorda State University, Kysylorda, Kazakhstan
artyak40@mail.ru

STATISTICS OF VARIATION RANGE OF F2- LAYER MAXIMUM HEIGHT OF THE IONOSPHERE

Abstract. The statistics of the nights when the ionosphere was sounded at the Institute of the Ionosphere in 2009–2016, and the nights during which the large scale traveling ionospheric disturbances (LS TIDs) were observed, were presented. Out of 1454 sessions of nighttime observations of the ionosphere, LS TIDs were observed in 185 sessions. The features of atmospheric and magnetospheric LS TIDs are found: a) high coherence of variations of critical frequencies and virtual heights ($h'(t)$), b) an increase in the amplitude of variations of $h'(t)$ with an increase in the sounding frequency, c) phase delay of variations of $h'(t)$ at lower frequencies relative to variations at high frequencies. A method has been developed for estimating the magnitude of the peak to peak variations in the height of the F-layer maximum, in terms of the range of variations of the virtual reflection height of the sounding signal $h'(t)$ at the maximum frequency reflected from the ionosphere. Distributions of the magnitude of the maximum height variations are obtained for magnetically quiet and magnetically active observation conditions of the LS TIDs. It was found that the maximum probabilities of the magnitude of peak to peak lie in the range of 40-50 km for a disturbed and 30-50 km for a quiet magnetic field.

Key words: ionosphere, vertical sounding, height of F layer maximum.

Introduction

It is known that large-scale traveling ionospheric disturbances (LS TIDs) are manifestations of atmospheric gravity waves (AGWs) generated in polar regions during geomagnetic storms [1], when the rapid amplification of polar electrojets leads to local atmosphere heating. The process of rapid expansion and subsequent compression of the atmosphere creates atmospheric gravity waves that propagate to the equator and generate the LS TIDs on its way. A number of observations have shown that the LS TIDs can also persist during magnetically quiet periods [2, 3]. The propagation of AGW in the neutral atmosphere and their ionospheric manifestations (LS TIDs) have been studied both experimentally and theoretically for many years. The results of these studies are presented in a series of reviews [1, 4, 5].

AGW at middle latitudes have a wavelength greater than ~ 1000 km. For such a wave, the motion of a neutral gas at the heights of the *F*-layer is a horizontal wind blowing south along the meridian when half of the wave passes over the observation point and north when the next half-wave passes. Plasma in the *F*-layer of the ionosphere is involved in the movement due to collisions of neutrals with ions. The plasma in the *F*-layer is magnetized and, therefore, can only move along magnetic lines of force. This movement is due to the component of the neutral wind, directed along the magnetic field. A neutral wind blowing towards the equator and the pole pushes the plasma along the magnetic field lines up and down, respectively, leading to periodic fluctuations in the height of the F-layer maximum. Information on oscillations of the meridional wind caused by the passage of AGW was obtained by us in [6, 7], in which a method was developed for processing data of the vertical sounding of the ionosphere and finding the distribution of the magnitude of variations in the height of the *F*-layer maximum has been done. The range of variations was estimated from the height profile of the electron concentration obtained as a result of laborious calculations. This paper proposes a simple method for estimating the range of variations from the initial ionogram data and presents the results obtained for the period 2009–2016.

Description of the equipment and analysis of the results of observations.

Nighttime observations of the LS TIDs in the *F*-layer of the ionosphere were carried out at the Institute of the Ionosphere (Alma-Ata 76 ° 55'E, 43 ° 15'N) on a digital ionosonde PARUS associated with a computer intended for collecting, storing and processing ionograms in digital form. The information necessary for calculating the various parameters of the LS TIDs was read from the ionograms by the semi-automatic method with the participation of an experienced operator. In [8], it was shown that such a method has a greater, as compared with the automatic method, reading accuracy of ionospheric parameters with ionograms and a large statistical yield of ionograms suitable for processing. The ionosphere was sounded every 5 min. The ionograms allow reading the values of the virtual reflection heights $h'(t)$ of the radio signal at a number of fixed operating frequencies and critical frequencies ($f_{o,x}F$). 1454 nighttime observations were carried out for the period 2009 - 2016, while 185 nights were characterized by wave activity associated with the LS TIDs.

The nights characterized by wave activity were divided into two groups according to the minimum value of the Dst index, which took place on a time interval beginning a few hours before the start of the observation session and ending at the end of the session. They represented observations with moderate and high geomagnetic activity (Dst ≤ - 40 nT) and low magnetic activity (Dst> - 40 nT). A typical example of the behavior of the *F*-layer parameters for such nights is shown in Fig. 1.

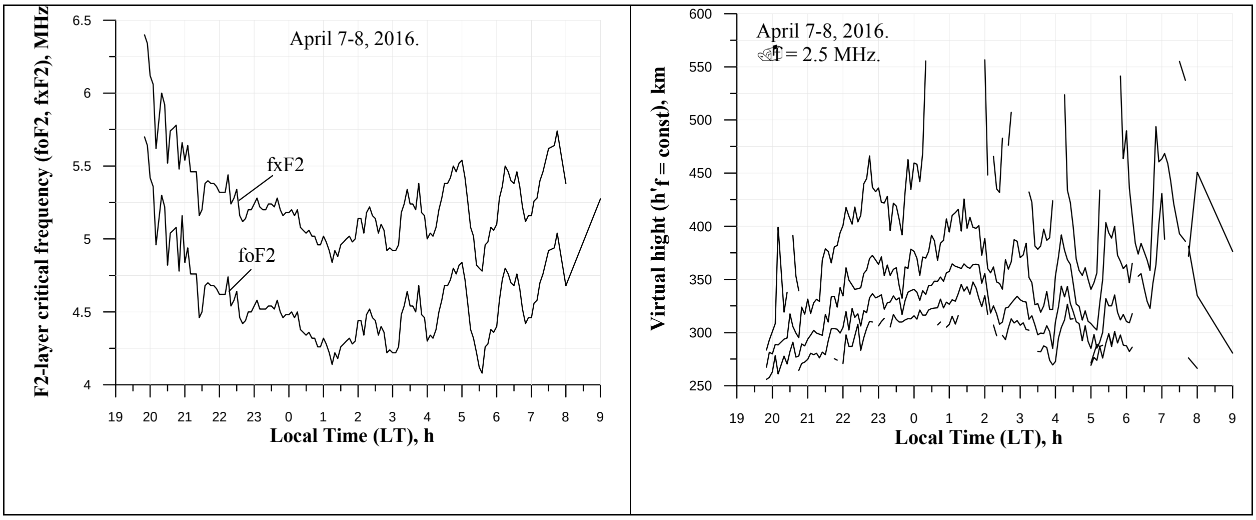

Figure 1 - Example of stochastic (LT = 20.00-01.30) and quasi-periodic (LT = 01.30-08.00) variations of critical frequencies (left panel) and effective heights of reflection from the ionosphere on a series of sounding frequencies (right panel).

Figure 1 shows the variations of critical frequencies (left panel) and operating altitudes (right panel) at night of April 7–8, 2016. Visual analysis allows us to conclude that in the first half of the night the critical frequencies decreased because the Sun, which represents the main source of ionizing radiation, did not illuminate the thermosphere on ionospheric altitudes. At the same time, the virtual reflection heights of the radio signal increased. Around 01.30, quasi-periodic variations of $f_{o,x}F$ and $h'(t)$ began at a number of sounding frequencies with an average period of ~ 1.5 h. Such characteristics of parameter variations as their high coherence and phase delays $h'(t)$ at lower frequencies with respect to variations on at high frequencies, allow to conclude that the variations represent LS TIDs caused by the propogation of AGW.

Critical frequencies and virtual heights are directly read from ionograms by the operator, but they do not allow to obtain data on variations in the height of the layer maximum. To consider the possible connection, we compared the parameters of variations obtained from the altitude ionization profiles (Fig. 2, left panel) with the parameters of variations $h'(t)$ (Fig. 2, right panel). The left panel shows variations in the height of the *F*-layer maximum (h_mF), the base of the layer ($h_{bot}F$), the half-thickness of the layer (Δh), and the critical frequency f_0F. We are only interested in h_mF. It follows from the figure that on this night three waves with maxima were clearly traced, both for variations h_mF and for variations $h'(t)$, occurring at the times of 21:00, 23:30 and 01:30.

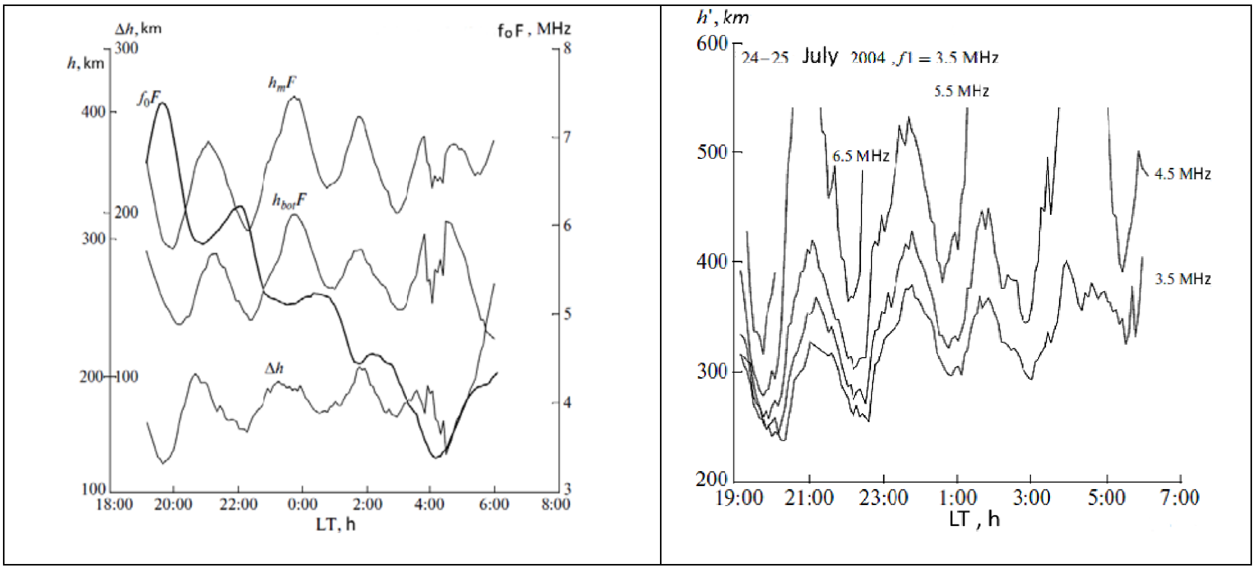

Figure 2 - Variations of the parameters of the ionosphere, calculated from the height profiles of the electron concentration (left panel) and variations of the virtual heights on a series of sounding frequencies (right panel) during the passage of atmospheric gravity waves

Let's turn to the right panel of the figure. It is seen that the variations of $h'(t)$ at the upper frequencies have discontinuities of various lengths. These discontinuities are due to the temporary behavior of the critical frequency (left panel). When the critical frequency becomes less than one or another frequency indicated on the right panel, the reflection at this frequency does not occur, and there are gaps in the behavior of $h'(t)$. It follows from the figure that with an increase in the working frequency, the range of variations increases. Tab. 1 shows the magnitude of variations for the height of the layer maximum (Δh_mF) and the virtual heights ($\Delta h'(t)$) for the three recorded waves. In this case, $\Delta h'_1$ refers to variations at a frequency of 3.5 MHz, $\Delta h'_2$ refers to variations at a frequency of 4.5 MHz, $\Delta h'_3$ refers to variations at a frequency of 5.5 MHz. The last frequency listed in the table for each wave corresponds to the maximum frequency that is still reflected from the ionosphere.

The next frequency is already experiencing breaks. For example, for waves 1, 2, the last frequency is 5.5 MHz, and for wave 3, this frequency is 4.5 MHz. Comparing the values given in the table, we come to the conclusion that the range of variations at the last frequency is about 2 times greater than the range of variations in the height of the layer maximum. This pattern was also observed for the other reviewed sessions of observations of the LS TIDs. Therefore, when processing a large statistical material, we used this ratio.

Table 1

LT	Δh_m (km)	$\Delta h'_1$ (km)	$\Delta h'_2$ (km)	$\Delta h'_3$ (km)
21:00	70	75	95	130
23:30	82	100	110	165
01:30	60	70	115	

Using this ratio, ΔhmF were calculated for all sessions with LS TIDs. In fig. Figure 3 shows the histograms of the distribution of the range of variations of the LS TIDs with low (left panel) and high (right panel) magnetic activity. The maximum probabilities ΔhmF lie in the range of 40-50 km for a disturbed and 30-50 km for a quiet magnetic field.

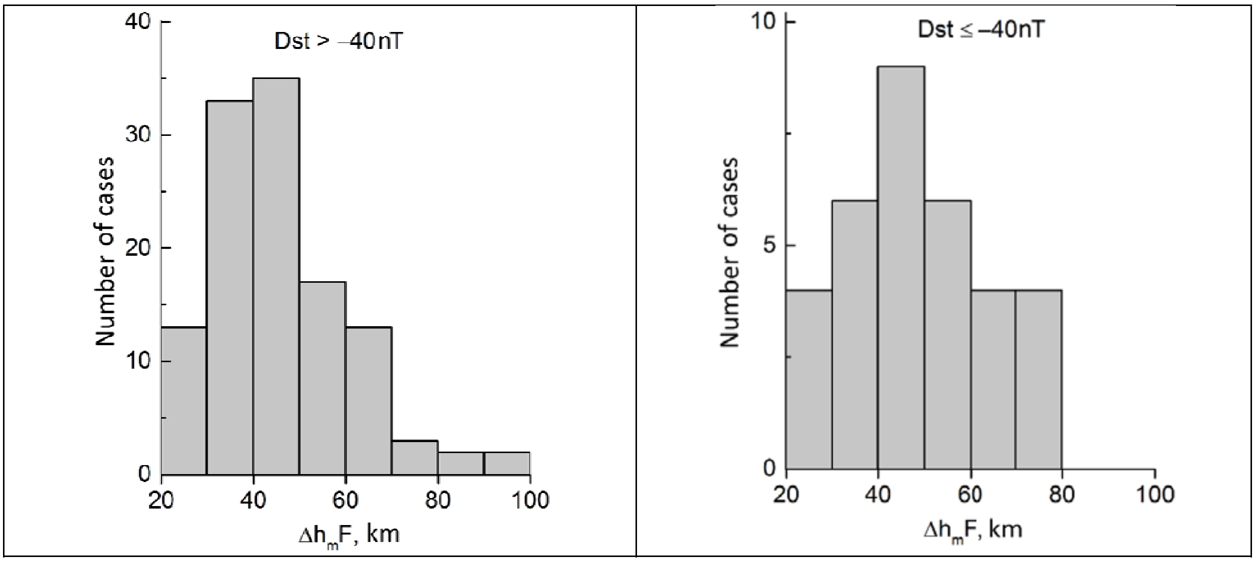

Figure 3 - Histograms of the distribution of the amplitude of variations of the LS TIDs with low (left panel) and high (right panel) magnetic activity

We analyzed all observation sessions, when quasi-periodic variations of ionospheric parameters were recorded. It was found that LS TIDs generated at low magnetic activity have the same properties as LS TIDs of magnetospheric origin, namely: a) high coherence of variations of critical frequencies and virtual heights ($h'(t)$) at heights covering the lower part of the F-layer, b) an increase in the amplitude of the variations $h'(t)$ with an increase in the sounding frequency; c) a phase delay of the variations $h'(t)$ at lower frequencies relative to variations at high frequencies. Thus, we came to the conclusion that the internal structure of the LS TIDs is the same for different sources of disturbances.

Conclusion

Thus, statistics was calculated for the nights when the ionosphere was frequently sounded at the Institute of the Ionosphere in 2009–2016, and for the nights during which traveling ionospheric disturbances were observed. Out of 1,454 sessions of nighttime observations of the ionosphere, 185 sessions with the LS TIDs were observed. The signs of atmospheric and magnetospheric origins of the LS TIDs are found: a) high coherence of variations of critical frequencies and virtual heights ($h'(t)$), b) an increase in the amplitude of variations $h'(t)$ with an increase in the sounding frequency, c) a phase delay of variations $h'(t)$ at lower frequencies relative to variations at high frequencies. A method has been developed for estimating the magnitude of the amplitude of variations in the height of the *F*-layer maximum, in terms of the amplitude of variations of the virtual reflection height of the sounding signal $h'(t)$ at certain sounding frequencies. Distributions of the magnitude of the amplitude height variations are obtained for magnetically quiet and magnetically active observation conditions of the LS TIDs.

The work was carried out in accordance with RBP-008 "Development of space technologies for monitoring and forecasting natural resources, technogenic environmental changes, creation of space technology and ground-based space infrastructure, research of long-distance and near-space objects" under the theme "Creation of a system of diagnostics and forecast of space weather for analysis and forecasting of conditions of functioning of space vehicles, navigation and communication systems (2018-2020), registration number (RN) 0118PK00800.

А.Ф. Яковец[1], А. Жаханшир[2], Г.И. Гордиенко[1],
Б.Т. Жумабаев[1], Ю.Г. Литвинов[1], Н. Абдрахманов[3]

[1]ЕЖШС «Ионосфера институты» «ҰҒЗТО» АҚ, Алматы, Қазақстан
[2]Буин Захра техникалық университеті, Иран
[3]Қорқыт Ата атындағы Қызылорда мемлекеттік университеті, Қызылорда, Қазақстан

ИОНОСФЕРАДАҒЫ F2- ҚАБАТЫНЫҢ ВАРИАЦИЯ АУҚЫМЫНЫҢ МАКСИМАЛДЫ БИІКТІГІН АЙҚЫНДАУ СТАТИСТИКАСЫ

Аннотация. Ионосфера институтында 2009-2016 жылдары жүргізілген ионосфераның жиі түндерін барлап байқау көрсетілген және де кең көлемді жылжымалы ионосфералық бұзылулар (КЖИБ) байқалған түндердің статистикасы ұсынылған. Ионосфераның түнгі бақылауларының 1454 сеансынан 185 (КЖИБ) сеансы байқалды. Кең көлемді жылжымалы ионосфералық бұзылулардың атмосфералық және магнитосфералық шығу белгілері анықталды: а) сыни жиіліктер мен биіктіктердің (*h'(t)*) қолданыстағы вариацияларының жоғары келісімділігі, б) вариация амплитудасының артуы *h'(t)* барлап байқау жиілігінің ұлғаюымен, в) жоғары жиіліктердегі вариацияларға қатысты төменгі жиіліктердегі вариацияларының *h'(t)* фазалық кешігуі. Ионосферадан көрінетін максималды жиіліктегі сигналының *h'(t)* тиімді көрсетілу биіктігіндегі вариация ауқымы бойынша, F-қабатының максималды биіктігіндегі вариация шамасын бағалау үшін әдіс әзірленді. Кең көлемді жылжымалы ионосфералық бұзылулардың магниттік тыныштықты және магниттік белсенді бақылау жағдайында, ауқымы бойынша максималды биіктік вариация шамаларының таралуы алынды. Максималды ықтималдығы бұзылған ауқым шамасы 40-50 км және тыныш магнит өрісі үшін 30-50 км болатындығы анықталды.

Түйін сөздер: ионосфера, тік барлап байқау, F2- қабатының максималды биіктігі

А.Ф. Яковец[1], А. Жаханшир[2], Г.И. Гордиенко[1],
Б.Т. Жумабаев[1], Ю.Г. Литвинов[1], Н. Абдрахманов[3]

[1]ДТОО «Институт ионосферы» АО «НЦКИТ», Алматы, Казахстан
[2]Буин Захра Технический Университет, Иран,
[3]Кызылординский государственный университет им. Коркыт ата, Кызылорда

СТАТИСТИКА РАЗМАХА ВАРИАЦИЙ ВЫСОТЫ МАКСИМУМА F2- СЛОЯ ИОНОСФЕРЫ

Аннотация. Представлена статистика ночей, когда проводилось учащенное зондирование ионосферы в Институте ионосферы в 2009-2016 годы, и ночей, в течение которых наблюдались крупномасштабные перемещающиеся ионосферные возмущения (КМПИВ). Из 1454 сеансов ночных наблюдений ионосферы в 185 сеансах наблюдались КМПИВ. Найдены признаки КМПИВ атмосферного и магнитосферного происхождения: а) высокая когерентность вариаций критических частот и действующих высот (*h'(t)*), б) увеличение амплитуды вариаций *h'(t)* с увеличением зондирующей частоты, в) фазовое запаздывание вариаций *h'(t)* на меньших частотах относительно вариаций на больших частотах. Разработан способ оценки величины размаха вариаций высоты максимума F-слоя, по размаху вариаций действующей высоты отражения зондирующего сигнала *h'(t)* на максимальной частоте, отражающейся от ионосферы. Получены распределения размаха вариаций высоты максимума для магнитоспокойных и магнитоактивных условий наблюдения КМПИВ. Найдено, что максимальные вероятности величины размаха лежат в диапазоне 40-50 км для возмущенного и 30-50 км для спокойного магнитного поля.

Ключевые слова: ионосфера, вертикальное зондирование, высота максимума F2-слоя

Information about authors:

Yakovets Arthur Fedorovich - cand. of phys.-mat. sciences, Leading Researcher, Institute of the Ionosphere JSC "NCSR", Almaty, artyak40@mail.ru. 1) The author made a significant contribution to the research concept, data analysis and interpretation, 2) the author wrote the first version of the article, 3) the author approved the final version of the article before submitting it for publication;

Arezu Jahanshir - PhD in Teoretical Physics and Mathematics, Buein Zahra Technical University, Iran, jahanshir@bzte.ac.ir 1) The author made a significant contribution to the concept and design of the study, the interpretation of data, 2) the author made a critical review of the article for important intellectual content, 3) the author approved the final version of the article before submitting it for publication;

Gordienko Galina Ivanovna - cand. of phys.-mat. sciences, Leading Researcher, Institute of the Ionosphere JSC "NCSR", Almaty, ggordienko@mail.ru. 1) The author made a significant contribution to the research concept, data acquisition and interpretation, 2) the author wrote the first version of the article; 3) the author approved the final version of the article before submitting it for publication;

Zhumabayev Beybit Tenelovich - cand. of phys.-mat. sciences, a head of laboratory, Institute of the Ionosphere JSC "NCSR", Almaty, beibit.zhu@mail.ru. 1) The author made a significant contribution to the study design, data acquisition, 2) the author wrote the first version of the article, 3) the author approved the final version of the article before submitting it for publication;

Litvinov Yurii Georgievich, cand. cand. of phys.-mat. sciences, senior researcher, Institute of the Ionosphere, JSC “NCSR”, Almaty, yurii-litvinov@mail.ru. 1) The author made a significant contribution to the acquisition of data and their analysis, 2) the author made a critical review of the article for important intellectual content, 3) the author approved the final version of the article before submitting it for publication;

Abdrakhmanov Nurtaza, cand. cand. of phys.-mat. sciences, senior researcher, Kyzylorda State University. Korkyt ata, Kyzylorda, abdrakhmanov.48@mail.ru. 1) The author made a significant contribution to data acquisition and interpretation, 2) the author made a critical review of the article for important intellectual content, 3) the author approved the final version of the article before submitting it for publication

REFERENCES

[1] Hunsucker R.D. Atmospheric gravity waves generated in the high latitude ionosphere: A review // Rev. Geophys. V. 20. № 2. P. 293–315. 1982.

[2] Tsugawa T., Saito A., Otsuka Y. A statistical study of large-scale traveling ionospheric disturbances using the GPS network in Japan // J. Geophys. Res. V. 109. № A06302, doi:10.1029/2003JA010302. 2004.

[3] Hawlitschka S. Travelling ionospheric disturbances (TIDs) and tides observed by a super-resolution HF direction finding system // J. Atmos. Solar-Terr. Phys. V. 68. № 3–5. P. 568–577. doi:10.1016/j.jastp.2005.03.022. 2006.

[4] Yeh K.C., Liu C.H. Acoustic-gravity waves in the upper atmosphere // Rev. Geophys. Space Phys. V. 12. P. 193–216. 1974.

[5] Hocke K., Schlegel K. A review of atmospheric gravity waves and traveling ionospheric disturbances: 1982–1995 // Ann. Geophysicae. V. 14. № 9. P. 917–940. 1996.

[6] A. F. Yakovets, V. V. Vodyannikov, G. I. Gordienko, and Yu. G. Litvinov. Thermospheric Wind Oscillations during the Propagation of Large-Scale Traveling Ionospheric Disturbances// Geomagnetism and Aeronomy, 2014, Vol. 54, No. 4, pp. 480–487.

[7] A. F. Yakovets, G. I. Gordienko, B.T. Zhumabaev and Yu. G. Litvinov. Comparison of altitude profiles of amplitude of two types of F2-layer ionospheric disturbances// News of the National Academy of Sciences of the Republic of Kazakhstan. Physico-Mathematical Series (In Russ) 2018, No 4, P. 79-84.

[8] Stankov S.M., Jodogne J.C., Kutiev I., Stegen K., Warnant R. Evaluation of automatic ionogram scaling for use in real-time ionospheric density profile specification: Dourbes DGS-256/ARTIST-4 performance // Ann. Geophys. V. 55. № 2. P. 283–291. doi:10.4401/ag-4976. 2012.

N E W S
OF THE NATIONAL ACADEMY OF SCIENCES OF THE REPUBLIC OF KAZAKHSTAN
PHYSICO-MATHEMATICAL SERIES
ISSN 1991-346X **https://doi.org/10.32014/2019.2518-1726.52**
Volume 4, Number 326 (2019), 135 – 142

UDC 004.9:519
IRSTI 20.53.00

M. Kalimoldayev, M. Akhmetzhanov, M. Kunelbayev

Institute Information and Computational Technologies CS MES RK,
Almaty, Republic of Kazakhstan

DEVELOPMENT AND RESEARCH OF A MATHEMATICAL MODEL OF A SOLAR PHOTO CONVERTER WITH AN INVERTER FOR CONVERTING DIRECT CURRENT TO ALTERNATING VOLTAGE

Abstract. This article presents a mathematical model of photovoltaic systems. For the analysis of energy processes in autonomous power transmission systems, it is now advisable to use computer simulation methods. The use of a simulation model makes it possible to provide an energy balance in an autonomous power transmission system with specific energy characteristics of ground and buffer sources of energy and a time scale from the power consumption of the load. This allows you to influence the energy characteristics of transmission systems to ensure the energy balance in the system in terms of temporary changes in the energy characteristics of energy sources, as well as the impact on the energy characteristics of the systems of transmission parameters such as solar energy. lighting, temperature, time of year, etc. This model is described by the current-voltage characteristic (CVC) at a given temperature, and the lighting conditions are the basis for calculating the parameters of the photoelectric energy in a wok. A new inverter was also designed and researched to convert direct current into alternating voltage, which allowed saving from 18.5% to 35.19% of expensive solar photo converters.
Keywords: solar cell; the current-voltage characteristics; mathematical model; MatLab.

1.Introduction

Solar cells in the production of electricity from renewable energy sources, is now developing rapidly and soon will be increased overall use [1]. For example, small solar cells used in watches, calculators, small toys, radios and portable TVs. While large objects are combined into modules and are used to supply the power system [2,3].

A solar cell is an electrical device that converts light energy into electricity using the photoelectric effect. The main material used for the production of solar cells is silicon.

I. The design and manufacture of silicon solar battery Large blocks of molten silicon carefully cooled and solidified is made from cast ingots of polycrystalline silicon square. Polycrystalline silicon is less costly than single crystal and are less effective [4,3,5]. Solar battery consists of the following elements [6,7,8].

- Silicon wafer (mono- or polycrystalline) with a p-n junctions on the surface.
- Front and back contact; front contact must have the correct shape to make the most of the incident radiation.
- Antireflection layer - cover the front surface. There are three major types of solar cells.
- Single crystal formed on a silicon crystal with a homogeneous structure. The basis for the formation of cells that are suitable silicon-sized blocks.
- They are cut into plates whose thickness is about 0.3 mm. Photovoltaic cells achieve the highest levels of performance and life [4,6].
- Polycrystalline are comprised of many small grains of silicon. These solar cells are less efficient than single crystal. The production process is simpler and have lower rates [4,6].

- Amorphous (thin film) - produced by incorporating multiple layers of silicon on the surface of another material, such as glass. In these solar batteries, we can not distinguish individual cells. Amorphous solar cells are generally used in small devices such as calculators and watches[4,6,9,10].As the metal contacts are made, the solar cells are interconnected by flat wires or metal ribbons, and assembled into modules or solar panels [7,11,12]. If the lower flow resistance of the current, the output current is a multiple of the current cell panel and associated with parallel connections of elements and modules. Similarly, the output voltage of the module depends on the amount series-connected cells and modules [3,13]. Photovoltaic solar cell generates electricity only when it is illuminated, electricity is not stored [13].

The current-voltage characteristics of the cell are shown the output current PV generator, depending on the voltage at the set temperature and lighting [2.14]. Short circuit current (ISC) - the output current of the photoelectric. Generative at a given temperature and irradiance, PMPP - point MPP (Maximum Power Point) is [2,6,15]. The output voltage is heavily dependent on the temperature of solar cells: increase results in a lower operating temperature and efficiency of [2,9].

The inverter is an inevitable component of the photovoltaic module.

There are many inverters available on the market. The cost of these inverters is a bit high due to the microcontroller-based SPWM generator [17,18,19]. In the article [20], researchers devoted to the design and construction of an inverter with a power of 100 W, 220 V and 50 Hz. The system is designed without a microcontroller and it has a cost-effective design architecture. The elementary purpose of this device is the conversion of 12 V DC to 220 V AC.

Solar Photovoltaic Modules (SPM) are popular in agriculture. For a lot of small farms, the main source of electrical energy is electric generators driven by Internal Combustion Engines (ICE), since installation of electrical networks is economically unprofitable. In these conditions, SPM are economically and environmentally promising, since it does not require the consumption of fuels and lubricants does not harm the environment. Determination of the main SPM operating parameters in 2 modes is considered in this research. In the cases when the panels oriented towards the sun (tracking mode) and in a stationary state with orientation to the south (without tracking mode). The dependences of current, voltage and power on time and density of solar radiation were measured. Accordingly, the voltage and current of Transportable Photovoltaic Unit (TPU), the charging current and the voltage of the batteries, the voltage at the output of the inverter, the temperature and humidity of the outside air and the electrical energy consumption by the electric receivers were recorded. The study of the TPU operation showed that the mode of orientation to the sun increases the daytime power generation by 25, ..., 33% in comparison with the fixed installation of Solar Panels (SP). The analysis showed the discrepancy between SP passport data and the experimental results. The decrease in electricity generation was 14% compared to the expected estimates [21]. The advent of unique technologies of the developing Solar Energy (SE), actual energy, faces economic and environmental problems. The main obstacle to the widespread use of SE is the low value of the average annual efficiency of known solar installations. In a sharply continental climate, they are exploited only in the warm season, about 6-7 months. Known combined systems, where additional conventional water heaters duplicate the operation of solar units, require additional costs for energy carriers. These disadvantages are not offered by the integrated system of SE use. In the article, the system was studied using the example of a cattle-breeding farm. The new system performs these functions; it recycles heat, organizes their movement and accumulation, and smooths out the uneven SE. The main components of the system are: Solar Power Plant (SPP), milk cooler, climate unit, Heat Pump (HP), the battery heat, automatic control system, and device heating and hot water. The main goal, i.e. lower cost of the energy produced and the elimination of the uneven SE, compared to the known SPP, is achieved through the flow of energy from the sources mentioned above [22].

2.Model Solar Battery

Photovoltaic generators for direct conversion of solar radiation into electrical energy, collected from a large number of series-connected photovoltaic solar cells (solar cells), are called solar cells (SC). Modern Security generate significant light on electrical power and are used both for power spacecraft (SC), and for many terrestrial autonomous devices for different purposes. Solar panels are made up of tens or hundreds of thousands of individual solar cells connected in parallel, in series in order to provide the required voltage and current ratings.

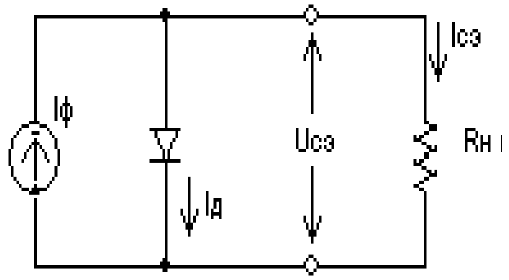

Figure 1 - Equivalent circuit of a solar cell

Figure 1 shows an equivalent circuit of the solar cell of substitution (SE). It is described by the following expression [16]:

$$I_{NY} = I_O(W) - I_0 \cdot \left[exp\frac{qU_{NY}}{kT} - 1\right] \leftrightarrow U_{NY} = \frac{kT}{q} ln\left[\frac{I_O(W)-I_{NY}}{I_0} + 1\right] \quad (1)$$

Where I_{NY} - current through an external load, I_0 - reverse saturation current, q - electron charge, T - the absolute temperature, ° K, k - is Boltzmann's constant, U_{NY}- voltage at the output element, I_O - current of minority carriers generated by the light (photocurrent).

Influence of irradiance on the FE value U_{NY} value expressed by the formula [13].

$$\mathrm{I_O(W) = W \cdot I_O} \quad (2)$$

where W - Illumination SE.

Figure 2 - The full-scale model of the solar panels

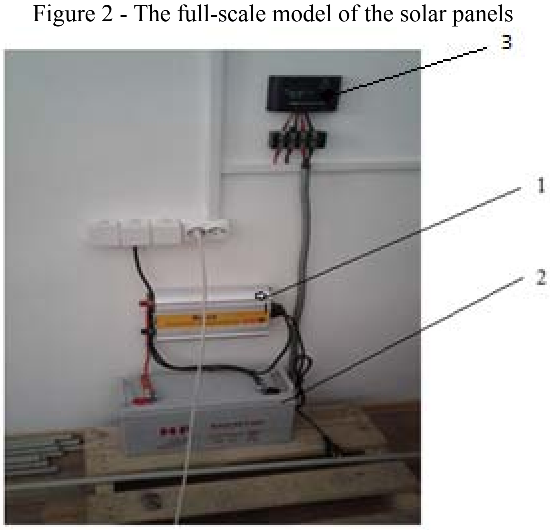

Fig. 3. The solar power systems:
1-inverter; 2- battery;3-controller

3. Inverter to convert DC to AC voltage

The objective of this study is to reduce the load on the power supply with maximum efficiency and increase the term of stability, simplify the design of the device, reduce the cost and expand the scope of their use in industry.

This task is achieved by the fact that when turning on the PWM controller that regulates the width of the pulses 1 to the logic elements 3, 4, the maximum sequence of gates of field-effect transistors is achieved.

As shown in Figure 1, the device has a PWM controller that regulates pulse width 1, voltage regulator 2, with field-effect transistors connected 3.4, to convert from DC to AC, capacitors 5, to filter the input voltage, diode bridge 6, transformer consisting of primary and secondary windings 7, switch 8, housing 9, you can use any material, plastic, iron, aluminum.

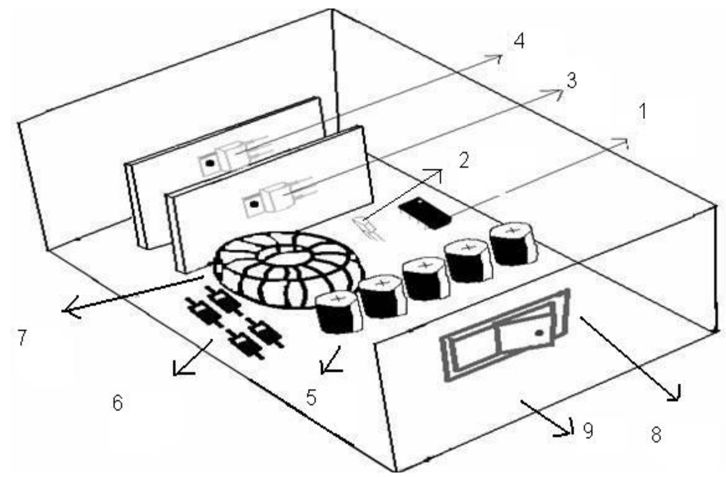

Figure 4 - Inverter to convert DC voltage to AC

Assembly and manufacture of the device is as follows. A PWM controller regulating pulse width 1 is connected via voltage regulator 2, and capacitors 5, for filtering and limiting the input voltage, followed by connecting field-effect transistors 3, 4, screwed to passive cooling, to prevent heating, and with parallel connection of the secondary winding transformer 7, the primary winding is connected directly to the diode bridge 6, with the connection to the input voltage circuit of the switch 8, with the subsequent location in the housing 9.

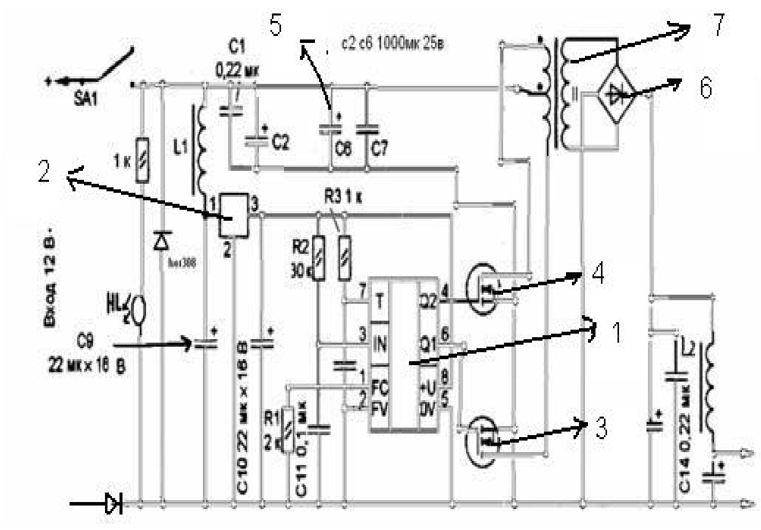

Figure 5 Schematic diagram of the inverter

The operation of the proposed device is as follows. When the input voltage is connected, with the switch 8 connected to the input voltage circuit, the current is fed to the PWM controller that controls the pulse width 1, through the capacitors 5, to filter the current, and the voltage regulator 2, then connect the field-effect transistors 3, 4 screwed to the passive cooling, to prevent heating, and with the parallel connection of the secondary winding of the transformer 7, the primary winding is connected directly to the diode bridge 6, with the connection to the input voltage circuit of the switch 8, followed by p As position in the housing 9.

According to the developed method of rational use of solar photo converters, calculations were carried out for a three-phase conversion system for various inversion schemes. According to calculations, it was found that with a three-phase conversion system, it is possible to save from 18.5% to 35.19% of expensive solar photo converters.

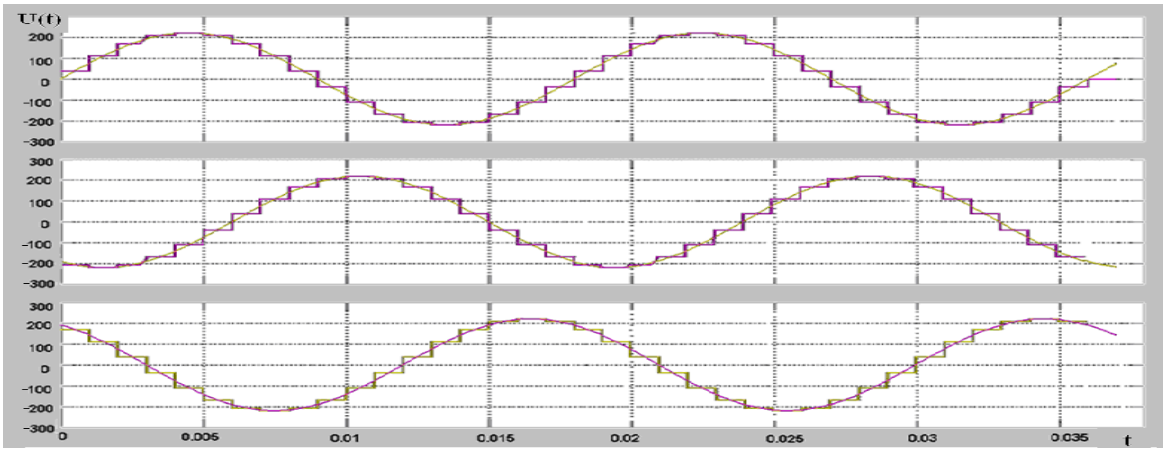

1- Output step voltage curve; 2- perfect sine curve

Figure 6 - The output voltage of a three-phase five-step model

In accordance with the graphical analysis, it can be asserted that with a three-phase load, as the steps grow, a voltage curve can be obtained that is close to a sinusoid.

4. Result

During the research, the following are recorded: the voltage and current of the FCM, the charging current and the voltage on the batteries, the voltage at the output of the inverter, the temperature of the outside air (from +5 to +35 0C) and the humidity of the outside air, and the electric power consumption of the electric receivers of the connected load.

In the experimental studies we used: a solar radiation meter SM-206, an ammeter and a DC voltmeter, a UT206 multimeter, a Saiman electric energy meter, a CENTER-350 infrared thermometer, and an MES-202 meteorometer. The measurement of solar radiation was carried out with a portable SM-206 instrument with an accuracy of ± 5% (measuring range 0.1 ... 399.9 W / m2, temperature - with an infrared thermometer CENTER-350 with an accuracy of ± 2% (measuring range -20 + 5000C) And the air humidity were measured with a psychrometer MV-4M with an error of ± 4% and a meteorometer MES-202, the limit of the permissible value of the absolute error of the pressure measurement is not more than ± 0,3 kPa in the temperature range from 0 to 60 0 C. Overall dimensions were measured with a tape measure of metal PM with an error ± 0.5 mm (measuring range 0 to 10m, the division price is 1mm) and a metal ruler (length 1m) with an error of ± 1mm.

The diagram of the connection of devices and equipment during laboratory-field testing is shown in Figure 1.

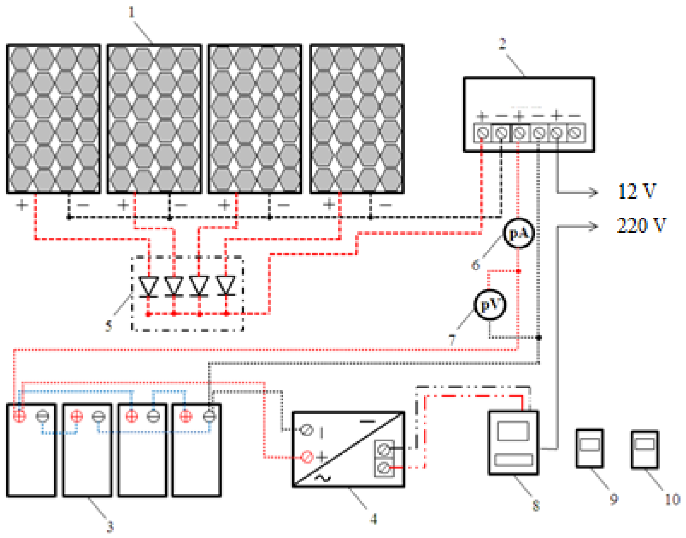

1-PV panel; 2- controller; 3- rechargeable battery; 4- inverter; 5- diodes; 6 - direct current ammeter;
7 - DC voltmeter; 8 - the counter of electric energy; 9 - solar radiation meter; 10 - a weather meter

Figure 7 - Scheme for mounting equipment and connecting devices

We are implementing the mathematical model of SE. As an example, we choose an SE with the following characteristics:

$$U_{xx} = 0{,}45B,$$
$$I_{kz} = 4{,}5A,$$
$$I_0 = 2{,}045 \cdot 10^{-9}A$$

The circuit that realizes the volt ampere characteristic of the solar cell described by the expression (1) is shown in Fig. 2. It allows one to estimate the influence on the operation of such parameters as the illumination level of the solar cell (nominal value W = 1360 kW / m ^ 2), the ambient temperature (Nominal value K = 298 K), as well as the angle of incidence of the light flux (nominal value α = 90 ° = π / 2 rad).

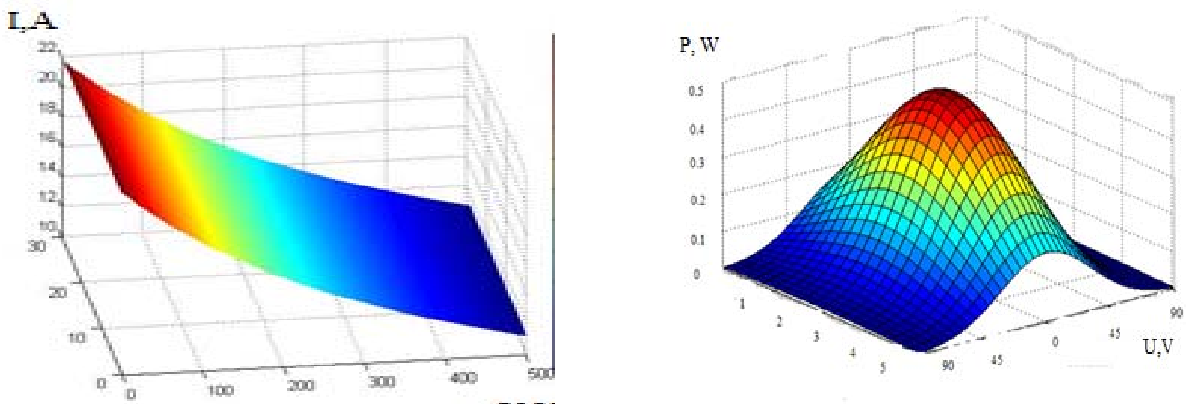

a b

a - current-voltage characteristic, b – volt watt characteristic
Fig. 8. Characteristics of the SE, described by the equation (2)

We test the solar battery consisting of 3 elements connected in series. In this case, the voltage at the output of the U_NA SB is determined by the formula$U_{NA} = U_{YEA} = U_{NY} \cdot N$, where N is the number of solar cells connected in series$I_{NA} = I_{YEA} = I_{NY}$.

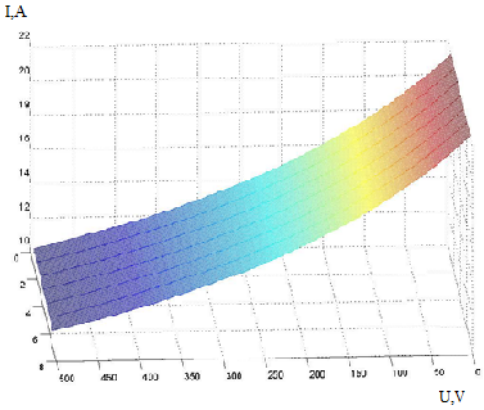

a

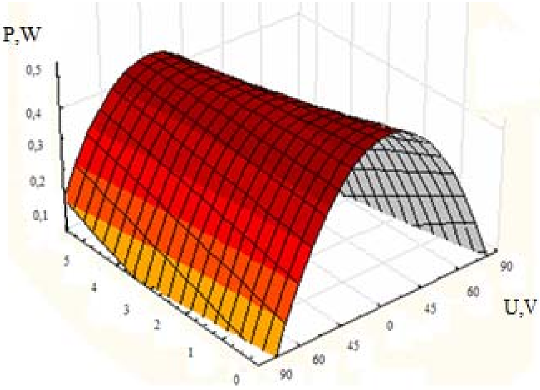

b

a - current-voltage characteristic, b – volt watt characteristic
Figure 9 - Characteristics of the circuit shown in Figure 4

As can be seen from Fig. 9, the idling voltage of the SB is 3 times greater The open circuit voltage of the solar cell (see Figure 3) => the model is compiled correctly.

V. CONCLUSION

Comparison with experimental data, processed by MATLAB, and with the characteristics of the PV panels, provided by manufacturers, has shown that the model implemented in MATLAB/Simulink can be an accurate tool for the prediction of energy production. A PV system model, using the same equations and parameters as in MATLAB/Simulink to define the PV module and characteristics, has also been developed and implemented in domestic consumers in agriculture to study load flow, steady-state voltage stability and dynamic behavior of a distributed power system. A comparison between both simulation models, implemented in MATLAB/Simulink and domestic consumers in agriculture , has shown a good similarity. That means that this work can be used for further development of tools for DER components in a distributed network. The developed mathematical model of the solar battery makes it possible to evaluate the influence on the characteristics of the SB both internal factors (U_{xx}, I_{kz}), and external (W, T, α). The model is designed for design of SES. The results of testing the model confirm its operability.

М. Калимолдаев, М. Ахметжанов, М. Кунелбаев

ТҰРАҚТЫ ТОК АЙНЫМАЛЫ КЕРНЕУГЕ ТҮРЛЕНДІРУ ҮШІН ТҮРЛЕНДІРГІШТІКПЕН КҮН ФОТОЭЛЕМЕНТТЕРІНІҢ МАТЕМАТИКАЛЫҚ МОДЕЛІН ӘЗІРЛЕУ ЖӘНЕ ЗЕРТТЕУ

Аннотация. Бұл мақалада фотовольтаикалық жүйелердің математикалық моделі берілген. Дербес энергетикалық жүйелердегі энергетикалық процестерді талдау үшін компьютерлік модельдеу әдістерін қолдану ұсынылады. Модельдеу моделін пайдалану автономды электр энергиясын беру жүйесінде энергетикалық тепе-теңдік қамтамасыз етуге мүмкіндік береді және энергияның буферлік көздері мен жүктің энергияны тұтынуының уақытша шкаласы. Бұл қуат көздерінің энергетикалық сипаттамалары бойынша уақытша өзгерістерге байланысты жүйедегі энергия теңгерімін қамтамасыз ету үшін трансмиссиялық жүйелердің энергетикалық сипаттамаларына, сондай-ақ, трансформатор параметрлері жүйелерінің энергия сипаттамаларына әсері сияқты, күннің энергия. жарықтандыру, температура, жыл уақыты және т.б. Бұл модель берілген температурада ағымдағы кернеу сипаттамасымен (CVC) сипатталады, ал жарықтандыру жағдайлары фотоэлектрлік энергияның параметрлерін есептеу кезінде негіз болады. Сондай-ақ жаңа ток түрлендіргішті айнымалы кернеуге айналдыру үшін әзірленген және зерттелді, бұл 18,5% -дан 35,19% қымбат күн фотоэлементтерін үнемдеуге мүмкіндік берді.

Түйін сөздер: күн батареясы; ток кернеуінің сипаттамалары; математикалық модель; MatLab.

М. Калимолдаев, М. Ахметжанов, М. Кунелбаев

Институт информационных и вычислительных технологий КН МОН РК

РАЗРАБОТКА И ИССЛЕДОВАНИЕ МАТЕМАТИЧЕСКОЙ МОДЕЛИ СОЛНЕЧНОГО ФОТОПРЕОБРАЗОВАТЕЛЯ С ИНВЕРТОРОМ ДЛЯ ПРЕОБРАЗОВАНИЯ ПОСТОЯННОГО ТОКА В ПЕРЕМЕННОЕ НАПРЯЖЕНИЕ

Аннотация. В данной статье представлена математическая модель фотоэлектрических систем. Для анализа энергетических процессов в автономных системах электропередачи сейчас целесообразно использовать методы компьютерного моделирования. Использование имитационной модели позволяет обеспечить энергетический баланс в автономной системе передачи энергии с конкретными энергетическими характеристиками наземных и буферных источников энергии и шкалой времени от потребляемой мощности нагрузки. Это позволяет влиять на энергетические характеристики систем передачи, чтобы обеспечить энергетический баланс в системе с точки зрения временных изменений энергетических характеристик источников энергии, а также влияния на энергетические характеристики систем параметров передачи, таких как солнечный энергия. освещение, температура, время года и т. д. Эта модель описывается вольт-амперной характеристикой (CVC) при данной температуре, и условия освещения являются основой для расчета параметров фотоэлектрической энергии в воке. Новый инвертор был также разработан и исследован для преобразования постоянного тока в переменное напряжение, что позволило сэкономить от 18,5% до 35,19% дорогих солнечных фотопреобразователей.

Ключевые слова: солнечный элемент; вольт-амперные характеристики; математическая модель; MatLab

REFERENCE

[1] Fundamentals of Photovoltaics: http://www.fotowoltaika. com.pl/podstawy.htm

[2] E. Klugmann-Radziemska, Photovoltaic, in theory and practice, Publishing House BTC, Legionowo, 2010 (in Polish).

[3]Photovoltaicshttp://www.acce.apsl.edu.pl/instrukcje/fotoogniwo_ogniwo%20sloneczne.pdf (in Polish).

[4] F. Wolanczyk, How to use the power of gifts, the solar collectors and photovoltaic cells, Publishing House KaBe, Krosno, 2011 (in Polish).

[5] M. Lipinski, Silicon nitride for photovoltaic application, Archives of Materials Science and Engineering 46/2 (2010) 69-87.

[6] T. Rodacki, A. Kandyba, Energy conversion in solar power, Wydaw. Politechniki Slaskiej, Gliwice, 2000 (in Polish).

[7] L.A. Dobrzanski, M. Szindler, Sol-gel and ALD antireflection coatings for silicon solar cells, Electronics: structures, technologies, applications 53/8 (2012) 125-127.

[8] T. Markvart, L. Castaner, Practical handbook of photovoltaics, fundamentals and applications, Oxford, Elsevier, 2006.

[9] Thin film solar cell - http://www.labfiz2p.if.pw.edu.pl/ ins/cos_nr_9.pdf (in Polish).

[10] R. Brende,l Thin-film crystalline silicon solar cells, physics and technology, Wiley-VCH, Weinheim, 2003.

[11] P. Würfel, Physics of solar cells: from basic principles to advanced concepts, Wiley-VCH Verlag, Weinheim, 2009.

[12] L.A. Dobrzanski, M. Musztyfaga, Effect of the front electrode metallisation process on electrical parameters of a silicon solar cell, Journal of Achievements in Materials and Manufacturing Engineering 48/2 (2011) 115-144.

[13] M. Waclawek, T. Rodziewicz, Solar cells: the impact of the environment on their work, Publishing House WNT, Warsaw, 2011 (in Polish).

[14] H.J. Moller, Photovoltaics - current status and perspectives, Environment Protection Engineering 32/1 (2006) 127-134.

[15] L.A. Dobrzanski, M. Musztyfaga, Effect of the front electrode metallisation process on electrical parameters of a silicon solar cell, Journal of Achievements in Materials and Manufacturing Engineering 48 /2 (2011) 115-144.

[16] L.A. Dobrzanski, M. Musztyfaga, A. Drygala, Final manufacturing process of front side metallisation on silicon solar cells using convectional and unconventional techniques, Journal of Mechanical Engineering 59 (2013) 3 175-182.

[17] Rafid Haider, Rajin Alam, Nafisa Binte Yousuf, Khosru M. Salim, "Design and Construction of Single Phase Pure Sine Wave Inverter for Photovoltaic Application" IEEE/OSA/IAPR International Conference on Infonnatics, Electronics & Vision.

[18] H. Dehbonei, L. J. Borle, "Design and implementation of a low cost sine Wave inverter," IEEE, 2003, pp. 280-285.

[19] A. A. Qazalbash et al., "Design and implementation of microcontroller based PWM technique for sine wave inverter," IEEE POWERENG, Lisbon. Portugal, pp. 163- 167, March 2009.

[20] Niaz Morshedul Haque, Ifthekhar Ahammad, Sayem Miah, Asad Ahmed Miki, Hasan Ahmed. International Journal Of Scientific & Technology Research Volume 6, Issue 10, October 2017, pp. 269-272.

[21] Omarov, R., Keshuov, S., Omar, D., Kunelbayev, M., . Determination of basic operating parameters of Solar Photovoltaic modules for farms. Journal of Engineering and Applied Sciences 12(Specialissue1), 2017, pp. 5761-5766.

[23] Omarov, R., Abdygaliyeva, S., Omar, D., Kunelbayev, M.. Integrated system for the use of solar energy in animal farm. Scientia Iranica, 2017, 24(6), pp. 3213-3222.

N E W S
OF THE NATIONAL ACADEMY OF SCIENCES OF THE REPUBLIC OF KAZAKHSTAN
PHYSICO-MATHEMATICAL SERIES
ISSN 1991-346X **https://doi.org/10.32014/2019.2518-1726.53**
Volume 4, Number 326 (2019), 143 – 150

УДК 539.12

M. Izbasarov, N.S. Pokrovsky, V.V. Samoilov,
T. Temiraliev, R.A. Tursunov, B.O. Zhautykov

Satbayev University, Institute of Physics and Technology, Almaty, Kazakhstan
alenzhutykov@gmail.com samoylov46@list.ru, rabik99@mail.ru

INVESTIGATION OF CORRELATIONS OF GENERATED NUCLEAR ACTIVE PARTICLES IN $\tilde{p}p$ - EVENTS ENRICHED BY ANNIHILATION AT MOMENTA 22.4 GeV/c AND 32 GeV/c

Abstract. Extraction of $\tilde{p}p$ - events, enriched by annihilation, allowed to carry out the analysis of multiparticle correlations for the generated particles. The correlation function $R_k(G)$ is characterizing the ratio of experimental differential distribution of quasi-rapidity intervals to differential background distribution $R_K(G) = \frac{F_K(G)}{F_K^{\phi}(G)} - 1$, where $G = \eta_{\iota+\kappa} - \eta_\iota$ - quasi-rapidities intervals, η_i and η_{i+k} - quasi-rapidity values for boundary particles in the interval with k - 1 charged particles.

The analysis of R_K dependence on G was carried out on events enriched by annihilation and non – annihilation $\tilde{p}p$ - interactions at momenta 22,4 GeV /c and 32 GeV / c, and also inelastic pp - collisions at momentum 69 GeV/c.

In interactions with “annihilation” more weak correlation of charged particles is observed, than in non-annihilation $\tilde{p}p$ - interactions. In proton – proton and non - annihilation antiproton – proton collisions similarity of correlation functions is observed.

Key words: annihilation, proton, antiproton, interaction, reaction, interval, correlation.

.

I. Introduction

The multiple production of hadrons in the interactions of elementary particles, in accordance with modern views, are results from hadronization of quarks and gluons [1-4], which are the parts of the interacting particles.

Investigation of secondary charged particles correlation in the multiple production processes at high energies gives the possibility to understand the internal dynamics of the studied processes. Just for this reason it is interesting to study particle correlations and to search non-statistical fluctuation effects in the processes of multiple hadron production.

It is known that antiproton – proton interactions include inelastic collisions with nucleons in final state (i.e. the baryon number conserves), and also annihilation events where the baryon number does not conserve. Information on events of antiproton – proton annihilation can be received by an exception of the inelastic non annihilation $\tilde{p}p$ - interactions from all data set.

Usually information about $\tilde{p}p$ - annihilation at sufficiently high energy ($E_0 > 10$ GeV) has been obtained by indirect methods [5-8]. In this regard the technique was developed [9] for division of “annihilation” proton - antiproton pair and non - annihilation processes in $\tilde{p}p$ - interactions.

Distinguishing by inverted commas of $\tilde{p}p$ - annihilation word everywhere in article authors mean the set of $\tilde{p}p$ - events enriched by annihilation.

Experimental material on $\tilde{p}p$ - interactions has been obtained using 2 metre hydrogen bubble chamber (HBC) «Ludmila» [10] (22.4 GeV/c) and HBC «Mirabelle» [11] (32 GeV/c), and on pp - inelastic event - HBC «Mirabelle» [12] (69 GeV/c). The bubble chambers were exposed at Serpukhov accelerator.

2. The procedure of extraction of $\tilde{p}p$ - "annihilation" events at 32 GeV / c.

Extraction of antiproton – proton "annihilation" events was carried out in two stages.

At the first stage events with identified proton or an antiproton were excluded. The interactions, remained after procedure of exclusion of events with protons and antiprotons, can be divided into three groups:

(I) - the group of annihilation reactions, in which neutrons (antineutrons) are absent in the final state $\tilde{p}p \to k(\pi^+\pi^-)x^0$, where *k* is the integer; x^0 - neutral system;

(II) - the group of non-annihilation reactions, containing neutrons (n) and antineutrons $(\tilde{n})$ in the final state $\tilde{p}p \to k(\pi^+\pi^-)n\tilde{n}x^0$;

(III) - the group with non-identified protons and antiprotons among charged particles.

At the second stage in mentioned three groups the values of missing masses were calculated on the charged particles

$$M_{miss} = [(E_0 - \sum_{i=1}^{n} E_i)^2 - (\overline{P}_0 - \sum_{i=1}^{n} \overline{P}_i)^2]^{1/2} \qquad (1)$$

Corresponding distributions are shown in Fig. 1.

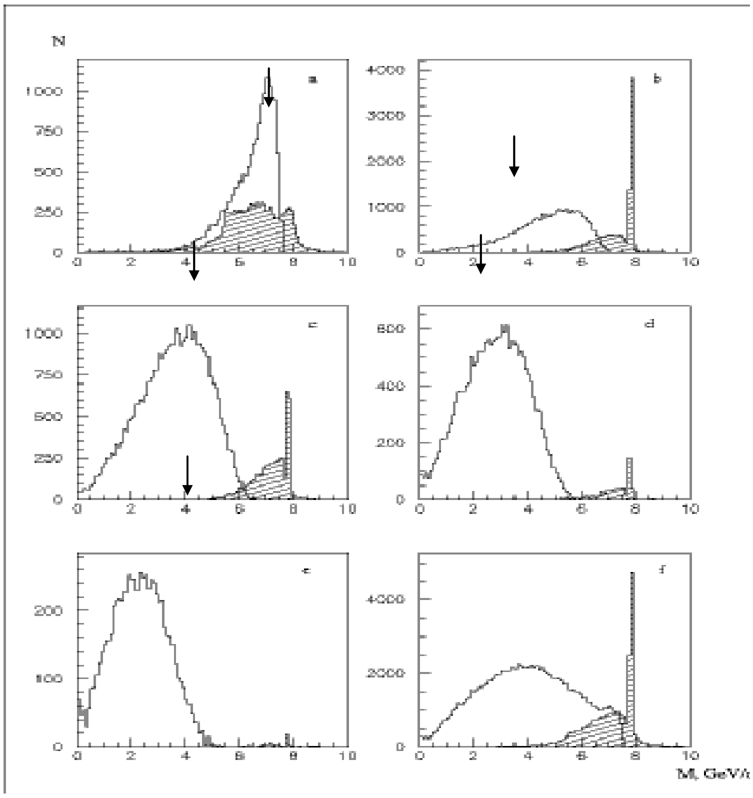

a) 2-prongs; b) 4-prongs; c) 6-prongs; d) 8-prongs; e) 10-prongs; f) summary distribution.

Figure 1 - Distributions on M. Unshaded histograms – distributions on $M_{miss.}$. The shaded histograms – distributions on the effective mass $M(p\tilde{p})$, which have to be similar to missing mass of neutron – antineutron pair

During separation on $M_{miss.}$ it was considered, that presence of a neutron and an antineutron among secondary particles should sharply increase the value of missing mass. For each multiplicity selection of antiproton-proton interactions, classified as annihilation events, began with events having smaller missing masses and stopped, when the total number of selected events corresponded to evaluate antiproton-proton “annihilation” cross-section [11,13]. Chosen boundary values of $M_{miss.}$ are shown by arrow in Fig. 1.

The final distribution of all antiproton-proton interactions on different channels at 32 GeV/c is given in Table 1.

Table 1 - Distribution of number of events on channels of reaction and boundary values of $M_{miss.}$ (in GeV/c).

	Reaction	Multiplicities						
		2	4	6	8	10	≥ 12	All mult..
(1)	$\tilde{p}p \to \tilde{p}pk(\pi^+\pi^-)x^0$	8553	15080	6781	3291	927	150	34782
(2)	$\tilde{p}p \to p\pi^- k(\pi^+\pi^-)\tilde{n}x^0$	9087	11369	7303	2001	386	63	30209
(3)	$\tilde{p}p \to \tilde{p}\pi^+ k(\pi^+\pi^-)nx^0$	9335	11914	7354	1973	281	53	30910
(4)	$\tilde{p}p \to k(\pi^+\pi^-)n\tilde{n}x^0$	8891	18054	19504	8555	1809	0	56813
(5)	$\tilde{p}p \to k(\pi^+\pi^-)x^0$	6616	9140	14134	10266	5251	1969	47376
	Total $M_{miss.}$ (boundary values)	42482 6,5	65557 4,4	55076 3,4	26086 3,0	8654 3,0	2235 3,0	200090 -

To confirm the correctness of the described approach for separation of “annihilation” interactions with small missing masses, the effective mass distributions $M(p\tilde{p})$ (shaded histograms in Fig.1) in events with protons and antiprotons (reaction 1) were compared with missing mass distributions (unshaded histograms in Fig.1), assuming that possible contribution of neutron-antineutron pairs is imitated by distribution of effective masses for proton-antiproton pairs.

It can be seen from Fig. 1 that in six-, eight-, and ten-prong events the admixture of non-annihilation processes into reactions corresponding to “annihilation”, is practically absent. This admixture equals to about 40% for 2-prong events, < 3% for 4 - prong events and ~ 12% for the total distribution.

3. Comparison of correlations in antiproton-proton “annihilation” events with corresponding data for inelastic pp - and non-annihilation $\tilde{p}p$ - interactions.

Separation of the events corresponding to antiproton-proton annihilation gives the possibility to carry out the analysis of multiparticle correlations for generated particles and to compare them with corresponding data for inelastic pp and non-annihilation $\tilde{p}p$ interactions.

The correlation function [14, 15]

$$R_K(G) = \frac{F_K(G)}{F_K^{\phi}(G)} - 1 , \tag{2}$$

where $G = \eta_{i+k} - \eta_i$ - the interval of quasirapidities; η_i and η_{i+k} - quasirapidities of boundary particles of the interval with (k - 1) charged particles inside it; $F_k(G)$ - measured differential distribution; $F_k^{\phi}(G)$ - expected differential distribution in the absence of correlations (background distribution).

The statistical error in finding of $R_k(G)$ is calculated according to formulae

$$\delta R_k(G) = (R_k(G)+1)\sqrt{(\frac{\delta F_k(G)}{F_k(G)})^2 + (\frac{\delta F_k^{\phi}(G)}{F_k^{\phi}(G)})^2} . \tag{3}$$

In Fig. 2 the results of R_k dependence on G for inclusive analysis of non-annihilation $\tilde{p}p$-interactions at momenta of primary antiprotons 22.4 GeV/c (Fig.2a), 32 GeV/c (Fig.2b) and for inelastic pp –interactions at momentum 69 GeV/c (Fig.2c) for k = (2 ÷ 5) are presented.

It is visible, that in the region of small rapidity intervals ($0 \div G_1$) and in the region of large rapidity intervals ($G > G_2$) positive correlation R_K (G) > 0 is observed, and in the region of ($G_1 > G > G_2$) the value of R_K (G) becomes negative for all considered values к=(2÷5). Here G_1 - the left point of function R_K (G) crossing with axis G; G_2 – the right point of function R_K (G) crossing with axis G.

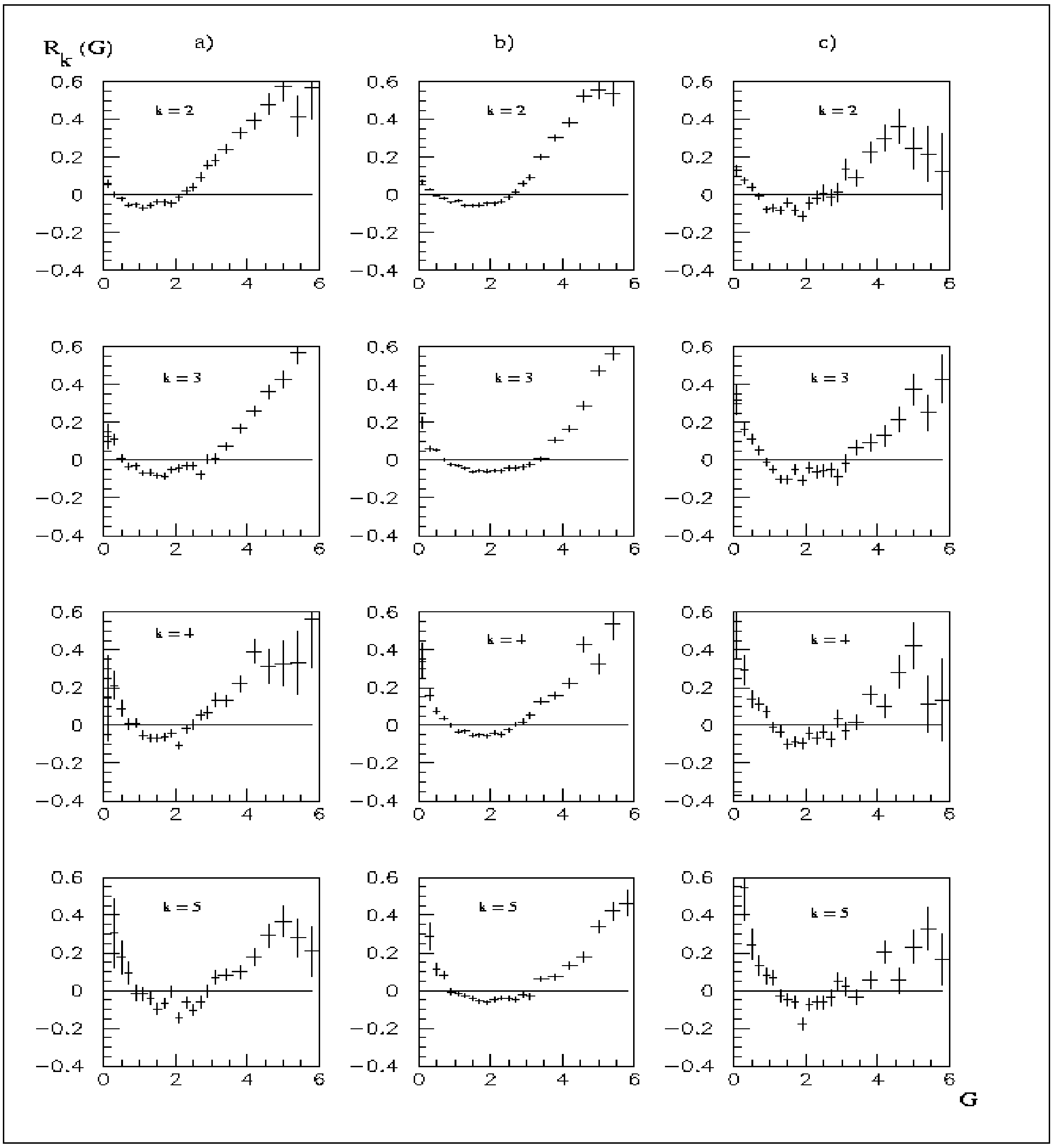

Figure 2.R_K dependence on G in non-annihilation channels
{$\tilde{p}p$ at 22.4 GeV/c – a); $\tilde{p}p$ at 32 GeV/c – b)} and in pp at 69 GeV/c – c).

In Table 2 the values of G_1 and G_2 and also the maximal value of $R_k^{\max}(G)$ inside region $0<G<G_1$ are given. The quantities G_1 and G_2 displace towards the larger values with increasing of primary particle energy (at the fixed value k). At the same time the mean quantity $\langle \Delta G \rangle = \langle G_2 - G_1 \rangle$ at k = (2 ÷ 5)

remains approximately the same in non-annihilation $\widetilde{p}p$ - interactions at 22.4 GeV/c, 32 GeV/c and in inelastic pp - collisions at 69 GeV/c and equals correspondingly to $\langle \Delta G \rangle$ = 1.8; $\langle \Delta G \rangle$ =2.0; $\langle \Delta G \rangle$ =2.2.

Table 2 - Values G_1, G_2 и R_{max} for non-annihilation interactions
(in brackets corresponding values for "annihilation" are resulted)

				$\widetilde{p}p$ 32 GeV/c			pp 69 GeV/c		
K	G_1	G_2	R_{max}	G_1	G_2	R_{max}	G_1	G_2	R_{max}
2	0.4 (0.2)	2.2 (1.2)	0.06±0.02 (0.01±0.02}	0.6 (0.2)	2.6 (1.4)	0.07±0.01 (0.02±0.02)	0.8	3.0	0.13±0.03
3	0.6 (0.6)	3.2 (1.6)	0.12±0.07 (0.00±0.02)	0.8 (0.4)	3.4 (1.8)	0.20±0.03 (0.10±0.03)	1.0	3.2	0.32±0.08
4	1.0 (0.6)	2.6 (2.0)	0.21±0.08 (0.02±0.04)	1.0 (0.4)	2.8 (2.0)	0.34±0.09 (0.35±0.10)	1.2	3.4	0.65±0.30
5	1.4 (0.8)	3.0 (2.0)	0.31±0.19 (0.00±0.01)	1.2 (0.6)	3.2 (2.4)	0.29±0.08 (0.40±0.25)	1.2	3.6	0.63±0.30

In Fig.3 the results obtained for dependence R_K on G at the analysis of reactions of antiproton-proton "annihilation" for k=(2÷5) at momenta 22.4 GeV/c (Fig 3a) and 32 GeV/c (Fig.3b) are presented.

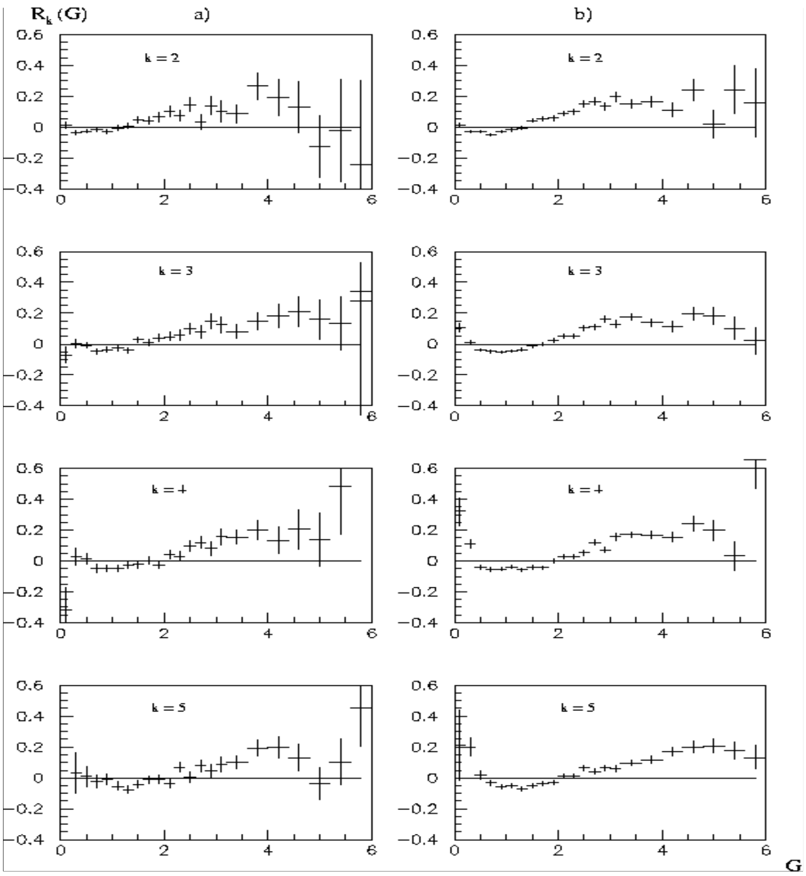

Figure 3 - R_K dependence on G:
a) $\widetilde{p}p$ -"annihilation" at 22.4 GeV/c; b) $\widetilde{p}p$ - "annihilation" at 32 GeV/c.

From comparison of Figures 2 and 3, and also the data in Table 2 can be seen that in non-annihilation $\widetilde{p}p$ - interactions the correlation is more noticeable, in comparison with "annihilation" events, the correlation of particles from non – annihilation events and qualitatively coinciding with correlation of particles in inelastic pp - interactions at 69 GeV/c.

The effect observed could probably be explained by the assumption that the mechanism of meson production goes mainly via intermediate creation of nucleon isobars, which contributes both to non-annihilation channel of $\tilde{p}p$ - collisions and to the inelastic pp - interactions.

In antiproton-proton "annihilation" events at 32 GeV/c the positive values of $R_K(G)$ in the region of small G at k=(3÷5) are observed (Fig.3b), whereas at antiproton – proton interactions at momentum 22.4 GeV/c (Fig.3a) such correlation is absent.

In Fig.4 the dependence of R_K on G is presented for each multiplicity at antiproton-proton "annihilation" at momentum 32 GeV/c with the purpose to find out the connection of observed correlations with multiplicity. In the region of small values G ($G < G_1$) correlation of particles is not observed for multiplicities 4 and 6 (the figures are not shown), but it is appreciable ($R_K(G) > 0$) for 8-prongs events at k =3 (Fig.4a) and is absent for the same 8-prongs interactions at k=4 and k=5. For events with multiplicities 10 (Fig.4b) and ≥ 12 (Fig.4c) the positive values of $R_K(G)$ are observed at k=3,4,5.

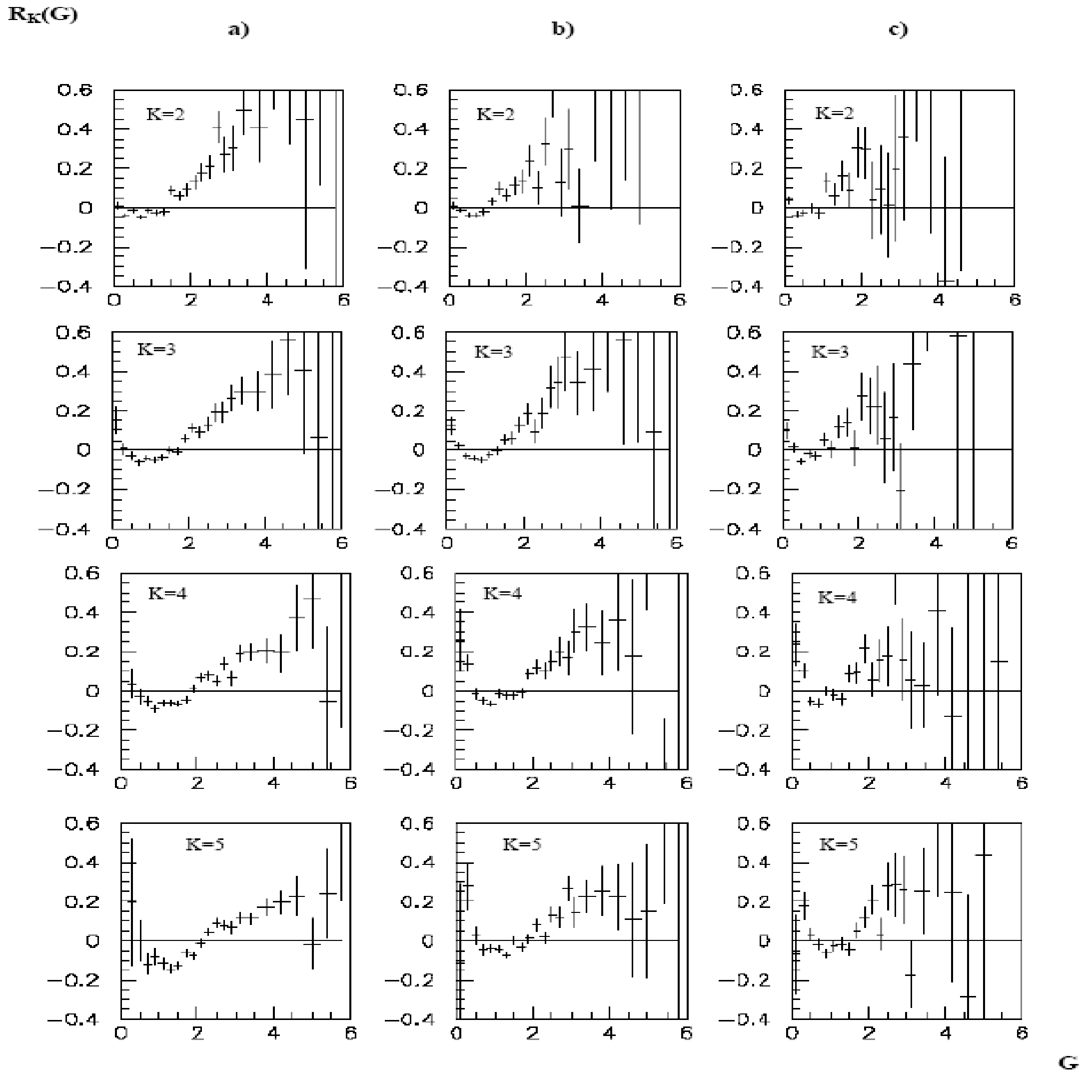

Figure 4 - R_K dependence on G for $\tilde{p}p$ -annihilation at 32 GeV/c:

a) 8-prongs; b) 10-prongs; c) ≥ 12-prongs

Thus, observed correlations of particles in inclusive channel of antiproton-proton "annihilation" are seen in interactions with multiplicities 8 and more. From here it is possible to make the conclusion that at momentum 32 GeV/c there is a new reaction channel with creation of meson resonances decaying onto 4 and more charged particles.

Summing up the results, we note the following.

In processes of anti-proton – proton “annihilation” at momentum 32 GeV /c the new reaction channel appears with formation of the meson resonances, decaying up to four and more charged particles.

In interactions of antiproton – proton “annihilation” the observed correlation of charged particles is more weak, than in non-annihilation interactions.

In proton – proton and non-annihilation antiproton – proton collisions similarity of correlation functions is observed.

The authors are sincerely grateful to participants of international collaborations «Ludmila» and «Mirabelle» for fruitful joint work in obtaining primary experimental data.

Б.О. Жаутыков, М. Избасаров, Н.С. Покровский, В.В. Самойлов, Т. Темиралиев, Р.А. Турсунов

Сәтбаев Университеті, Физика-техникалық институты, Алматы, Қазақстан

22,4 ГэВ/с ЖӘНЕ 32 ГэВ/с ИМПУЛЬСТА АННИГИЛЯЦИЯМЕН БАЙЫТЫЛҒАН $\tilde{p}p$ - ӘСЕРЛЕСУДЕГІ ЯДРО-БЕЛСЕНДІ БӨЛШЕКТЕРДІҢ КОРРЕЛЯЦИЯСЫН ЗЕРТТЕУ

Аннотация. Аннигиляциямен байытылған $\tilde{p}p$ - әсерлесуді анықтау өндірілген бөлшектер үшін көпбөлшекті корреляция талдауын жүргізуге мүмкіндік берді. Корреляциялық $R_k(G)$ функциясы квазижылдам интервалдың тәжірибелік таралуының дифференциалдық $R_K(G) = \frac{F_K(G)}{F_K^{\varphi}(G)} - 1$ аялық таралуға қатынасын сипаттайды, мұндағы $G = \eta_{i+k} - \eta_\imath$ квазижылдамдық интервалы, ал η_i и η_{i+k} мәндері k – 1 бөлшектер интервалындағы шектік бөлшектер үшін квазижылдамдық мәні.

R_K функциясының G тәуелді талдауы аннигиляциямен байытылған ортада және аннигиляцияланбаған $\tilde{p}p$ -әсерлесуде 22,4 ГэВ/с және 32 ГэВ/с импульста, сондай-ақ, 69 ГэВ/с импульста серпімсіз pp - әсерлесуде жүргізілді.

Аннигиляцияланбаған pp-әсерлесудегі корреляцияға қарағанда «аннигиляциялы» әсерлесуде біршама әлсіз корреляция байқалды. Протон-протондық және аннигиляцияланбаған антипротон-протондық соқтығысуларда корреляциялық функциялардың ұқсастығы байқалды.

Түйін сөздер: аннигиляция, протон, антипротон, әсерлесу, реакция, интервал, корреляция.

Б.О.Жаутыков, М.Избасаров, Н.С.Покровский, В.В.Самойлов, Т.Темиралиев, Р.А.Турсунов

Сәтбаев Университеті, Физико-технический институт, Алматы, Казахстан

ИССЛЕДОВАНИЕ КОРРЕЛЯЦИЙ ЯДЕРНО-АКТИВНЫХ ЧАСТИЦ В $\tilde{p}p$ -ВЗАИМОДЕЙСТВИЯХ, ОБОГАЩЕННЫХ АННИГИЛЯЦИЕЙ ПРИ ИМПУЛЬСЕ 22,4 ГэВ/с и 32 ГэВ/с

Аннотация. Выделение $\tilde{p}p$ -взаимодействий, обогащенных аннигиляцией, позволило провести анализ многочастичных корреляций для генерированных частиц. Корреляционная функция $R_k(G)$ характеризует отношение экспериментального распределения квазибыстротных интервалов к дифференциальному фоновому распределению $R_K(G) = \frac{F_K(G)}{F_K^{\varphi}(G)} - 1$, где $G = \eta_{i+k} - \eta_\imath$ квазибыстротный интервал, а η_i и η_{i+k} значения квазибыстрот для граничных частиц в интервале с k – 1 частицей.

Анализ функции R_K в зависимости от G проводился на обогащенных аннигиляцией и не аннигиляционных $\tilde{p}p$ - взаимодействиях при импульсе 22,4 ГэВ/с и 32 ГэВ/с, а также на неупругих pp - взаимодействиях при импульсе 69 ГэВ/с.

Во взаимодействиях с “аннигиляцией” наблюдается более слабая корреляция по сравнению с корреляцией в неаннигиляционных pp-взаимодействиях. В протон-протонных и неаннигиляционных

антипротон-протонных столкновениях наблюдается сходство корреляционных функций.

Ключевые слова: аннигиляция, протон, антипротон, взаимодействие, реакция, интервал, корреляция.

Information about authors:

Boulat Zhautykov - Satbayev University, Institute of Physics and Technology, Almaty, Kazakhstan, https://orcid.org/0000-0002-8838-7443;

Tursynhan Temiraliev – Satbayev University, Institute of Physics and Technology, Almaty, Kazakhstan, https://orcid.org/0000-0002-2226-1143;

Rabik Tursunov - Satbayev University, Institute of Physics and Technology, Almaty, Kazakhstan, https://orcid.org/0000-0002-2276-6512;

Mambet Izbasarov - Satbayev University, Institute of Physics and Technology, Almaty, Kazakhstan, https://orcid.org/0000-0002-7433-1238;

Vladimir Samoilov - Satbayev University, Institute of Physics and Technology, Almaty, Kazakhstan, https://orcid.org/0000-0001-7259-239X;

Nikolai Pokrovsky - Satbayev University, Institute of Physics and Technology, Almaty, Kazakhstan, https://orcid.org/0000-0003-1214-4936

REFERENCES

[1] Troitsky S.V. Unsolved problems in particle physics // Phys. Usp., 2012, V. 55, №1-2, P. 72–95.

[2] Mangano M.L. QCD and the physics of hadronic collisions // Phys. Usp. 2010, V. 53, № 2б P. *109*–132.

[3] Dremin I M, Kaidalov A B Quantum chromodynamics and phenomenology of strong interactions // Phys. Usp. 2006, V. 49, № 3, P. 263–273.

[4] Rubakov V.A. Cosmology and the Large Hadron Collider // Phys. Usp., 2011, V. 54 № 6, P. 633–641.

[5] Raja R. Estimation of the Annihilation Component in $\bar{P}P$ Interactions // Phys.Rev., 1977, V. D16, P. 142 – 153.

[6] Boos E.G., Ermilova D.I. et al. Charge asymmetry at large p_T in inelastic *pp* - *r*eactions at 22.4 GeV/c. // Nucl. Phys. B, 1977, V. 128, № 2, P. 269 – 274.

[7] Smirrnova L.N. The Dynamics of $\tilde{p}p$ - annihilation at High Energies // Yaderrnya Fizika, 1988, V. 47, P. 419 – 430. (In Russian)

[8] Ward, C.P. *et al.* General Features Of Charged Particle Production In Anti-p P Interactions At 100-gev/c // Nucl. Phys. B, 1979, V. 153, P. 299 – 333.

[9] Boos E.G., Temiraliev T. et al. The Method of $\tilde{p}p$ - annihilation Separation at 22,4 GeV/c Momentum. // Izvestiya MON RK, NAN RK, seriya fiziko-matematicheskaya, 2000, №2, P. 35 – 44. (In Russian)

[10] Batyunya B.V., Boguslavsky I.V. et. al. Charged particle multiplicity distribution in anti pp interactions at 22.4 GeV/c // Preprint JINR E1-739, 1981, Dubna.

[11] Hanumaiah B., Sarycheva L.I. et al. Charged-particle multiplicities in pp interactions at 32 GeV/c // Nuovo Cimento A, 1982, V. 68, № 2, P. 161 – 175.

[12] Bumazhnov V.A., Ermolov P.F. et al. Negative Pion Production in Proton Proton Interactions at 69 GeV/c // Phys. Lett. B, 1974, V. 50, P. 283 - 286.

[13] Boos E.G., Temiraliev T. et al.. Cross-Section of $\tilde{p}p$ - annihilation at 32 GeV/c // Izvestiya NAN RK, seriya fiziko-matematicheskaya, 2006, № 6, P. 64 – 69. (In Russian)

[14] Boos E.G., Vinitsky A.H. et al. Study of Nuclear Density Effects on Secondary Hadrons Many-Particle Correlations // Z.Phys. 1995, V. A351, P. 209 – 216.

[15] Tasmambetov Zh.N., Rajbov N., Issenova A.A. The Construction of a Solution of a Related System of the Laguerre Type // News of the National Academy of Sciences of the Republic of Kzakhstan. Series of physic – mathematical sciences. Volume 1, Number 323 (2019) pp. 38-50. ISSN 1991-346X https://doi.org/10.32014/2019.2518-1726.5

МАЗМҰНЫ

Зазулин Д.М., Буртебаев Н., Петерсон Р.Ж., Артемов С.В., Игамов С., Керимкулов Ж.К., Алимов Д.К., Мухамеджанов Е.С., Насурлла Маулен, Сабидолда А., Насурлла Маржан, Ходжаев Р. Төмен энергиялардағы Р-^{12}С радиациялық қарпуының жаңа нәтижелері........ 5

Жадыранова А.А. n = 3 және N = 2 жағдайлары үшін енгізгізілген жаңа жүйе a_t, b_t, c_t $V_0 = 0$ болғандағы WDVV ассоциативтілік теңдеуінің иерархиясы........ 14

Шалданбаев А.Ш., Ақылбаев М.И., Шалданбаева А.А., Бейсебаева А.Ж. Кіші мүшелі толқын операторының спектрәлдік қасиеттері........ 22

Шалданбаев А.Ш., Шалданбаева А.А., Шалданбай Б.А. Потенциалы симметриялы, ал шекаралық шарттары ажырамайтын Штурм-Лиувилл операторының кері есебі туралы........ 30

Дасибеков А., Юнусов А.А., Юнусова А.А., Корганбаев Б.Н., Куатбеков Н.А., Такибаева Г.А., Еспембетова Д.Н. Серпімділік қасиеттері бар және шектестік жағдайлары әртекті топрақ қабатың тығыздау........ 42

Мамырбаев Ө.Ж., Шаяхметова Ә.С., Сейсенбекова П.Б. Байес тәсіліне негізделген ақпараттық технологиялар бағытында білім алушылардың құзыреттілігін арттыру үшін зияткерлік ортаны құру әдістемесі........ 50

Калимолдаев М., Ахметжанов М., Кунелбаев М. Екі роторлық шағын гидроэлектростанция үшін сұйықтық ағынымен гидро турбиналы тордың энергетикалық өзара әрекеттесуін анықтау........ 59

Исахов А.А., Абай А., Омарова П.Т., Бекжигитова Ж.Е. Тұрғын үй аумағындағы ластаушы заттардың таралуының сандық моделдеуі........ 68

Бекболат Б., Кангужин Б., Токмагамбетов Н. Толқын теңдеуі үшін көп нүктелі аралас шекаралық есеп........ 76

Тасмамбетов Ж.Н., Раджабов Н., Убаева Ж.К. Үшінші ретті дербес туындылы екі дифференциалдық теңдеулердің бірлескен шешімі........ 83

Бекболат Б., Нурахметов Д. Б., Токмагамбетов Н., Аймал Раса Г. Х. Ойылған аймақтағы Лаплас операторының түбір функциялар жүйесінің минималдылығы........ 92

Марат Нуртас, Байшемиров Ж.Д. Семей полигоны аумағының температуралық режимін зерттеу және математикалық модельді және оның сандық шешімін сипаттау........ 110

Серикбаев Д., Токмагамбетов Н. Штурм-Луивилл операторлы псевдо-параболалық теңдеу үшін кері есеп........ 122

Яковец А.Ф., Жаханшир А., Гордиенко Г.И., Жумабаев Б.Т., Литвинов Ю.Г., Абдрахманов Н. Ионосферадағы F2-қабатының вариация ауқымының максималды биіктігін айқындау статистикасы........ 129

Калимолдаев М., Ахметжанов М., Кунелбаев М. Тұрақты ток айнымалы кернеуге түрлендіру үшін түрлендіргіштікпен күн фотоэлементтерінің математикалық моделін әзірлеу және зерттеу........ 135

Жаутыков Б.О., Избасаров М., Покровский Н.С., Самойлов В.В., Темиралиев Т., Турсунов Р.А. 22,4 ГэВ/с және 32 ГэВ/с импульста аннигиляциямен байытылған $\tilde{p}p$ - әсерлесудегі ядро-белсенді бөлшектердің корреляциясын зерттеу........ 143

СОДЕРЖАНИЕ

Зазулин Д.М., Буртебаев Н., Петерсон Р.Ж., Артемов С.В., Игамов С., Керимкулов Ж.К. , Алимов Д.К., Мухамеджанов Е.С., Насурлла Маулен, Сабидолда А., Насурлла Маржан, Ходжаев Р. Новые результаты для радиационного захвата p-^{12}C при низких энергиях........ 5

Жадыранова А.А. Иерархия уравнений ассоциативности WDVV для случая n = 3 и N = 2 при V_0 = 0 с новой системой a_t, b_t, c_t........ 14

Шалданбаев А.Ш., Ақылбаев М.И., Шалданбаева А.А., Бейсебаева А.Ж. О спектральных свойствах волнового оператора, возмущённого младшим членом........ 22

Шалданбаев А.Ш., Шалданбаева А.А., Шалданбай Б.А. Обратная задача оператора Штурма-Лиувилля с не разделенными краевыми условиями и симметричным потенциалом........ 30

Дасибеков А., Юнусов А.А., Юнусова А.А., Корганбаев Б.Н., Куатбеков Н.А., Такибаева Г.А., Еспембетова Д.Н. Уплотнение слоя грунта, обладающего упругим свойством и неоднородностью граничных условий........ 42

Мамырбаев О.Ж., Шаяхметова А.С., Сейсенбекова П.Б. Методология создания интеллектуальной среды повышения компетентности обучающегося по направлению it на основе байесовского подхода........ 50

Калимолдаев М., Ахметжанов М. , Кунелбаев М. Определение силового взаимодействия гидротурбинной сетки с потоком жидкости для двухроторной микро ГЭС........ 59

Исахов А.А., Абай А., Омарова П.Т., Бекжигитова Ж.Е. Численное моделирование распространение загрязняющих веществ в жилых районах........ 68

Бекболат Б., Кангужин Б., Токмагамбетов Н. О многоточечной задаче смешанной границы для волнового уравнения........ 76

Тасмамбетов Ж.Н., Раджабов Н., УбаеваЖ.К. Совместное решение двух дифференциальных уравнений в частных производных третьего порядка........ 83

Бекболат Б., Нурахметов Д. Б., Токмагамбетов Н., Аймал Раса Г. Х. О минимальности систем корневых функций оператора Лапласа в проколотой области........ 92

Марат Нуртас, Байшемиров Ж.Д. Исследование температурного режима территории семипалатинского полигона и описание математической модели и его численного решения........ 110

Серикбаев Д., Токмагамбетов Н. Обратная задача для псевдо-параболического уравнения для оператора Штурма-Лиувиля........ 122

Яковец А.Ф., Жаханшир А., Гордиенко Г.И., Жумабаев Б.Т., Литвинов Ю.Г., Абдрахманов Н. Статистика размаха вариаций высоты максимума F2-слоя ионосферы........ 129

Калимолдаев М., Ахметжанов М., Кунелбаев М. Разработка и исследование математической модели солнечного фотопреобразователя с инвертором для преобразования постоянного тока в переменное напряжение........ 135

Жаутыков Б.О., Избасаров М., Покровский Н.С., Самойлов В.В., Темиралиев Т., Турсунов Р.А. Исследование корреляций ядерно-активных частиц в $\widetilde{p}p$ -взаимодействиях, обогащенных аннигиляцией при импульсе 22,4 ГэВ/с и 32 ГэВ/с........ 143

CONTENTS

Zazulin D. M., Burtebayev N., Peterson R. J., Artemov S. V., Igamov S., Kerimkulov Zh.K., Alimov D. K., Mukhamejanov E. S., Nassurlla Maulen, Sabidolda A., Nassurlla Marzhan, Khojayev R. New results for the P-^{12}C radiative capture at low energies 5

Zhadyranova A.A. Hierarcy of WDVV associativity equations for n = 3 and N = 3 case when $V_0 = 0$ with new system a_t, b_t, c_t 14

Shaldanbayev A.Sh., Akylbayev M.I., Shaldanbayeva A.A., Beisebayeva A.Zh. On the spectral properties of a wave operator perturbed by a lower-order term........ 22

Shaldanbayev A.Sh., Shaldanbayeva A.A., Shaldanbay B.A. Inverse problem of the Sturm-Liouville operator with unseparated boundary value conditions and symmetric potential........ 30

Dasibekov A., Yunusov A.A., Yunusova A.A., Korganbayev B.N., Kuatbekov N.A., Takibayeva G.A., Espembetova D.N. Sealing of a layer of a sound with effect of elastic properties and inhomogeneous border conditions........ 42

Mamyrbayev O. Zh., Shayakhmetova A.S., Seisenbekova P.B. The methodology of creating an intellectual environment of increasing the competence of students based on a bayesian approach........ 50

Kalimoldayev M., Akhmetzhanov M., Kunelbayev M. Determination of the power interaction of the hydro turbine GRID with a fluid flow for a double-rotor micro hydro power plant........ 59

Issakhov A.A., Abay A., Omarova P.T, Bekzhigitova Zh. E. Numerical modeling of contaminating substances distribution in residential areas........ 68

Bekbolat B., Kanguzhin B., Tokmagambetov N. To the question of a multipoint mixed boundary value problem for a wave equation........ 76

Tasmambetov Zh.N., Rajabov N., Ubayeva Zh.K. The coordinated solution of two differential equations in private derivatives of the third order........ 83

Bekbolat B., Nurakhmetov, D. B., Tokmagambetov N., Aimal Rasa G. H. On the minimality of systems of root functions of the Laplace operator in the punctured domain........ 92

Marat Nurtas, Baishemirov Zh.D. Investigation of the temperature regime of the territory of the semipalatinsk polygon and description of the mathematical model and its numerical solution........ 110

Serikbaev D., Tokmagambetov N. An inverse problem for the pseudo–parabolic equation for a Sturm-Liouville operator........ 122

Yakovets A.F., Jahanshir A., Gordienko G.I., Zhumabayev B.T., Litvinov Yu.G., Abdrakhmanov N. Statistics of variation range of F2- layer maximum height of the ionosphere........ 129

Kalimoldayev M., Akhmetzhanov M. , Kunelbayev M. Development and research of a mathematical model of a solar photo converter with an inverter for converting direct current to alternating voltage........ 135

Izbasarov M., Pokrovsky N.S., Samoilov V.V., Temiraliev T., Tursunov R.A., Zhautykov B.O. Investigation of correlations of generated nuclear active particles in $\tilde{p}p$ - events enriched by annihilation at momenta 22.4 GeV/c AND 32 GeV/c....... 143

Publication Ethics and Publication Malpractice
in the journals of the National Academy of Sciences of the Republic of Kazakhstan

For information on Ethics in publishing and Ethical guidelines for journal publication see http://www.elsevier.com/publishingethics and http://www.elsevier.com/journal-authors/ethics.

Submission of an article to the National Academy of Sciences of the Republic of Kazakhstan implies that the described work has not been published previously (except in the form of an abstract or as part of a published lecture or academic thesis or as an electronic preprint, see http://www.elsevier.com/postingpolicy), that it is not under consideration for publication elsewhere, that its publication is approved by all authors and tacitly or explicitly by the responsible authorities where the work was carried out, and that, if accepted, it will not be published elsewhere in the same form, in English or in any other language, including electronically without the written consent of the copyright-holder. In particular, translations into English of papers already published in another language are not accepted.

No other forms of scientific misconduct are allowed, such as plagiarism, falsification, fraudulent data, incorrect interpretation of other works, incorrect citations, etc. The National Academy of Sciences of the Republic of Kazakhstan follows the Code of Conduct of the Committee on Publication Ethics (COPE), and follows the COPE Flowcharts for Resolving Cases of Suspected Misconduct (http://publicationethics.org/files/u2/New_Code.pdf). To verify originality, your article may be checked by the Cross Check originality detection service http://www.elsevier.com/editors/plagdetect.

The authors are obliged to participate in peer review process and be ready to provide corrections, clarifications, retractions and apologies when needed. All authors of a paper should have significantly contributed to the research.

The reviewers should provide objective judgments and should point out relevant published works which are not yet cited. Reviewed articles should be treated confidentially. The reviewers will be chosen in such a way that there is no conflict of interests with respect to the research, the authors and/or the research funders.

The editors have complete responsibility and authority to reject or accept a paper, and they will only accept a paper when reasonably certain. They will preserve anonymity of reviewers and promote publication of corrections, clarifications, retractions and apologies when needed. The acceptance of a paper automatically implies the copyright transfer to the National Academy of Sciences of the Republic of Kazakhstan.

The Editorial Board of the National Academy of Sciences of the Republic of Kazakhstan will monitor and safeguard publishing ethics.

Правила оформления статьи для публикации в журнале смотреть на сайтах:

www:nauka-nanrk.kz

http://physics-mathematics.kz/index.php/en/archive

ISSN 2518-1726 (Online), ISSN 1991-346X (Print)

Редакторы *М. С. Ахметова, Т.А. Апендиев, Д.С. Аленов*
Верстка на компьютере *А.М. Кульгинбаевой*

Подписано в печать 10.08.2019.
Формат 60х881/8. Бумага офсетная. Печать – ризограф.
9,6 п.л. Тираж 300. Заказ 4.

Национальная академия наук РК
050010, Алматы, ул. Шевченко, 28, т. 272-13-18, 272-13-19